

This information product has been peer reviewed and approved for publication as a preprint by the U.S. Geological Survey. The final published information product will be published as a Scientific Investigation Report by the U.S. Geological Survey after editorial review, therefore the final version of this information product may have slightly different content and formatting. Feel free to contact the authors with any questions you may have.

*This information product has been peer reviewed and approved for publication as a preprint by the U.S. Geological Survey. Any use of trade, firm, or product names is for descriptive purposes only and does not imply endorsement by the U.S. Government.*

# **Salinas Valley Integrated Hydrologic and Reservoir Operations Models, Monterey and San Luis Obispo Counties, California**

By Wesley R. Henson, Randy Hanson, Scott Boyce, Joseph Hevesi, and Elizabeth R. Jachens

**Prepared in cooperation with Monterey County Resources Agency, Monterey County  
and the Salinas Valley Basin Groundwater Sustainability Agency**

Contents

Motivation..... 22

Previous Model Studies..... 27

Climate ..... 32

Land Use..... 35

    Irrigated Land Use ..... 37

Surface Water and Watershed ..... 39

Geology of Groundwater Basins ..... 42

Groundwater ..... 43

    Groundwater Recharge..... 44

    Observed Trends in Groundwater Levels ..... 44

    Groundwater Use and Natural Discharge ..... 45

    Groundwater Budget..... 47

    Sea Water Intrusion ..... 47

Simulation Code..... 50

Discretization..... 51

    Temporal Discretization ..... 52

    Spatial Discretization and Layering..... 53

    Analysis Regions ..... 54

    Water Balance Subregions ..... 55

Landscape..... 56

    Farm Process Overview..... 56

        Input Parameters ..... 57

        Landscape Consumptive Use..... 58

Water Demands.....	58
Water Supply.....	59
Runoff and Recharge .....	60
Surface Water Operations .....	61
Climate Data .....	62
Reference Evapotranspiration .....	63
Land Use .....	64
Simulation of Crop Acreage.....	67
Crop Coefficients.....	68
Fractions of Transpiration, Precipitation, and Evaporation .....	70
Irrigation Efficiencies .....	71
Surface Water Inflows and Outflows.....	72
Surface Water Flow Data.....	73
Surface Water Flow Simulation .....	74
Surface-Water Agricultural Supply.....	77
Groundwater Pumpage Agricultural Supply.....	77
Geologic Framework .....	78
Hydrogeologic Units.....	78
Geologic Structures .....	80
Hydrogeologic Texture.....	81
Groundwater Inflows and Outflows.....	83
Groundwater Data .....	83
Specified Groundwater Pumpage for Water Supply .....	84
Groundwater Flow Simulation.....	85

No-Flow Boundaries .....	85
General-Head Boundaries .....	86
Groundwater Wells .....	89
Drain Return Flows .....	91
Hydraulic Properties .....	92
Zones .....	93
Texture-Based Hydraulic Properties .....	94
Groundwater Storage .....	95
Hydraulic Conductivity .....	97
Faults .....	99
Initial Conditions .....	100
Parameter Estimation and History Matching—Salinas Valley Integrated Hydrologic Model .....	101
Parameter Estimation .....	102
Observation Data .....	104
Surface Water .....	105
Groundwater .....	106
Agricultural Pumpage .....	107
Observation Weighting .....	108
Parameters .....	109
Landscape-Process Parameters .....	110
Hydraulic Parameters .....	111
Horizontal-Flow Barrier Parameters .....	113
Regional Groundwater Flow and Seawater Coastal Inflow Parameters .....	113
Single and Multiple-Aquifer Well Parameters .....	114

Surface-Water Network and Drain Return Flow Parameters.....	115
Parameter Sensitivity Analysis .....	115
History Matching Results .....	117
Streamflow.....	118
Groundwater.....	121
Groundwater Levels.....	121
Groundwater-Level Maps.....	125
Agricultural Pumpage .....	127
Hydrologic Flow Budgets—Salinas Valley Integrated Hydrologic Model .....	129
Analysis Periods .....	130
Salinas Valley Landscape Budget .....	132
Landscape Budget Components .....	132
Climate Variability.....	133
Total Delivery Requirement .....	134
Salinas Valley Groundwater Budget .....	135
Groundwater Budget Components .....	136
Groundwater Budget Bar Plots.....	137
Groundwater Budget Summary Tables .....	138
Groundwater Budget Flow Charts .....	139
Integrated Hydrologic Model Domain Groundwater Budget.....	139
Riparian Analysis Region.....	141
Pressure Analysis Region.....	143
East Side-Langley Analysis Region .....	144
Forebay Analysis Region .....	146

Upper Valley Analysis Region.....	147
Salinas Valley Operational Model.....	149
Reservoir Release Simulation.....	150
Baseline Reservoir Results.....	152
Data Uncertainty and Limitations.....	155
FMP Suitability and Limitations .....	159
Hydrologic Model Limitations .....	162
Potential Improvements.....	166
Surface Water Summary .....	176
Agricultural Demand Summary .....	177
Groundwater-Level Summary .....	178
Groundwater Budget Summary.....	179
Conclusions.....	180

## Figures

**Figure 1.** Map of Salinas River watershed in Monterey and San Luis Obispo counties, showing the Salinas Valley Groundwater Basin (California Department of Water Resources, 2020), Zone 2C water management area (Henson and Jachens, 2022), Salinas, Nacimiento and San Antonio Reservoirs, Castroville Seawater Intrusion Project (CSIP)(Henson and Jachens, 2022), Salinas River Diversion Facility (SRDF), Clark Colony, and Tembladero Slough diversions (Henson and others, 2023). ..... 22

**Figure 2.** Salinas Valley showing the Monterey County groundwater sustainability management area, Zone 2C Water Management Area, integrated hydrologic model domain, Salinas Valley Integrated Groundwater Model domain, and Seaside adjudicated groundwater subbasin. .... 28

**Figure 3.** Integrated hydrologic model domain annual average gridded precipitation at 530-foot resolution for water years 1968 through 2018, coastal and inland climate zones based on aggregation of California Irrigation Management Information System (CIMIS) climate zones, CIMIS stations, selected climate stations, Remote Automatic Weather Stations (RAWS), Cooperative Observer Network (COOP) stations, and two analysis COOP stations: Salinas Airport (USW00023233) and King City (USC00044555)..... 34

**Figure 4.**Annual precipitation at selected Cooperative Observer Network stations (COOP; National Oceanic and Atmospheric Administration, 2020) for water years 1968 through 2018 for A) Salinas Airport (USW00023233) and B) King City (USC00044555). Shaded regions illustrate two relatively dry periods in the Salinas Valley defined based on generally decreasing or flat cumulative precipitation departure from the mean and annual precipitation less than mean precipitation from water years 1968 through 2018. C) Cumulative precipitation departure from the mean at Salinas Airport (USW00023233) and King City (USC00044555) showing delineation of analysis periods A, B, C, and D for the study. .... 34

**Figure 5.** Integrated hydrologic model domain annual average gridded potential evapotranspiration at 530-foot resolution for water years 1968 to 2018, coastal and inland climate zones based on aggregation of California Irrigation Management Information System (CIMIS) climate zones, CIMIS evaluation locations, Remote Automatic Weather Stations (RAWS), and Cooperative Observer Network (COOP) stations..... 35

**Figure 6.** Integrated hydrologic model domain land use (Henson and others, 2024) for calendar years A) 1968, B) 1984, C) 1998, and D) 2014 that includes additional remotely sensed irrigated areas within the study area and outside of Zone 2C Water Management Area..... 36

**Figure 7.**Cropped acreage estimates in the integrated hydrologic model domain showing total harvested acres in Monterey County during the study period..... 38

**Figure 8.** Comparison of total annual watershed inflows into the integrated hydrologic model domain from the Salinas Valley Watershed Model and observed Salinas River flows at the first gage on Salinas River in the study area (USGS 11150500 Salinas River near Bradley, California) (USGS, 2018) to show the relative



contribution of surface water from adjacent watershed inflows and inflows from the upper watershed outside of the study area for water years 1968 through 2018.....	40
<b>Figure 9.</b> Comparison of annual mean storage in Lakes San Antonio and Nacimiento for water years 1968 through 2018.....	42
<b>Figure 10.</b> Surface water deliveries from agricultural diversions for Clark Colony and Salinas River Diversion Facility (SRDF), channel wetting diversions for Tembladero Slough, and recycled water deliveries for the Castroville Seawater Intrusion Project (CSIP) from water year 1968 to 2018 (Henson and others, 2023).....	42
<b>Figure 11.</b> Groundwater basins and subbasins within and adjacent to the Salinas Valley.....	43
<b>Figure 12.</b> Estimated groundwater level contours in the integrated hydrologic model domain for A) shallow aquifers (less than 200 feet deep) and B) deep aquifers (greater than 200 feet deep) in fall 1994. The Salinas River, Salinas Valley groundwater subbasins, and selected observation wells are also shown. ....	45
<b>Figure 13.</b> Observed water levels during the study period for A) well BDA331 in the 180-Foot/400-Foot Aquifer groundwater subbasin, B) well ZES1572 in the East Side Aquifer groundwater subbasin, C) ZFS1001 in the Forebay Aquifer groundwater subbasin, and D) well ZSE733 in the Upper Valley Aquifer groundwater subbasin. ....	45
<b>Figure 14.</b> Annual total municipal, industrial, and agricultural pumpage in Zone 2C Water Management Area from water year 1970 through 2018. Pumpage is estimated before 1994 and reported for water years 1995 to 2018.....	46
<b>Figure 15.</b> Analysis regions and other areas that are simulated within the integrated hydrologic model domain.....	54
<b>Figure 16.</b> Thirty-one (31) water balance subregions of the integrated hydrologic model domain. ....	56

**Figure 17.** California Irrigation Management Information System (CIMIS, 2020) field-scale reference evapotranspiration (ET<sub>ref</sub>) and potential evapotranspiration (PET) estimated using the 270-meter-resolution Basin Characterization Model (BCM; Hevesi and others, 2022) at the same location. A) Correlation and comparison of stations with long-term records used for more detailed comparisons. Comparisons of time series are shown for B) Castroville (CIMIS 019), C) Arroyo Seco (CIMIS 114), D) Salinas South (CIMIS 089), E) King City-Oasis Rd. (CIMIS 113), and F) Salinas North (CIMIS 116)..... 64

**Figure 18.** Comparison of time series of physical acreage, simulated acreage assuming a multi-cropping factor of 1.97, and harvested acreage for selected land use types in the Salinas Valley for water years 1968 through 2014. .... 68

**Figure 19.** Crop coefficients by land use type for A) high frequency land use, B) annually stable land use, C) multi-year land use, D) urban and managed land use, and E) native land cover in Salinas Valley, California. .... 69

**Figure 20.** Surface water drainage network channel types within the Salinas Valley study area, USGS National Water Information System streamgages, stream diversion locations, and point locations of watershed inflows from outside the active model domain. .... 73

**Figure 21.** Annual average net stream leakage normalized by segment length in the surface water drainage network in acre-feet per year per foot (afyf), diversion locations, and selected streamgages used for analysis. .... 76

**Figure 22.** A) surface extent of hydrogeologic units and fault traces of the Salinas Valley study area in Monterey and San Luis Obispo Counties, California, adapted from the Salinas Valley Geologic Framework (Sweetkind, 2023) and B) conceptual cross section through hydrogeologic units of the Salinas Valley Geologic Framework along the central axis of the Salinas Valley. Vertical exaggeration is approximately 100 times. .... 79

**Figure 23.** Hydrogeologic unit thickness and percentage of coarse material for hydrogeologic units in the Salinas Valley, California that are not fully consolidated (Sweetkind, 2023): *A*) shallow aquifer, *B*) upper confining unit, *C*) 180-Foot Aquifer, *D*) middle confining unit, *E*) 400-Foot Aquifer, *F*) lower confining unit, and *G*) Paso Robles Formation; and *H*) maps showing hydrogeologic unit thickness for Purisima Formation and bedrock hydrogeologic units. The Purisima Formation and bedrock hydrogeologic units represent composite rock aquifers without a textural classification so the percentage of coarse materials is not shown. .... 82

**Figure 24.** Wells within the integrated hydrologic model domain for *A*) municipal, industrial, and agricultural wells, and a subset of wells used to estimate municipal and industrial pumpage from water year 1968 to 1994 (pre-1995 wells); and *B*) location of observation wells. .... 84

**Figure 25.** Specification of general head boundaries (GHB) in the integrated hydrologic model domain. The location of GHB wells and the cells used to define the offshore GHB, coastal GHB, and inland GHB in the Salinas Valley Integrated Hydrologic Model domain are shown. .... 87

**Figure 26.** General head boundary (GHB) time series in the Salinas Valley, California for *A*) coastal GHB boundary well 33H1, *B*) coastal GHB boundary well 16D1, *C*) coastal GHB boundary well 4L1, *D*) coastal GHB boundary well 12D1 (Henson and others, 2023), and *E*) mean monthly sea level (National Oceanic and Atmospheric Administration, 2019). .... 87

**Figure 27.** Distribution of parameter zones used for estimation of hydraulic properties in the integrated hydrologic domain for the six aquifer hydrogeologic units in the Salinas Valley, California *A*) shallow aquifer (model layer 1), *B*) 180-Foot Aquifer (model layer 3), *C*) 400-Foot Aquifer (model layer 5), *D*) Paso Robles Formation (model layer 7), *E*) Purisima Formation (model layer 8), and *F*) bedrock (model layer 9) (Henson and Culling, 2025). .... 93

**Figure 28.** Hydrogeologic unit *A*) specific yield and *B*) thickness for the uppermost layer of each model cell in the integrated hydrologic model domain for the Salinas Valley, California. The uppermost layer is a

composite of hydrogeologic units in the uppermost cell in layers 1, 3, 5, 7, 8, or 9 (Henson and Culling, 2025). ..... 97

Figure 29. Horizontal and vertical hydraulic conductivity in six aquifer hydrogeologic units in the Salinas Valley, California A) shallow aquifer, B) 180-Foot Aquifer, C) 400-Foot Aquifer, D) Paso Robles Formation, E) Purisima Formation, and F) bedrock (Henson and Culling, 2025). ..... 99

**Figure 30.** Analysis regions with locations of selected observation wells in Salinas Valley, California. .... 107

**Figure 31.** Magnitudes of the relative composite scaled sensitivity for selected parameters used in Salinas Valley integrated and reservoir operations models for Monterey and San Luis Obispo Counties, California. Refer to table 6 for a full description of the sensitive parameter names and values. All model parameters described by Henson and Culling (2025). ..... 110

**Figure 32.** Observed and simulated equivalent streamflow hydrographs for selected river gages and diversions within the Salinas Valley Integrated Hydrologic Model domain for water years 1968 to 2018. A) Correlation among simulated and observed streamflows for all stream observations. Simulated and observed streamflow at B) USGS 11150500, C) USGS 11151700, D) USGS 11152300, E) USGS 11152500, F) USGS 11152000, and G) USGS 11152050 gages. Simulated and observed stream difference for H) USGS 11150500 – USGS 11151700, I) USGS 11151700 – USGS 11152300, J) USGS 11152300 – USGS 11152500, and K) USGS 11152000 – USGS 11152050. Simulated and observed diversions from L) Arroyo Seco for Clark Colony and M) Salinas River at the Salinas River Diversion Facility (Henson and Culling, 2025). ..... 119

**Figure 33.** Groundwater observations and simulated equivalent values from the Salinas Valley Integrated Hydrologic Model. A) Graph of correlation among groundwater-level measurements and simulated equivalent groundwater-level hydrographs for selected wells. Hydrographs are shown for wells B) CSI239, C) BDA331, D) ZPN1529, and E) ZPN441 in the Pressure analysis region; wells F) ZES1572 and G) ZES871 in the East Side-Langley analysis region; wells H) ZNE1267 and I) ZSE355 in the Forebay

analysis region; and wells J) ZSE355 and K) ZSE733 in the Upper Valley analysis region (Henson and Culling, 2025). ..... 121

**Figure 34.** Mean residuals computed as the difference between observed and simulated equivalent values in the Salinas Valley Integrated Hydrologic Model for all observation wells for the parameter estimation period from water year 1968 through 2014 (Henson and Culling, 2025). ..... 125

**Figure 35.** Historical model groundwater contours in Salinas Valley, California developed from simulated equivalent December groundwater levels to Monterey County Water Resource Agency (MCWRA) fall composite contoured groundwater levels. The shallow aquifer composite contour map was computed by MCWRA using measurements in aquifers that are less than 200 feet deep. The shallow contours are compared to groundwater level contours from model cells within the 180-Footer Aquifer hydrogeologic unit (layer 3). The deep aquifer composite contour map was computed by MCWRA using measurements greater than 200 but less than 420 feet deep. The deep contours are compared to groundwater level contours from model cells within the 400-Footer Aquifer hydrogeologic unit (layer 5). These maps show A) shallow aquifer composite contours and simulated equivalent contours in fall of 1994, B) deep aquifer composite contours and simulated equivalent contours in fall 1994, C) shallow aquifer composite contours and simulated equivalent contours in fall of 2003, D) deep aquifer composite contours and simulated equivalent contours in fall 2003, and E) shallow aquifer composite contours and simulated equivalent contours in fall 2011, and F) deep aquifer composite contours and simulated equivalent contours in fall 2011..... 126

**Figure 36.** Reported and simulated equivalent agricultural pumpage within the Salinas Valley Integrated Hydrologic Model. A) Correlation among monthly reported and simulated equivalent groundwater pumpage. Time series of monthly observed and simulated equivalent farm deliveries for the B) Pressure analysis region, C) East Side-Langley analysis region, D) Forebay analysis region, and E) Upper Valley analysis region. Times series of annual observed and simulated equivalent pumpage for F) entire integrated

hydrologic model domain, G) Pressure analysis region, H) East Side-Langley analysis region, I) Forebay analysis region, and J) Upper Valley analysis region (Henson and others, 2023; Henson and Culling, 2025).

..... 128

**Figure 37.** Four hydrologic budget analysis subperiods in the study that is informed by the cumulative departure of precipitation at Cooperative Observer Network stations for the Salinas Airport (USW00023233) and King City (USC00044555), California. The subperiods represent A) the start of land use conversion to more multi-cropping, 1970–1983; B) historical dry period, 1984–1994; C) start of reported withdrawal data collection with relatively wetter conditions, 1995–2009; and D) initiation and operation of the Salinas River Diversion Facility and recent recycled water deliveries, 2010–2018. .... 131

**Figure 38.** Distribution of landscape-budget inflow and outflow components for the Salinas Valley Integrated Hydrologic Model for water years 1970 to 2018 showing the A) entire integrated hydrologic model domain, B) Riparian analysis region, C) Pressure analysis region, D) East Side-Langley analysis region, E) Forebay analysis region, and F) Upper Valley analysis region (Henson and Culling, 2025). .... 133

**Figure 39.** Distribution of groundwater-budget components of inflows and outflows for the flow system of the Salinas Valley Integrated Hydrologic Model for water year 1970 to 2018. A) Entire integrated hydrologic model domain, B) Riparian analysis region, C) Pressure analysis region, D) East Side-Langley analysis region, E) Forebay analysis region, and F) Upper Valley analysis region (Henson and Culling, 2025). .... 138

**Figure 40.** Average groundwater budget from water year 1970 through 2018 showing budget components (in thousands of acre-feet) for the A) entire Salinas Valley Integrated Hydrologic Model domain, B) Riparian analysis region, C) East Side-Langley analysis region, D) Pressure analysis region, E) Forebay analysis region, and F) Upper Valley analysis region (Henson and Culling, 2025). .... 141

**Figure 41.** Salinas Valley Operational Model implementation, showing storage parameters that are used to simulate reservoir storage and operational rule parameters that are used to evaluate operational rules for conservation, demand, and floods to generate a time series of reservoir releases. .... 151

**Figure 42.** Salinas Valley Operational Model (SVOM) reservoir observed data (Henson and others, 2023) and simulated equivalent values in Lake San Antonio and Lake Nacimiento reservoirs for A) monthly storage, B) annual mean reservoir storage, and C) total annual mean reservoir releases. Reservoir storage and releases in the SVOM are not intended to replicate historical conditions. The historical time series is shown to illustrate that the SVOM results reasonably reproduce flows and storage within the boundaries of historical conditions (Henson and Culling, 2025)..... 153

**Figure 43.** Selected statistics related to reservoir operations describing A) total reservoir releases, B) mean annual reservoir storage, C) simulated days per year where specified streamflow values are met to support phases of steelhead (*Oncorhynchus mykiss*) life cycle, and D) total annual number of days the Salinas River Diversion Facility (SRDF) is active. For each box plot, the shaded box represents the interquartile range, where 50 percent of the data occurs within the range. The lower portion of the shaded box represents the 25th to 50th percentile range, and the upper portion represents the 50th to 75th percentile range. The whiskers display the range that is within 1.5 times the interquartile range. All the data points are plotted on each box plot. Any data points outside of the whisker range are statistical outliers (Henson and Culling, 2025)..... 154

**Tables**

**Table 1.** Summary of MODFLOW-One Water Hydrologic Model (MF-OWHM) packages and processes used in the Salinas Valley Integrated Hydrologic Model and Salinas Valley Operational Model..... 51

**Table 2.** Summary of analysis regions, Salinas Valley groundwater subbasins, named subareas, water-balance subregions, and their available water sources to meet demands..... 54

**Table 3.** Summary of geologic formations and hydrogeologic units in the Salinas Valley Geologic Framework (Sweetkind, 2023)..... 79

<b>Table 4.</b> Summary of hydrogeologic units, model layers, and aquifer properties in the Salinas Valley Integrated Hydrologic Model and Salinas Valley Operational Model with corresponding layers and properties from the previously developed Salinas Valley Integrated Groundwater and Surface Model (SVIGSM; Montgomery Watson, 1997). .....	93
<b>Table 5.</b> Summary of IBOUND parameter and zone codes used to represent the hydrogeologic properties in the Salinas Valley, California used in the integrated hydrologic models. ....	95
<b>Table 6.</b> Summary of sensitive calibration parameters from composite scaled sensitivity analyses for the Salinas Valley, California Integrated Hydrologic Model. ....	110
<b>Table 7.</b> Summary of streamflow history matching showing streamflow statistics for the period from 1970 to 2018, mean residual streamflow computed as observed minus the simulated equivalent value, root mean squared error, scaled root mean square error, and Nash-Sutcliffe model efficiency for U.S. Geological Survey gages and diversions in the Salinas Valley Integrated Hydrologic Model. ....	120
<b>Table 8.</b> Summary of selected observation wells used to illustrate Salinas Valley Integrated Hydrologic Model history matching, indicating number of observations, representative model layers, hydrogeologic units, mean residual computed as observed minus the simulated equivalent value, and root mean square error. ....	122
<b>Table 9.</b> Summary of groundwater level history matching showing drawdown mean residual (computed as observed minus the simulated equivalent value), root mean square error, and scaled root mean square error for the Salinas Valley integrated hydrologic model domain and analysis regions. ....	122
<b>Table 10.</b> Summary of monthly agricultural pumpage history matching by analysis region showing mean residual computed as observed minus the simulated equivalent value, root mean square error, and scaled root mean square error for the integrated hydrologic model domain. ....	129



<b>Table 11.</b> Summary of groundwater budget data for the entire Salinas Valley Integrated Hydrologic Model domain for the simulation period 1970–2018, analysis periods A–D, and high and low precipitation years representing conditions before and after the Salinas River Diversion Facility was implemented.....	140
<b>Table 12.</b> Summary of groundwater budget data for the Riparian analysis region for the simulation period 1970–2018, analysis periods A–D, and high and low precipitation years representing conditions before and after the Salinas River Diversion Facility was implemented.....	143
<b>Table 13.</b> Summary of groundwater budget data for the Pressure analysis region for the simulation period 1970–2018, analysis periods A–D, and high and low precipitation years representing conditions before and after the Salinas River Diversion Facility was implemented.....	144
<b>Table 14.</b> Summary of groundwater budget data for the East Side-Langlely analysis region for the simulation period 1970–2018, analysis periods A–D, and high and low precipitation years representing conditions before and after the Salinas River Diversion Facility was implemented.....	146
<b>Table 15.</b> Summary of groundwater budget data for the Forebay analysis region for the period 1970–2018, analysis periods A–D, and high and low precipitation years representing conditions before and after the Salinas River Diversion Facility was implemented.....	147
<b>Table 16.</b> Summary of groundwater budget data for the Upper Valley analysis region for the simulation period 1970–2018, analysis periods A–D, and high and low precipitation years representing conditions before and after the Salinas River Diversion Facility was implemented.....	149
<b>Table 17.</b> Description of Salinas Valley Operational Model (SVOM) operational rules that define reservoir releases triggered based on flow conditions and downstream water demands. ....	152

## Datum

Horizontal coordinate information is referenced to the North American Datum of 1983 (NAD 83).

Vertical coordinate information is referenced to the North American Vertical Datum of 1988 (NAVD 88).

## Supplemental Information

A water year is the 12-month period from October 1 through September 30 and is designated by the calendar year in which it ends.

## Abbreviations

Afyf acre-feet per year per foot

CalPUR California Pesticide Use Reporting

CalPUR-LUE California Pesticide Use Reporting land use estimator

CIMIS California Irrigation Management Information System

COOP Cooperative Observer Network

CSIP Castroville Seawater Intrusion Project

DEM digital elevation model

DRT Drain Return Flow package

ETref reference evapotranspiration

FEI area fraction of evaporation from irrigation

FEP area fraction of evaporation from precipitation

FMP MODFLOW farm process

FTR area fraction of transpiration

GHB general head boundary

GIS geographic information system

HSPF Hydrologic Simulation Program-FORTRAN

Kc crop coefficient

lidar light detection and ranging

M & I municipal and industrial

MCWRA Monterey County Water Resources Agency

mg/L Milligrams per liter

MNW2 Multi-node well package

NLCD National Land Cover Database

NSME Nash-Sutcliffe model efficiency

MF-OWHM MODFLOW-One Water Hydrologic Model

OFE on-farm efficiency factor

PET potential evapotranspiration

PRISM Parameter-elevation Regressions on Independent Slopes Model

RMSE Root mean square error

SFR2 Stream Flow Routing Package

SGMA Sustainable Groundwater Management Act

SRDF Salinas River Diversion Facility

SVWP Salinas Valley Water Project

SVIGSM Salinas Valley Integrated Groundwater Model and Surface Model

SVIHM Salinas Valley Integrated Hydrologic Model

SVGF Salinas Valley Geologic Framework

SVOM Salinas Valley Operational Model

SVWM Salinas Valley Watershed Model

SWO surface water operations

TAFY thousand acre-feet per year

TAW total applied water

TDR total delivery requirement

USGS U.S. Geological Survey

WY water year

WBS water balance subregion

## **Abstract**

The area surrounding the Salinas Valley groundwater basin in Monterey and San Luis Obispo Counties of California is a highly productive agricultural area, contributes significantly to the local economy, and provides a substantial portion of vegetables and other agricultural commodities to the Nation. This region of California provides about half of the Nation's lettuce, celery, broccoli, and spinach each year. Thus, this agricultural area provides significant volumes of agricultural products not just for California but the entire United States.

Changes in population and increased agricultural development, which includes a shift toward more water-intensive crops, and climate variability, have put increasing demand on both surface water and groundwater resources in the valley. This has resulted in water management challenges in the Salinas Valley that are predominantly related to distribution of water supply throughout the basin. Where and when the water is present in the surface and subsurface does not coincide with where and when the water is needed. To deal with the distribution issue, historically water has been used conjunctively in the valley. Conjunctive use is a water

management strategy that coordinates surface water and groundwater use to maximize water availability. Groundwater is used throughout the Salinas Valley to meet water demands when surface water supplies are insufficient. Availability of surface water is constrained by climate. Precipitation and streamflow vary seasonally and year to year. Although there are two reservoirs in the Salinas Valley to capture and store water during wet periods, the only conveyance of reservoir water to coastal agricultural areas is the Salinas River. Increasing demand on groundwater and surface water resources throughout the Salinas Valley has resulted in undesirable effects of unsustainable water use, such as surface water depletion, groundwater level declines, storage depletion in the principal aquifers, and seawater intrusion. To address these escalating issues, local communities, water management agencies, and groundwater sustainability agencies are evaluating how to sustainably manage both their surface water and groundwater resources. To meet water demands and reduce undesirable effects of unsustainable water use, continued conjunctive management of surface water and groundwater would ideally incorporate strategies to deal with increases in demand and a variable climate.

To evaluate the challenging water management issues in the Salinas Valley, the U.S. Geological Survey, Monterey County Water Resource Agency, and the Salinas Valley Basin Groundwater Sustainability Agency developed a comprehensive suite of models that represent the Salinas Valley hydrogeologic system called the Salinas Valley System Model. The Salinas Valley Geologic Framework was developed to characterize the subsurface using various topographic and geologic data sources, including information on hydrogeologic units, their surfaces and extents, geologic structures, lithology, and elevations from borehole data and cross sections, as well as details on faults and existing models. The Salinas Valley Watershed Model simulates the entire Salinas River watershed. Monthly surface water inflows into the integrated

hydrologic model domain were simulated using the Salinas Valley Watershed Model. The historical model uses historical climate data, water and land use data, and reservoir releases to simulate agricultural operations, including landscape water demands, diversions, and reclaimed wastewater. The operational model adds an embedded reservoir operations framework to the simulation of the historical model that allows specified operational rules to simulate reservoir releases and changes in reservoir storage. The operational model assumes current reservoir operations and constant land use, which differs from historical conditions. Thus, the operational model is a hypothetical baseline model that can be used by local water managers to evaluate and quantify potential benefits of water supply projects. Together, the geologic framework, watershed, historical, and operational models form a tool that can be used to simulate irrigated agriculture and associated reservoir operations of the integrated hydrologic system of the Salinas Valley.

## **Introduction**

The Salinas Valley that surrounds the Salinas Valley groundwater basin in Monterey and San Luis Obispo Counties, California (fig. 1), is one of the most productive agricultural basins in California (California Department of Food and Agriculture, 2022) because of its fertile soil, temperate climate, and availability of water for irrigation (Lapham and Heileman, 1901; Cook, 1978). Agricultural production supports more than 76,000 local jobs (nearly one in four households) and contributes an estimated \$5.7 billion per year to Monterey County's economic output and \$8.12 billion to the local economy (Monterey County Agricultural Commission, 2022). In addition, the Salinas Valley provides a substantial number of agricultural products for the Nation. Salinas Valley agriculture produces approximately 150 types of crops that include

large percentages of the Nation’s crops, including 61 percent of leaf lettuce, 57 percent of celery, 56 percent of head lettuce, 48 percent of broccoli, 38 percent of spinach, 30 percent of cauliflower, 28 percent of strawberries, and 3.6 percent of wine grapes (California Department of Food and Agriculture, 2022). Therefore, water supply sustainability in the Salinas Valley is critical for local and national agricultural supplies. Changes in population (U.S. Census Bureau, 2018), increased agricultural development that includes a shift toward more water-intensive crops (Monterey County Agricultural Commission, 2022), and climate variability have put increasing demand on water resources throughout the basin.

**Figure 1.** Map of Salinas River watershed in Monterey and San Luis Obispo counties, showing the Salinas Valley Groundwater Basin (California Department of Water Resources, 2020), Zone 2C water management area (Henson and Jachens, 2022), Salinas, Nacimiento and San Antonio Reservoirs, Castroville Seawater Intrusion Project (CSIP)(Henson and Jachens, 2022), Salinas River Diversion Facility (SRDF), Clark Colony, and Tembladero Slough diversions (Henson and others, 2023).

## **Motivation**

Water management challenges in the Salinas Valley include coordinating conjunctive use of surface water and groundwater throughout the basin. Surface water and groundwater are used conjunctively to support coordinated management of reservoirs for flood mitigation, agricultural water supply, and habitat for federally listed threatened steelhead populations while mitigating aquifer storage losses that have resulted in groundwater level declines, seawater intrusion (California Department of Public Works, 1946; Leedshill-Herkenhoff, Inc., 1985; Monterey County Water Resource Agency [MCWRA], 1995, 1996), and nitrate contamination (California

Department of Water Resources, 1971a; Kulongoski and Belitz, 2007; Moran and others, 2011; Harter and others, 2012). Surface water is plentiful during wet periods, but precipitation and streamflow vary seasonally and year to year (California Department of Public Works, 1946; MCWRA, 1995). Thus, many people, industries, and ecosystems depend directly or indirectly on groundwater because surface water supplies are variable in space and time. Surface water sources used to meet agricultural water demands and support riparian habitat include reservoir releases from two reservoirs in the study area, recycled water deliveries near the coast, surface water diversions from Arroyo Seco, and diversions from the Salinas River (MCWRA, 1995; Henson and others, 2023). Surface water resources are insufficient to meet water demands for all municipal, industrial, and agricultural needs in the basin (California Department of Public Works, 1946). Although there are two reservoirs within the study area that capture and store water during wet periods, the only conveyance of reservoir water to coastal agricultural areas is the Salinas River. The riverbed near the reservoirs is highly permeable with stream leakage that recharges nearby unconfined aquifers (California Department of Public Works, 1946; MCWRA, 1995). This stream leakage results in reduction of streamflow through infiltration in the river as it drains toward the coast near Monterey Bay (MCWRA, 1995). The delivery of surface water to the coastal areas is limited by conveyance during dry periods and by surface water storage capacity during wet periods (MCWRA, 1995).

Groundwater pumpage is used extensively to supplement surface water supplies to meet water demands where and when surface water is unavailable. Limitations on the spatial and temporal availability of surface water and associated dependence on groundwater has resulted in substantial groundwater storage losses in several groundwater basins (California Department of Public Works, 1946; MCWRA, 1995). Groundwater provides about 95 percent of the water used



in the Salinas Valley (California Department of Water Resources, 1973) and groundwater extraction has been occurring in the area for at least a century. Extraction was estimated at 353 thousand acre-feet per year (TAFY) in the 1930s (California Department of Public Works, 1946) and groundwater use has increased through time. The average annual estimated groundwater pumpage from 1970 to 1994 was 519 TAFY (Montgomery Watson, 1997) to 535 TAFY (MCWRA, 1995). The estimated Salinas Valley water budget for 2013 indicated a total reported pumpage of 509 TAFY with an estimated cumulative storage depletion of 559,000 acre-feet from 1944 to 2013 (Baillie and others, 2015). Extensive use of groundwater has resulted in declines of groundwater levels (California Department of Public Works, 1946; MCWRA, 1995), groundwater storage depletion (Baillie and others, 2015), and sea water intrusion into aquifers near the coast (California Department of Public Works, 1946; California Department of Water Resources, 1973; Leedshill-Herkenhoff, Inc., 1985; MCWRA, 1995).

In the Salinas Valley near the Pacific coast, seawater intrusion has been observed in the primary water-bearing units of the Salinas Valley 180-Foot/400-Foot groundwater subbasin—the 180- and 400-foot aquifers (Leedshill-Herkenhoff, Inc., 1985; MCWRA, 1995, 2020). The landward extent of the estimated acreage affected by sea water intrusion from 1944 to 2015 is estimated to be 28,257 and 17,125 acres in the 180- and 400-foot aquifers, respectively (MCWRA, 2020). Sea water intrusion advances inland preferentially along geologic pathways that allow for easier movement of water, affecting land over the 180-foot aquifer at a rate of approximately 265 acres per year in the 180-foot aquifer and the land over the 400-foot aquifer at a rate of 414 acres per year. Several projects have been implemented that aim to reduce coastal groundwater pumping and sea water intrusion. The Monterey County Reclamation Project consists of the Salinas Valley Reclamation Project recycled water plant and the Castroville

Seawater Intrusion Project distribution system (CSIP). The Salinas Valley Water Project includes the Salinas River Diversion Facility (SRDF) to divert Salinas River water for treatment at the recycled water plant for distribution through CSIP to coastal agricultural fields and to offset groundwater pumpage.

Water quality changes from seawater intrusion are not the only concern for water managers in the Salinas Valley. Nitrate contamination continues to be a major concern (Harter and others, 2012). The State of California Water Resources Control Board is working to assess and monitor nitrate concentrations in groundwater and surface water in the Salinas Valley. Nitrate has been measured in groundwater and surface water with some areas exceeding 130 milligrams per liter (mg/L), which is above the regulatory limit for drinking water of 45 mg/L (Moran and others, 2011). Although an evaluation of nitrate is not an aspect of this study, quantifying hydrologic flows and recharge rates are vital to understanding the timing and extent of nitrate contamination.

Water managers are challenged with operating Lake San Antonio and Lake Nacimiento reservoirs to attain a variety of objectives. The reservoirs have mandated operational rules to control releases and storage for flood mitigation and water supply and to promote habitat for federally listed steelhead (*Oncorhynchus mykiss*) populations (Henson and others, 2023). These objectives have priorities, water rights, and regulatory requirements. The stream leakage from reservoir releases into the riverbed as water is conveyed through the Salinas River to meet these objectives can be substantial. Managing the timing and volume of releases is key to meeting objectives.

Conjunctive use of surface water and groundwater has been used in the Salinas Valley to help manage groundwater resources. In 2014, the California legislature passed the Sustainable

Groundwater Management Act (SGMA). California Department of Water Resources (2023) provides a complete description of how SGMA is being implemented. As a part of SGMA, each groundwater basin throughout the State must develop a plan to assess historical groundwater conditions and develop groundwater sustainability plans to sustainably manage groundwater by 2040 or 2042, depending on its priority as assigned by California Department of Water Resources. To understand the historical conjunctive use of groundwater and surface water, it is important to define the quantity of the groundwater and surface water supplies and to assess the efficiency of water resource use in the context of changing population, land use, crop type, irrigation practices, reservoir management, and climate. Analysis of the complex relationship between the use and movement of water in the Salinas Valley requires an integrated hydrologic model capable of tracking the three-dimensional flow of water in the aquifers, surface-water drainage networks, engineered conveyance structures, and reservoirs. Moreover, a comprehensive set of tools is needed to evaluate water supply projects and understand feedback between water quality and water supply. These evaluations are vital to the development of groundwater sustainability plans.

The evaluation of the Salinas Valley hydrologic system requires an integrated approach to describe the surface and subsurface and simulate natural and managed hydrologic flows. To simulate this system, a collection of integrated, geologic texture, surface water, groundwater, and operational models and data were developed into a comprehensive Salinas Valley System Model. This study and associated geohydrologic and hydrologic submodels of the Salinas Valley System Model were specifically developed to understand groundwater availability and use, support decision making throughout the Salinas Valley, and provide tools that can be used to evaluate sustainability plans and water supply projects. This study provides a description of the

hydrologic conditions in the Salinas Valley, including an evaluation of total water demand for existing uses, sea water intrusion on an annual basis for the study period, and groundwater levels. The integrated hydrologic and reservoir operation models developed for this study will aide entities throughout Monterey County in evaluating water resources and groundwater sustainability in the Salinas Valley.

### **Previous Model Studies**

Geologic mapping within the Salinas Valley occurred as early as 1900 (Nutter, 1901) and continued in the 1970s in the northern Salinas Valley (Durham, 1974) and southern Salinas Valley (Tinsley, 1975). Geologic mapping and hydrologic studies in the early 2000s (Feeney and Rosenberg, 2003; Kennedy/Jenks, 2004a, b) helped define the aquifer system and controls on groundwater flow. These geologic and hydrogeologic studies, among others, contribute to the conceptualization of the hydrogeologic units in the Salinas Valley Geologic Framework (Sweetkind, 2023).

There have been several modeling studies in the Salinas Valley. The first basin-scale model was developed by the U.S. Army Corps of Engineers and U.S. Geological Survey (USGS) in 1978. This model comprised a stream tributary model and a Salinas River model, and two-dimensional and three-dimensional finite difference groundwater models were developed as part of the study (Durbin and others, 1978). In 1986, Boyle Engineering Corporation used these models as the basis to develop a finite element model of the Salinas Valley Integrated Groundwater Model and Surface Model (SVIGSM, fig. 2; Boyle Engineering Corporation, 1987). Yates (1988) updated Durbin and others' (1978) original two-dimensional model. In 1997, the SVIGSM was updated with refined input data, updated model parameters were

developed through recalibration, and the model was extended through 1994 (Montgomery Watson, 1997). In addition to the basin-scale models for the Salinas Valley, the adjudicated Seaside groundwater subbasin of the Salinas Valley (fig. 2) has a locally focused groundwater model that is used to develop the adjudication. In 2009, a MODFLOW-2005 (Harbaugh, 2005) groundwater model for the Seaside subbasin was developed to support the adjudication of water rights by the Seaside subbasin by the watermaster (Hydrometrics, 2009). Although the area that contains the Seaside subbasin is included in the newly developed integrated hydrologic model domain in this study, the Seaside subbasin was not specifically evaluated. The development of the watershed and integrated hydrologic models included the refinement of previous conceptual models (Durbin and others, 1978; Yates, 1988; Montgomery Watson, 1997). The conceptual model for the integrated hydrologic models required the incorporation of natural and engineered features in the region, such as the SRDF, and reservoirs simulated in the operational model.

**Figure 2.** Salinas Valley showing the Monterey County groundwater sustainability management area, Zone 2C Water Management Area, integrated hydrologic model domain, Salinas Valley Integrated Groundwater Model domain, and Seaside adjudicated groundwater subbasin.

Prior models of the Salinas Valley groundwater basin were developed with the best tools available at the time of publication. Although the fundamental framework for simulating surface and groundwater flow was represented in these models, the spatial resolution was coarse (approximately 1,600 finite elements with areas ranging from 56 to 550 acres), aquifer representation was simplified to one to three layers, model simulation periods were limited by challenges in updating and maintaining the model, and the representation of land use categories, agricultural demands, and reservoirs was simplified. Previous efforts within the region have either integrated all crop demands using an approach that considers consumptive use (SVIGSM;

Montgomery Watson, 1997) or used virtual crop coefficients to represent water demands based on assumed or estimated distributions of crops (Hanson and others, 2004, 2014a, b). Although, simulations that group agricultural demands can provide a reasonable estimate of basin-scale water needs, discerning the effect of changing acreages and harvest frequency of individual crops on water demands is limited.

In the Salinas Valley, surface and groundwater are managed conjunctively to meet water demands, water demands are spatially variable and driven by land use, complex operational frameworks are applied to diversions, reservoir releases, and agricultural practices, and reservoirs are managed to meet multiple environmental and water supply objectives. Estimating crop production and water needs are key to managing groundwater and surface water sustainably and forecasting future water supply needs under climate variability and change. A comprehensive tool is needed that can represent the regional hydrologic system, where (1) the geologic framework is well defined, discretely representing all major aquifers as hydrogeologic units, (2) hydrologic processes and operations are represented at high resolution, (3) hydrologic budgets are aggregated to meaningful subareas with minimal processing, (4) hydrologic flows can be evaluated among groundwater and surface water regionally and among subareas, (5) land use input is comprehensive with representation of the entire land surface and the numerous crops grown in the basin, (6) crop demands and irrigation efficiencies are computed, (7) complex water supply projects can be implemented and evaluated, and (8) multi-objective reservoir operations can be simulated using established operational rules or configured to evaluate alternative rules. The integrated hydrologic models developed for this study meet these goals by building on the conceptual understanding of previous modeling efforts and leveraging recently developed software.

## **Purpose and Scope**

The purpose of this report is to document (1) the implementation of the geologic framework model and texture-based property characterization from the Salinas Valley Geologic Framework (SVGF; Sweetkind, 2023) into hydrogeologic units representing aquifers in integrated hydrologic models, (2) the evaluation of the hydrology and hydrogeology of the groundwater system, (3) the development of the historical and operational integrated hydrologic models, and (4) the analysis of historical water availability from the results of the integrated hydrologic models. There were three hydrologic models developed as part of this effort. The Salinas Valley Watershed Model (SVWM) simulates the entire Salinas River watershed (fig. 1) and is documented in a separate report (Hevesi and others, 2025a, b). The two integrated hydrologic models developed in this study and documented here are the Salinas Valley Integrated Hydrologic Model (SVIHM) and the Salinas Valley Operational Model (SVOM). These models represent the Salinas Valley groundwater basin (fig. 1) with primary focus on the primary water-producing subareas of MCWRA Zone 2C Water Management Area (Henson and Jachens, 2022) and the groundwater sustainability management area (California Department of Water Resources, 2020) (fig. 2). The integrated hydrologic models simulate the integrated surface water and groundwater system for water years (WY) 1968 through 2018.

## **Description of Study Area**

The Salinas River watershed (fig. 1) includes the drainage areas of the entire Salinas River in San Luis Obispo and Monterey Counties and includes upland tracts of surrounding hills and mountains, coastal lowlands, and offshore areas within Monterey Bay and the drainage areas of other creeks and canals within the Salinas Valley. The Salinas River watershed (fig. 1) and

adjacent coastal drainages, including the areas of agricultural and groundwater development, comprise a total area of 4,529 square miles (Hevesi and others, 2025a). The watershed encompasses the entire Salinas River and the portion of the watershed in Monterey County is referred to as the Salinas Valley. The Salinas River is the largest river within the California's Central Coast region (California Department of Water Resources, 2020). The Salinas River begins in San Luis Obispo County at the Santa Margarita Lake and enters the Salinas Valley near the boundary between San Luis Obispo and Monterey Counties. The Salinas Valley extends approximately 150 miles from the border of San Luis Obispo County north-northwest to its mouth at Monterey Bay, with a total area of 4,200 square miles in Monterey and San Luis Obispo Counties. The Salinas Valley is bounded on the west by the Santa Lucia Range and Sierra de Salinas and on the east by the Gabilan and Diablo Ranges. Monterey Bay acts as the northwestern boundary of the Salinas Valley (Manning, 1963) and the Monterey County border is the southern boundary (California Department of Water Resources, 2020). In the southern Salinas Valley, there are two reservoirs that release flow into tributaries of the Salinas River, Lake San Antonio and Lake Nacimiento (fig. 1).

Several subareas of interest are the Zone 2C Water Management Area, Salinas Valley groundwater sustainability basin management boundary, and the integrated hydrologic model domain. The Zone 2C Water Management Area was defined by Monterey County (Ordinance 3717, fig. 2) as a benefit assessment zone for water resource management of surface water and groundwater among the streams, reservoirs, and groundwater subbasins of the Salinas Valley within Monterey County (California Department of Water Resources, 2020). Some of the Salinas Valley groundwater subbasins have similar names to the hydrogeologic units defined for the Salinas Valley (Sweetkind, 2023). For example, the Salinas Valley 180/400-Foot Aquifer



groundwater subbasin represents an area defined by California Department of Water Resources (2020) and the 180-Foot Aquifer hydrogeologic unit (Sweetkind, 2023) describes the lateral extent of the subsurface 180-Foot Aquifer. The extent of the subsurface 180-Foot Aquifer may continue beyond the boundary of the 180-Foot/400-Foot Aquifer groundwater subbasin. For consistency, all references to the hydrogeologic units for the 180-Foot Aquifer and 400-Foot Aquifer are capitalized. To provide clear management boundaries for assessing surface water, groundwater, and their interaction in the Salinas Valley, California Department of Water Resources defined the groundwater sustainability management boundary in this study area as the portion of the Salinas Valley groundwater basin located in Monterey County (fig. 2; California Department of Water Resources, 2020); the rest of the Salinas Valley groundwater basin in San Luis Obispo County is separately managed. In this report, the term “Salinas Valley” is used to generally refer to the area represented by the integrated hydrologic model domain that surrounds the groundwater sustainability management boundary. The integrated hydrologic model domain surrounds both the Zone 2C Water Management Area and the Salinas Valley and extends to the ridges of the surrounding hillsides and offshore (fig. 2). The integrated hydrologic model domain described in this report focuses on the Salinas River, two reservoirs, and groundwater basins within the Salinas Valley (fig. 2).

## **Climate**

The Salinas Valley has a Mediterranean climate, with generally dry and mild summers, and wet, cool winters (Yates, 1988). Topography and proximity to the Pacific Ocean have a strong effect on the spatial distribution of precipitation within the integrated hydrologic model domain (fig. 3). Mean annual gridded precipitation at a 530 by 530 feet (ft) resolution for WY 1968 through 2018 within the study area (fig. 3) shows higher precipitation values in adjacent

mountain ranges and the coastal area of the integrated hydrologic model area (16 to 26 inches per year) with lower values in the center and upper valley of the integrated hydrologic model area (10 to 15 inches per year) (Henson and others, 2022c). Throughout the integrated hydrologic model area precipitation is almost entirely rain, with approximately 90 percent falling during the 6-month period from November to April (Manning, 1963; Yates, 1988). Climate zones were defined to analyze variations in climate throughout the Salinas Valley. California Irrigation Management Information System (CIMIS) climate zones in the Salinas Valley (CIMIS, 2020) were aggregated into “inland” and “coastal” climate zones and clipped to the integrated hydrologic model area boundary for this study (fig. 3; Henson and others, 2024). The aggregation of CIMIS climate zones was informed by analysis of the spatial distribution of precipitation and potential evapotranspiration (PET) and showed precipitation and PET change in the middle of the basin. Precipitation and cumulative departure of precipitation are shown for two Cooperative Observer Network (COOP) climate stations (fig. 4): one station is near the coast at the Salinas Airport (COOP station USW00023233) and one station is inland near King City (COOP station USC00044555). Climate data show that (1) year-to-year variability in precipitation is prevalent, (2) cumulative precipitation departure from the mean shows multiple wet and dry periods, and (3) there is a precipitation gradient such that mean precipitation is higher near the coast than inland. Mean precipitation at climate stations is 12.27 inches near the coast (fig. 4A) and 11.27 inches inland (fig. 4B). Similarly, long term average gridded climate data show average precipitation as 14 to 15 inches near the coast and 10–13 inches inland (fig. 3). Climate data show that year-to-year variability in precipitation is prevalent (figs. 4A, 4B). Cumulative precipitation departure from the mean at both stations show relatively dry periods when cumulative precipitation departure from the mean is decreasing over multiple years.

Periods where the cumulative precipitation departure from the mean is flat represent average conditions and are interpreted using antecedent conditions. Shaded tan areas in figure 4 highlight the relatively dry conditions for WY 1984 to 1992 with dry conditions from WY 1984 to 1992 and from 2012 to 2018.

**Figure 3.** Integrated hydrologic model domain annual average gridded precipitation at 530-foot resolution for water years 1968 through 2018, coastal and inland climate zones based on aggregation of California Irrigation Management Information System (CIMIS) climate zones, CIMIS stations, selected climate stations, Remote Automatic Weather Stations (RAWS), Cooperative Observer Network (COOP) stations, and two analysis COOP stations: Salinas Airport (USW00023233) and King City (USC00044555).

**Figure 4.** Annual precipitation at selected Cooperative Observer Network stations (COOP; National Oceanic and Atmospheric Administration, 2020) for water years 1968 through 2018 for A) Salinas Airport (USW00023233) and B) King City (USC00044555). Shaded regions illustrate two relatively dry periods in the Salinas Valley defined based on generally decreasing or flat cumulative precipitation departure from the mean and annual precipitation less than mean precipitation from water years 1968 through 2018. C) Cumulative precipitation departure from the mean at Salinas Airport (USW00023233) and King City (USC00044555) showing delineation of analysis periods A, B, C, and D for the study.

Climate year types (wet, normal, or dry) influence availability of surface water, magnitudes of groundwater recharge, and agricultural practices and are used by MCWRA to guide operation of Lake San Antonio and Lake Nacimiento. Moreover, climate year types can be used to analyze changes caused by wet or dry periods in data and results. Climate year types are defined by the percentile of annual mean flow at the Arroyo Seco near Soledad gage (USGS 11152000) (fig. 2). A wet year is defined as years with annual mean flow greater than or equal to the 75th percentile of flow. Dry years are defined as years with annual mean flow less than or

equal to the 25th percentile. Normal WYs are defined as having annual mean flow between the 25th and 75th percentiles, preliminarily determined on March 15th and officially on April 1st (MCWRA, 2005, 2018). The MCWRA assesses climate year types using a five-tiered WY classification (dry, dry-normal, normal, wet-normal, wet); for the integrated hydrologic models we reclassify these into a three-tiered classification: dry, normal (which includes dry-normal, normal, and wet-normal), and wet. These climate types are based on flow conditions at streamgauge USGS 11152000, not precipitation at climate stations, so there may be years when precipitation is low, but the climate year type is normal.

A critical component of the hydrologic cycle in the region is evapotranspiration. Available monthly gridded 530-ft resolution PET data (Henson and others, 2022c) were aggregated to mean annual values. Mean annual PET for WYs 1968 to 2018 within the study area (fig. 5) shows relationships between topography and proximity to the Pacific Ocean, with higher PET values in adjacent mountain ranges and the upper valley (52 to 65 inches per year) and lower values in the center of the valley and coastal region (39 to 51 inches per year). Throughout the domain, PET is higher than precipitation (figs. 3, 5).

**Figure 5.** Integrated hydrologic model domain annual average gridded potential evapotranspiration at 530-foot resolution for water years 1968 to 2018, coastal and inland climate zones based on aggregation of California Irrigation Management Information System (CIMIS) climate zones, CIMIS evaluation locations, Remote Automatic Weather Stations (RAWS), and Cooperative Observer Network (COOP) stations.

## Land Use

Land use data compiled for the study include maps of native, urban, and managed land cover from the National Land Cover Database (NLCD) (USGS, 2000, 2003, 2011, 2014; Dewitz

and U.S. Geological Survey, 2021) that were integrated with locally developed periodic land use maps (California Department of Water Resources, 1971b, 1997, 2014). Additionally, we incorporated land use data obtained by MCWRA from the Association of Monterey Bay Area Governments for 1992 and for the recent update to the Salinas Valley Integrated Geologic System Model in 2012. We then supplemented our analysis using National Agriculture Imagery Program aerial photography (U.S. Department of Agriculture, 2016), economic reports (Monterey County Agricultural Commission, 2022), and pesticide application records (California Department of Pesticide Regulation, 2018).

Categorized and summarized land use data for the years 1968, 1984, 2000, and 2014 illustrate land use change in the Salinas Valley in figures 6A–D, respectively. On each land use map, a pie chart highlights land use categories to illustrate total land use change through time. This study evaluates irrigated agriculture where agricultural demand data are available in Zone 2C Water Management Area. Data from a national irrigated lands dataset (Xie and others, 2022) is shown (fig. 6D) to illustrate additional potential irrigated areas within the study area that are not evaluated in this study. The development of land use data and model input are summarized in the “Model Development” section in the “Land Use Data” subsection of this report and are fully described by Henson and others (2024a).

**Figure 6.** Integrated hydrologic model domain land use (Henson and others, 2024) for calendar years *A*) 1968, *B*) 1984, *C*) 1998, and *D*) 2014 that includes additional remotely sensed irrigated areas within the study area and outside of Zone 2C Water Management Area.

#### Native Land Cover and Urban and Managed Land Use

Native land cover and urban and managed land use categories in the Salinas Valley have been stable through time (figs. 6A–D). The native land cover category includes water bodies,

riparian areas, upland grasslands/shrub lands, woodlands, beach-dunes, and barren-burned land cover and represents approximately 54 to 56 percent of land cover (figs. 6A–D). The managed land use category includes pasture, non-irrigated, semiagricultural, idle-fallow, and quarries; the urban land use category includes golf course turf/parks, and urban land uses. The largest urban areas are the cities of Monterey, Salinas, and King City (Kulongoski and Belitz, 2007). Urban areas represent the maximum extent of urban areas for the period 1968 to 2014 based on aerial imagery. The combined urban and managed land use category represents more area in 1968 (approximately 15 percent of land use) due to pasture distributed throughout the Salinas Valley. After 1968, the pasture is supplanted by irrigated land uses and both the urban and managed land use category areas are relatively stable (approximately representing 6 to 8 percent of land use; figs. 6B–D).

## Irrigated Land Use

The variety of crops grown within the Salinas Valley have changed substantially throughout the simulation period; however, leafy vegetables, such as lettuce, have been a primary crop of the Salinas Valley for more than 70 years (Manning, 1963). Other important crops in the Salinas Valley include artichokes, crucifers (broccoli and cauliflower), vineyards, celery, onions, and strawberries (Monterey County Agricultural Commission, 2022). Multi-cropping, more than one harvest of one or more crops on a given field, is a common practice in the Salinas Valley (California Department of Water Resources, 1997; Smukler and others, 2008). Land use maps (figs. 6A–D) represent physical extent of planted acreage not the harvested acreage that is reported in agricultural reports (Monterey County Agricultural Commission, 2022). To illustrate potential changes in land use due to multi-cropping, land use data were categorized based on frequency with which they were likely to change within one growing

season. There were three irrigated land use subcategories delineated: annually stable, high frequency rotational, and multi-year. If multiple crops can occupy the same area within a year, the land use was defined as “high frequency rotational.” If crops are stable for at least one year but can change year to year, the land use was defined as “annually stable.” If crops are likely to change over multiple years to decades, the land use was defined as “multi-year.”

The sum of the irrigated areas represented by the three irrigated land use subcategories was relatively stable through time ranging from approximately 31 to 37 percent of land use (figs. 6A–D). Although the total irrigated land use area did not vary substantially, there were changes in the distribution of irrigated land use subcategory areas and the implementation of multi-cropping increased. The distribution of irrigated land use subcategories for multi-year and annually stable crops increased through time. The most substantial increases in these subcategories occurred between 1968 (fig. 6A) and 1984 (fig. 6B). The percentage of areas represented by multi-year vineyards increased by approximately 5 percent and annually stable strawberries increased to represent approximately 1 percent of the land use. These trends of increased land use area for multi-year vineyards and annually stable strawberries continued into the year 2000 (fig. 6C) and remained relatively stable from 2000 to 2014 (fig. 6D). Over the same period from 1968 to 2000, the practice of multi-cropping increased, as shown by the total reported harvested acres (fig. 7; Monterey County Agricultural Commission, 2022), which increased more than the area represented by the “high frequency rotational” irrigated land use subcategory (approximately 27 to 31 percent of land use, figs. 6A–D).

**Figure 7.** Cropped acreage estimates in the integrated hydrologic model domain showing total harvested acres in Monterey County during the study period.

## Surface Water and Watershed

The characteristics of high relief and mountainous terrain combined with a focused distribution of annual precipitation to a limited number of winter (December to March) storms results in large variations in Salinas River streamflow, both seasonally and between peak and mean streamflow conditions (Hevesi and others, 2025a). Streamflow enters the Salinas River from ephemeral runoff from valley slopes, local ungaged surface water drainage networks, such as the Arroyo Seco and San Lorenzo Creek tributaries, and local reservoirs, such as Santa Margarita Lake, Lake Nacimiento, and Lake San Antonio (fig. 1). Flows into the Salinas Valley from ephemeral drainages and intermittent creeks that feed into the Salinas River can be substantial but vary in time. Figure 8 shows a comparison between total annual estimated ungaged inflows to the watershed inflows (Henson and others, 2025) and total annual streamflow at the first streamgauge on the Salinas River within the study area (USGS 11150500 near Bradley; USGS, 2018) to illustrate the relative magnitude of stream and watershed inflows into the Salinas River within the Salinas Valley. This comparison confirms that watershed inflows are intermittent but there are periods where watershed inflows can provide substantial runoff to the Salinas Valley. Arroyo Seco has long been considered a substantial tributary for water supply in the study area (California Department of Public Works, 1946). Surface water flows measured in Arroyo Seco (USGS 11152000, fig. 1; USGS, 2018) are used to manage reservoir operational decisions (MCWRA, 2005, 2018; Henson and others, 2023). Three reservoirs are connected to the Salinas River: Santa Margarita Lake completed in 1941, Lake Nacimiento dam and reservoir completed in 1957, and Lake San Antonio dam and reservoir completed in 1967 (fig. 1). Santa Margarita Lake is not represented in the hydrologic models presented in this report because it is



located outside of the integrated hydrologic model domain; however, it is the upper boundary of the Salinas River.

**Figure 8.** Comparison of total annual watershed inflows into the integrated hydrologic model domain from the Salinas Valley Watershed Model and observed Salinas River flows at the first gage on Salinas River in the study area (USGS 11150500 Salinas River near Bradley, California) (USGS, 2018) to show the relative contribution of surface water from adjacent watershed inflows and inflows from the upper watershed outside of the study area for water years 1968 through 2018.

Flow from the Salinas River travels down approximately 115 miles of stream channel within the study area before discharging to Monterey Bay. Streamflow is highly variable both spatially and temporally in the Salinas River due to variation in climate and streamflow gains and losses. At the uppermost Salinas River gage in the integrated hydrologic model area (USGS 11150500 near Bradley) for WY 1968 through 2018, monthly average streamflow is 518 cubic feet per second (ft<sup>3</sup>/s) but is highly variable, ranging from less than 1 to 10,185 ft<sup>3</sup>/s (USGS, 2018). Stream gains and losses vary along the length of the river. Between the USGS 11150500 (near Bradley) and USGS 11151700 (near Soledad) gages, the average monthly streamflow difference is 117 ft<sup>3</sup>/s and ranges between 859 ft<sup>3</sup>/s (loss) and -1,655 ft<sup>3</sup>/s (gain) with losing conditions occurring between the gages for 83 percent of months with observations (USGS, 2018). Between USGS 11150500 gage near Soledad and the last gage on Salinas River, USGS 11152500 near Spreckels, the average monthly streamflow difference is positive, indicating losing stream conditions with a mean reduction in streamflow of 88 ft<sup>3</sup>/s and maximum of 683 ft<sup>3</sup>/s over all observations. The streamflow gains occur typically from intermittent storm flow and streamflow losses are due to stream leakage through coarse materials in the streambed.

Historically, surface water supply from the Salinas River and its tributaries was limited due to variability and uncertainty in streamflow year to year (Manning, 1963). To support irrigated agriculture, there is a continued need to develop new water supplies using conjunctive use strategies to meet existing and projected water demand. Currently, these strategies focus on increasing storage of surface water in reservoirs during wet periods, deliveries of recycled water from urban areas to coastal regions to offset groundwater pumpage, and regular surface water diversions from the Salinas River and its tributaries.

Lakes Nacimiento and San Antonio provide flood control for the Salinas Valley, hydroelectric power, and have a maximum storage capacity of 377,900 and 335,000 acre-feet, respectively. Throughout the study period, average annual reservoir storage varied with climate and ranged from approximately 14,000 to 300,000 acre-feet in Lake San Antonio and 22,000 to 300,000 in Lake Nacimiento (fig. 9; Henson and others, 2022b). In 1998, the Monterey County Water Recycling Project began delivering a new supply of tertiary treated wastewater to 12,000 acres of coastal farmland as part of the CSIP to reduce the need for groundwater pumping and mitigate seawater intrusion. Reported diversion from Arroyo Seco at Clark Colony (Clark Colony diversion) has been used to meet agricultural demands and a 1 ft<sup>3</sup>/s diversion from Tembladero Slough has been used for maintaining wetted channel conditions. These two diversions represent the most continuous reported surface water source for irrigation (fig. 10; Henson and others, 2023). The Salinas Valley Water Project (SVWP) was started in 2003 to deliver supplemental water to meet irrigation needs and recharge the basin (MCWRA, 2001). In 2010, enhancements to the SVWP involved installation of a rubber spillway gate and dam near the SRDF that diverts flow from the Salinas River to be treated and delivered to coastal farmland as part of CSIP.

**Figure 9.** Comparison of annual mean storage in Lakes San Antonio and Nacimiento for water years 1968 through 2018.

**Figure 10.** Surface water deliveries from agricultural diversions for Clark Colony and Salinas River Diversion Facility (SRDF), channel wetting diversions for Tembladero Slough, and recycled water deliveries for the Castroville Seawater Intrusion Project (CSIP) from water year 1968 to 2018 (Henson and others, 2023).

### **Geology of Groundwater Basins**

The Salinas Valley is a large intermontane valley that extends southeastward from Monterey Bay to Paso Robles. The groundwater basins of the Salinas Valley are some of the largest coastal groundwater basins in Central California (fig. 11; California Department of Water Resources, 2020). The groundwater basins are structural basins formed, in part, by normal faulting along the western margin of the valley from King City to Monterey Bay (California Department of Water Resources, 2020). Downward movement of the valley-side fault block resulted in the deposition of a westward thickening alluvial wedge above crystalline bedrock (Showalter and others, 1983) that is as thick as 10,000 ft (3,048 meters [m]) on the east side of the basin and as thick as 15,000 ft (4,572 m) on the west side. These Tertiary and Quaternary marine and terrestrial sediments include as much as 2,000 ft (609 m) of saturated alluvium (Showalter and others, 1983). The sediments that contain the aquifers of the Salinas Valley are a combination of gravels, sands, silts, and clays that are organized into sequences of relatively coarse-grained and fine-grained materials. The three-dimensional distribution of sediment texture and hydrogeologic units in the Salinas Valley are defined in the SVGF (Sweetkind, 2023). A

summary of the geologic framework is provided in the “Geologic Framework” section and fully described by Sweetkind (2023).

**Figure 11.** Groundwater basins and subbasins within and adjacent to the Salinas Valley.

## **Groundwater**

Groundwater movement is generally from the southern part of the Salinas Valley north toward Monterey Bay. Components of the groundwater flow system include groundwater recharge, groundwater use, and natural groundwater discharge. Groundwater budget components include total recharge, total pumpage, aquifer storage changes, seawater coastal inflow (an analogue for seawater intrusion), and groundwater exchanges among groundwater subbasins within the Salinas Valley. The Salinas Valley groundwater basin is divided into seven subbasins that represent both hydrologic and management boundaries: the 180- and 400-Foot Aquifer subbasin, East Side Aquifer subbasin, Forebay Aquifer subbasin, Langley Area subbasin, Monterey subbasin, Seaside subbasin, and Upper Valley Aquifer subbasin (fig. 11; California Department of Water Resources, 2020). These groundwater subbasins are used to manage groundwater sustainability by groundwater sustainability agencies and water agencies. The tools developed for this study support the evaluation of groundwater and surface water availability and conjunctive use of groundwater throughout these groundwater subbasins. The geologic framework developed alongside this study (Sweetkind, 2023) contains the entire Salinas Valley groundwater basin and the hydrogeologic units that span its subbasins. Therefore, the individual groundwater subbasins are not described in detail in this report. A full description of the groundwater subbasins is provided by California Department of Water Resources (2020).

## Groundwater Recharge

Recharge to the groundwater system is primarily from stream-channel infiltration from the major rivers and their tributaries and from infiltration of water from precipitation and irrigation (MCWRA, 1995). Infiltration of runoff along with percolation of a fraction of precipitation and irrigation below the root zone contribute to groundwater recharge. Mountain block recharge into the East Side Aquifer and Langley Area subbasins occurs along the Gabilan Range (fig. 11). Additional regional groundwater flow occurs under the Salinas River where the river enters the Salinas Valley at the southern integrated hydrologic model boundary (fig. 2).

## Observed Trends in Groundwater Levels

Groundwater level contours (figs. 12A, 12B) for 1994 conditions were developed by MCWRA. Shallow and deep groundwater contours show that lateral gradients in the aquifer generally follow the gradient of the Salinas River stream channel through the valley. Where contoured groundwater data are available for the deeper aquifers, contours show vertical hydraulic gradients are downward from the shallow (180-Foot Aquifer) to the deep (400-Foot Aquifer) in the 180-Foot/400-Foot Aquifer groundwater subbasin. The combined effects of groundwater pumping for irrigation and water supply have periodically depressed the groundwater levels in and near the 180-Foot/400-Foot Aquifer, East Side Aquifer, and Forebay Aquifer groundwater subbasins of the Salinas Valley during dry periods, where most agriculture and urban development has been centered since the 1920s (California Department of Public Works, 1946; Manning, 1963). A region of lower groundwater levels is observed in both aquifers near the city of Salinas. Long-term groundwater level declines over the study period have been observed in monitoring wells (MCWRA, 1996) throughout the 180-Foot/400-Foot Aquifer and

East Side Aquifer groundwater subbasins (figs. 13A, 13B), resulting from lowering of groundwater levels during the 1984 to 1994 dry period. The groundwater levels did not recover to levels observed before the dry period. The long-term groundwater level decline in the 180-Foot/400-Foot Aquifer groundwater subbasin is approximately 10 ft and stabilized after 1995 (fig. 13A); declines in the East Side Aquifer groundwater subbasin are approximately 50 ft (fig. 13B) and are larger than the annual variability. Wells in the Forebay Aquifer groundwater subbasin (fig. 13C) show groundwater levels decreased in response to the 1984 to 1994 dry period but groundwater recovered afterward. Wells in the Upper Valley Aquifer groundwater subbasin (fig. 13D) show stable groundwater levels through the study period and a faster recovery after the dry period relative to other groundwater subbasins, likely due to groundwater recharge from reservoir operations in the Upper Valley Aquifer groundwater subbasin.

**Figure 12.** Estimated groundwater level contours in the integrated hydrologic model domain for A) shallow aquifers (less than 200 feet deep) and B) deep aquifers (greater than 200 feet deep) in fall 1994. The Salinas River, Salinas Valley groundwater subbasins, and selected observation wells are also shown.

**Figure 13.** Observed water levels during the study period for A) well BDA331 in the 180-Foot/400-Foot Aquifer groundwater subbasin, B) well ZES1572 in the East Side Aquifer groundwater subbasin, C) ZFS1001 in the Forebay Aquifer groundwater subbasin, and D) well ZSE733 in the Upper Valley Aquifer groundwater subbasin.

## Groundwater Use and Natural Discharge

The primary sources of groundwater discharge are irrigation and municipal supply wells, evapotranspiration, and discharge to streams. There is a long history of irrigation in the study area and groundwater is the primary source of water for irrigating agricultural crops and meeting

domestic, municipal, and industrial water demands (Manning, 1963; California Department of Water Resources, 1973). Groundwater outflow to the ocean is small and occurs in shallow alluvium along the coast (Baillie and others, 2015). Water also leaves the system through evapotranspiration from native vegetation, urban landscapes, and irrigated agriculture.

To monitor groundwater pumpage throughout the basin, the Groundwater Extraction Management System database was developed in 1994 to comply with MCWRA ordinance 3717. All groundwater withdrawals in the Zone 2C Water Management Area for municipal and industrial (M & I) and agricultural water use in the Salinas Valley are currently reported and maintained in this database (MCWRA, 1996). Prior to 1994, M & I pumpage was estimated using census data (fig. 14; U.S. Census Bureau, 2018; Henson and others, 2023). Domestic pumpage is not reported nor directly simulated in this study. However, census-based population estimates in the year 2000 suggest 92 percent of the population is in cities served by reported M & I wells (Henson and others, 2023). Overall, M & I water use is approximately 10 to 15 percent of agricultural pumpage but is important to subregional groundwater budgets (fig. 14). Monthly agricultural pumpage has been reported since WY 1995, and shows total agricultural pumpage ranges from approximately 379 to 571 TAFY and is the most substantial use of groundwater within the Salinas Valley.

**Figure 14.** Annual total municipal, industrial, and agricultural pumpage in Zone 2C Water Management Area from water year 1970 through 2018. Pumpage is estimated before 1994 and reported for water years 1995 to 2018.

## Groundwater Budget

The groundwater system has been under stress since the 1920s, but extensive development of the groundwater system did not begin in earnest until the 1940s and 1950s (Manning, 1963). In the late 1900s and early 2000s, groundwater pumping accounted for 95 percent of outflow from the basin and the remaining loss was from evapotranspiration (Ferriz, 2001; Baillie and others, 2015). The California Department of Public Works (1946) estimated groundwater recharge to be approximately 220 TAFY with negligible regional groundwater flow from the groundwater basins south of San Ardo. At that time, groundwater overdraft was estimated to be about 55 TAFY in the 180-Foot Aquifer. Groundwater modeling and water budget analyses by MCWRA (1995) further quantified components of recharge and discharge in the basin. Groundwater recharge was estimated to be 454 TAFY, of which 144 TAFY was agricultural return flows, 244 TAFY was streamflow infiltration, and 66 TAFY was precipitation recharge. Over the same period from 1970 to 1994, average groundwater overdraft basinwide was 44 TAFY.

## Sea Water Intrusion

Substantial pumping in aquifers of the coastal region has caused significant sea water intrusion and groundwater-level declines that was first documented in the 1930s (California Department of Public Works, 1946). The landward extent of sea water intrusion in the 180-Foot and 400-Foot Aquifers is estimated by MCWRA using spatial sampling of chloride concentrations in coastal monitoring wells. Since it was first studied in 1946 (California Department of Public Works, 1946), sea water intrusion had advanced nearly 6 miles inland by 1995 and affected the groundwater wells supplying approximately 20,000 acres of coastal



farmland (MCWRA, 1995). Chloride concentrations of greater than 500 milligrams per liter (mg/L) in those wells indicated groundwater was impaired in approximately 20,000 acres of the 180-Foot Aquifer and 10,000 acres of the 400-Foot Aquifer (MCWRA, 1995). An analogue for evaluating sea water intrusion is seawater coastal inflow, which is the aquifer freshwater volume displaced by sea water intrusion. In 1946, an estimated 6 to 12 TAFY annual seawater coastal inflow occurred. When estimated in 1995, the average annual seawater coastal inflow from 1970 to 1992 was 15 TAFY.

## **Integrated Hydrologic and Operational Model Development**

The integrated hydrologic and operational models were developed to support analysis of groundwater and surface water availability and use, quantify regional groundwater flow among groundwater subbasins, and examine current and proposed operational schemes for managing reservoir and water supply projects. The Salinas Valley Integrated Hydrologic Model (SVIHM), referred to herein as the “historical model,” simulates historical conditions for groundwater levels and hydrologic budgets. The Salinas Valley Operational Model (SVOM), referred to herein as the “operational model,” simulates the engineered surface-water and reservoir operations for two reservoirs. This operational model implements current reservoir operations and uses 2014 fixed land use and current water supply projects with observed historical climate records to provide baseline information for project benefit analyses and evaluation of water supply projects and reservoir operations. The historical and operational models are referred to together herein as the “integrated hydrologic models.” The integrated hydrologic models represent aquifers and confining units using hydrogeologic units and spatially distributed estimates of sediment texture. These data are fully defined in the Salinas Valley Geologic

Framework (SVGF) by Sweetkind (2023). Monthly surface water inflows into the integrated hydrologic model domain were simulated using the Salinas Valley Watershed Model (SVWM), herein referred to as the “watershed model,” that is documented by Hevesi and others (2024a).

The focus of this report is the development of inputs and calibration of the integrated hydrologic models. The historical model parameter estimation is used to define properties that are then used in the operational model (discussed in the “Salinas Valley Operational Model” section). The integrated hydrologic models share many model files and are explained together. Differences among the integrated hydrologic models are noted using the specific model name where relevant, otherwise the same description of model construction applies to both models. The integrated hydrologic models simulate transient conditions dependent on the interactions among head-and-flow-dependent components of hydrologic processes simulated in the model, including engineered systems and management constraints on operations and water availability. The integrated hydrologic models were developed to analyze conjunctive water use and the movement of water throughout the landscape, including the surface-water drainage network and aquifers. The integrated hydrologic models simulate water budgets, changes in groundwater storage and related seawater coastal inflow (an analogue for sea water intrusion), and agricultural, municipal, and industrial water demands in different hydrologic regions of Salinas Valley, California.

The integrated hydrologic models are supported by a watershed model documented by Hevesi and others (2024a). The integrated hydrologic models have a smaller footprint than the watershed model and are geographically focused near the Zone 2C Water Management Area and associated groundwater basins of the Salinas Valley (fig. 2). Specifically, the watershed model provides basinwide estimates of monthly watershed inflows for ungaged streams and tributaries

that flow into the integrated hydrologic model area from the watershed outside of the active simulation area (fig. 2). The watershed model was built using the Hydrologic Simulation Program-FORTRAN (HSPF; Bicknell and others, 1997) and the model simulates the period from October 1, 1948, to September 30, 2018. This period encompasses several years before the Lake Nacimiento reservoir was built through WY 2018. The watershed and integrated hydrologic models use the same regional climate input (Hevesi and others, 2022) and surface water drainage network (Henson and Jachens, 2022).

## **Simulation Code**

The integrated hydrologic models were built using MODFLOW-One-Water Hydrologic Flow Model version 2.3 (MF-OWHM; Hanson and others, 2014a; Boyce and others, 2020; Boyce, 2023) with the latest version of the MODFLOW Farm Process (FMP). MF-OWHM is a MODFLOW-2005 based integrated hydrologic model designed to dynamically simulate the conjunctive use of surface water and groundwater to meet agricultural demands (Hanson and others, 2014a; Boyce and others, 2020). The term “integrated” refers to the tight coupling of groundwater flow, surface-water flow, landscape processes such as agricultural management and evapotranspiration, and reservoir operations. Within the active integrated hydrologic model domain (fig. 2), surface and subsurface hydrologic processes, operations, and water use constraints are simulated simultaneously, allowing for consideration of conjunctive-use, water-management, water-food-security, and climate-crop-water scenarios in the Salinas Valley. The FMP simulates a land-use-based water supply and demand framework for water balance subregions (WBSs) that can be specified for subareas of the model domain. Within each WBS, quantities of interest for agricultural water supply management are computed, such as the total delivery requirement (TDR) to meet agricultural demands, total applied water (TAW), surface-

water and groundwater supply, and excess applied irrigation water. These quantities of interest for agricultural water supply management depend on simulated head- and flow-dependent inflows and outflows. For example, direct uptake of groundwater to meet crop demands can occur when simulated water levels are above the bottom of the root zone, which reduces the amount of water required to be diverted or pumped to meet land use water demands. The FMP simulates the operational and water allocation constraints on water resources available to each WBS. For example, the water available for diversions or volume and timing of reservoir releases could be dependent on flow constraints in designated locations and times of the year. These constraints guide the simulation of the conjunctive use of groundwater and surface water to meet agricultural demands. A full list of the processes and packages of MF-OWHM used in the integrated hydrologic models are provided in table 1.

**Table 1.** Summary of MODFLOW-One Water Hydrologic Model (MF-OWHM) packages and processes used in the Salinas Valley Integrated Hydrologic Model and Salinas Valley Operational Model.

## **Discretization**

The study area is shown in figure 1. The study area contains a watershed model domain that represents the Salinas River watershed (fig. 1) and an integrated hydrologic model domain that simulates the Salinas Valley and Salinas River within the surrounding Salinas Valley groundwater basins, as well as Lake San Antonio and Lake Nacimiento reservoirs (fig. 2). The active integrated hydrologic model domain completely contains the current Salinas Valley groundwater sustainability management area (fig. 2; California Department of Water Resources, 2020).

## Temporal Discretization

The total simulation period for the integrated hydrologic models was from October 1, 1967, through September 30, 2018. The 51-year simulation period encompasses the period just after the construction of the second reservoir in the integrated hydrologic model area, Lake San Antonio, to the recent period. To better represent the dynamics of the changing climate, streamflow, and growing season (irrigation supply and demand components) the integrated hydrologic models are discretized into 612 monthly stress periods to reflect the common frequency of some of the reported data, such as groundwater pumpage. A model stress period is an interval of time in which the user-specified inflows and outflows are held constant and time steps are units for which groundwater levels and flows are calculated throughout all model cells (Harbaugh, 2005). We discretize monthly aquifer stresses into input for each stress period. The historical model has two equal-length semi-monthly time steps (approximately 15-days) for each monthly stress period. Semi-monthly time steps are commonly used in regional scale historical models that include agriculture (Faunt and others 2009a; Hanson and others, 2014b, c, d). To represent reservoir operations, the operational model has a smaller time step than the historical model. For each monthly operational model stress period, a model time step of 5 or 6 days is used for the temporal discretization of the operational model to account for the approximately 5-day transit time for reservoir releases through the integrated hydrologic model area (Howard Franklin, MCWRA, oral communication, 2018) and to comply with steelhead fish passage requirements specified in the National Oceanic and Atmospheric Administration National Marine Fisheries Service (2007) biological opinion.

## Spatial Discretization and Layering

The integrated hydrologic model area encompasses the Salinas Valley groundwater basin and its offshore extent (fig. 2). The total active modeled area is 957 square miles. The top of the integrated hydrologic models is represented by the elevation of the land surface. The finite-difference model grid used to represent the land surface and subsurface deposits consists of a series of orthogonal 530-ft (6.46 acres) square model cells of variable thickness. Spatial discretization was held constant through time. There are 976 rows, 272 columns, and 9 layers that have a varying number of active cells in each layer, for a total of 589,720 active model cells. Active model cells within the model grid are defined using the IBOUND parameter in the MODFLOW basic package. Where model cells are active, the IBOUND parameter is set to a value greater than 0. The uppermost active model cell could be within model layers one, three, five, seven, eight, and nine. Where hydrogeologic units pinch out, a “pinched” cell type was defined to transmit water between layers. Where confined hydrogeologic units are not present, the layer is specified as an approximately 1-ft-thick layer. Based on the Salinas Valley Geologic Framework (Sweetkind, 2023), the nine model layers were defined to represent each of the nine hydrogeologic units of the regional aquifer system: three confining units—upper (layer 2), middle (layer 4), and lower (layer 6)—and six aquifers—surficial aquifer (layer 1), 180-Foot Aquifer (layer 3), 400-Foot Aquifer (layer 5), Paso Robles Formation (layer 7), Purisima Formation (layer 8), and basement aquifer (layer 9). These hydrogeologic units are further described in the “Geological Framework” section of this report.

## Analysis Regions

All historical model results and hydrologic budgets are discussed for five analysis regions and the entire integrated hydrologic model domain. The five analysis regions represent the riparian area that includes the Salinas River and the four primary water-producing subareas of the Zone 2C Water Management Area (fig. 15). The five analysis regions are the Riparian, Pressure, East Side-Langley, Forebay, and Upper Valley. The analysis regions are aligned with Salinas Valley groundwater subbasins shown in figure 11. Table 2 shows the relationship between analysis regions, Salinas Valley groundwater subbasins, named subareas, and water balance subregions as implemented in the integrated hydrologic models.

**Figure 15.** Analysis regions and other areas that are simulated within the integrated hydrologic model domain.

**Table 2.** Summary of analysis regions, Salinas Valley groundwater subbasins, named subareas, water-balance subregions, and their available water sources to meet demands.

The five analysis regions (fig. 15) represent nearly the entire integrated hydrologic model area (93 percent of Zone 2C Water Management Area and 74 percent of the onshore study area) (Henson and Jachens, 2022). The analysis regions account for more than 98 percent of reported groundwater usage within Zone 2C Water Management Area recorded in the Groundwater Extraction Management System (MCWRA, 2005, 2018; Henson and others, 2023). There are other regions within the integrated hydrologic model domain that are hydrologically connected but are outside of the analysis regions (fig. 15). These other areas include the area outside of analysis regions but within the integrated hydrologic model domain: the separately adjudicated Seaside groundwater subbasin (Seaside), the area below Lakes Nacimiento and San Antonio

(Below dam), the area outside of Zone 2C Water Management Area (Outside Zone 2C), and the offshore region (offshore).

## Water Balance Subregions

The MF-OWHM Farm Process was used to define the landscape processes in the integrated hydrologic model area using water balance subregions (WBS). WBS are used to represent analysis regions (fig. 15), named subareas, and other areas that are within the integrated hydrologic model domain (fig. 16, table 2). Each analysis region comprises one or more WBS. Results are aggregated for each analysis region from its associated WBSs. Each WBS represents an area on the model's surface that has common water use properties, crop properties, water supply, and runoff and recharge characteristics. Within each WBS, water supply and demand calculations are made, deliveries from connected water sources (for example, groundwater; table 2) are applied to meet demands, and recharge and runoff are simulated. The integrated hydrologic models are discretized into 31 WBSs (fig. 16) to better associate the location of water demands with the location of water sources used to satisfy them. This approach ensures that groundwater pumpage from one side of the river is not used to meet crop demands on the other side of the river. The Salinas River riparian area was delineated as a separate WBS, WBS 1, so that net groundwater regional groundwater flow and water balances within the Salinas River riparian area could be specifically evaluated. Some WBS were delineated to represent specific named subareas within the Salinas Valley, including the area for the CSIP (fig. 1), the area around Arroyo Seco in the Forebay analysis region, and Clark Colony (table 2). Although the extent and number of WBSs defined in this version of the models are held constant, the model input for WBSs can be adjusted by users to vary the extent and number of WBSs through time (Boyce and others, 2020). This flexibility presents opportunities to specifically



delineate changes in future model efforts for areas of interest, such as growing urban centers. The delineation of multiple WBSs throughout the integrated hydrologic model domain can support refined analyses of water supply projects in the future. In analyses in this report, WBS landscape and groundwater budgets are aggregated to their associated analysis regions and the entire integrated hydrologic model domain. However, in the model output, landscape and groundwater budgets are output for each WBS.

**Figure 16.** Thirty-one (31) water balance subregions of the integrated hydrologic model domain.

## **Landscape**

The MF-OWHM Farm Process (FMP) provides coupled simulation of the groundwater and surface-water components of the hydrologic cycle and managed flows and operations by water managers for irrigated and non-irrigated lands (for example, native vegetation). The FMP estimates water demands and allocates water supply, simulates runoff and recharge, simulates groundwater evapotranspiration, and computes surface water deliveries and groundwater pumpage for agricultural supply for each WBS in the active model domain. The FMP has a demand-driven and supply-constrained representation of the landscape. The FMP uses land use and water demands to partition precipitation and groundwater and surface water deliveries into evapotranspiration, runoff, and recharge.

## **Farm Process Overview**

Within each model cell for each WBS, FMP estimates landscape consumptive use as uptake and transpiration by plants and the associated evaporation. For each land use category in every active model cell, a landscape consumptive use of water is estimated based on a modified United Nations Food and Agriculture Organization method (Allen and others, 1998) that has

been widely applied throughout California (Faunt and others, 2009a, 2024; Hanson and others, 2014b, c, d). A summary of FMP landscape consumptive use and water demand simulation is provided here; a complete explanation of the method is provided by Boyce and others (2020).

## Input Parameters

The landscape consumptive use for every model stress period is computed using (1) reference evapotranspiration ( $ET_{ref}$ ) for each model cell that is approximated using PET, (2) a seasonally varying crop coefficient ( $K_c$ ), which is a scalar value that is multiplied by  $ET_{ref}$  to estimate a landscape consumptive use, (3) specification of the fraction of the maximum leaf area in each cell (that is, fraction of transpiration; FTR) and fractions representing the remainder of the area subject to evaporation from precipitation (FEP) and irrigation (FEI), and (4) the land use area.

The  $ET_{ref}$  is a reference value that assumes a well-watered grass surface and is used for landscape consumptive use calculation. The  $K_c$  value represents a stage of crop growth and associated landscape consumptive use. The FTR represents the fraction of land use “leaf area” in each model cell where plant transpiration occurs and varies between 0 and 1. The FTR is assumed to be independent of whether the transpiratory portion of landscape consumptive use is satisfied by irrigation, precipitation, or groundwater uptake. The remaining fraction ( $1-FTR$ ) of each cell is assumed to represent the fraction of area subject to evaporation from precipitation (FEP) and irrigation (FEI). The FEP represents the fraction of the land use area over which evaporation occurs and is calculated internally by FMP as  $1-FTR$ . The FEI can be conceptualized as the irrigated area that is not planted, such as the irrigated area between plants or planting beds. FEI is specified as a fraction less than or equal to FEP. The FTRs vary linearly

with the respective area occupied by crops and the area open to soil evaporation (Schmid and others, 2006). The fraction of the landscape consumptive use that is transpiratory (FTR) or evaporative (FEP and FEI) depends strongly on type of land use and associated crop growth stage. When the vegetation cover approaches 100 percent,  $FTR = 1$  and  $FEP$  and  $FEI = 0$ . As a result, the fractions of transpiration and evaporation vary by land use type for different months of the year.

### Landscape Consumptive Use

The landscape consumptive use is the sum of transpiration and evaporation consumptive use. The transpiration consumptive use by plants is estimated based on FTR,  $ET_{ref}$ , and  $K_c$  parameters. The transpiration consumptive use is computed as  $ET_{ref}$  multiplied by each land use area and  $K_c$  in each cell. The transpiration consumptive use is then prorated by the monthly FTR for each land use type. The evaporative consumptive use is computed using the FEP and FEI parameters that are multiplied by the volumes of precipitation and irrigation that are applied to each cell. The consumptive use due to transpiration and evaporation are summed to estimate a landscape consumptive use in each model cell.

### Water Demands

In FMP, landscape consumptive uses can be satisfied from natural sources, such as precipitation and direct uptake from shallow groundwater above a specified rooting depth. If natural sources of water are not available to meet the calculated landscape consumptive use for a WBS, a TDR is computed. For each model time step, FMP determines a residual of total landscape consumptive use that cannot be satisfied by natural sources—the TDR. For irrigated land uses, this residual water demand is increased using an on-farm efficiency factor (OFE) to

account for crop, WBS-specific, and irrigation-type inefficiency losses to estimate the amount that must be supplied to meet demand. Available supplies are used to meet the TDR for the entire WBS. The total applied water (TAW) represents the amount of water applied to meet land use water demands. In the integrated hydrologic models, the deficit-irrigation scenario is used; when demand cannot be satisfied with available supplies for a WBS, demand is reduced to the supply and the deficit is shared among all land uses in the WBS. If the irrigated water demand cannot be satisfied with available water supply, then the TAW will be less than the TDR. Due to the prevalence of groundwater wells with substantial pumping capacity throughout the study area, this deficit irrigation scenario is unlikely to occur under current conditions. If constraints were placed on well pumpage in future simulations, this deficit scenario would affect the calculation of demands. More details for how the FMP accounts for inflows and outflows for each WBS are available in the MF-OWHM documentation (Schmid and others, 2006; Schmid and Hanson, 2009; Hanson and others, 2014a; Boyce and others, 2020).

## Water Supply

The TDR in irrigated lands can be satisfied by additional water supplies, such as semi-routed surface water deliveries from streams or canals (diversions), reservoir releases, non-routed delivery from external sources (for example, wastewater reclamation or pipelines), or groundwater pumpage by wells. Where the conjunctive use of surface water and groundwater are major sources of water used for irrigation, FMP attempts to satisfy the TDR by using surface water diversions or non-routed deliveries (such as pipelines and recycled water) first, with residual water demand satisfied by groundwater. Surface-water deliveries can be limited to a specified allocation (surface-water allotments) to the agricultural WBSs that use both surface water and groundwater (Hanson and others, 2014b, c, d). If diverted flows to a WBS through a

semi-routed delivery are more than land use water demands, diverted surface water is returned to the surface-water drainage network for potential reuse downstream. For each WBS, the FMP computes the collective potential pumping capacity of all wells that can provide groundwater for supplemental irrigation water. The residual water demand is distributed to every well in the WBS, and all active wells are pumped. The volume of groundwater pumpage is only limited by well capacity and any imposed volumetric constraints specified using groundwater allotments.

### Runoff and Recharge

Runoff and recharge from each WBS are partitioned based on a specified fraction of excess water after all demands have been satisfied. Runoff is routed on a segment-length weighted basis to all streams within a WBS. Recharge results from excess irrigation and excess precipitation, reduced by losses to surface-water runoff and evapotranspiration from groundwater (Schmid and others, 2006). The evapotranspiration from groundwater is subtracted from the potential net downward flux as deep percolation to the uppermost aquifer. Hence, recharge to groundwater can be affected both by user-specified and head-dependent processes. This definition of recharge requires the following assumptions: deep percolation below the active root zone is equal to groundwater recharge; evapotranspiration from groundwater equals an instantaneous outflow from aquifer storage in any time step; and the net change in soil-moisture storage for irrigated, well-managed agricultural areas for periods of weeks to months is negligible (Schmid and others, 2006). The recharge to the aquifers is applied on a cell-by-cell basis to the uppermost active model cell in each WBS. Recharge is computed after evapotranspiration consumption losses. Therefore, recharge can be negative if groundwater evapotranspiration is greater than deep percolation. When this occurs, it is constrained to specific areas. For example, in the model cells near the stream in the Riparian analysis region, the amount

of groundwater evapotranspiration from riparian vegetation may be higher than the amount of deep percolation into those cells, resulting in a negative recharge value; however, stream leakage is also occurring in those cells. Therefore, the recharge may be negative, but the total recharge (stream leakage plus recharge) is positive.

## Surface Water Operations

The FMP also includes a surface water operations (SWO) module that allows for simulation of large-scale surface-water storage and distribution systems—including simulation of surface-water storage, allocation, release, and distribution—to meet agricultural, municipal, and industrial water demand, maintain a minimum streamflow requirement, and reserve a portion of storage for flood protection. This additional functionality facilitates improved analysis of basin-scale conjunctive use and large-scale surface-water management. SWO interacts with the Stream Flow Routing Package (SFR2; Niswonger and Prudic, 2005) and with the Farm Process (FMP) to simulate two-way interactions and feedback between surface-water and groundwater management and use. Reservoir dynamics are simulated using SWO—by simulating surface-water storage, management objectives, allocation, and reservoir release—which determines downstream diversion amounts and makes reservoir releases as inflow to SFR2 that routes flow through a surface water drainage network—to simulate distribution—and SFR2 calculates the associated groundwater-surface water interaction. The appropriate reservoir releases and downstream diversion amounts are determined by SWO based on the surface water conveyance calculated from SFR2. Reservoirs simulated by SWO can provide supply to FMP WBSs. Each connected WBS has a computed water demand and SWO can deliver the appropriate water based on allocation, storage, and SFR2 stream gains and losses.

SWO was developed to allow analysis of the complete feedback cycle between surface-water and groundwater management and use, including effects of groundwater management and use on reservoir storage, allocation, and releases and corresponding effects of surface-water management on groundwater recharge and demand. SWO can be used to evaluate how changes in groundwater pumping affect surface-water management, including storage, allocation, release, and distribution of surface water supplies. Notably, SWO also allows for analysis of how changes in surface-water management affect groundwater recharge via stream leakage and deep percolation of applied water and thus how surface-water management affects groundwater storage and movement. SWO further allows for analysis of how changes in surface-water management affect groundwater demand and use due to changes in surface water allocations and deliveries, thus providing for complete two-way interactions between groundwater and surface-water management and use.

## Climate Data

For the entire Salinas River watershed, high-resolution, 270-m (886-ft) gridded maps of daily precipitation, daily maximum and minimum air temperature, and daily PET were developed (Hevesi and others, 2022). These regional climate input data were derived using methods from a regional-scale Basin Characterization Model developed for the State of California (Flint and Flint, 2007, 2012; Flint and others, 2021). Climate input data were developed using the Gradient-Inverse-Distance-Squared method (Nalder and Wein, 1998) and daily climate records from a network of 155 climate stations were used to spatially interpolate daily precipitation and maximum and minimum daily air temperature onto a 270-m digital elevation model (DEM) grid (USGS, 2013). The gridded daily and PET maps are inputs to the watershed model. These same gridded climate datasets were also used as input for the FMP in

the integrated hydrologic models. However, since the model's stress periods are monthly, the daily climate input data were averaged to monthly values and assigned to each of the model cells in the integrated hydrologic models using an area-weighted approach. The complete description of the development of climate datasets is provided with the regional climate data (uniform grid with 270 m resolution; Hevesi and others, 2022) and monthly climate data (uniform grid with 530 ft resolution; Henson and others, 2022c).

### Reference Evapotranspiration

There are two related measures that describe the potential for evapotranspiration, ET<sub>ref</sub> and PET. The ET<sub>ref</sub> is a reference value that assumes a well-watered grass surface and is used for crop demand calculation. The PET is the total potential for evaporation from a surface if evaporation is not limited by water availability (Allen and others, 1998). The two quantities are related but PET values may be higher seasonally. For all locations within the integrated hydrologic model area, the average annual ET<sub>ref</sub> rate, calculated by the California Irrigation Management Information System (CIMIS), exceeds average annual precipitation (Baillie and others, 2015; CIMIS, 2020). The highest ET<sub>ref</sub> rates of 53 to 62 inches per year occur in the lowlands that define the valley floor in the central and southern parts of the integrated hydrologic model domain (CIMIS, 2020). Mean monthly ET<sub>ref</sub> rates for these locations vary from 1 to 1.5 inches for December to 8 to 9 inches for July (CIMIS, 2020).

The ET<sub>ref</sub> values in the integrated hydrologic models are estimated using adjusted PET, as described here. Measured field-scale ET<sub>ref</sub> from CIMIS (2020) was compared to 270-m resolution PET (Hevesi and others, 2022) at CIMIS stations within the study area (figs. 3, 5). These 270-m climate data were mapped using an area-weighted approach to the uniform 530-ft



model grid. Comparison of WY-averaged ET<sub>ref</sub> and PET for stations in the study area that have long-term records (greater than 9 years) show reasonable correspondence with an R<sup>2</sup> value of 0.897 (fig. 17A). Regressions for all stations did not have good correlation so only long-term stations with records greater than 9 years were evaluated. The time series of values at stations with long records were further evaluated at Castroville (CIMIS 019, fig. 17B), Arroyo Seco (CIMIS 114, fig. 17C), Salinas South (CIMIS 089, fig. 17D), King City-Oasis Rd. (CIMIS 113, fig. 17E), and Salinas North (CIMIS 116, fig. 17F) stations. The ET<sub>ref</sub> records and PET estimates at these sites show reasonable correspondence, although PET is slightly underestimated in the winter and slightly overestimated in the summer. Accordingly, seasonal bias adjustment factors are used to adjust PET values to estimate ET<sub>ref</sub> for crop demand calculations in this study (further discussed in the “Crop Coefficients” section of this report).

**Figure 17.** California Irrigation Management Information System (CIMIS, 2020) field-scale reference evapotranspiration (ET<sub>ref</sub>) and potential evapotranspiration (PET) estimated using the 270-meter-resolution Basin Characterization Model (BCM; Hevesi and others, 2022) at the same location. A) Correlation and comparison of stations with long-term records used for more detailed comparisons. Comparisons of time series are shown for B) Castroville (CIMIS 019), C) Arroyo Seco (CIMIS 114), D) Salinas South (CIMIS 089), E) King City-Oasis Rd. (CIMIS 113), and F) Salinas North (CIMIS 116).

## Land Use

Land use data were compiled from available local, State, and Federal datasets. A complete description of the development of land use input data for the models are provided by Henson and others (2024a). Available multi-year composite land use data were integrated with national-scale land use and land cover data (USGS, 2000, 2003, 2011, 2014; Dewitz and U.S.

Geological Survey, 2021) and supplemented with information from the California Pesticide Use Reporting (CalPUR) database (California Department of Pesticide Regulation, 2018; Henson and Voss, 2023) to provide a comprehensive edge-to-edge land use map for each year (Henson and others, 2024). Native vegetation was defined using NLCD data and intersected in a geographic information system (GIS) with other available land use data. All land areas were presumed to be stable year to year until updated land use data showed changes in their distribution. If available land use data for an irrigated crop was present where NLCD data showed a native land use cover class, the irrigated land area was preserved. There were 56 land use identifiers developed to represent native vegetation, urban areas, and crops in the Salinas Valley (Henson and others, 2024). As described above, land use analysis categories were grouped based on native or urban classes and the frequency that crops may change: high frequency rotational, annually stable, multi-year. There is a climate gradient across the valley that could lead to differences in crop management and demands in coastal and inland areas—for example, gradients in precipitation (fig. 3) and PET (fig. 5). Additionally, coastal areas can have differences in fog occurrence and cloud cover relative to inland areas. Inland and coastal climate zones (figs. 3, 5) were used to support delineation of cropping and growth in land uses. Of the 56 land use identifiers, 40 were defined as irrigated land use categories with an inland and coastal member. Discriminating crops between these regions and climate zones allows for specification of crop properties specific to the climate region and resulting simulation of potential differences in climate, water demands, and crop management.

In land use data, irrigated land use is often broadly classified into categories with similar uses, such as “irrigated land” or “truck and vegetable crop.” For regions in the study area with these broad categorizations of land use, available land use data were supplemented with CalPUR

data (California Department of Pesticide Regulation, 2018). Applications of pesticides, including the date, crop, and application area are reported by each grower in the CalPUR database. Crop categories for the study area were defined by grouping reported crops from the CalPUR database into classes of vegetation with similar water demand and cultivation practices. Tabular data for Monterey County from 1974 to 2018 were obtained (California Department of Pesticide Regulation, 2018, [www.cdpr.ca.gov/docs/pur/purmain.htm](http://www.cdpr.ca.gov/docs/pur/purmain.htm)). The CalPUR land use estimator (CalPUR-LUE; Henson and Voss, 2023) was used to filter and aggregate the tabular data to an approximately 1-mile resolution defined by the public land survey system. Each row in each annual table is an application record and is associated with a public land survey system section (approximately 1 square mile or 640 acres). For each section, all crop applications were tabulated, and a cropped area fraction was computed for each of the irrigated land use types in the integrated hydrologic models (land use identifiers 1–48; Henson and others, 2024). These fractions were applied to each model cell within each section to provide more detailed information where land use is more broadly defined in NLCD or other land use data. To capture the intra-annual changes in the distribution of crops (for example, early spring and late fall), these fractions were computed for the January to June and June to December period each year. This results in two land use maps for every simulation year where land use is mapped to each model cell supporting the potential for multiple land uses in each model cell.

Urban areas are represented using two land use categories: an urban and a golf course turf/parks land-use type that are used to estimate outdoor irrigation and runoff. The extent of cities and settlements in the Salinas Valley were delineated based on NLCD data and aerial imagery. The extent of these developed areas was specified as both an urban or golf course turf/parks land-use type and an urban WBS. It is assumed that urban and golf course turf/parks

land areas have access to shallow groundwater and groundwater pumpage by wells from the municipal systems where they are located.

Streams and riparian areas were delineated using aerial imagery (U.S. Department of Agriculture, 2016) and the National Hydrography Database (USGS, 2019b). A riparian buffer of 530 ft was applied to the main channel of the Salinas River, resulting in 3,252 riparian model cells. These cells were grouped into their own WBS to support evaluation of the riparian areas in subsequent studies. A riparian land use type was developed using other hydrologic models in the region (Hanson and others, 2004, 2014b, c, d) and vegetation data surveys from the Salinas River that show substantial woody and shrub vegetation with the invasive giant reed species *Arundo donax* L. (Howard Franklin, MCWRA, oral communication, 2018).

#### Simulation of Crop Acreage

To show the relation between physical land use acreage compiled for the study and harvested acres, time series for eight crops are compared for calendar year 1967 to 2014 (fig. 18). To better illustrate the representation of multi-cropping in the simulation, simulated acres for multi-cropped land uses were estimated for high frequency rotational and annually stable crops that can have multiple harvests. To estimate the simulated crop acres, the physical crop acres were multiplied by a multi-cropping factor of 1.97, as defined and used in the previous Salinas Valley hydrologic model (SVIGSM; Boyle Engineering Corporation, 1987; Yates, 1988; Montgomery Watson, 1997). The time series show the comparison of estimated harvested acres from county crop reports, estimated physical acres using CalPUR data and land use GIS data (Henson and others, 2024), and simulated acres assuming a multi-cropping factor of 1.97 applied to the estimated physical acres (fig. 18). The data show that harvested and simulated acres have

similar trends, variability, and magnitudes. The trends of increased strawberries and vineyard acreage starting in the 1980s, the reduction in root vegetables (for example, sugar beets), and steady increase in lettuce production correspond well (fig. 18). Although some of the simulated acreage values are lower than the harvested acres (for example, crucifers), these comparisons are for demonstration. The model simulates a long growing season with multiple harvests that accounts for the water demands due to multi-cropping but does not simulate individual harvests. After 2014, the strawberry and vineyard physical acreages do not increase as much in the model as the harvested acres reported in crop reports. Some of this effect could be due to differences between multiple harvests that may be counted in harvested acres. Physical acreage area is always the area that the crop occupies regardless of harvest. Although some differences among crop group harvested and simulated acres are present, the land use captures much more of the distribution and variability in crop group acreage than the common practices of estimating a crop group area that remains the same between land use datasets (for example, step functions in crop group acreage or linearly interpolating crop group acreages between land use datasets).

**Figure 18.** Comparison of time series of physical acreage, simulated acreage assuming a multi-cropping factor of 1.97, and harvested acreage for selected land use types in the Salinas Valley for water years 1968 through 2014.

### Crop Coefficients

Each of the land use categories in the study are represented by seasonally varying crop properties. The closer association between crop type and properties used in this study allows for better definition of individual crops of interest and supports future refinements of crop properties in the model as data become available. When available, published crop coefficient ( $K_c$ ) values for similar coastal areas were used (Brouwer and others, 1985; Brouwer and Heibloem, 1986;

Snyder and others, 1987a, b; Allen and others, 1998; Michael Cahn, University of California Agriculture and Natural Resources, Crop Manage, written communication, 2018). When no published Kc values for coastal areas were available, published Kc values for the western San Joaquin Valley compiled by Brush and others (2004) were used. Additional specific Kc values were used for greenhouse crops (Orgaz and others, 2005), turfgrass (Gibeault and others, 1989), and strawberries (Snyder and Schullbach, 1992; Hanson and Bendixen, 2004). The Kc values from the literature were adjusted to account for differences between field-measured CIMIS ETref and 530-ft resolution gridded PET used in this study using a seasonal bias adjustment factor. A seasonal bias adjustment factor for winter, spring, summer, and fall was computed to reduce the sum of squares error from the simulated PET and estimated ETref from CIMIS station data at five long-term stations throughout the Salinas Valley. The seasonal bias adjustment factors for PET were highest in the winter (1.00) and lowest in the summer (0.88), with a value of 0.94 for the spring and 0.97 for the fall. The seasonal bias adjustment factor for each season was multiplied by the Kc value to account for the difference between PET and ETref and the Kc values for each of the land uses in each land use category was defined (fig. 19; Henson and Culling, 2025).

**Figure 19.** Crop coefficients by land use type for A) high frequency land use, B) annually stable land use, C) multi-year land use, D) urban and managed land use, and E) native land cover in Salinas Valley, California.

Superimposed on the consumptive-use estimates are additional climatic-stress scale factors applied to Kc values as seasonal wet, normal, or dry scale-factor parameters that were estimated during parameter estimation and analysis. These climate-stress scale factors are applied to adjust Kc values for the period before and after 1995 in the model input (further

described in the “Landscape-Process Parameters” section and defined in the model archive by Henson and Culling [2024]). Climate year type is defined using methods defined by MCWRA for reservoir operations (MCWRA, 2005, 2018; Henson and Jachens, 2022). Each year was defined as wet, normal, or dry based on the minimum storage in Lakes San Antonio and Nacimiento and the percentile of April 1st streamflow in Arroyo Seco. These seasonal scale factors are used to reflect potential differences in agricultural practices more appropriately among defined WBSs embedded in the consumptive-use estimates and the year-to-year changes in surface-water allocations and deliveries during the 1967–2018 simulation period. This approach is consistent with several studies of the region (Hanson and others, 2004, 2014b, c, d; Faunt and others, 2009a, c).

#### Fractions of Transpiration, Precipitation, and Evaporation

The complete time series of FTR and FEI values are provided in the model archive (Henson and Culling, 2025); a summary is provided here. The FEP is calculated internally by FMP as  $1 - \text{FTR}$ . There are no specific data for FTR available in the literature. The FTR was developed based on expert knowledge, crop type and month, informed by other model applications in the region that use MF-OWHM (Hanson and others, 2004, 2014b, c, d; Faunt and others, 2009a, c), and adjusted during parameter estimation using reported withdrawal data. The FTR values for cropped land uses range from 0.39 to 0.73. To explain this conceptually, this means that the leaf area of each land use in each cell can vary between 39 and 73 percent of the land use area. For non-irrigated land uses, the FTR only influences the consumption of precipitation and shallow groundwater from the root zone. Thus, the FTR values mainly influence runoff to the streams generated from these land uses. For many of the non-irrigated land uses (for example, beach-dunes, barren-burned, quarries, semiagricultural, and idle-fallow),

constant values of 0.3 are assumed for land use. This assumes that grasses and weedy vegetation covers as much as 30 percent of these areas. Constant values of 0.08 are assumed for urban areas, which assumes that about 8 percent of the urban areas are subject to evapotranspiration from precipitation and 92 percent are subject to evaporation of precipitation. It is assumed that the urban water uses that include irrigation are included in M & I pumpage. The FEI is computed by crop for each irrigated land use type and can be conceptualized as the non-vegetated area that is irrigated (for example, sprinkler overspray). Through the simulation period, harvested acres have increased (fig. 7), yet water use has been relatively stable (fig. 14). Thus, FEI was reduced through time alongside assumed changes in irrigation methods. This was done to represent the effects of shifting from sprinkler to drip irrigation and implementation of irrigation water conservation practices to reduce wetted areas that are not planted. This is supported by documented increases in irrigation efficiency between 2001 and 2010 as noted by Sandoval-Solis and others (2013) and Tindula and others (2013). FEI values for crops range from 0.05 to 0.15 before the year 2000 and 0.01 to 0.05 after 2000.

### Irrigation Efficiencies

In general, irrigation efficiencies and irrigation system types are poorly known (Williamson and others, 1989; California Department of Water Resources, 1994; Brush and others, 2004). Data describing the association between crops and irrigation system type, distribution of irrigation systems, and associated efficiencies in the integrated hydrologic model area are not available. We used expert input from agricultural producers, regional information, and a statewide report (Sandoval-Solis and others, 2013) to estimate irrigation system type throughout the simulation period. Specification of OFE and their variation in time was informed by similarly constructed hydrologic and agricultural models in this region of California, the



Central Valley Hydrologic Model (Faunt and others, 2009a, c, 2024), Cuyama Valley (Hanson and others, 2014b), and the Pajaro Valley Hydrologic Model (Hanson and others, 2014c, d) and were adjusted during model parameter estimation. Williamson and others (1989) report values averaging 59 percent and ranging from 38 to 92 percent for the 1961–77 period. California Department of Water Resources reports overall efficiencies of 60–70 percent for parts of the Central Valley (California Department of Water Resources, 1994). The irrigation types specified in the integrated hydrologic models are a sprinkler and drip irrigation type for each of the two climate regions (inland and coastal) and nursery, flood, and urban for a total of seven specified irrigation types. For each of those irrigation types, an OFE was specified for each WBS. The OFE in the integrated hydrologic models vary between 0.3 for flood irrigation and 0.95 for drip irrigation. The OFE increase in time alongside assumed changes in irrigation methods (for example, shifting from sprinkler to drip irrigation) and improvements in irrigation water conservation practices. All OFE values used in the model are provided by Henson and Culling (2025).

## Surface Water Inflows and Outflows

The simulation of surface water inflows and outflows in the integrated hydrologic models relies on observed streamflows at gages, reported diversions, reservoir outflows, and monthly average simulated watershed inflows as well as structural information about the surface water drainage network, watershed inflow point, and reservoir release locations. The simulation of surface water budgets relies on the simulation of streamflow gains and losses and flow from the surface water drainage network into the ocean. Direct evaporation of surface water is not simulated within the surface water drainage network. In the operational model, the simulation of surface water outflows includes simulation of evaporation from reservoirs. Runoff to streams is

simulated by FMP as a fraction of inefficient irrigation and precipitation for each model cell. However, runoff is not explicitly routed across the land surface, it is distributed equally to all stream reaches within each WBS where the runoff was generated. The surface water drainage network is simulated with the SFR2 package (Niswonger and Prudic, 2005).

### Surface Water Flow Data

Surface water flow data used as input to the integrated hydrologic models include available monthly records of the three surface water diversions (Henson and others, 2023), simulated monthly average watershed inflows (Hevesi and others, 2025b; Henson and others, 2025), and monthly historical reservoir inflows and releases (Henson and others, 2023). Simulated daily watershed inflows from the watershed model are aggregated to monthly average inflow time series at 148 watershed inflow points along the boundary of the integrated hydrologic model domain (fig. 20; Henson and Jachens, 2022). These monthly watershed inflow time series are input to the streams within the integrated hydrologic model simulation (Henson and others, 2025). There are two watershed inflow points that are coincident with the location of reservoir releases. At these inflow points, watershed model simulated monthly average natural flows are summed with monthly average historical reservoir flows. For the historical model, the watershed model inflows are summed with historical monthly average reservoir releases. For the operational model, the watershed model inflows are summed with simulated reservoir releases.

**Figure 20.** Surface water drainage network channel types within the Salinas Valley study area, USGS National Water Information System streamgages, stream diversion locations, and point locations of watershed inflows from outside the active model domain.

## Surface Water Flow Simulation

The surface water drainage network in the integrated hydrologic model area represents the Salinas River, major canals, diversion channels, drains, and tributaries that drain each surrounding upland watershed outside the integrated hydrologic model area (Henson and others, 2022a). The topology of the surface water drainage network (Henson and others, 2022a) was developed using analysis of surficial geology and land-surface elevations from the SVGF, National Hydrography Dataset stream line data (USGS, 2019b), and aerial imagery (U.S. Department of Agriculture, 2016). The surface water drainage network simulates the distribution and conveyance of surface water within the integrated hydrologic model area (fig. 20). This network is represented by a collection of stream cells (referred to as reaches), which are combined to form a collection of cells or reaches known as a segment. The total surface-water drainage network contains 524 segments, 9,008 reaches (model cells), 3 diversions, 148 watershed inflows, and 2 outflows to the ocean (fig. 20). There are a total of 93 collector segments that collect surface runoff but do not discharge to the Salinas River or its tributaries. These collector segments represent abandoned drainage canals, intermittent arroyo channels not present in National Hydrography Dataset stream data, and were specifically delineated to facilitate simulation of intermittent recharge so that the magnitude of recharge from these features can be evaluated as part of future sustainability analyses. These collector segments have high streambed permeability to facilitate infiltration. Estimated watershed inflows from 42 of the 148 watershed inflows are routed into intermittent runoff from these ungaged watersheds at watershed inflow points connected to the surface water drainage network. All streamflow that does not infiltrate into the underlying aquifer or flow into another stream is assumed to be lost to evapotranspiration. Riparian vegetation evapotranspiration in streams outside of the Salinas

River is not directly simulated. The flows into collector segments are intermittent such that flow in any collector segment was greater than 10 ft<sup>3</sup>/s in only 24 of the 1,224 model time steps (Henson and others, 2025). Within the surface water drainage network, channel bed elevations are specified on a model cell-by-cell (reach) basis using 1-meter horizontal resolution light detection and ranging (lidar) data (USGS, 2019a), where available, or a 10-meter horizontal resolution DEM (USGS, 2013). Streambeds were specified to be 1 foot thick throughout the network.

The surface water flow simulation and water balance calculation used in SFR2 allow for streamflow routing, streamflow infiltration into the aquifer (losing stream reaches), and any potential base flow as groundwater discharge to streams (gaining stream reaches). Hydraulic flows among segments of the surface-water drainage network were simulated using two approaches based on available data for each stream segment: (1) a rating table approach that relates channel depth, width, and flow for a range of flow values (SFR2 ICALC parameter equal to 4) and (2) an approach that assumes Manning's equation and a wide rectangular channel (SFR2 ICALC parameter equal to 1). The rating table approach was applied to seven stream segments in the surface water drainage network that contain a USGS streamgage with long term streamflow records (USGS 11150500, USGS 11151700, USGS 11152300, USGS 11152500, USGS 11152050, USGS 11152000, USGS 11152650; USGS, 2018; Henson and others, 2022b). The Manning's equation approach was used for the rest of the stream segments. These stream segments were grouped based on the channel type (tributary, main channel, canal, ditch, or segment) that collects surface runoff and facilitate recharge but does not have a downgradient connection. Manning's roughness coefficient for each segment was specified using literature values for natural channels, developed channels, and canals for each segment (Arcement and

Schneider, 1989). Roughness coefficient values varied within the range of 0.02–0.05. When supported by local conditions, for example, in the upper Salinas Valley where vegetation in the channel can increase roughness, a value of about 0.05 was specified. The channel type was evaluated using adjacent land use through visual inspection of aerial imagery (U.S. Department of Agriculture, 2016). Hydraulic properties for these groups of segments have been parameterized to help with the parameter estimation of surface-water flow parameters.

To illustrate the spatial distribution of net stream leakage into the aquifer, the long-term (WY 1968 to 2018) annual average stream leakage in each stream segment was computed using output from the historical model. The net stream leakage for each segment was divided by the segment length to provide a normalized value in acre-feet per year per foot (afyf) of stream segment length. The resulting long-term stream leakage map is shown in figure 21. Stream leakage varies along the length of the river, such that substantial leakage in the Salinas River (greater than 0.5 alyf) and even greater leakage (greater than 1.5 alyf) occurs in the center of the model domain, and much lower leakage (less than 0.25 alyf) occurs in the tributary segments and canals. This aligns with the streamflow analysis described in the “Surface Water and Watershed” section of this report, which showed substantial leakage in several segments of the Salinas River between USGS 11150500 (near Bradley), USGS 11151700 (near Soledad), and the gage farthest downstream on the Salinas River (USGS 11152500) near Spreckels.

**Figure 21.** Annual average net stream leakage normalized by segment length in the surface water drainage network in acre-feet per year per foot (afyf), diversion locations, and selected streamgages used for analysis.

## Surface-Water Agricultural Supply

There are three major surface water supply sources in the integrated hydrologic models: diversions, reclaimed wastewater, and two reservoirs. Each surface water source provides water to only one WBS. Surface-water diversions were simulated for two WBSs. To support the implementation of surface water diversions for agriculture, a semi-routed delivery segment was added to the SFR2 stream for each of the two WBS that receive surface water for irrigation. The addition of the semi-routed delivery allows for water deliveries to FMP to be constrained by available water in the SFR2 package and to be returned to the surface water drainage network, which maintains the MF-OWHM framework of demand-driven and supply-constrained conjunctive use. Diversions for CSIP (WBS 2) are supplied by the SRDF. Diversions for Clark Colony (WBS 15) are supplied by Clark Colony Canal diversion on Arroyo Seco. Reclaimed wastewater is simulated as an additional source to the CSIP (WBS 2). Reclaimed wastewater deliveries are simulated as a non-routed delivery where a volume of water is specified for each month that is available to meet water demands. Lastly, reservoir releases from Lakes Nacimiento and San Antonio are used to meet streamflow targets at the SRDF and support surface water deliveries to CSIP to offset groundwater pumpage.

## Groundwater Pumpage Agricultural Supply

Monthly reported agricultural groundwater pumpage for each WBS was used to evaluate and calibrate the historical model (Henson and others, 2023). A specific representation of groundwater pumpage from individual wells was not an objective of this study nor is it appropriate given the regional scale and application of the integrated hydrologic models. The estimated well pumping capacities are provided with the well data by Henson and others (2023).

Currently, there are no groundwater allotments declared in the integrated hydrologic models. The overall required pumpage within a WBS is distributed among all wells associated with the WBS using the “PRORATE ByCapacity” option in the FMP and divides the pumping requirement of the WBS to each well proportional to the specified maximum capacity of each well (Boyce and others, 2020). Thus, wells with more specified capacity supply more of the groundwater for irrigation. Simulated groundwater pumpage by each irrigation well may substantially differ from the actual pumping value because the aggregated demands for a WBS are distributed among all irrigation wells. This assumption may result in local-scale error in simulated groundwater levels near actual pumping wells but will result in accurate overall regional groundwater-level simulation.

## **Geologic Framework**

Multiple sources of topographic and geologic data were used to define the geologic framework and the hydrogeologic units that are simulated in the integrated hydrologic models. Input to the final geologic framework included faults, hydrogeologic unit surfaces and extents, and hydrogeologic texture interpreted from borehole data, existing cross sections, and models. A brief discussion of the geologic framework is provided here; the full enumeration of the development of the geologic framework is described by Sweetkind (2023).

## **Hydrogeologic Units**

A hydrogeologic map of the study area (fig. 22A) was created from digital geologic maps using a GIS to merge the mapped stratigraphic units into the nine hydrogeologic units defined in table 3. Geologic map data for the onshore part of the study area were compiled from the digital geologic map of Monterey County (Wagner and others, 2002). South of this map, the California

State geologic map (Jennings, 2010) was the primary source of geologic map data, locally augmented by larger scale maps (Dibblee, 1971, 1972; Hart, 1985; Clark and others, 1997, 2000). Geologic map data for the offshore part of the study area were compiled from Greene (1970, 1977), Greene and Clark (1979), Wagner and others (2002), Golden and Cochrane (2013), Dartnell and others (2016), and Johnson and others (2016). Geologic maps were combined and consolidated into a single hydrogeologic unit map (fig. 22A).

**Figure 22.** A) surface extent of hydrogeologic units and fault traces of the Salinas Valley study area in Monterey and San Luis Obispo Counties, California, adapted from the Salinas Valley Geologic Framework (Sweetkind, 2023) and B) conceptual cross section through hydrogeologic units of the Salinas Valley Geologic Framework along the central axis of the Salinas Valley. Vertical exaggeration is approximately 100 times.

**Table 3.** Summary of geologic formations and hydrogeologic units in the Salinas Valley Geologic Framework (Sweetkind, 2023).

A topographic model of the land surface at the model resolution was developed to describe the top of the uppermost hydrogeologic unit. Digital elevation data for the study area were extracted from a seamless 1:24,000-scale USGS National Elevation Dataset DEM resampled using spatial averaging to the 530 foot by 530 foot model grid, and processed using the Cascade Routing Tool for eight direction (D-8) routing (Henson and others, 2013). Elevations of contacts between hydrogeologic units were compiled from structure-contour maps and well borehole data. The elevation of specific hydrogeologic unit tops were obtained from published structure contour maps of the onshore Salinas Valley as follows: base of Purisima Formation (Feeney and Rosenberg, 2003); base of Paso Robles Formation in the Paso Robles basin (Fugro West, Inc. and Cleath and Associates, 2002); and elevation of tops of the 400-Foot



Aquifer, the Middle aquitard, and the 180-Foot Aquifer (Baillie and others, 2015). For the Seaside basin, contour maps of the tops of the Monterey Formation, Purisima Formation, and Paso Robles Formation were digitized (Hydrometrics, 2009). For the offshore region, geologic surface data were obtained from the elevation of the top of granitic basement and thickness contours of Miocene and Pliocene sedimentary rocks and Pleistocene and Holocene sediments (Greene and Clark, 1979). Contours representing modeled depth to pre-Cenozoic basement based on analysis of gravity data were digitized from Watt and others (2010). A surface for each hydrogeologic unit was estimated using correlation of borehole data and augmented using geologic sections from eight reports (Thorup, 1983, 1985; Cleath and Associates, 1991; Hall, 1992; Staal, Gardner, and Dunne, Inc., 1993; Feeney and Rosenberg, 2003; Kennedy/Jenks, 2004a, b; GEOSCIENCE Support Services, Inc., 2013). A conceptual diagram of the SVGF along the central axis of the Salinas Valley is shown (fig. 22B) to illustrate the distribution of hydrogeologic units and their thickness from the coastal area to the edge of the integrated hydrologic model domain.

## Geologic Structures

Structures, predominantly faults for the onshore part of the study area, were compiled from the digital geologic map of Monterey County (Wagner and others, 2002) and from the California State geologic map (Jennings, 2010). Offshore faults were compiled from digital offshore geologic map data (Wagner and others, 2002; Golden and Cochrane, 2013; Dartnell and others, 2016; Johnson and others, 2016) and digitized from georeferenced maps of the offshore region (Greene, 1970, 1977; Greene and Clark, 1979). Faults were attributed according to their recency, defined by the youngest geologic unit that the fault cuts completely (fig. 22A). Fault recency was determined through comparison with the Quaternary fault and fold database of the

United States (U.S. Geological Survey and California Geological Survey, 2021) and through inspection of the structural offset of each fault as shown on geologic cross sections (Thorup, 1983, 1985; Cleath and Associates, 1991; Hall, 1992; Staal, Gardner, and Dunne, Inc., 1993; Feeney and Rosenberg, 2003; Kennedy/Jenks, 2004a, b; GEOSCIENCE Support Services, Inc., 2013).

## Hydrogeologic Texture

Lithologic data were compiled from a database of monitoring and water wells provided by MCWRA and augmented by data transcribed from water wells obtained from the California Department of Water Resources Well Completion Report database

(<https://water.ca.gov/Programs/Groundwater-Management/Wells/Well-Completion-Reports>).

Downhole stratigraphy was transcribed for monitoring and water wells that appear on cross sections where aquifer and confining units were interpreted on cross sections in the following reports: Thorup (1983, 1985), Cleath and Associates (1991), Hall (1992), Staal, Gardner, and Dunne, Inc. (1993), Harding ESE (2001), Feeney and Rosenberg (2003), Kennedy/Jenks (2004a, b), and GEOSCIENCE Support Services, Inc. (2013). Geohydrologic information for the deeper aquifers near the coast was obtained from Hanson and others (2002). Stratigraphic information for deeper hydrogeologic units in the southern, upstream part of the Salinas Valley was compiled from 336 oil and gas exploration wells obtained from the California Department of Conservation Geologic Energy Management Division

(<https://www.conservation.ca.gov/calgem/Pages/WellFinder.aspx>). Drilled depths to the tops of formations penetrated in the well were compiled. The source of the formation depth data for each well depended on the year the well was completed. Before 1964, summary tables of data for oil and gas prospect wells were used. From 1964 to 1980 year-by-year tables from California

Division of Oil, Gas and Geothermal Resources (1982) were used. For all other wells, the interpretation of formations was evaluated using electric logs obtained through the California Department of Conservation Geologic Energy Management Division. The deepest hydrogeologic units, basement and the Purisima Formation, were assumed to be mostly consolidated with potential secondary alteration of porosity; thus, textural information was not developed for them. The remaining hydrogeologic units were considered less consolidated where sediment texture substantially influences the distribution of permeability. Textural properties of the seven remaining hydrogeologic units were derived from lithologic data in the basin using methods developed in nearby basins in California (Phillips and Belitz, 1991; Burow and others, 2004; Faunt and others, 2009b, 2015; Sweetkind and others, 2013). Downhole lithologic data from nearly 1,400 wells were used to calculate the percentage of coarse-grained deposits within each hydrogeologic unit at each borehole. This percentage was interpolated using two-dimensional kriging from each borehole onto the model cells to create gridded estimates of the percentage of coarse-grained materials in each hydrogeologic unit. The hydraulic properties in the integrated hydrologic models were estimated based on the percentage of coarse-grained deposits like was done for the Cuyama Valley (Sweetkind and others, 2013), Pajaro Valley (Hanson and others, 2014c, d), and Borrego Valley (Faunt and others, 2015). The hydrogeologic unit thickness and texture are shown side by side for the less consolidated hydrogeologic units (figs. 23A–G) that had textural classification in the SVGF. The thickness for the basement and Purisima Formation hydrogeologic units is provided in figure 23H.

**Figure 23.** Hydrogeologic unit thickness and percentage of coarse material for hydrogeologic units in the Salinas Valley, California that are not fully consolidated (Sweetkind, 2023): A) shallow aquifer, B) upper confining unit, C) 180-Foot Aquifer, D) middle confining unit, E) 400-Foot Aquifer, F) lower confining unit,

and G) Paso Robles Formation; and H) maps showing hydrogeologic unit thickness for Purisima Formation and bedrock hydrogeologic units. The Purisima Formation and bedrock hydrogeologic units represent composite rock aquifers without a textural classification so the percentage of coarse materials is not shown.

## **Groundwater Inflows and Outflows**

The simulation of groundwater pumpage and levels in the integrated hydrologic models relies on specification of boundary conditions, reported pumpage that is specified as model input, and simulated groundwater pumpage and recharge using FMP. Simulation of agricultural groundwater pumpage in MF-OWHM is constrained by reported aggregated pumpage by WBS when available. Simulation of M & I groundwater pumpage is specified based on estimated or reported data when available. Simulation of groundwater recharge is constrained by observed water levels. Groundwater flows within the study area are computed using simulation of regional groundwater flow to adjacent groundwater basins, vertical exchanges among hydrogeologic units, pumpage, and evaporation of groundwater in the shallow root zone.

## **Groundwater Data**

Groundwater pumpage data were obtained for the period from October 1, 1967, to September 30, 2018 (Henson and others, 2023), and reported groundwater pumpage data from as many as 353 M & I wells were used to specify groundwater pumpage (fig. 24A). Reported data aggregated to the WBS scale from as many as 2,002 agricultural wells (fig. 24A) were used to evaluate the performance of simulated agricultural demand. A subset of wells was used to estimate M & I pumpage prior to 1995. Reported groundwater levels from 439 wells were used to evaluate groundwater levels in the simulation (fig. 24B). Of the 439 observation wells, 340 were also specified as agricultural wells and pumped to meet simulated agricultural demands

(fig. 24B) because many are used as agricultural supply wells and information about available pumping wells in the basin was limited. Groundwater pumpage in the integrated hydrologic models is (1) FMP simulated pumpage from irrigation wells (herein referred to as agricultural supply) and (2) estimated and specified M & I and domestic pumpage (herein referred to as water supply). Because the integrated hydrologic models use monthly stress periods, pumping information from available data sources was converted into monthly values to define model input.

**Figure 24.** Wells within the integrated hydrologic model domain for A) municipal, industrial, and agricultural wells, and a subset of wells used to estimate municipal and industrial pumpage from water year 1968 to 1994 (pre-1995 wells); and B) location of observation wells.

#### Specified Groundwater Pumpage for Water Supply

Groundwater pumpage for M & I is specified based on reported and estimated values. Domestic pumpage from individual landowners is not explicitly estimated. The M & I pumpage estimates prior to 1995 are based on population and include potential domestic groundwater pumpage. After 1995, domestic pumpage is assumed to be less than 10 percent of M & I pumpage. For example, domestic pumpage only meets water demands for approximately 31,000 of the 402,000 people estimated to live in Monterey County in the year 2000 (Henson and others, 2023). Groundwater pumpage information for each M & I well was estimated for the model period before November 1994 and specified using observations for the remainder of the simulation. For the model period before November 1994, the volume of groundwater pumpage was estimated using census population data and estimated gallons per capita per day for years 1970, 1980, and 1990 (Henson and others, 2023). After November 1994, M & I pumpage was specified based on reported data. A complete description of the M & I estimation methods and

pumpage data is provided by Henson and others (2023). The estimated monthly pumpage rate was divided among the wells in each area on a monthly time step and assigned to wells that were known or assumed to exist at that time.

## Groundwater Flow Simulation

Groundwater flow within the Salinas Valley occurs within the sediments of the nine hydrogeologic units and is assumed to be bounded at depth by the basement hydrogeologic unit and laterally by the outermost extent of the seven groundwater subbasins and mountain ridgelines that bound the Salinas Valley. Within the Salinas Valley, fault systems can act as barriers that affect groundwater flow and levels. Groundwater recharge and inflows can occur in hydrogeologic units exposed in the hillsides that bound the catchment of the Salinas Valley, through ephemeral, intermittent, and perennial stream channels, through surface alluvium, and as underflow from Monterey Bay, the Paso Robles Area groundwater subbasin, and the Corralitos-Pajaro Valley groundwater subbasin (fig. 11). Groundwater outflow occurs as streamflow discharge, drain return flows, discharge to Monterey Bay, groundwater pumpage, and evapotranspiration. Groundwater pumpage for M & I supply is specified. Groundwater flow, hydraulic properties, and initial and boundary conditions are described in this section. Groundwater recharge, pumpage for agricultural water supply, and evapotranspiration are simulated together using the representation of the land surface and land use water demands in the integrated hydrologic models, as described in the “Farm Process Overview” section.

## No-Flow Boundaries

No-flow boundaries in the integrated hydrologic models were used for the bottom of the basement hydrogeologic unit (layer 9) that represents the basement aquifer and for the lateral

boundaries of the active model domain. The lateral no-flow boundaries are defined at the topographic ridges of ranges that bound the Salinas Valley and represent the contact between the low-permeability basement hydrogeologic unit and the aquifers at the edges of the groundwater basin (fig. 22A). No-flow boundaries were also specified for faults that bound parts of the foothills surrounding the Salinas Valley. The lower boundary of the model was limited to 500 ft below the top of the basement hydrogeologic unit, which is deeper than the deepest supply wells.

### General-Head Boundaries

Lateral and vertical head-dependent flow boundaries are implemented to represent net regional groundwater flow from adjacent groundwater subbasins. Using the General Head Boundary Package of MODFLOW (Harbaugh, 2005), head-dependent flow boundaries were simulated in three locations in the model: a coastal, inland, and offshore general head boundary (GHB). The net coastal and inland GHB groundwater flow data were summed to create an “interbasin underflow” groundwater budget category and the offshore GHB net groundwater flow data were summed for all model layers to create a “seawater coastal inflow” groundwater budget category. This seawater coastal inflow groundwater budget category is an analogue for seawater intrusion. Seawater intrusion is usually quantified as an area of the aquifer that has water quality degradation due to contamination by saline water, and the seawater coastal inflow budget category reflects the total volume of water that enters the landward portion of the model domain from the ocean. The hydraulic conductance for each group of GHB cells was based on the hydraulic conductivity of the aquifer sediments (described in the “Hydraulic Properties” section) and the cell geometry. Hydraulic conductance for each GHB boundary was adjusted during model parameter estimation.

For the coastal GHB, lateral head-dependent flow boundaries were specified in selected cells in layers 1, 3, 5, 7, and 8 near the northern boundary of the study area near the coast in the 180-Foot/400-Foot Aquifer and Langley Area groundwater subbasins (fig. 25). The coastal GHB represents interbasin underflow between the integrated hydrologic model domain and the Pajaro Valley groundwater subbasin to the north. For the coastal GHB, four GHB were specified with spatially constant and time-varying boundary heads obtained from nearby monitoring well groundwater levels (figs. 26A–D; Henson and others, 2023). The hydraulic conductance for the group of cells associated with each monitoring well in each layer is considered constant.

**Figure 25.** Specification of general head boundaries (GHB) in the integrated hydrologic model domain. The location of GHB wells and the cells used to define the offshore GHB, coastal GHB, and inland GHB in the Salinas Valley Integrated Hydrologic Model domain are shown.

**Figure 26.** General head boundary (GHB) time series in the Salinas Valley, California for A) coastal GHB boundary well 33H1, B) coastal GHB boundary well 16D1, C) coastal GHB boundary well 4L1, D) coastal GHB boundary well 12D1 (Henson and others, 2023), and E) mean monthly sea level (National Oceanic and Atmospheric Administration, 2019).

For the inland GHB, lateral head-dependent flow boundaries were also specified in layer 7 near the Salinas River at the southern boundary of the integrated hydrologic model domain. This inland GHB represents interbasin underflow between the integrated hydrologic model domain and the Paso Robles Area groundwater subbasin to the south. For the inland GHB (fig. 25), a GHB is defined for seven cells in layer 7 perpendicular to the first river reach. The inland GHB time-series value was a constant 400 ft through time, estimated as the mean hydraulic head near the river from the Paso Robles hydrologic model of the upper Salinas Valley (GEOSCIENCE Support Services, Inc., 2016; Henson and others, 2023).



For the offshore GHB, vertical head-dependent flow boundaries were specified for the exposed offshore geologic units to estimate seawater coastal inflow in the aquifers along the coast. The offshore GHB is used to estimate coastal inflow exchanges among the onshore and offshore areas of each hydrogeologic unit. The integrated hydrologic models do not explicitly simulate the density of seawater for the simulation of exchanges between the onshore and offshore areas of the model domain. For each model cell exposed on the seafloor, a vertical GHB boundary was applied. A monthly time series of sea-level variation was estimated using the mean monthly sea level elevation data (fig. 26E; National Oceanic and Atmospheric Administration, 2019) in San Francisco Bay before 1974 (identifier 9414290) and in Monterey Bay after 1974 (station 9413450). An equivalent freshwater hydraulic head was used to account for the density of seawater in the offshore hydraulic heads using the methods described by Motz and Sedighi (2009). The elevation value was based on the North American Vertical Datum of 1988. This approximation of equivalent freshwater hydraulic head was determined to yield accurate values for hydraulic heads in a coastal aquifer based on experiments in three-dimensional groundwater flow models. The GHB along the coastline was computed using equation 1:

$$h_{fw} = \frac{\rho}{\rho_f} h - \frac{\rho - \rho_f}{\rho_f} Z_i \quad (1)$$

where

$h_{fw}$  is the hydraulic head of freshwater equivalence,

$h$  is the pressure head at a point N above a datum,

$\rho$  is the density of saline groundwater at point N above a datum,

$\rho_f$  is the density of freshwater, and

$Z_i$  is the node of each GHB cell along the coast.

The equivalent freshwater head used to compute the GHB value was variable for each cell with an offshore GHB. The equivalent GHB value depends on the height of the column of water above the center of cell  $Z_i$  where the GHB was applied. If the top of the cell where the GHB was applied was closer to the ocean surface (for example, near the shoreline), the GHB value was lower. If the top of the cell where the GHB was applied was deep under the sea level (for example, far from shore), the GHB value was higher. The range of GHB values over all offshore GHBs ranged from 2.5 to 97.4 ft.

### Groundwater Wells

Irrigation, municipal, and industrial wells are simulated as multiple-aquifer wells that can extract water from more than one hydrogeologic unit (figs. 24A). All single and multiple-aquifer wells were simulated by the multi-node well (MNW2) package (Konikow and others, 2009). The MNW2 simulates two processes: (1) the produced groundwater from single or multiple aquifers during pumping and (2) the flow of water between aquifers via boreholes when multiple aquifers are connected to the same well and have different hydraulic heads. For many of the wells, data for each well describing the operational history, open screen intervals, construction information, and radius were estimated where they were incomplete. This section summarizes the methods used for estimating the missing well data to create a complete set of well-related data and properties needed for model construction. The resulting complete set of well information was published by Henson and others (2023).

Estimated operational history information (drill dates, active pumping periods, and destruction dates, if applicable) was used to construct the monthly pumping time series for each well. The number of active wells for any given stress period varied through time based on

reported drill dates and destruction dates. Well construction and destruction dates were used where available to specify when wells are active in the simulation. Specifying wells with undefined construction information as active for the entire simulation is warranted based on historical reports of extensive agricultural groundwater development (California Department of Water Resources, 1968). Available open-screen interval data were used to identify the model layers from which water was withdrawn, with the assumption that wells fully penetrate each layer they pump from. If a well contained multiple open-screen intervals, all layers from the top of the uppermost open interval to the bottom of the lowermost interval are assumed to be completely screened and fully penetrating in those model layers. When well-screen intervals span multiple model layers, the well is simulated as a multiple-aquifer well, allowing pumping to be dynamically distributed along with intra-wellbore flow between all corresponding layers. Thus, pumpage for each well was dynamically allocated to individual model layers based on available construction information to determine which layers contribute to potential pumpage or intra-wellbore flow within a well. There is substantial uncertainty of which hydrogeologic unit each well is connected to. This can contribute to uncertainty in the magnitude of simulated well drawdowns, distribution of pumpage, and intra-borehole exchanges of water among layers. To mitigate this uncertainty to the extent possible, wells with missing construction information were assigned open screen intervals based on their WBS, construction date, depth, and the nearby MCWRA-estimated 500 mg/L chloride concentration contour (fig. 24A; MCWRA, 2023; Henson and others, 2023). Where available, the well pumping capacity and casing diameter of each well was obtained from MCWRA. Missing well pumping capacity and casing diameter of each MNW2 well was estimated based on properties of similar wells from the MCWRA well database (Henson and others, 2023). If the casing diameter was not available for a well, the well

was either assigned a casing diameter from a nearby well or assumed to have the median casing diameter of all wells with the same well-use category. The diameter of the well skin, representing the region of disturbed aquifer material surrounding the well casing due to drilling activities, was assumed based on the drill date and casing diameter of the well.

### Drain Return Flows

Groundwater discharge to the land surface was simulated using the MODFLOW Drain Return Flow package (DRT; Banta, 2000; Hanson and others, 2014a). This drainage boundary condition was applied to each of the uppermost model cells in the integrated hydrologic models with the drain elevation set to the land surface elevation plus 1 foot inside the riparian area and cells containing streams and the land surface elevation everywhere else. This model setup allows routing of groundwater discharge to streams when using DRT. The DRT applies a drain boundary condition to compute groundwater-level rise above the land surface and routes this drain flow to adjacent streams. This drain flow becomes streamflow that is managed by the SFR2 package.

To better quantify the magnitude and timing of groundwater discharge to streams in different locations of the study area, the model cells specified in DRT were grouped into three different budget group categories in the model output. Each cell in the riparian WBS was defined as a “riparian drain” and assigned to a “riparian drainage” groundwater budget category in the analysis. Each cell coincident with or adjacent to a stream cell that is not a part of the riparian WBS was defined as a “tributary drain” and assigned to a “tributary drainage” groundwater outflow budget category. Every other cell in the model domain was defined as a “surface drain” and assigned to a “surface drainage” groundwater outflow budget category. These budget

categories are used to evaluate the role of different locations of groundwater discharge to streams in hydrologic budgets throughout the basin.

### Hydraulic Properties

The Layer Property Flow package (Harbaugh, 2005) was used to define storage and hydraulic conductivity properties in each of the aquifers represented in the integrated hydrologic models. The Layer Property Flow package, along with the Parameter Value (Harbaugh, 2005) and Multiplier (Harbaugh, 2005) packages, was used to calculate and specify the aquifer storage and hydraulic conductivity parameters. Lateral and vertical variations in sediment texture affect the direction and rate of groundwater flow by constraining the magnitude and distribution of aquifer-system permeability, porosity, and storativity. The hydrogeologic units defined in the SVGF (fig. 22A, table 2; Sweetkind, 2023) were used as surrogates to define the vertical and lateral hydraulic conductivity and storage property distributions within the integrated hydrologic models. Each hydrogeologic unit can be characterized by variations in hydraulic properties, which are based on the textural distribution of coarse- and fine-grained sediments in zones that represent subregions in which sediments accumulated in particular depositional environments, referred to as facies (Sweetkind, 2017). For this study, facies are generally represented by the Salinas Valley groundwater subbasins (fig. 11) and are implemented as parameter zones using the ZONE package (Harbaugh, 2005). Hydraulic properties for the three model layers of the most recent Salinas Valley hydrologic model (SVIGSM; Montgomery Watson, 1997) were used as initial values for the integrated hydrologic models (table 4). Hydraulic properties were then estimated as separate parameters that were adjusted by groundwater subbasin using regional-scale factors.

**Table 4.** Summary of hydrogeologic units, model layers, and aquifer properties in the Salinas Valley Integrated Hydrologic Model and Salinas Valley Operational Model with corresponding layers and properties from the previously developed Salinas Valley Integrated Groundwater and Surface Model (SVIGSM; Montgomery Watson, 1997).

### *Zones*

The distributions of storage properties and horizontal and vertical hydraulic conductivities vary with the distribution of subregions or zones of each hydrogeologic unit (figs. 27A–F). The parameters used to represent these subregions within each model layer represent unconfined aquifers in outcrop areas and subareas of confined aquifers that underlie other aquifers. Therefore, the hydraulic properties of each of these subareas were estimated with separate model parameters during model parameter estimation. In subareas where hydrogeologic units (layers) pinch out or were otherwise missing, the hydraulic properties are represented by a zone of “pinched” cells with relatively small storativity, high vertical hydraulic conductivity, and low horizontal hydraulic conductivity that allow communication between the layers that are present. To define model parameters, zones were combined with information about sediment texture from the SVGF.

**Figure 27.** Distribution of parameter zones used for estimation of hydraulic properties in the integrated hydrologic domain for the six aquifer hydrogeologic units in the Salinas Valley, California *A*) shallow aquifer (model layer 1), *B*) 180-Foot Aquifer (model layer 3), *C*) 400-Foot Aquifer (model layer 5), *D*) Paso Robles Formation (model layer 7), *E*) Purisima Formation (model layer 8), and *F*) bedrock (model layer 9) (Henson and Culling, 2025).

### *Texture-Based Hydraulic Properties*

The hydraulic water-transmitting properties of aquifer sediments are represented by hydraulic storage properties and horizontal and vertical hydraulic conductivity of the hydrogeologic units. The relation between hydrogeologic units in the aquifer system, lithology, texture, and hydraulic properties has been developed in many previous studies that include both the properties of the aquifers and those of any fine-grained interbeds or confining units (Hanson and others, 1990, 2003, 2004, 2014a, b; Laudon and Belitz, 1991; Phillips and Belitz, 1991; Hanson and Benedict, 1994; Leighton and others, 1995; Belitz and Phillips, 1995; Burow and others, 2004; Phillips and others, 2007; Faunt and others, 2009a, b). The storage and hydraulic conductivity parameter values for each model cell in each hydrogeologic unit are assumed to be correlated to sediment texture in the SVGF, using the fraction of coarse-grained to fine-grained sediment. The percentage of coarse material estimated from the SVGF (fig. 23) were used to develop values for storage and hydraulic conductivity properties. All hydrogeologic units except the Purisima and basement aquifers have separate estimates of the percentage of coarse material. The zones are used to distribute hydraulic properties in the Purisima and basement aquifer hydrogeologic units and the zones and estimates of the percentage of coarse material in each model cell are used for all other hydrogeologic units. Within each model layer, these distributed values are scaled within defined zones (table 5, figs. 27A–F) to estimate final values derived from parameter estimation ( figs. 21A–H). The final parameters from parameter estimation representing hydraulic properties and related scale factors are discussed in the “Parameter Estimation and Sensitivity—Salinas Valley Integrated Hydrologic Model” section.

**Table 5.** Summary of IBOUND parameter and zone codes used to represent the hydrogeologic properties in the Salinas Valley, California used in the integrated hydrologic models.

### *Groundwater Storage*

Simulation of groundwater storage consisted of two storage terms (Helm, 1975; Hanson, 1988): specific yield ( $S_y$ ) for unconfined subregions and elastic specific storage ( $S$ ) that includes the compressibility of water for unconfined and confined subregions. The  $S_y$  and  $S$  are storage terms that represent and govern the reversible uptake and release of water to and from storage (eq. 2). The  $S_y$  storage term represents unconfined storage and represents gravity-driven draining or filling (resaturation) of sediments as changes to the water table occur. The  $S_y$  is a function of sediment porosity and moisture-retention characteristics; it cannot exceed the porosity. Specific yield typically is orders of magnitude larger than specific storage and is volumetrically the dominant storage parameter for aquifers in outcrops of basement, Purisima Formation, Paso Robles Formation, and recent alluvium. The  $S$  storage term represents the component of confined storage owing to the compressibility of water and to the reversible compressibility of the matrix or the skeletal framework of the aquifer system (Jacob, 1940; Hanson, 1988). The inelastic storage coefficient is another storage term that is sometimes defined and included in the storage formulation. The inelastic storage coefficient governs the irreversible release of water from the inelastic compaction of the fine-grained deposits or permanent reduction of pore space, which can also lead to land subsidence. There has not been land subsidence documented in the Salinas Valley where assessments have occurred (Brandt and others, 2021) and this version of the integrated hydrologic models does not simulate subsidence; thus, the inelastic storage coefficient storage term was not considered in the composite storage formulation shown in equation 2.



The resulting equation for composite storage is represented (Hanson, 1988) as:

$$S^* = S + S_y \quad (2)$$

where

$S^*$  is the total storage of the aquifer layer,

$S$  is the elastic specific storage, and

$S_y$  is the specific yield from water table drainage for unconfined portions of an aquifer.

The elastic specific storage ( $S$ ) from equation 2 can be further represented by its respective components as:

$$S = b * S_s = \rho g(a + n\beta) * b \quad (3)$$

where

$\rho g$  is the weight of water,

$\alpha$  is the compressibility of coarse- or fine-grained facies matrix material,

$n$  is the total porosity of the coarse- or fine-grained facies,

$b$  is the cell-by-cell thickness of the aquifer layer,

$\beta$  is the compressibility of water, and

$S_s$  is the total specific storage.

The elastic specific storage of water (eq. 3) is dependent on the specified porosities for the coarse- and fine-grained facies of each hydrogeologic unit (model layer). The product of average porosity and the compressibility of water ( $1.4 \times 10^{-6} \text{ ft}^{-1}$ ) yields one part of the composite aquifer specific storage value. Accordingly, the porosity and compressibility of the fine and coarse end members of each hydrogeologic unit were estimated during parameter

estimation. Storage properties in the outcrop subregions (fig. 28A) of the uppermost layers (layers 1, 3, 5, 7, or 9) are represented by specific yield and are adjusted as necessary to represent the unconfined portion of the system. For the parts of hydrogeologic units that represent areas of the aquifers that are unconfined, aquifers were simulated as confined. This simplifying assumption that has been applied in complex regional integrated hydrologic models (Hanson and others, 2004, 2014b, c, d; Faunt and others, 2009a, 2024) is further discussed in the “Model Uncertainty, Limitations, and Potential Improvements” section.

**Figure 28.** Hydrogeologic unit A) specific yield and B) thickness for the uppermost layer of each model cell in the integrated hydrologic model domain for the Salinas Valley, California. The uppermost layer is a composite of hydrogeologic units in the uppermost cell in layers 1, 3, 5, 7, 8, or 9 (Henson and Culling, 2025).

### *Hydraulic Conductivity*

Hydraulic conductivities generally decrease with depth and with increasing distance from the original sediment source (eroded and [or] transported from the adjacent mountain ranges and river channels), which is consistent with colluvial, fluvial, and eolian processes that resulted in fining upward and fining toward the center (distal) sequences observed in aquifer sediments in the SVGF. These expected behaviors can be observed in the horizontal and vertical hydraulic conductivity plots of each aquifer (fig. 29A–F). In several subregions, smaller values of hydraulic conductivity were estimated in fine-grained facies that may also reflect secondary alteration, such as cementation. Coarse-grained sediments are represented near stream channels in the alluvium. Coarse and fine end member values of hydraulic conductivity were used to make initial estimates of the horizontal and vertical hydraulic conductivity for each cell in each hydrogeologic unit in the model. Faunt and others (2009a) identify the power mean as a useful

means for estimating hydraulic conductivity values. This approach specifies a power exponent for each hydrogeologic unit that is adjusted during model parameter estimation. A power exponent equal to 1.0 indicates the hydraulic conductivity is the weighted arithmetic mean of the hydraulic conductivities of the coarse-grained and fine-grained lithologic end members and the sediment texture for each model cell. In each hydrogeologic unit, the fine-grained lithologic end member hydraulic conductivity is much smaller than the coarse-grained lithologic end member hydraulic conductivity; thus, the arithmetic mean heavily weights the coarse-grained end member. For horizontal hydraulic conductivity, the arithmetic mean was assumed. Vertical hydraulic conductivity between model layers was calculated as the weighted power mean of the hydraulic conductivities of the coarse- and fine-grained lithologic end members (Faunt and others, 2009b). The harmonic mean is a weighted power mean with the power law exponent equal to  $-1.0$  and results in increased vertical anisotropy. The geometric mean is a weighted power mean with the power law exponent equal to  $0.0$  and results in decreased vertical anisotropy. Phillips and Belitz (1991) determined that vertical conductivities could be calculated by using either weighted harmonic or weighted geometric means. Belitz and others (1993) represented the vertical conductivities with the weighted harmonic mean. Faunt and others (2009a) calculated the vertical conductivities as power means in which the power mean exponent varied between  $-1.0$  (the harmonic mean) and  $0.0$  (the geometric mean). The vertical hydraulic conductivity is sensitive to the averaging method used. Both the harmonic and geometric means more heavily weight the fine-grained end member and, as a result, the calculated vertical hydraulic conductivity is much lower than the horizontal. Dimitrakopoulos and Desbarats (1993) determined that the value of the power law exponent depended to some extent on the size and thickness of the grid blocks used to discretize the model domain; smaller grid cells resulted in

smaller values of the power law exponent. An initial value of the power law exponent was set for each model layer and adjusted during model parameter estimation.

Figure 29. Horizontal and vertical hydraulic conductivity in six aquifer hydrogeologic units in the Salinas Valley, California A) shallow aquifer, B) 180-Foot Aquifer, C) 400-Foot Aquifer, D) Paso Robles Formation, E) Purisima Formation, and F) bedrock (Henson and Culling, 2025).

### *Faults*

Some faults within the model domain cut across some of the hydrogeologic units; these faults are simulated as potential hydrologic flow barriers (fig. 22A). Many faults are on the western edge of the model and offshore. For computational convenience and to maintain consistency with published interpretations (Greene, 1977; Feeney and Rosenberg, 2003), all faults in the study area were generalized as vertical boundaries with locations shown on figure 22A. Some faults intersect more than one hydrogeologic unit and extend outside of the defined groundwater basins. The MODFLOW Horizontal Flow Barrier package (Hsieh and Freckelton, 1993) was used to simulate resistance to horizontal flow across these structures. The effectiveness of these faults as partial flow barriers to horizontal flow was then estimated by five parameters representing the conductance of the vertical model cell faces aligned with the fault trace. These parameters were specified based on the hydrogeologic unit onshore (180-Foot Aquifer, 400-Foot Aquifer, Purisima Formation, and basement aquifer) and by age in the offshore region (Quaternary or older). Groundwater levels at selected wells that straddle the faults show lateral head differences that may also reflect a combination of screened depths and the faults acting as flow barriers. Barriers to horizontal groundwater flow in the integrated

hydrologic models were represented using the Horizontal Flow Barrier package across the model cell faces of 34,932 model cells.

### *Initial Conditions*

The initial October 1967 groundwater levels in all active cells were set as a composite of water-table contours estimated using available groundwater elevation records and of an assumed correspondence between potentiometric surface contours and surface topography in upland areas of aquifers where limited measurements were available. The initial condition of groundwater elevations in the model was refined during parameter estimation. Defining a steady-state initial condition for the model is not warranted because substantial groundwater pumpage was already occurring before 1967. Salinas Valley groundwater development started in the 1890s with groundwater pumpage from windmills, and more development occurred in the 1920s and 1940s (Manning, 1963). A steady-state or pre-development initial condition assumes that groundwater flows are primarily influenced by the natural cycles of climate variability with no effects of regulated streamflows or groundwater pumpage affecting changes in groundwater levels.

Although multiple periods of historical conditions could be defined to represent pre-development conditions and stages of development, data are limited and the period of interest in this study is focused on more recent periods when reservoirs were operating. Defining a steady-state initial condition for the model is highly uncertain. The initial conditions used in the integrated hydrologic models represent composite estimates of hydrologic conditions after extensive groundwater development for irrigation in the 1920s. With little historical information about aquifer stresses, such as pumpage or climate variability, arriving at a potentially less uncertain set of initial conditions is difficult. The initial conditions were further refined by periodically adjusting scale factors for each layer and region as refinements to estimates of initial heads

during parameter estimation. This adjustment of scaling parameters of the overall elevation of initial groundwater levels helped refine the initial heads for all nine model layers during parameter estimation.

For transient models, initial conditions define the system state at the beginning of the simulation. When the simulation is started, the simulated heads and flows change in response to the initially specified and simulated inflows and outflows. Because the irrigation and pumping stress on the system change rapidly, the inconsistencies between the initially specified conditions and the simulated initial processes and properties generally are not problematic because the magnitudes of the next stress regime (for example, pattern of pumpage) soon dominates the solution (Hill and Tiedeman, 2007). As a result, comparing observed and simulated values becomes meaningful after a relatively short simulation time. This study and previous studies (Belitz and Phillips, 1995; Hanson and others, 2004, 2014b, c, d; Faunt and others, 2009a, 2024) show that the time frame for stabilization is typically less than several months to several years of the simulation, depending on the magnitude of the changes in the stresses that drive inflows and outflows and the overall hydraulic diffusivity of the aquifer systems. The initial conditions are regularly updated during model parameter estimation to develop stable starting conditions. For the water budget analyses in the historical model, WYs 1968 and 1969 are considered spin-up years and analysis of water budgets begins with WY 1970.

### **Parameter Estimation and History Matching—Salinas Valley Integrated Hydrologic Model**

The historical model (SVIHM) was used to simulate historical conditions and represent historical observations (history matching). Therefore, parameter estimation used to calibrate the integrated hydrologic models is focused on the historical model. The operational model (SVOM)

relies on the historical model properties derived from parameter estimation. Simulation with integrated hydrologic models can require specification of several hundred parameters that vary spatially and temporally, some of which are correlated through their process-based relations; thus, developing an optimized set of calibrated parameter values within an integrated hydrologic model can be challenging. Accordingly, a parameterization procedure was employed that allows a limited number of parameter values to control the temporal and spatial variability of a much larger number of model properties specified as inputs. The parameterization procedure followed that of Hill and Tiedeman (2007) in defining the term “parameters” to mean model inputs of hydraulic and hydrologic properties; this definition was extended to include landscape and land-use-related properties from the FMP.

## Parameter Estimation

The following subsections summarize the (1) parameter estimation method and application, (2) observations used for parameter estimation, including how observations were processed and weighted, (3) description of parameters, and (4) parameter sensitivity analysis. Parameter estimation employed a combination of trial-and-error and computer-assisted processes of minimizing differences between “real-world” observations and their simulated equivalent values. Parameter estimation requires more than just matching historical observations by estimating parameters, it also requires adjustments in the conceptual framework of the integrated hydrologic models to integrate information obtained during parameter estimation and to improve numerical instabilities—for example, making small alterations to hydrogeologic unit layer elevations within the uncertainty of the geologic framework from which they are defined. The result of this iterative process is a more consistent framework for parameter estimation. Once the

structural framework is consistent, then observations and parameters can be compiled and grouped.

The parameter estimation software package PEST-HP (Doherty, 2024) was used for the computer-assisted parameter estimation and sensitivity analyses. The PEST-HP is a serial parameter-estimation program, that allows execution of parallel model runs on multiple computers. PEST-HP uses the Gauss-Levenberg-Marquardt algorithm to systematically adjust parameter values to find a minimum of an objective function over a space of parameters. To improve parameter estimation, the correlation among parameters was addressed, where possible, using singular value decomposition to reduce the total number of parameters into “super-parameters” that represent more than one parameter. Tikhonov regularization (Doherty, 2024) was employed to prevent parameter overfitting. Regularization also adds stability to the parameter estimation process because parameters that are insensitive to observations do not change values during each PEST-HP iteration (Doherty, 2024). The objective function is the sum of squared, weighted residuals between observed values and their simulated equivalents. For each parameter, an initial value and range is specified. The observations are grouped and weighted to ensure that the observation measurement scale does not influence its contribution to the objective function and that the simulation focuses on the information obtained from observations that can be replicated by the simulation.

Many simulated hydrologic fluxes are head dependent or were correlated through their exchange of water (flow dependent); thus, parameters controlling each set of processes were adjusted through automated and trial-and-error analysis. Initial parameter estimation was performed in a stepwise format that started with the landscape processes, followed by adjustment of hydraulic properties, streambed properties, multiple-aquifer well properties, general-head



boundary conductance, and fault conductance. The parameter estimation process also required modifications to the parameter framework. For example, parameters and observations for the surface water drainage network were further partitioned, and climate and efficiency factors were included for improved consumptive-use and related agricultural pumpage estimates. Parameter estimation was later limited to a subset of parameters using composite scaled sensitivity analyses to define meaningfully sensitive parameters. Even though some parameters demonstrated significant correlations, those parameters selected for parameter estimation were assumed to be independent or were calibrated in a stepwise manner to minimize the effect of parameter correlation. Observations were classified, grouped, and weighted to ensure that simulated hydrologic flows in the integrated hydrologic models represent the important hydrologic flows (for example, agricultural water supply) and changes in regional groundwater levels. The weighting of observation groups in parameter estimation is described further in the “Observation Weighting” section. Parameter adjustments were based on the comparison of observed values to their simulated equivalents. The simulated equivalent values were compared to all observed values and provided a measure of model performance through various historical time intervals and model analysis regions. The resulting error distributions constrain model parameters, and the comparison between simulated and observed values provided a basis for a sensitivity analysis of selected parameters.

## Observation Data

The parameter estimation includes observation data for the period from October 1967 to December 2014. Observations representing groundwater conditions include groundwater levels, temporal changes in groundwater levels (drawdowns), vertical gradients in groundwater levels between units, published changes in groundwater level contours, aggregated agricultural

groundwater pumpage by WBS, and streamflow differences among upstream and downstream gages. Observations representing surface water conditions include surface-water flows along the Salinas River and in rivers within the integrated hydrologic model domain at USGS streamgaging stations, canals/laterals, and drains where data were available, as well as flow-differences between gages (fig. 20; Henson and Culling, 2025).

### *Surface Water*

Surface water flow data used to develop observations for parameter estimation include monthly averaged streamflow data (USGS, 2018) at gages along the Salinas River and its tributaries Arroyo Seco and Reliz Creek (fig. 20), available surface water diversions records (Henson and others, 2023), and flow differences between selected streamgages (USGS, 2018). Where sufficient measurements were available, surface water data were averaged to quarterly and annual mean values as additional observations for parameter estimation. Five pairs of USGS gages were selected for flow-difference observations on the major tributaries Arroyo Seco and Reliz Creek (USGS 11152050 and USGS 11152000) and the USGS gages along the Salinas River (USGS 11150500, USGS 11151700, USGS 11152300, and USGS 11152500). Streamflow differences were computed as upstream minus downstream, meaning that negative values represent streamflow gains in the surface water drainage network between the gages. There were 5,736 streamflow observations, 291 diversion observations, 2,508 streamflow difference observations, 2,011 quarterly mean streamflow observations, and 527 annual mean streamflow observations. Each observation was classified into subgroups based on observed low flow (flow less than 25 ft<sup>3</sup>/s), stream name (Salinas River or Arroyo Seco), differences, or diversions.

## *Groundwater*

Groundwater-level histories are largely restricted to the Salinas Valley floor. The largest set of observed values used for parameter estimation were groundwater levels and changes in groundwater levels over time. The dataset used for parameter estimation consists of groundwater-level measurements from WY 1968 to 2014 from 439 single and multiple-aquifer wells and multi-well monitoring sites (figs. 24A, 24B). These groundwater-level measurements were developed into groundwater-level observations and drawdown observations. Where the frequency of measurement at a given well was sufficient, mean quarterly and mean annual groundwater level and drawdown observations were generated. Drawdown observations measure the change in groundwater level relative to the first head observation for the time span of measurements from each well. A negative drawdown value represents a lowering of groundwater levels. To represent the overall trend in heads throughout the region and to minimize the potential effects of initial conditions, a set of drawdown observations were made for each well. There were 459 monthly groundwater-level observations and 50,992 monthly drawdown observations, 11,942 quarterly mean groundwater-level observations and 11,942 quarterly drawdown observations, 5,415 annual mean groundwater-level observations and 5,415 annual mean drawdown observations, and 1,576 head difference observations.

During the development of groundwater-level and drawdown observations for parameter estimation, the effects of local and regional pumpage was considered. The density of pumping wells in each of the analysis regions can be substantial (figs. 24A, 24B). Moreover, 340 of the 439 observation wells are also agricultural supply wells. For these wells, there is an unknown pumping time series and no information about when these wells or adjacent wells were pumping relative to the time of groundwater-level measurement. Thus, data from these wells were

carefully managed during parameter estimation. Seasonal oscillations in these wells are not expected to be well matched because the well pumping rates simulated in the models are not simulated using time series from individual well owners but are based on the water demands of the WBS across all available wells. The groundwater-level and drawdown observations are classified into one of two classes depending on if they were potentially influenced by pumping (“pumping influenced”) or not. This classification is based on the following conditions: the observation well is also an agricultural supply well and the measurement occurs in the peak growing season from March through September. This classification does not capture every measurement that could be influenced by pumping as pumping occurs year-round. However, it does help delineate the measurements that are most likely to be. Groundwater level and drawdown observations for a historical dry period from WY 1984 to 1994 were grouped by analysis region and whether they were pumping-influenced, then further grouped by quarterly mean values and by annual mean values.

**Figure 30.** Analysis regions with locations of selected observation wells in Salinas Valley, California.

### *Agricultural Pumpage*

The monthly agricultural pumpage reported by the Groundwater Extraction Management System was aggregated by WBS (Henson and others, 2023), spanning the period from November 1994 through December 2014. Prior to November 1994, when monthly agricultural pumpage observations were not available, simulated annual agricultural pumpage was compared to published long-term estimates (MCWRA, 1995). The monthly agricultural pumpage data were averaged to generate quarterly and annual average observations for each WBS. In addition, monthly observations from each WBS were aggregated to the analysis regions (fig. 15; Henson

and Jachens, 2022). There are 3,630 monthly, 1,215 quarterly, and 315 annual agricultural observations.

### Observation Weighting

During parameter estimation, observations were weighted. The sensitivity of a parameter is also dependent on the observation weights. Observation weights are used for a variety of purposes, including accounting for differences in measurement units and quantification of measurement error, and are sometimes imposed to help distribute the importance of observations across the many different types of observations (for example, to remove the effects of spatial or temporal clustering of measurements or to emphasize areas where a model will be used to make predictions). The weighting of observations helps to determine how the contribution to the objective function is distributed among the various types of observations. This weighting procedure also helps ensure that the parameter estimation only considers observations that the model can reproduce given data and model limitations. Including observations that the model cannot reproduce can lead to parameter compensation and model structural error (White and others, 2021). Therefore, some observations were weighted near zero or scaled to focus parameter estimation on observations of interest. For example, observations for the first 2 years of the simulation had reduced weights to allow for the parameter estimation to focus on the period after the assumed 2-year model spin-up. There were many parameter estimation iterations that alternated between trial and error and PEST-HP. Through this process, observations were regularly reweighted so that the objective function was updated and the contribution of error from each observation group was equalized.

Each observation group type (surface-water, groundwater, and agricultural pumpage) was weighted to represent about 1/3 of the total error; subgroups (for example, low flows) within

each observation group were weighted differently. Within the stream observation group, selected streamflow observations in the stream network were given relatively more importance to the parameter estimation if they influence pumpage and groundwater levels, specifically those within the main channel of the Salinas River, diversion locations, and places where reservoir operational target flows are defined. The low flows and all other flows were equally weighted, ensuring parameters that control high and low flows influence model parameter estimation. High flows are driven primarily by precipitation runoff, whereas low flows are typically driven by irrigation runoff and groundwater and surface-water exchange. Many of the groundwater level observations in the model were influenced by pumping or occurred in wells that were used for groundwater supply. The observations associated with these agricultural supply wells were weighted lower than other wells, and the observations that represented annual minima of groundwater levels were assigned zero weights. The observations associated with annual mean groundwater levels and drawdowns were increased to twice the weight of other groundwater level and drawdown observations. The monthly and quarterly mean agricultural pumpage observations were weighted based on their fraction of total agricultural pumpage reported in the Groundwater Extraction Management System. These weights were doubled for annual average agricultural pumpage observations.

## Parameters

The number of adjustable parameters changed during parameter estimation. A total of 311 parameters were initially created to facilitate model parameter estimation, and after initial global sensitivity and parameter estimation, about 40 parameters were determined to be relatively sensitive and were included in the computer-assisted and trial-and-error parameter estimation process (fig. 31, table 6). All other parameters were less sensitive than the least

sensitive parameter shown in figure 31. The full enumeration of parameters is provided by Henson and Culling (2024). These parameters included aquifer conductivity, aquifer storage, climate scale factors, drain conductance, runoff, and stream conductance parameters. As discussed, hydraulic properties were initially assigned values based on previous modeling studies, then adjusted during model parameter estimation. Model parameters were adjusted within ranges of reasonable values to best-fit historical hydrologic conditions (history matching) and observations in the groundwater, surface-water network, and landscape.

**Figure 31.** Magnitudes of the relative composite scaled sensitivity for selected parameters used in Salinas Valley integrated and reservoir operations models for Monterey and San Luis Obispo Counties, California. Refer to table 6 for a full description of the sensitive parameter names and values. All model parameters described by Henson and Culling (2025).

**Table 6.** Summary of sensitive calibration parameters from composite scaled sensitivity analyses for the Salinas Valley, California Integrated Hydrologic Model.

#### *Landscape-Process Parameters*

Landscape process parameters within FMP that were adjusted during parameter estimation included selected properties related to land use. Some parameters were fixed to initial estimated values, some were adjusted manually, and some were adjusted using PEST-HP. These included seasonal climate-stress scale factors and fractions of inefficient losses to runoff from irrigation and precipitation that vary by crop type. Climate-stress scale factors for crop demands represent factors such as irrigation stress and climate-based changes in the crop demands—for example, hot and dry conditions. The climate-stress scale factors adjust crop demands in response to different climate regimes (for example wet, normal, or dry, and winter, spring,

summer, or fall) and represent the influence of K<sub>c</sub> stress factors (Allen and others, 1998) that amplify or reduce K<sub>c</sub> values used to estimate agricultural demands. Estimation of K<sub>c</sub> values typically occurs under unstressed conditions. These factors were adjusted during parameter estimation to improve the simulation of estimated pumpage. Adjustment factors for K<sub>c</sub> were decreased from as much as –25 percent and increased by as much as 55 percent, depending on the season and climate year type, to align estimated agricultural pumpage with reported monthly pumpage and groundwater-level declines. Many of these climate-stress scale factors were sensitive and are shown in table 6. The fractions of irrigation losses and precipitation losses to surface-water runoff for all land uses are provided in the model archive (Henson and Culling, 2025). The fraction of irrigation losses to surface-water runoff were assumed to be relatively small and range from 0.1 percent for indoor nursery crops to 7 percent of outdoor nursery crops, with most values equal to 5 percent. The fraction of precipitation losses to surface-water runoff were assumed to be greater than the irrigation losses, with precipitation losses to surface water ranging from 5 to 7 percent for agricultural areas, 40 percent for grasslands, and 100 percent for the riparian areas. Excess applied irrigation was assumed to mostly contribute to deep percolation to groundwater along with subsequent lateral flow and capture by nearby drain canals.

### *Hydraulic Parameters*

The historical model was calibrated to estimate values of hydraulic properties within each hydrogeologic zone within each model layer. Parameters include the values of horizontal and vertical hydraulic conductivity and specific storage for each facies zone within each hydrogeologic unit and the power law exponents for vertical hydraulic conductivity. Defining these three parameters for each of the 47 textural zones across all hydrogeologic units (figs.



27A–F) yields 88 parameter values for horizontal and vertical hydraulic conductivities and 9 multipliers for storage properties. An additional group of 18 parameters for specific storage, porosities, and specific yields were included using the MODFLOW MULT package that was used to build the specific storage values and horizontal and vertical values for hydraulic conductivity. For the specific storage formulation, the compressibility of water was held constant. Specific yield was specified as a component of the storage properties proportional to the estimated porosity.

The parameter estimation of hydraulic properties required the adjustment of horizontal and vertical hydraulic conductivity and rescaling of specific storage based on groundwater-level hydrographs and vertical head differences. The most sensitive parameters were vertical hydraulic conductivities that, in part, controlled the seasonal amplitudes and vertical water-level differences between aquifer layers. Other sensitive parameters include the hydrogeologic unit power law exponents used to define vertical hydraulic conductivity values in each cell (using a weighted power mean of the hydraulic conductivities of coarse- and fine-grained lithologic end members; Faunt and others, 2009b). Reductions in vertical hydraulic conductivity and storage properties were required for some confined zones and scaled increases in these properties were required for certain unconfined zones. Horizontal hydraulic conductivities (represented by the hydraulic conductivity of the subregional facies) were increased during model parameter estimation in many of the hydrogeologic units. Specific yield was assigned to each upper active cell. During calibration, a multiplier was used for each zone to determine the final range in specific yield. Specific yield values ranged from a maximum 0.14 for the shallow aquifer to 0.05 for the basement aquifer (table 4).

### *Horizontal-Flow Barrier Parameters*

The model cells represented by the horizontal flow barrier package were combined by faults and fault groups into six parameter groups that have hydraulic characteristics specified as adjustable parameters. The characteristic values are used to rescale the model-cell face row and column conductances between the adjacent model cells that are coincident with the trace of the barrier. In addition, the faults were combined into groups first based on their assigned recency of faulting (youngest age of faulted units) and then grouped based on orientation of faulting. Based on their tectonic setting, the north-south trending faults were assumed to be a barrier with lower characteristic values; computer-assisted and manual parameter estimation confirmed relatively low parameter values (Henson and others, 2025). Fault conductances were initially model-estimated parameters, but ultimately were specified at low values that were held constant for final calibration. These low conductances are consistent with discontinuities observed in groundwater levels of selected wells in the Langley Area groundwater subbasin.

### *Regional Groundwater Flow and Seawater Coastal Inflow Parameters*

The conductance factors in the GHB package, which simulated regional groundwater flow, were specified in groups of model cells and were manually adjusted as constant values within each group of boundary cells (fig. 25). These GHB conductance values controlled the small inflows to and from the Pajaro River groundwater basin in the northwest corner of the integrated hydrologic model domain and underflow in the aquifer beneath the Salinas River from the Paso Robles Area groundwater subbasin in the southeast part of the model domain. These GHB conductance values range from 1.9 to 552 square feet per day (ft<sup>2</sup>/d) near the Pajaro River groundwater basin (WBS 6) and are 535 ft<sup>2</sup>/d near the Paso Robles Area groundwater subbasin

(WBS 29). For seawater coastal inflow, the general head boundaries represent vertical boundaries instead of horizontal boundaries. Therefore, conductance values for the seawater coastal inflow GHB have a larger magnitude because the cross-sectional areas they represent at the boundary are different. The offshore GHB conductance values range from 596 to 6,590 ft<sup>2</sup>/d.

#### *Single and Multiple-Aquifer Well Parameters*

The flowrate to each single and multiple-aquifer well from each aquifer depends on aquifer properties, including hydraulic head. This flowrate is restricted by flow through the well screen and the narrow zone of formation damage that was created during the well drilling process. This zone of restriction is collectively known as the skin, and the hydraulic conductivity of the skin is selected as the only adjustable parameter for multiple-aquifer wells. The skin factor affects the interlayer flow that occurs as wellbore flow and related vertical water-level difference between model layers. Eighteen skin factors were used as parameters to control the delay of wellbore flow within all layers screened for all multiple-aquifer wells (table 8). Wells were assigned skin-factor parameters based on whether they were constructed before 1960 (old) or after 1960 (new) and have casing diameters less than or equal to 5 inches (small) or greater than 5 inches (large). This resulted in five parameter groups. The calibrated values of these parameters were relatively large in order to maintain the observed vertical head differences and to control wellbore flow between layers. The final calibrated skin factors ranged from 25.3 to 40 feet per day (ft/d) for the older, small-diameter wells and from 10.3 to 89.5 ft/d for the newer, large-diameter wells.

### *Surface-Water Network and Drain Return Flow Parameters*

For the surface-water drainage network infrastructure, all channel geometry parameters were held constant, and the only adjustable parameter is the vertical hydraulic conductivity of the bed material. This conductivity controls the leakage rate to or from the surface water feature, which, in turn, controls artificial recharge, shallow groundwater heads, and conveyance of water throughout the network. Stream, canal, drain, and arroyo segments were combined into groups with similar channel properties, yielding 26 adjustable parameters for streambed hydraulic conductivity (Henson and others, 2025). Natural stream channels were separated into groups representing the Salinas River and its tributaries or adjacent surface water drainage networks within the model domain. This resulted in 26 groups of multiple segments that span 524 segments. The parameter grouping of segments within the Salinas River was based on the general distributions of gains and losses estimated from seepage runs. The parameterization of the Salinas River streambed was subdivided into four parameter groups representing the upper middle, lower, and tidal portions of the valley. The final distribution of parameter groups of streambed vertical hydraulic conductivities for the calibrated values ranges from 0.0001 ft/d at the coast in the Pressure analysis region of the Salinas River to as much as 11.34 ft/d along some tributaries in the East Side-Langley analysis region (Henson and others, 2025). For the DRT input, drain conductances were specified for each drain type: riparian was 1,180 ft<sup>2</sup>/d, tributary was 3,780 ft<sup>2</sup>/d, and land surface was 3,390 ft<sup>2</sup>/d.

### Parameter Sensitivity Analysis

Computer-assisted parameter-estimation techniques using PEST-HP (Doherty and Hunt, 2010; Doherty, 2024) were primarily used to estimate selected model parameters and related

sensitivities, but additional insight was provided by trial-and-error analyses. PEST-HP computes the sensitivity of simulated values to changes in model parameters at the locations of measurements. Sensitive parameters were identified (fig. 31), which helped guide which parameters were adjusted during the parameter estimation process (Hill and others, 2000). The measure of parameter sensitivity used to remove insensitive parameters was composite scaled sensitivities (Hill and Tiedeman, 2007). Composite scaled sensitivities indicate the information content of all the observations for the estimation of a parameter and provide insight into parameter importance and sensitivity.

The most sensitive parameter was the power law exponent for distributing the texture distribution within layer 7 in the Pressure and Forebay analysis regions. This is the aquifer that is closest to the surface in the Upper Valley analysis region (fig. 22A), so the textural distribution where layer 7 is deeper may be important for transmission of recharge in the Upper Valley analysis region toward the coast in deeper aquifers. The next set of important parameters were the climate scale factors that represent seasonal stress adjustments for  $K_c$  values. An additional sensitive parameter was the streambed conductance in the Upper Valley analysis region between the USGS 11150500 and USGS 11151700 gages, where substantial stream leakage has been documented (fig. 21; MCWRA, 1995). Similarly, the sensitivity of the streambed conductance between the USGS 11151700 and USGS 11152300 gages was substantial for the same reasons. Other sensitive parameters include hydraulic conductivity ( $kc_{ly1}$ ,  $11hkpressure$ ), specific storage ( $11ss$ ), and specific yield ( $sy_{ly1c}$ ) of the shallow aquifer. The sensitivity of the parameters that govern (1) recharge and storage in the shallow aquifer, (2) streambed conductance, and (3) climate factors that influence agricultural demand simulation is to be expected given that the primary recharge to the aquifer from precipitation and agricultural return

flows are influenced by storage and hydraulic conductivity of layer 1 and the Salinas River and agricultural demands are such a substantial portion of the total water demand.

## History Matching Results

The ability of the integrated hydrologic models to simulate the hydrologic system was evaluated based on comparisons of historical model results to spatially and temporally distributed observations of groundwater levels, surface-water flows, diversions, and observed pumpage throughout the integrated hydrologic model domain. These comparisons were used to assess the capacity of the historical model to simulate effects of changing inflows and outflows on the hydrologic system. The goodness of fit between observed values and their simulated equivalents was evaluated using (1) correlation plots, (2) matching groups of hydrographs for subregions and model layers, (3) mean residuals (or the average of the differences between the simulated equivalent values and observation values), (4) minimal root mean square errors (RMSE; Anderson and Woessner, 1992), (5) scaled RMSE (or RMSE divided by observation maxima minus minima), and (6) the Nash-Sutcliffe model efficiency (NSME) statistic (Nash and Sutcliffe, 1970; Markstrom and others, 2008), which is a standardized mean squared-error statistic varying between 0 and 1. An NSME value greater than 0.5 indicates the model provides a better match to the observed streamflow values than the mean of the observed streamflow values (Nash and Sutcliffe, 1970). The closer the NSME is to 1.0, the better the match is between simulated and observed values, with a value of 1.0 indicating a perfect match. The NSME is not evaluated for evaluation of groundwater level history matching. Additionally, the correspondence between simulated groundwater levels and MCWRA estimated groundwater-level contours for the shallow and deep aquifers (MCWRA, 2005, 2018; Henson and others, 2023) was evaluated by visual inspection. The groundwater-level maps were used for qualitative

comparisons. However, these maps were considered less reliable than time-series data because the composite water-level measurements and manually drawn contour lines represent various combinations of depth- and time-averaged conditions.

The parameter estimation focuses on minimizing the absolute value of the mean residual, RMSE, and scaled RMSE and maximizing the NSME value for hydrologic flow observations. Some observations are challenging to simulate in regional-scale models, especially when they represent intermittent extreme values. The simulated equivalent values for these extreme observed values can be biased low due to limitations of model formulation and temporal and spatial averaging. Many observations developed for parameter estimation and history matching aggregate daily observed values to monthly averages or resolve measurements at point-scale spatial units (for example, streamgages) to the model discretization (for example, stream reaches). The overall history matching is evaluated using the mean residual, RMSE, and normalized RMSE that is less sensitive to singular observations. The NSME is sensitive to high flows as noted by Krause and others (2005). Therefore, if observed values and their simulated equivalents have substantial range or if the magnitude of simulated equivalent values for extreme values is biased low, then the NSME values can be low. Therefore, the model performance for groups of hydrologic flow observations with extreme high and low values (such as stream differences) that have low NSME values are evaluated using the mean residual, RMSE, and normalized RMSE.

### Streamflow

Correlation plots show good correspondence among observed and simulated equivalent streamflow values (fig. 32A) across the range of highly variable streamflows within the Salinas

Valley. There is more spread around the 1:1 line for high peak streamflows. Figures 32B–G show observed and simulated equivalent flows at selected observation gages of the Salinas River and its major tributary Arroyo Seco. Streamflow differences for four pairs of gages are shown in figures 32H–K. These hydrographs illustrate a reasonable match of streamflows through time within the region from the uppermost to lowermost gage in the system. Monthly peak streamflows are well characterized but low flows are commonly overestimated. This effect of low flow overestimation increases downstream along the Salinas River due to accumulation of simulation error.

**Figure 32.** Observed and simulated equivalent streamflow hydrographs for selected river gages and diversions within the Salinas Valley Integrated Hydrologic Model domain for water years 1968 to 2018. A) Correlation among simulated and observed streamflows for all stream observations. Simulated and observed streamflow at B) USGS 11150500, C) USGS 11151700, D) USGS 11152300, E) USGS 11152500, F) USGS 11152000, and G) USGS 11152050 gages. Simulated and observed stream difference for H) USGS 11150500 – USGS 11151700, I) USGS 11151700 – USGS 11152300, J) USGS 11152300 – USGS 11152500, and K) USGS 11152000 – USGS 11152050. Simulated and observed diversions from L) Arroyo Seco for Clark Colony and M) Salinas River at the Salinas River Diversion Facility (Henson and Culling, 2025).

Streamflow hydrographs indicate a good visual fit of monthly observed values and their simulated equivalents (figs. 32B–K) such that the absolute value of all mean residuals is less than or equal to 81 ft<sup>3</sup>/s, RMSE is less than or equal to 437 ft<sup>3</sup>/s, scaled RMSE is less than or equal to 5 percent, and NMSE values are greater than or equal to 0.87 (table 7). Streamflow difference plots (figs. 32H–K) show a good visual fit of observed values and their simulated equivalents, such that the absolute value of all mean residuals is less than or equal to 48 ft<sup>3</sup>/s, RMSE is less



than or equal to 238 ft<sup>3</sup>/s, and scaled RMSE is less than or equal to 8 percent (table 7). The NMSE values for streamflow differences are lower (less than 0.5) because of the effect of extreme values that are not simulated well by the model. Stream differences are challenging to match because errors propagate downstream, leading to even larger differences in USGS gages lower in the Salinas Valley. Also, stream gains and losses can be influenced by localized runoff or withdrawal from shallow wells adjacent to the river that may not be represented by the model.

**Table 7.** Summary of streamflow history matching showing streamflow statistics for the period from 1970 to 2018, mean residual streamflow computed as observed minus the simulated equivalent value, root mean squared error, scaled root mean square error, and Nash-Sutcliffe model efficiency for U.S. Geological Survey gages and diversions in the Salinas Valley Integrated Hydrologic Model.

Diversions are well matched where inflow data to the channel are sufficiently accurate. The historical model has a good visual fit for diversions at Clark Colony (fig. 32L); the mean residual is 3 ft<sup>3</sup>/s, RMSE is 8 units, scaled RMSE is 13 percent, and NMSE is 0.52. The higher scaled RMSE and lower NSME are because Clark Colony diversions were estimated, and the estimated diversion values are commonly higher than the observed flow in the upgradient channel at USGS 11152000. Nonetheless, the low mean residual and RMSE for Clark Colony diversions imply that the diversion is reasonably represented even though the estimated diversions were typically higher than the available flow. Diversions at the SRDF (fig. 27H) are well matched, with a mean residual and RMSE less than 1 ft<sup>3</sup>/s, scaled RMSE of about 2 percent, and NMSE equal to 0.99. This indicates that the FMP is computing the full amount of the surface diversions used to meet demands at CSIP. Overall, these results indicate that the surface-water flow system is well represented in the integrated hydrologic model.

## Groundwater

### *Groundwater Levels*

Hydrographs that show both simulated and observed heads for selected wells help to illustrate the match of groundwater levels throughout the model subareas of the historical model. An analysis well subset of hydrographs for 10 wells (fig. 33) were selected as representative due to their long period of record, regular measurements, and representation of the important aquifers in each region. Table 9 summarizes the hydrogeologic units and model layers for each well in the analysis well subset. Analysis wells were selected in each analysis region to evaluate the 180-Foot Aquifer, 400-Foot Aquifer, and deeper hydrogeologic units (Paso Robles Formation, Purisima Formation, and basement). The four wells selected in the Pressure analysis region represent hydrogeologic units of the 180-Foot Aquifer (CSI239 and ZPN1529) and the 400-Foot Aquifer (ZPN441 and CSI239). The hydrographs for the East Side-Langley analysis region represent the composite of the 180-Foot Aquifer, 400-Foot Aquifer, and Paso Robles Formation hydrogeologic units (ZES871 and ZES1572). The hydrographs for the Forebay analysis region represent the 400-Foot Aquifer hydrogeologic unit (ZFS1001) and the composite Paso Robles Formation and Purisima Formation hydrogeologic units (ZNE1267). The hydrographs for the Upper Valley analysis region represent the Purisima Formation hydrogeologic unit (ZSE355 and ZSE733). The hydrographs for all observation wells can be obtained in the head observation output file in the model archive (Henson and Culling, 2025).

**Figure 33.** Groundwater observations and simulated equivalent values from the Salinas Valley Integrated Hydrologic Model. A) Graph of correlation among groundwater-level measurements and simulated equivalent groundwater-level hydrographs for selected wells. Hydrographs are shown for wells B) CSI239, C) BDA331, D) ZPN1529, and E) ZPN441 in the Pressure analysis region; wells F) ZES1572 and G)

ZES871 in the East Side-Langley analysis region; wells H) ZNE1267 and I) ZSE355 in the Forebay analysis region; and wells J) ZSE355 and K) ZSE733 in the Upper Valley analysis region (Henson and Culling, 2025).

**Table 8.** Summary of selected observation wells used to illustrate Salinas Valley Integrated Hydrologic Model history matching, indicating number of observations, representative model layers, hydrogeologic units, mean residual computed as observed minus the simulated equivalent value, and root mean square error.

**Table 9.** Summary of groundwater level history matching showing drawdown mean residual (computed as observed minus the simulated equivalent value), root mean square error, and scaled root mean square error for the Salinas Valley integrated hydrologic model domain and analysis regions.

Correlation plots (fig. 33A) and examples of hydrographs from the East Side-Langley, Pressure, Forebay, and Upper Valley analysis regions (figs. 33B–K) are used to illustrate the temporal fit of groundwater-level observations and their simulated equivalents. The observed and simulated equivalent groundwater-level correlation is good across the range of groundwater levels (fig. 33A). The monthly to interannual fluctuations in observed groundwater levels indicate the influence of groundwater pumping, followed by climate variability (figs. 33B–K) and streamflow infiltration (for example, wells CSI239, ZPN1529, and ZSE733 near the Salinas River). Even though there are places where the groundwater levels are over- or underpredicted, the change in groundwater levels from the first measurement in each observation well (drawdown) have low mean residuals (tables 8, 9).

Groundwater levels and drawdowns generally show good agreement between observed and simulated equivalent values. There are some areas of the Forebay analysis region where groundwater levels are overpredicted by about 10 ft (fig. 33I) and in the Upper Valley analysis

region they are overpredicted by 20 ft (fig. 33K). The absolute value of the mean residual for all drawdown observations is less than 1 ft, with a RMSE of 15 ft and a scaled RMSE of 6 percent. There are drawdowns in the Pressure analysis region that are underpredicted by approximately 19 ft (fig. 33C, table 8) or 21 ft (fig. 33D, table 8) or overpredicted by 6 ft (fig. 33B, table 8) or less than 1 ft (fig. 33E, table 8). This under- or overprediction of mean drawdowns is influenced by the capability of the model to simulate the seasonal oscillations in these observation wells where pumping is occurring at unknown rates. The magnitude of seasonal oscillations in some wells were not matched everywhere. For example, seasonal oscillations in groundwater levels in the East Side-Langley analysis region are commonly 40 ft or more (fig. 33F). This effect results in the spread of simulated and observed groundwater levels across the 1:1 correlation line in the correlation plot (fig. 33A). This poor representation of seasonal oscillations is likely because 340 of the 439 observation wells are also agricultural supply wells and pumping rates in the models are not simulated using time series from individual well owners. The aim of this study was to represent subregional water demands rather than individual well reported withdrawals. The differences between simulated and observed seasonal oscillations are caused by using subregional distributed pumping rates to replicate the pumpage rates applied to each well. Observations that were assumed to be “pumping influenced” were delineated to help focus the parameter estimation and analysis. Pumping occurs year-round so the assumptions for pumping influence did not capture all wells where large oscillations due to pumping can be observed. The effects of pumping and oscillations are still observed in some wells, especially in the Pressure and East Side-Langley analysis regions (fig. 33A). The effect of this difference between observed and simulated can be observed in hydrographs that have multiple measurements per year (figs. 33B, 33C, 33G, and 33J). Many of these wells are in the Pressure and East Side-

Langley analysis regions, where mean residual drawdowns are low (from 1 ft to -1 ft, respectively) and RMSE values (15 ft and 18 ft, respectively; table 9) are higher in these regions. Nonetheless, the scaled RMSE for the Pressure and East Side-Langley analysis regions are 8 and 7 percent, respectively. Mean residual drawdowns in the Forebay analysis region were -3 ft with a RMSE of 10 ft and scaled RMSE of 9 percent. Mean residual drawdowns in the Upper Valley analysis region were 1 ft with a RMSE of 7 ft and a scaled RMSE of 13 percent. The scaled RMSE is higher here because there are fewer wells in this region that have known properties added to the integrated hydrologic models. Thus, all observation wells in the Upper Valley analysis region were specified as agricultural supply wells with pumping rates specified on analysis region demands that are likely to be different from pumping time series applied at those wells. The specification of simultaneous pumping and observation wells was unavoidable as there are fewer reported supply wells in the Upper Valley analysis region (figs. 24A, 24B) among which to distribute estimated agricultural demands. This resulted in oscillations in some wells that differ from measured values.

Model results in early time periods are sensitive to estimates of initial conditions. Although the rates of decline and the elevations are like those in historical records, some of the temporal changes are not reflected in the simulated values. The magnitude of substantial drawdowns and subsequent recovery in the dry period from WY 1984 to 1994 is not captured in some wells (for example, figs. 33F-H). This could be due to an interaction between the time of the groundwater level measurement and residual pumping effects of the observation well and adjacent wells. Other places where simulated and observed groundwater levels diverge could be a function of changes in actual land use or irrigation practices that are not well represented in the available land use data, variability in Kc values that estimate crop demands, and divergence

between the rates of actual groundwater pumpage at a specific well and the wells simulating groundwater pumpage. Although there are some places where seasonal oscillations are not well matched, or drawdowns are well matched and groundwater levels are elevated or depressed, overall historical model results show reasonable correspondence among simulated and observed groundwater levels throughout the integrated hydrologic model domain.

Groundwater observation well mean residuals also show reasonable correspondence across all analysis regions (fig. 34); 77 percent of observation wells have mean residual drawdowns of -30 to 30 ft and 56 percent of wells have mean residual drawdowns between -15 and 15 ft. These residuals are substantially influenced by the aforementioned challenges in representing seasonal oscillations in observations wells that are also pumping wells. In the Langley Area groundwater subbasin of the East Side-Langley analysis region, some water levels are not well matched but several faults in the groundwater basin here cause water level offsets of more than 100 ft in adjacent wells. There are three isolated wells in this area that have absolute mean drawdown residuals greater than 50 ft (fig. 34), indicating that the model residual bias is limited spatially.

**Figure 34.** Mean residuals computed as the difference between observed and simulated equivalent values in the Salinas Valley Integrated Hydrologic Model for all observation wells for the parameter estimation period from water year 1968 through 2014 (Henson and Culling, 2025).

### *Groundwater-Level Maps*

To allow for a spatial comparison of the simulated historical model values to observed data, groundwater-level maps were developed for fall of 1994, 2003, and 2011 (fig. 35A-F). The observed data in these plots are contours generated by MCWRA for a composite of shallow aquifers (depth less than 201 ft) and deep aquifers (depth greater than 201 ft and less than 420

ft). The shallow contours from the historical model are approximated using the December simulated equivalent groundwater levels in the 180-Foot Aquifer (model layer 3). The deep contours from the historical model are approximated by the December simulated equivalent groundwater levels in the 400-Foot Aquifer (model layer 5). These maps were used during historical model parameter estimation to provide additional information on the effects of internal flow boundaries along faults and to help adjust selected model hydraulic properties, such as vertical hydraulic conductivities.

**Figure 35.** Historical model groundwater contours in Salinas Valley, California developed from simulated equivalent December groundwater levels to Monterey County Water Resource Agency (MCWRA) fall composite contoured groundwater levels. The shallow aquifer composite contour map was computed by MCWRA using measurements in aquifers that are less than 200 feet deep. The shallow contours are compared to groundwater level contours from model cells within the 180-Foot Aquifer hydrogeologic unit (layer 3). The deep aquifer composite contour map was computed by MCWRA using measurements greater than 200 but less than 420 feet deep. The deep contours are compared to groundwater level contours from model cells within the 400-Foot Aquifer hydrogeologic unit (layer 5). These maps show A) shallow aquifer composite contours and simulated equivalent contours in fall of 1994, B) deep aquifer composite contours and simulated equivalent contours in fall 1994, C) shallow aquifer composite contours and simulated equivalent contours in fall of 2003, D) deep aquifer composite contours and simulated equivalent contours in fall 2003, and E) shallow aquifer composite contours and simulated equivalent contours in fall 2011, and F) deep aquifer composite contours and simulated equivalent contours in fall 2011.

The MCWRA and simulated groundwater level contour maps show good correspondence among the shallow and deep aquifers in 1994, 2003, and 2011 (fig. 35). The simulated

groundwater levels have similar areas of over- and underprediction, as described in the “Groundwater Levels” section. The historical model data and contours both show that water level declines are concentrated in the Pressure and East Side-Langley analysis regions and increase in magnitude toward the city of Salinas. Additional declines in groundwater levels are observed in the East Side-Langley analysis region through time. Simulated groundwater levels in 1994, 2003, and 2011 overestimate the MCWRA contours in the Upper Valley analysis region of the historical model by about 20–30 ft, where additional refinement of aquifer properties, land use, or recharge may be required.

### Agricultural Pumpage

The reported monthly agricultural pumpage was aggregated by WBS, resulting in 3,630 observations spanning the period from November 1994 through December 2014 that were compared to FMP simulated equivalent agricultural pumpage values during calibration. Prior to November 1994 when monthly agricultural pumpage observations were not available, simulated equivalent annual agricultural pumpage was compared to published long-term estimates. The historical model matches the total reported annual agricultural pumpage from November 1994 through September 2018 for Salinas Valley within 99 percent and has general agreement among monthly reported and simulated agricultural pumpage throughout the model domain (fig. 36A–E). Simulated equivalent annual agricultural pumpage varies from year to year with an average of approximately 470 TAFY for the period between 1970 and 1994. This value is consistent with prior modeling efforts (Montgomery Watson, 1997) and MCWRA reports (MCWRA, 1995). After November 1994, annual reported agricultural pumpage has varied from 380 TAFY in 2001 to as much as 529 TAFY in 1997, with an average of 439 TAFY (fig. 36B). The annual mean residual (annual reported pumpage minus simulated equivalent annual pumpage) for the history



matching period (WY 1995 to 2014) was  $-4.3$  TAFY which is approximately 1 percent of the mean annual pumpage. There is reasonable correspondence among monthly simulated equivalent and reported agricultural pumpage (fig. 36A). The monthly reported and simulated equivalent agricultural pumpage for each analysis region for the entire simulation with reported observations is shown in figures 36C–G. The absolute value of all monthly mean residuals for the entire integrated hydrologic model domain and the analysis regions is less than or equal to 181 acre-feet, with RMSE less than 1,350 acre-feet and all scaled RMSE less than 9 percent (table 10). Approximately 73 percent of all simulated equivalent monthly agricultural pumping is within 700 acre-feet of the reported monthly values. The close correspondence of reported and simulated equivalent annual total pumpage indicates that monthly errors tend to cancel themselves out over the growing season. There is reasonable correspondence between simulated and observed pumpage among areas in analysis regions exclusively irrigated by groundwater (East Side-Langley and Upper Valley analysis regions; figs. 36D and 36F, respectively) and among areas that have irrigation from surface water diversions and recycled water deliveries (Pressure and Forebay analysis regions; figs. 36C and 36E, respectively).

**Figure 36.** Reported and simulated equivalent agricultural pumpage within the Salinas Valley Integrated Hydrologic Model. A) Correlation among monthly reported and simulated equivalent groundwater pumpage. Time series of monthly observed and simulated equivalent farm deliveries for the B) Pressure analysis region, C) East Side-Langley analysis region, D) Forebay analysis region, and E) Upper Valley analysis region. Times series of annual observed and simulated equivalent pumpage for F) entire integrated hydrologic model domain, G) Pressure analysis region, H) East Side-Langley analysis region, I) Forebay analysis region, and J) Upper Valley analysis region (Henson and others, 2023; Henson and Culling, 2025).

**Table 10.** Summary of monthly agricultural pumpage history matching by analysis region showing mean residual computed as observed minus the simulated equivalent value, root mean square error, and scaled root mean square error for the integrated hydrologic model domain.

### **Hydrologic Flow Budgets—Salinas Valley Integrated Hydrologic Model**

The natural and man-made inflows and outflows in the hydrologic budgets represent the supply and demand components of water use and variability of groundwater and surface water in the Salinas Valley. The historical model simulation of the conjunctive use and movement of water in Salinas Valley shows cyclic storage depletion that is driven by reduced supply during dry periods combined with sustained and increased agriculture and related demand for water. Although periodic events of recharge occur from natural climate cycles, the recent and historical sustained demand for water exceeds the long-term replenishment rate associated with quasi-periodic climate cycles. The historical model results confirm that overdraft conditions have periodically occurred since the onset of increased groundwater development in the 1960s through the end of the historical simulation period (2018) and are related to periodic dry periods and increased agricultural production. The historical model results indicate a level of pumpage that is consistent with estimates from the selected years of reported total annual agricultural increase in water demand with increased agricultural development. The periodic groundwater storage depletion is predominantly the result of cycles of storage depletion in the 180-Foot, 400-Foot, and deeper Paso Robles Formation, Purisima Formation, and basement aquifers. Annual landscape and groundwater budgets were computed for the entire model domain and for each of the five analysis regions along with a summary of groundwater budgets for the entire domain and all analysis regions.

## Analysis Periods

The groundwater budgets for the study are evaluated over five periods: the entire simulation after the model spin-up period (1970–2018) and four analysis periods when changes throughout the Salinas Valley have occurred (fig. 37). The periods examine changes in groundwater budgets due to land use change, dry periods, and development of water supply projects. The first analysis period (A) is a period of land use change from WY 1970 through 1983 where changes in cropping practices such as multi-cropping and development of vineyards occurred. In analysis period A, there were 3 dry years, 7 normal years, and 4 wet years. During this period, land use within the Salinas Valley started to shift toward more quick-duration water-intensive crops, such as lettuce and herbs. Over 20 years, a steep increase in harvested acres of vineyards, leafy commodity crops such as lettuce and broccoli, and quick herb crops is observed (fig. 7). This resulted in increased demands and associated groundwater pumping through this period (fig. 36). This transition in agricultural commodities continued through analysis period B. This second analysis period (B) is a historical dry period from WY 1984 through 1994. In analysis period B, there were 5 dry years, 4 normal years, and only 2 wet years. Of the 5 dry years, four are the driest consecutive years on record, resulting in the most severe dry period during the simulation period. The third analysis period (C) is a relatively wet period of aquifer recovery with groundwater pumpage reporting and development of a new recycled water supply for CSIP. Analysis period C had 1 dry year, 10 normal years, and 4 wet years. During this period, several initiatives began to encourage better data collection and water use reporting. Monitoring networks were expanded; 19 monitoring wells were added in 1993 alone. The Groundwater Extraction Management System was established, and growers and urban communities began to report monthly water usage. Agricultural irrigation efficiency

improvements and urban conservation efforts were implemented, leading to reductions in agricultural groundwater pumpage from the year 1998 onward and reductions in M & I pumpage from 2004 onward (fig. 14). Conversion of a larger area to drip or low flow irrigation systems increased agricultural efficiency (Edinger-Marshall and Letey, 1997; Orang and others, 2008; Sandoval-Solis and others, 2013; Tindula and others, 2013). The fourth analysis period (D) is a relatively dry period from WY 2010 through 2018 where further implementation of the SVWP increased reservoir storage and the SRDF was developed to deliver Salinas River diversions to CSIP. Accordingly, groundwater budget analysis of period D can provide insight into the effect of the recent developments of the SVWP on groundwater resources. Analysis period D is the driest period of them all (66 percent of the time), with 6 dry years, 1 normal year, and 2 wet years. Five of the 6 dry years occurred during the last 5 years of the model simulation period, 2014–18, resulting in another dry period. Observation data after 1994 were much more frequent and comprehensive for water level measurements, M & I pumpage, agricultural pumpage, and land use. Thus, there is more confidence in the budgets of the two most recent analysis periods after 1994 (analysis periods C and D) (fig. 37).

**Figure 37.** Four hydrologic budget analysis subperiods in the study that is informed by the cumulative departure of precipitation at Cooperative Observer Network stations for the Salinas Airport (USW00023233) and King City (USC00044555), California. The subperiods represent A) the start of land use conversion to more multi-cropping, 1970–1983; B) historical dry period, 1984–1994; C) start of reported withdrawal data collection with relatively wetter conditions, 1995–2009; and D) initiation and operation of the Salinas River Diversion Facility and recent recycled water deliveries, 2010–2018.

## Salinas Valley Landscape Budget

The landscape is a specific area of the land surface (except for stream channels) that is modeled as a container different from the groundwater system for which we estimate a water budget with inflows and outflows. This landscape budget includes items of interest that are represented as net flows in the groundwater budgets, such as volumes associated with components of evapotranspiration and runoff to streams. Landscape budgets are computed in this study to support analyses of landscape water demands and supplies and to assess the effects of changes in land use, climate, and water management. Landscape budgets are presented for the entire integrated hydrologic model domain and the analysis regions using bar charts showing the inflows and outflows.

### Landscape Budget Components

No water storage is considered in the landscape budget. Streams exist within the landscape; however, stream inflows and outflows are counted in the surface water budget. Groundwater entering and exiting streams (gains and losses) also is not accounted for in the landscape budget (to avoid double counting with the groundwater budget). Runoff here is defined as overland runoff that goes into streams and thus out of the reference landscape area. Pumpage and surface water diversions are taken from groundwater and streams (outside of the container) and flow into the container. Deep percolation flows out of the container and into groundwater. Instead, the landscape budget represents the flows into and out of the landscape throughout the historical model. Inflows to the landscape are precipitation, shallow groundwater, agricultural pumpage, surface water diversions, and recycled water. Outflows from the landscape are evapotranspiration of precipitation, groundwater, irrigation, deep percolation to groundwater,

and runoff to streams. Irrigation TDR to meet agricultural demands is represented by the sum of agricultural pumpage, recycled water deliveries, and surface water deliveries in figure 38. The TDR analysis allows for evaluation of the landscape components that support deliveries to meet agricultural demands.

**Figure 38.** Distribution of landscape-budget inflow and outflow components for the Salinas Valley Integrated Hydrologic Model for water years 1970 to 2018 showing the A) entire integrated hydrologic model domain, B) Riparian analysis region, C) Pressure analysis region, D) East Side-Langley analysis region, E) Forebay analysis region, and F) Upper Valley analysis region (Henson and Culling, 2025).

### Climate Variability

The temporal distribution of inflows and outflows to the landscape and surface-water systems indicates a strong climatic influence with higher values overall in wet periods. Overall, precipitation aligns with reported data. However, 2013 shows lower precipitation than expected given that it was a normal climate year. This is likely an anomaly in the estimated climate data. The watershed inflows and other surface water flows align with historical records and are consistent with periods before and after 2013. The climate year type that is used for reservoir operations (based on surface water flow percentiles as described in the “Climate” subsection of the “Description of Study Area” section) is not always aligned with observed climate within the basin. This is especially true for normal and dry climate year types; for example, 1984 (normal) and 1988 (dry) have similar precipitation magnitudes for the entire integrated hydrologic model domain (fig. 38A). There is also subregional inconsistency where the climate year type does not align with analysis region conditions; for example, 1984 precipitation in the Pressure analysis region is less than the 1988 precipitation (fig. 38C). Generally, runoff is higher in normal and wet years than dry years. However, substantial runoff can occur in dry years from inefficient

irrigation. Analysis of landscape budgets among all analysis regions show similar trends with the entire basin (figs. 38B–F), including a strong relationship between climate and TDR with increased pumpage during dry periods.

### Total Delivery Requirement

The influence of climate on TDR is evident in the simulation results. Although some variability does occur among analysis regions, the TDR commonly exceeds precipitation over the entire basin, with 1988–90 and 2007 having annual TDR values more than 1.5 times the precipitation those years. The TDR is greater than 1.5 times precipitation for 15 years in the Pressure analysis region (fig. 38C), 7 years in the East Side-Langley analysis region (fig. 38D), 33 years in the Forebay analysis region (fig. 38E), and 18 years in the Upper Valley analysis region (fig. 38F). This spatial variability in the ratio of precipitation to TDR in each analysis region further illustrates the water management challenges in delivering water to meet demands throughout the basin (California Department of Public Works, 1946). Because local TDR commonly exceeds precipitation, groundwater is used extensively in the basin to meet demands. More instances of years with TDR greater than 1.5 times the precipitation in the analysis regions than the entire integrated hydrologic model domain suggest an interconnected water supply with water demands supported by flows from adjacent areas. Water demands in each analysis region are supported by recharge from precipitation in the uplands outside of the analysis regions (other areas, fig. 15) and potentially underflow from the Riparian analysis region and groundwater subbasins in adjacent analysis regions. This interbasin underflow is evaluated using the groundwater budgets in the next section.

Offsetting groundwater use, surface water deliveries (recycled water deliveries and surface-water diversions) have steadily increased since 1998, reaching nearly 4 percent of the TDR by the end of the simulation period, with a maximum of as much as 23,000 acre-feet in 2013 (fig. 38A). Especially in the Pressure analysis region, the TDR supplied by groundwater has been substantially reduced since 1998 through increases in recycled water deliveries and development of surface water diversions supported by the Salinas Valley Reclamation Project at the SRDF. These new surface water supplies provide a substantial portion of the TDR. The surface water supplies have supported decreases in observed pumpage in the Pressure analysis region.

### Salinas Valley Groundwater Budget

Each groundwater budget treats the subsurface system as a container. The frame of reference for all net flows, storage changes, and outflows in the aquifers is represented by the hydrogeologic units. Groundwater budgets are computed in this study to support analysis of groundwater availability and use and to assess the effects of changes in land use, climate, and water management. Quantifying groundwater budget components and metrics is vital to assessing historical conditions and evaluating the effects that water supply projects (SVWP, SRDF, CSIP) and reservoir operations have on groundwater and surface water availability. Groundwater budgets are presented in three ways for the entire integrated hydrologic model domain and the analysis regions: (1) bar charts showing the inflows and outflows, (2) summary tables with additional metrics that provide average groundwater budget components and metrics for the entire simulation period, the four analysis periods, and for the years with highest and lowest precipitation that occurred before and after the implementation of water supply projects, and (3) average groundwater budget flow charts of inflows, outflows, and storage loss that can



be readily compared to similar plots published for prior analyses (MCWRA, 1995; Montgomery Watson, 1997).

### Groundwater Budget Components

Some items in the groundwater budget bar graphs and summary tables are presented as net values where the sum of inflow and outflow for each budget component are added to compute a net gain or loss. Positive values equal a gain in flow and negative values equal a loss in flow. These net budget components include recharge, stream leakage, interbasin underflow, subbasin underflow, riparian underflow, seawater coastal inflow, and aquifer storage change. Recharge is computed as the difference between direct groundwater uptake by vegetation and the amount of water that percolates into the subsurface. Recharge is generally positive in the groundwater budget but can be negative if groundwater evapotranspiration is greater than the amount of percolation. Stream leakage is the amount of water that infiltrates in all stream segments and is comprised of Salinas River infiltration and other channel infiltration. Interbasin underflow is the onshore flow into the model domain from adjacent groundwater basins outside of the active model domain that is simulated by the inland GHB (fig. 25). Subbasin underflow is the regional groundwater flow to the analysis region within the active model domain. Riparian underflow is the regional groundwater flow to an analysis region from the riparian area. Seawater coastal inflow is landward flow from the ocean simulated at the coastal GHB (fig. 25). Aquifer storage change is the difference between all outflows and inflows. The sign convention for aquifer storage can lead to positive and negative values that are counterintuitive; they are explained in the “Groundwater Budget Bar Plots” section.

The components of outflows in groundwater budgets include surface drainage, riparian drainage, tributary drainage, surface drainage, M & I pumpage, and agricultural pumpage. Surface drainage occurs when groundwater is above the land surface in a model cell that is not associated with a stream. Riparian drainage occurs when groundwater is above the land surface in a model cell in the riparian area. Tributary drainage occurs when groundwater is above the land surface in a model cell that contains a stream segment outside of the Salinas River. Municipal and industrial pumpage is specified using furnished and estimated data (Henson and others, 2023). Agricultural pumpage is simulated to meet demands by FMP. Important groundwater budget components for water managers include total recharge, stream recharge (which is recharge from the surface water drainage network outside of the Salinas River), riparian underflow to each analysis region sourced from recharge in the Salinas River, total pumpage, pumpage-recharge fraction (which is the fraction of analysis region pumping to recharge), aquifer storage change, and groundwater depletion.

### Groundwater Budget Bar Plots

Groundwater budget bar plots (fig. 39) show the volumes of each groundwater budget component. In these plots, aquifer storage change is negative if there are more inflows than outflows. This sign convention for the groundwater budget bar plots ensures that the sum of inflows equals the sum of outflows. In the cumulative storage change line plots for each groundwater budget bar plot and in the groundwater budget summary tables (tables 11–16), the sign for aquifer storage change and cumulative storage change are reversed (multiplied by  $-1$ ) so that the changes in storage are shown as expected, with positive values indicating an increase in storage and negative values indicating a decrease in storage. The cumulative storage curves

plotted on each groundwater budget bar plot show the actual change in groundwater volume starting in 1970.

**Figure 39.** Distribution of groundwater-budget components of inflows and outflows for the flow system of the Salinas Valley Integrated Hydrologic Model for water year 1970 to 2018. A) Entire integrated hydrologic model domain, B) Riparian analysis region, C) Pressure analysis region, D) East Side-Langley analysis region, E) Forebay analysis region, and F) Upper Valley analysis region (Henson and Culling, 2025).

### Groundwater Budget Summary Tables

Groundwater budget summary tables provide quantities of interest averaged over analysis periods and for selected high and low precipitation years. Comparison of quantities of interest over analysis periods and for selected high and low precipitation years allows the evaluation of these quantities under different historical conditions. The quantities of interest distill information from the budgets to inform decision making and sustainability efforts. These quantities of interest include net average groundwater inflows and outflows described in the “Groundwater Budgets Components” section and summarized values such as local stream recharge, total recharge, total pumpage, pumpage-recharge fraction, storage loss, and groundwater depletion. Analyses of recharge, pumping, and groundwater depletion are supported by these summarized quantities of interest.

The local stream recharge is the stream leakage from all other surface water drainage features except the Salinas River minus the sum of riparian and tributary drainage. Total recharge is computed as the sum of components of groundwater recharge, the recharge and stream recharge groundwater budget components. Total pumpage is the sum of M & I and agricultural pumpage. Total recharge, total pumpage, and their ratio (pumpage-recharge fraction)

provide information about drivers of aquifer storage change and local groundwater sustainability. Storage loss is the absolute value of the aquifer storage change groundwater budget component if aquifer storage change is negative. Groundwater depletion is the sum of storage loss and the seawater coastal inflow groundwater budget component. Groundwater depletion is an important quantity for sustainability analyses and to quantify the effect of water management strategies on undesirable effects of unsustainable groundwater use, such as seawater coastal inflow and storage loss.

### Groundwater Budget Flow Charts

The groundwater budget flow charts show the average annual budget components and summarized values for the entire integrated hydrologic model domain and each of the five analysis regions. Each flow chart has defined inflows and outflows and provides a concise view of the groundwater budgets. The groundwater budget terms and summarized values are represented using boxes with arrows that indicate the direction of flow (in or out). This simple view of the budget facilitates an easy comparison to budgets evaluated in prior Salinas Valley analyses.

### Integrated Hydrologic Model Domain Groundwater Budget

The groundwater budget bar plots for the entire integrated hydrologic model domain show pumpage and cycles of wet and dry years with cumulative storage change increasing in period A, decreasing during the dry period (period B), recovering in period C, and declining again in the most recent dry period (period D) (fig. 39A). Groundwater budget analysis for the entire integrated hydrologic model domain (table 11) shows that average aquifer storage changes over the four analysis periods range from 139 TAFY (out) to 158 TAFY (in). There is substantial

variability within the high and low precipitation end-member years before and after the SRDF, with pre-SRDF values ranging from 451 TAFY (out) in 1989 to 214 TAFY (in) in 1983, and post-SRDF values ranging from 275 TAFY (out) in 2013 to 112 TAFY (in) in 2013. The average storage losses were high during dry periods—139 TAFY (out) in analysis period B and 83 TAFY (out) in analysis period D. The driest year in period B (1989) had a substantial storage depletion of 469 TAFY. The driest year in period D (2013) had substantial but lower storage depletion of 275 TAFY. The effects of this depletion can be observed in the lowering of groundwater levels throughout the basin (figs. 33A–E). The lowest recorded measurements of groundwater levels occurred during the dry years of analysis period B. The long-term average groundwater depletion is about 15 TAFY, comprised of mostly seawater coastal inflow. The average seawater coastal inflow varied over the analysis periods and individual years from 12 to 18 TAFY. There are slightly lower average values after the implementation of the SRDF (analysis period D) even though the conditions were dry for much of that analysis period. The magnitude of seawater coastal inflow is higher in years with higher overdraft (fig. 39A), so the cumulative effect of multiple years of overdraft may have a more substantial effect on usable storage of the aquifer than the long-term average implies.

**Table 11.** Summary of groundwater budget data for the entire Salinas Valley Integrated Hydrologic Model domain for the simulation period 1970–2018, analysis periods A–D, and high and low precipitation years representing conditions before and after the Salinas River Diversion Facility was implemented.

Over the entire simulation analysis period, the average total recharge was 597 TAFY, average recharge was 93 TAFY, and average stream recharge was 504 TAFY (table 11 fig. 40A). Total recharge varied from year to year over the individual wet and dry analysis years, ranging from 250 TAFY in 1989 to 913 TAFY in 1983. The average total recharge for analysis periods A

and B (1970–94), 732 and 501 TAFY, respectively, are higher than previous groundwater budget tabulations that were 454 TAFY for the period 1970–92 (MCWRA, 1995; Montgomery Watson, 1997). However, the model domain in this study is about 40 percent larger than the SVIGSM from which that estimate was determined.

**Figure 40.** Average groundwater budget from water year 1970 through 2018 showing budget components (in thousands of acre-feet) for the A) entire Salinas Valley Integrated Hydrologic Model domain, B) Riparian analysis region, C) East Side-Langley analysis region, D) Pressure analysis region, E) Forebay analysis region, and F) Upper Valley analysis region (Henson and Culling, 2025).

#### *Riparian Analysis Region*

The Salinas River is an important source of recharge in the integrated hydrologic model domain. The riparian area of the Salinas River is its own WBS so the regional groundwater flow to adjacent analysis regions is clearly represented. The contribution of the Salinas River recharge to each analysis region is represented by the riparian underflow budget component. The contribution of all other surface water drainage features in each analysis region is represented by the “stream recharge” budget component. The year-by-year groundwater budget is shown in [figure 39B](#) and illustrates substantial contributions from stream leakage and subbasin underflow to adjacent analysis regions. [Table 12](#) provides a summary of the groundwater budget for the Riparian analysis region to support evaluation of annual average groundwater budgets over the period from WY 1970 to 2018 ([fig. 40B](#)).

In the Riparian analysis region, riparian vegetation water demands near streams are greater than deep percolation, resulting in a negative average recharge value among all analysis periods that ranges from 98 to 104 TAFY (out). To prevent confusion caused by the negative

recharge values in discussion of this analysis region, total recharge is assumed to be equal to the sum of recharge, stream leakage, and riparian and tributary drainage. The average annual total recharge is 297 TAFY and ranges from 224 and 356 TAFY among all analysis periods. Subbasin underflow out to adjacent analysis regions is an average of 291 TAFY and varies between 221 and 339 TAFY among the analysis periods (table 12). Total pumpage is less than 14 TAFY, which is approximately 2 percent of the average total pumpage in the basin (tables 11–12). However, this amount of pumpage in the riparian area is based on the defined riparian area of the riparian WBS and reported groundwater use where required. This volume may not represent the total volume of pumpage occurring within or near the riparian area. Aerial imagery indicates there are agricultural fields, wells, and storage ponds near the stream channels with water use that may not be subject to mandatory reporting. However, the pumpage-recharge fraction is still very low in this analysis region. The cumulative groundwater storage change line plot shows increases and decreases in response to wetter and drier analysis periods but minimal groundwater storage depletion overall. Storage loss is low, averaging 5 TAFY, with a minimum average near zero in analysis period A and maximum average of 24 TAFY in the driest analysis period B (table 12). Seawater coastal inflow is relatively consistent (2 TAFY) and is a small portion of the total simulated values for the entire integrated hydrologic model domain.

**Table 12.** Summary of groundwater budget data for the Riparian analysis region for the simulation period 1970–2018, analysis periods A–D, and high and low precipitation years representing conditions before and after the Salinas River Diversion Facility was implemented.

### *Pressure Analysis Region*

The Pressure analysis region is located along the Monterey Bay coast and is a substantial area of agricultural production with several water supply projects, including CSIP and SRDF. The 180-Foot/400-Foot Aquifer groundwater basin represented by this analysis region has had substantial seawater coastal inflow. The year-by-year groundwater budget is shown in figure 39C and illustrates substantial contributions from riparian underflow and agricultural pumpage. Table 13 provides a summary of the groundwater budget for the Pressure analysis region to support evaluation of annual average groundwater budgets over the period from WY 1970 to 2018 (fig. 40C).

Average total recharge for the simulation and all analysis periods ranges from 54 to 94 TAFY, with local stream recharge representing about 30 percent of total recharge. Riparian underflow is a substantial inflow, with averages that range from 76 to 122 TAFY and an average of 105 TAFY over the entire simulation period. The average subbasin underflow to adjacent analysis regions is minimal, with a simulation period average of 11 TAFY (out) that varies between 8 and 14 TAFY (out) among the analysis periods (table 13). The average total pumpage simulation period average is 150 TAFY and varies between 134 and 176 TAFY among all analysis periods. Pressure analysis region average pumpage-recharge fraction for the entire simulation period is 2.1. The maximum average pumpage-recharge fraction among all analysis periods is 2.5 and occurred during the dry years of analysis period B and D. Higher riparian underflow and negative (out) subbasin underflow suggests that riparian underflow and



groundwater storage are used to meet a portion of current pumping demands on an average basis and reductions in Salinas River streamflow may contribute to storage loss. The cumulative groundwater storage change line plot shows an increase in analysis period A, substantial storage loss in analysis period B, recovery in analysis period C, and storage declines in the most recent analysis period D (fig. 39C). Historical storage declines (fig. 39C) are supported by changes in groundwater levels. A steep decline in groundwater levels was observed in response to the dry period B; however, overall average drawdown observations for the region suggest that groundwater levels have recovered (figs. 33B–E) but are still low in the area near the city of Salinas (fig. 35). Average seawater coastal inflow ranges from 10 to 11 TAFY among all analysis periods, with an average of 11 TAFY over the simulation period. Groundwater depletion ranged from 11 to 44 TAFY among all analysis periods, with an average of 11 TAFY over the simulation period (table 13, fig. 40C).

**Table 13.** Summary of groundwater budget data for the Pressure analysis region for the simulation period 1970–2018, analysis periods A–D, and high and low precipitation years representing conditions before and after the Salinas River Diversion Facility was implemented.

#### *East Side-Langley Analysis Region*

The East Side-Langley analysis region is along the northern edge of the integrated hydrologic model on the flanks of the Gabilan Range and relatively disconnected from the Salinas River; thus, it does not receive much riparian underflow (averaging <1 TAFY for the simulation and analysis periods) (table 14). The year-by-year groundwater budget is shown in figure 39C and illustrates substantial contributions from subbasin underflow, recharge, and

agricultural pumpage. Table 14 provides a summary of the groundwater budget for the Eastside-Langley analysis region to support evaluation of annual average groundwater budgets over the period from WY 1970 to 2018 (fig. 40D).

Average total recharge for the simulation and all analysis periods ranges from 34 to 72 TAFY, with local stream recharge representing about 20 to 30 percent of total recharge. Subbasin underflow is a substantial inflow with average values that range from 22 to 23 TAFY with an average of 22 TAFY over the entire simulation period (table 14). The average total pumpage over the simulation period is 83 TAFY and varies between 73 and 99 TAFY among all analysis periods. The average pumpage-recharge fraction for the East Side-Langley analysis region for the entire simulation period is 1.6. The maximum average pumpage-recharge fraction among all analysis periods is 2.1 and occurred during the recent dry years of analysis period D. Low riparian underflow (<1 TAFY) and positive (in) subbasin underflow suggest that subbasin underflow and storage loss are used to meet a portion of current pumping demands on an average basis. This suggests that groundwater budgets may be more influenced by activities in adjacent analysis regions and underscores the role of analysis region connectivity in regional sustainability efforts. The cumulative groundwater storage change line plot shows a moderate increase in analysis period A and substantial storage declines for the rest of the simulation (fig. 39D). Historical storage declines (fig. 39D) are supported by changes in groundwater levels. A steep decline in groundwater levels was observed in response to dry analysis period B and have not recovered since (figs. 33F, 33G). Groundwater depletion ranged from 8 to 26 TAFY among all analysis periods with an average of 9 TAFY over the simulation period (table 14, fig. 40D).

**Table 14.** Summary of groundwater budget data for the East Side-Langley analysis region for the simulation period 1970–2018, analysis periods A–D, and high and low precipitation years representing conditions before and after the Salinas River Diversion Facility was implemented.

#### *Forebay Analysis Region*

The Forebay analysis region is located near the center of the basin. This region receives stream recharge from Arroyo Seco and the Salinas River and represents the transition between where deeper hydrogeologic units (Paso Robles and Purisima Formations) are closer to the surface (fig. 22B) and the 180-Foot Aquifer and 400-Foot Aquifer hydrogeologic units thin or pinch out (figs. 23D, 33E). The year-by-year groundwater budget is shown in figure 39E and illustrates substantial contributions from subbasin underflow, recharge, and agricultural pumpage. Table 15 provides a summary of the groundwater budget for the Forebay analysis region to support evaluation of annual average groundwater budgets over the period from WY 1970 to 2018 (fig. 40E).

Average total recharge for the simulation and all analysis periods ranges from 64 to 106 TAFY, with local stream recharge representing a majority of total recharge. Subbasin underflow is out of the analysis region and not substantial, with average values among analysis periods that range from 4 to 6 TAFY for all analysis periods (table 15). Riparian underflow is a substantial inflow, with average values among analysis periods that range from 82 to 128 TAFY and an average of 110 TAFY over the entire simulation period. The average total pumpage over the simulation period is 155 TAFY and varies between 139 and 170 TAFY among all analysis periods. The average pumpage-recharge fraction for the Forebay analysis region for the entire simulation period is 1.8. The maximum average pumpage-recharge fraction among all analysis periods is 2.4 and occurred during the dry years of recent analysis period D. Higher riparian

underflow and negative (out) subbasin underflow suggests that riparian underflow is used to meet a portion of current pumping demands on an average basis and reductions in Salinas River streamflow may contribute to storage loss. The cumulative groundwater storage change line plot shows an increase in analysis period A, substantial storage loss in analysis period B, recovery in analysis period C, and storage declines in the most recent analysis period D. Historical storage declines and increases (fig. 39E) are supported by changes in groundwater levels. A steep decline in groundwater levels was observed in response to dry period B and have recovered in many areas (figs. 33H, 33I). Groundwater depletion ranged from 27 to 33 TAFY among all analysis periods and averaged less than 1 TAFY over the simulation period (table 15, fig. 40E).

**Table 15.** Summary of groundwater budget data for the Forebay analysis region for the period 1970–2018, analysis periods A–D, and high and low precipitation years representing conditions before and after the Salinas River Diversion Facility was implemented.

#### *Upper Valley Analysis Region*

In the Upper Valley analysis region, deeper hydrogeologic units (Paso Robles and Purisima Formations) are closer to the surface (fig. 22B) and 180-Foot Aquifer and 400-Foot Aquifer hydrogeologic units thin or pinch out (figs. 23D, 23E). Also, the number of known and specified supply and observation wells and groundwater level observations are more limited in the Upper Valley analysis region (table 9). All these factors should be considered in the evaluation of the groundwater budgets. The year-by-year groundwater budget is shown in figure 39F and illustrates substantial contributions from agricultural pumpage, riparian underflow, and recharge. Table 16 provides a summary of the groundwater budget for the Upper Valley analysis region to support evaluation of average groundwater budgets over the period from WY 1970 to 2018 (fig. 40F).

Average total recharge for the simulation and all analysis periods ranges from 32 to 52 TAFY, with local stream recharge representing about 25 percent of total recharge. Subbasin underflow is not substantial, with average values  $>1$  TAFY for the simulation and all analysis periods (table 16). Riparian underflow is a substantial inflow, with average values among analysis periods that range from 61 to 83 TAFY and an average of 74 TAFY over the entire simulation period. The average total pumpage over the simulation period is 97 TAFY, and ranges between 81 and 106 TAFY among all analysis periods. The average pumpage-recharge fraction for the Upper Valley analysis region is 2.3 for the entire simulation period. The maximum average pumpage-recharge fraction among all analysis periods is 3.2 and occurred during the dry years of recent analysis period D. The presence of substantial riparian underflow and minimal subbasin underflow (simulation period average of 4 TAFY) suggests that riparian underflow and groundwater storage are used to meet a portion of current pumping demands on an average basis and reductions in Salinas River streamflow may contribute to storage loss. The cumulative groundwater storage change line plot shows an increase in analysis period A, substantial storage loss in analysis period B, recovery in analysis period C, and storage declines in the most recent analysis period D (fig. 39F). Historical storage declines and increases (fig. 39F) are supported by changes in groundwater levels. A steep decline in groundwater levels was observed in response to the dry period B and have recovered in many areas (figs. 33J, 33K). Groundwater depletion ranged from 20 to 26 TAFY among all analysis periods, with an average of 4 TAFY over the simulation period (table 16, fig. 40F).

**Table 16.** Summary of groundwater budget data for the Upper Valley analysis region for the simulation period 1970–2018, analysis periods A–D, and high and low precipitation years representing conditions before and after the Salinas River Diversion Facility was implemented.

### **Salinas Valley Operational Model**

The Salinas Valley operational model (SVOM) was developed to simulate current projects and reservoir operations for the Lake San Antonio and Lake Nacimiento reservoirs, such as reservoir storage and releases, flood mitigation, and management of Salinas River flows to support habitat conservation, fish passage, and downstream diversions for the SRDF. The operational model is a hypothetical baseline model developed to examine the benefit of different reservoir operations for the availability of water resources. The operational model is only to be used for scenario evaluation under hypothetical conditions that are informed and driven by historical conditions. It is a baseline model that will be used to evaluate how different hypothetical reservoir operation frameworks influence hydrologic flows and budgets.

The notable differences between the integrated hydrologic models (SVIHM and SVOM) are the model time-step length, a few boundary conditions related to the implementation of current projects and land use, and the direct simulation of reservoir inflows to the surface water drainage network. Specifically, the SVOM has (1) the same initial conditions, historical climate, and climate year types as the SVIHM, (2) time steps that range from 5 to 6 days for the temporal discretization instead of bimonthly time steps used in the historical model, (3) constant 2014 land use, (4) current reservoir operational rules for flood management, required ecological flow targets, and downstream demands, (5) operation of SVWP (that includes the SRDF and CSIP) for the entire simulated period, and (6) simulated reservoir releases instead of specified reservoir

releases that are used in the historical model. The properties in the calibrated historical model provide the basis for the operational model.

## Reservoir Release Simulation

The reservoir releases for the operational model are dynamically simulated using the surface water operations capabilities of MF-OWHM (Boyce and others, 2020; Boyce, 2023). The operations model reservoir operation decisions are defined in a set of rules that are based on current reservoir operation rules and legal constraints, allowing for reservoir releases into the surface water drainage network to be simulated internally to account for changes in reservoir storage and reservoir releases for conservation, demands, and flood management. Each rule has a set of logic statements that determine the magnitude and volume of reservoir releases (Henson and others, 2022a). The operational model rules are based on WY condition, as either dry, normal, or wet (based on surface water flow percentiles as described in the “Climate” subsection of the “Description of Study Area” section). Both juvenile and smolt fish passage rules have a year type condition. However, the logic only specifies “dry” and “wet” as a trigger.

To simulate reservoir releases for the operational model, reservoir storage changes are simulated using storage input parameters that describe climate, watershed inflows, and reservoir evaporation (fig. 41). After reservoir storage is computed, conditions for operations are evaluated using operational rule parameters. The reservoir operation rule parameters include streamflow at designated gages, current reservoir storage, and WY type. Reservoir operation rule parameters are evaluated using the operational model rules. For each rule, if conditions are met, a target reservoir release amount is calculated. Each release from both reservoirs is simulated internally to account for changes in reservoir storage and compute reservoir releases for conservation,

demands, and flood mitigation. Within the conservation, demand, and flood mitigation releases, there are several rules that apply: flood release, fish passage, water rights, reservoir release fractions, spillway release thresholds, and the SRDF (table 17). Each rule includes logic statements that evaluate the reservoir operation inputs to determine if the conditions for the rule are met.

**Figure 41.** Salinas Valley Operational Model implementation, showing storage parameters that are used to simulate reservoir storage and operational rule parameters that are used to evaluate operational rules for conservation, demand, and floods to generate a time series of reservoir releases.

The fish passage rules describe flow requirements for managing steelhead (*Oncorhynchus mykiss*) in the Salinas River. The fish passage rules follow the National Marine Fisheries Service Requirements (National Marine Fisheries Service, 2007) across four stages of the steelhead lifecycle: the adult steelhead upstream migration, downstream migration of smolt steelhead, downstream migration of juvenile and post-spawn adult steelhead, and spawning and rearing in freshwater habitats. The adult steelhead upstream migration requires a minimum flow rate at the Salinas River near Chualar (USGS 11152300, fig. 20) for a minimum duration when the river mouth is open to the ocean. The downstream migration of smolt steelhead requires minimum streamflow at various streamflow locations for 10 days or until the lagoon closes to the ocean during normal WY classification. Downstream migration of juvenile and post-spawn adult steelhead flow requires a minimum lagoon streamflow delivery for a specified duration in normal and wet WY classifications and a smaller minimum lagoon delivery flow in dry WY classifications. For spawning and rearing habitat below the Nacimiento Dam, additional reservoir releases are triggered.



**Table 17.** Description of Salinas Valley Operational Model (SVOM) operational rules that define reservoir releases triggered based on flow conditions and downstream water demands.

After the logic of operational rules is evaluated to determine if reservoir releases are triggered, the reservoir releases are calculated to meet the flow requirement. If multiple operational rules are initiated for the same time step, then reservoir releases are computed as the minimum release that attains all operational targets. The streamflow into the channel where reservoir discharges occur is simulated as the sum of flows estimated by the watershed model for the entire simulated period (October 1, 1967, through September 30, 2018) and the reservoir releases from Lakes San Antonio or Nacimiento reservoirs. In the operational model, reservoir releases are dynamically simulated using reservoir data and operational rules. Reservoir releases are not explicitly represented in the historical model (SVIHM). In the historical model, a time series of historical releases is added to the surface water drainage network at the downstream segment from each reservoir as part of the calculated inflow from the watershed model.

### Baseline Reservoir Results

For the operational model (SVOM), reservoir releases are a function of the reservoir storage parameters and the operational rule parameters (fig. 3). Reservoir storage and releases in the operational model are not meant to replicate the historical conditions. The reservoirs were not operated by the rules throughout time. In addition, reservoir operation decisions in the real world are made based on daily assessment of conditions and forecasts. In the operational model, reservoir operation decisions are made based on objective model conditions in the Salinas River based on 5–6 day average flows and monthly mean inflows to the integrated hydrologic model area from Arroyo Seco. However, there is good monthly and annual agreement between

simulated reservoir storage and releases and historical conditions, indicating that the reservoir operations for the operational model are within the reasonable range for operating and are producing flows within the system's capacity (fig. 42; Henson and others, 2023). For reservoir storage, both Lakes Nacimiento and San Antonio follow the monthly and annual patterns of the historical conditions (figs. 42A, 42B). This suggests that the operational model and the associated rules are using the climate and reservoir inputs to simulate reservoir levels within the expected ranges and variations. Reservoir releases for Lake Nacimiento tend to resemble the annual releases more closely for historical conditions than for Lake San Antonio, with the average simulated reservoir releases lower than historical releases (fig. 42C). On average, reservoir releases for Lake San Antonio are higher than historical releases. One reason for these differences is that the reservoir operation rules for the operational model are trying to optimize water storage and releases, which were controlled manually under historical conditions.

**Figure 42.** Salinas Valley Operational Model (SVOM) reservoir observed data (Henson and others, 2023) and simulated equivalent values in Lake San Antonio and Lake Nacimiento reservoirs for A) monthly storage, B) annual mean reservoir storage, and C) total annual mean reservoir releases. Reservoir storage and releases in the SVOM are not intended to replicate historical conditions. The historical time series is shown to illustrate that the SVOM results reasonably reproduce flows and storage within the boundaries of historical conditions (Henson and Culling, 2025).

Trends in reservoir releases differ between the two reservoirs, with Lake Nacimiento releases being overall greater than Lake San Antonio with greater peak releases. Lake Nacimiento releases range from 7 to 649 TAFY. Lake Nacimiento has a higher storage capacity and generally maintains a larger storage volume compared to Lake San Antonio (figs. 42A, 42C, 43B). Lake San Antonio releases range from 2 to 296 TAFY (figs. 42B, 43A). The reservoir

releases and gains and losses along the river network play a key role for determining the total streamflow downstream to meet fish flow requirements. For adult fish, the median days per year that meet flow requirements (overall 51 years of the historical simulation) is 17 days; with an upper quartile of 38 days (75th percentile) and a maximum of 59 days (fig. 43C). For kelt fish, the median days per year that meet flow requirements is 15 days, the upper quartile is 35 days (75th percentile), and the maximum is 81 days (fig. 43C). For smolt fish, the median days per year that meet flow requirements is 15 days, the upper quartile is 36 days (75th percentile), and the maximum is 41 days (fig. 43C). For juvenile fish, flow requirements were met 0 days per year for each year in the historical simulation. When combined reservoir releases and streamflow meet a minimum threshold, the SRDF can divert water. The number of active SRDF days per year ranges from 0 to 42 days, with a median of 42 days per year (fig. 43D).

**Figure 43.** Selected statistics related to reservoir operations describing *A*) total reservoir releases, *B*) mean annual reservoir storage, *C*) simulated days per year where specified streamflow values are met to support phases of steelhead (*Oncorhynchus mykiss*) life cycle, and *D*) total annual number of days the Salinas River Diversion Facility (SRDF) is active. For each box plot, the shaded box represents the interquartile range, where 50 percent of the data occurs within the range. The lower portion of the shaded box represents the 25th to 50th percentile range, and the upper portion represents the 50th to 75th percentile range. The whiskers display the range that is within 1.5 times the interquartile range. All the data points are plotted on each box plot. Any data points outside of the whisker range are statistical outliers (Henson and Culling, 2025).

## **Model Uncertainty, Limitations, and Potential Improvements**

The integrated hydrologic models (SVIHM and SVOM) have been developed in cooperation with Monterey County Water Resources Agency and Salinas Valley Groundwater Sustainability Agency staff. Although the historical model was calibrated to available observations, model uncertainty exists because of the inherent uncertainty in some model properties because selected observations and inputs were not available to further constrain or delineate landscape processes. Additional uncertainty occurs due to the necessary simplifications and assumptions needed to represent a complex hydrologic system within a numerical model. This is especially true for the simulation of complex systems that have constraints on the movement and availability of water resources that are not governed by the physics of hydrological processes. The influence of potential uncertainties and errors in furnished data on model inputs or outputs was not directly evaluated in this study. Therefore, model results represent the best available data at the time of publishing.

### **Data Uncertainty and Limitations**

Model development benefited from the guidance of a Technical Advisory Committee representing agricultural stakeholders, Monterey County, the Monterey County Agricultural Commission, regional water utilities, and the National Oceanic and Atmospheric Administration National Marine Fisheries Service. Although considerable conceptual information was provided through the Technical Advisory Committee and our cooperators, there are limitations in the spatial and temporal distribution of necessary data for a regional model and measurement error and uncertainty. Model inputs are based on spatially and temporally distributed data for climate; surface water flows, diversions, and recycled water; groundwater wells and levels; groundwater

pumping; surface and subsurface hydraulic properties; and reservoir characteristics and operations. Specific details on the uncertainty of agricultural demands, the most substantial water budget category in the integrated hydrologic models, is presented in the next section (“FMP Suitability and Limitations”).

Climate data were developed using all available climate stations in the Remote Automatic Weather Stations (RAWS) (Desert Research Institute, 2020), COOP (National Oceanic and Atmospheric Administration, 2020), and CIMIS (CIMIS, 2020) networks. These data were supplemented with spatially distributed Parameter-elevation Relationships on Independent Slopes Model (PRISM) (Daly and others, 2008; PRISM Climate Group, 2020) data to generate monthly maps for precipitation and PET (Hevesi and others, 2022; Henson and others, 2022c). There is uncertainty associated with using climate models to distribute climate station data to spatially distributed model input.

Surface water flows include streamflows, reported reservoir releases, surface water diversions, and recycled water. Daily streamflows were obtained from gages in the National Water Information System (USGS, 2023) and aggregated to monthly mean values. Streamflows have uncertainty due to measurement error of each observation associated with each gage and errors due to temporal averaging of daily streamflows to monthly values. Measurement error of each streamflow observation is classified into four groups ranging from 2 percent error to greater than 8 percent error. Reservoir releases, surface water diversions, and recycled water deliveries were furnished by MCWRA (Henson and others, 2022c, 2023) and assigned to the model.

An additional component of model uncertainty arises because of how well model-input values and features represent the actual hydrologic system. The accuracy of the calibrated model also is contingent on the accuracy of the specified inflows and of specified observed flows and

groundwater levels used for model comparison. For example, observed surface-water flows may only be accurate to within 5 to 20 percent. The accuracy of the integrated hydrologic models could benefit from additional observations of streamflow from other major ungaged drainages, especially if more constraints are needed to improve the overall hydrologic budget and estimates of local recharge and runoff.

Groundwater levels are measured in wells throughout the MCWRA well network, which includes both observation wells (non-pumping) and agricultural and M & I supply wells (pumping wells). The properties of many wells, such as screened intervals and associated aquifers, had to be estimated in many cases. Henson and others (2023) provide a summary of the assumptions and development of wells simulated in the integrated hydrologic models. Groundwater levels used in this study were furnished by MCWRA and are included in the model archive (Henson and Culling, 2025). Groundwater level measurements are obtained quarterly to annually depending on the well; therefore, groundwater levels between measurements are unknown. Groundwater level measurement procedures are not currently implemented to ensure that measurements are taken after well recovery from pumping in current and nearby wells, so measured groundwater levels in many wells are pumping influenced.

Groundwater pumpage data were classified by water use as M & I or agricultural supply. There is some unreported domestic and agricultural pumping in the model domain because the reporting ordinances only apply to a portion of the Zone 2C Water Management Area within the integrated hydrologic model domain. Before directly reported data were available in November 1994, M & I water demands were estimated using U.S. Census data and agricultural supply was simulated and compared to long-term estimated values. After November 1994, monthly M & I pumpage has been reported to MCWRA by municipalities and monthly agricultural pumpage has

been reported on a voluntary basis within much of the Zone 2C Water Management Area. Interpretation of groundwater and surface water budgets before and after 1994 for the historical model should be considered with these data limitations.

Surface and subsurface hydraulic properties were developed for the integrated hydrologic models. These data include defining the surface water drainage network topology and channel properties (Henson and others, 2022b), many of which are unknown and require estimation. Subsurface hydraulic properties were estimated based on prior published data and models and updated using parameter estimation (Henson and others, 2025). Although properties were constrained by data where available, there is uncertainty in model properties that should be explored in future model development. For the parts of hydrogeologic units that represent areas of the aquifers that are unconfined, aquifer storage properties were developed to simulate the aquifers as confined. Although this approach has been widely used in complex regional models (Hanson and others 2004, 2014b, c, d; Faunt and others, 2009a, 2024), the confined assumption results in the saturated thickness being held constant during declining or rising groundwater levels. This simplifying assumption allows for more reasonable model run times but warrants consideration for sustainability analyses that examine drawdowns in the upper aquifer.

Reservoir characteristics, such as storage, area, capacity, and operation rules, for the reservoirs in the operational model are defined (MCWRA, 2005, 2018; Henson and others, 2022c). However, the reservoirs are simulated as separate entities with their own mass balance and the only connection to the integrated hydrologic models is through reservoir releases to stream channels. Seepage through the bottom of the reservoir is not directly simulated. Reservoir operations are simulated using predefined rules that describe operations for flood release and

required fish passage. These rules represent reservoir operations under ideal conditions and are limited by simulated water available in the model.

## **FMP Suitability and Limitations**

The Salinas Valley has extensive agriculture with limited reporting of water use and a complex water supply portfolio with multiple environmental and operational constraints. In the Salinas Valley, it is assumed that irrigated lands are considered well managed, with soil moisture being maintained by irrigation so that it is essentially steady state during the growing season for the 2-week time steps implemented in the model. Irrigated agriculture occurs over periods of weeks to months. Thus, the historical model (SVIHM) evaluates water demands, supplies, and flows like other typical regional scale applications of MF-OWHM with typical weekly to monthly time periods (Hanson and others, 2004, 2014b, c, d; Faunt and others, 2009a, 2024).

In FMP, there is no explicit representation of soil moisture storage, and runoff and recharge are specified as fractions of excess precipitation and excess irrigation greater than actual irrigation evapotranspiration by crop type (Schmid and others, 2006; Schmid and Hanson, 2009; Boyce and others, 2020). For weekly to monthly time steps, the simplifying assumptions that near-surface soil moisture is well managed and steady are reasonable. Moreover, the approximation that runoff and recharge can be considered as fractions of excess water after consumption at these time scales is reasonable because the model is evaluating the longer term monthly to seasonal responses, not individual events. Uncertainty analyses that focus on these fractions could clarify the validity of these assumptions. The estimation of runoff and runoff routing using more physically based methods that consider soil moisture and topology could improve the timing of streamflow response in the model.



The integrated hydrologic models are regional in scale with water supplies and demands aggregated to WBS. Although this is helpful because field-scale data are not available, simplifications must be made to facilitate the regional-scale analyses. The crop areas, crop rotations, and land management and irrigation practices of individual agricultural producers are not represented. Water demand calculations in the integrated hydrologic models rely on defining the aerial extent and properties of land uses, landscape consumptive use estimates for each land use, and other factors to estimate the additional water required to account for the efficiency of water management, estimated irrigation methods, and local conditions under variable climate conditions (wet or dry).

Land use data were estimated using a composite of multiple available land use datasets supplemented by information from the California Pesticide Use Reporting database (California Department of Pesticide Regulation, 2018). Although new methods were developed in this study for semi-annual land-use input data, the data were only a regionally developed estimate. Growing periods and land use are estimated using the best available data. However, spatially discrete and temporally dense measurements of crop harvesting are limited to the data incorporated from California Department of Pesticide Regulation (2018). In this study, the cropping patterns and changes were supplemented from Monterey County Agricultural Commissioner agricultural reports (Monterey County Agricultural Commission, 2022) that are only provided at the county scale. These data gaps contribute to potential inaccuracy and uncertainty of growing periods and estimates of actual evapotranspiration that are used to simulate landscape consumptive use.

In addition to land use, simulation of landscape consumptive use requires data to characterize agricultural practices that are highly dynamic and changing. Data are not available

to describe complex agricultural management practices at a monthly time scale for each approximately 6-acre grid cell, so there is some model error that would take substantial effort and outreach to quantify. Landscape consumptive use estimates represent the amount of water a land use requires under perfect conditions and depend on land use properties that are initially estimated based on published values and other regional studies with similarly constructed integrated hydrologic models (Hanson and others, 2004, 2014b, c, d; Faunt and others, 2009a, 2024).

The water demand is the landscape consumptive use divided by the overall efficiency. The overall efficiency represents the additional water required to account for the efficiency of water management, estimated irrigation methods and sources, and local conditions under variable climate conditions (wet or dry). The efficiency of water management in each WBS (that is, OFE) was a factor applied to crop water demands to represent efficiencies that are influenced by local conditions and irrigation type. This includes the effects of seasonal activities and irrigation types on efficiency. Seasonal agricultural field preparation activities are not directly represented in the crop growth model and had to be included in overall WBS efficiency calculations. Regional data for irrigation methods and irrigation sources (such as farm storage ponds) were limited. Therefore, assumptions were made using available data from available literature (Sandoval-Solis and others, 2013; Tindula and others, 2013) and models of comparable agricultural basins in this region (for example, Hanson and others, 2004, 2014b, c, d; Faunt and others, 2009a, 2024). In addition, landscape consumptive use and agricultural practices respond to climate stress (wet or dry conditions). Thus, to account for climate stress, Kc climate scale factors were used to try to match annual pumpage and some of the initial land use parameter

values were adjusted during parameter estimation. The integrated hydrologic models would benefit from refinements of these efficiency input data.

FMP provides a reasonable and defensible estimate of water demands, landscape water fluxes, and operations. Despite the limitations, voluntary reported agricultural pumping estimates provided valuable observations for simulating total delivery requirements for each WBS. These agricultural pumping estimates were consistent with the simulated water demands estimated using land use and climate.

### **Hydrologic Model Limitations**

As with any model, the integrated hydrologic models are a simplification of the real flow system and, as such, have some inherent limitations. The accuracy of simulation results is related strongly to the quality and resolution (both spatial and temporal) of input data and of measurements of the system (such as precipitation, groundwater levels, streamflow, and pumpage) used to drive and constrain the simulation and related calibration. The inflows and outflows in the integrated hydrologic models were a combination of measured values, simulated flows from adjustments to parameters to represent conceptualizations of the system, estimated inflows provided by the watershed model, and values specified using MF-OWHM. Differences between simulated and actual hydrologic conditions arise from several sources and are collectively known as model error and model uncertainty. Whereas the historical model was designed with the capability to be accurate at the WBS and subregion scales, the conceptual and numerical models were developed based on assumptions and simplifications that may restrict the use of the historical model to regional and subregional levels of spatial analysis within seasonal to interannual temporal scales.

The historical model (SVIHM) was designed to evaluate annual to decadal patterns in regional water availability. Processes that vary at a spatial scale smaller than grid spacing (approximately 6 acres, with variably thick layers) and a temporal scale smaller than the stress periods (1 month) cannot be explicitly represented with the historical model. Model discretization in space and time can be a potential source of error and uncertainty. Models represent a hydrologic system as a series of discrete spatial units, through which intrinsic properties and flows are assumed to be uniform. The use of a discretized model to represent a hydrologic system introduces limitations for features that occur at scales smaller than the current discretization. Transient models are further discretized into a series of discrete units of time, during which specified hydrologic inflows and outflows are held constant. The use of monthly stress periods and two biweekly time steps per month in the historical model assumes that the variations of inflows and outflows and changes in groundwater levels are piecewise linear changes. Changes at smaller time scales are not simulated, and are not discernable in historical model results, which may contribute to some additional temporal uncertainty. For example, the distribution of daily precipitation and soil moisture within each monthly period used by the historical model can result in large variations in simulated recharge and runoff (for example, precipitation occurring as a large 1-day storm rather than as a series of smaller storms), and this cannot be accounted for with the existing model. The temporal scale used in the historical model was expressly designed to separate the supply and demand components of water use and movement for agriculture within the model domain.

Model parameter estimation and history matching of observations from the historical model constrain the differences between the real-world and simulated volumetric flows. Thus, the degree to which a simulated condition provides a reasonable representation of the hydrologic

system can be evaluated by comparing simulated hydrologic conditions with those observed and measured in the field, which, in turn, provides a volume-constrained calibration. Thus, the performance and accuracy of the integrated hydrologic models are constrained primarily by groundwater levels and surface-water flows, differences in surface-water flows (gains and losses), and to a lesser degree by estimates in annual agricultural pumpage and vertical groundwater-level differences. For example, small sources of error and uncertainty in the integrated hydrologic models could result from not simulating delayed recharge that is potentially associated with unconfined conditions outside of the model domain, not representing selected faults as potential conduits for vertical flow, or not including layer-specific skin factors for multiple-aquifer wells that could further accentuate the vertical distribution of groundwater pumpage.

Differences between simulated and observed hydrologic features also arise from the numerical solution that attempts to provide a cell-by-cell mass balance of inflows and outflows. Mass-balance errors are minimized by ensuring the model solution reaches a reasonable state of mass balance within each biweekly period. The twice-per-month time steps were used to remain consistent with the assumptions of the current version of the FMP process. The cumulative mass balance of the historical model was less than 1 percent of the total flow over the 51 years of historical simulation (October 1967–September 2018). It is also important to note that groundwater budget components vary substantially in scale. For example, the average agricultural supply pumpage is 454 TAFY and the average seawater coastal inflow is 12 TAFY, which is approximately 3 percent of the average groundwater pumpage. Estimating seawater coastal inflow is important for sustainability assessments; however, uncertainty in groundwater

pumpage may be greater than the estimated seawater coastal inflow. This underscores the importance of accurate groundwater pumpage estimates, specifically in the coastal region.

The operational model (SVOM) is a hypothetical baseline model used to evaluate water supply project alternatives and alternate reservoir operational rules by MCWRA. The intent of the operational model is not to directly represent historical conditions; the reservoirs and land use were not always as they were in 2014. The reservoir releases and storage are compared to the historical data for the purpose of evaluating if they are reasonable. There may be differences in groundwater levels, groundwater storage, and surface water flows among the two integrated hydrologic models. The purpose of the operational model is to quantify potential benefits of water supply projects within a framework that considers historical climate and benefits from representation of the system using as much of the calibrated historical model input as feasible. Despite the differences among the purpose and implementation of the integrated hydrologic models, the operational model reasonably reproduces the historical conditions for which it was developed—reservoir operations and reservoir-provided flows to downgradient diversions at the SRDF (to offset groundwater pumpage in the coastal region).

Despite these potential limitations, the integrated hydrologic models are sufficient for the intended purposes of simulating surface water and groundwater interactions on annual to decadal scales at the subregional scale. Hydrologic budget analysis is needed for planning and evaluating alternatives for managing conjunctive use within the analysis regions evaluated in this study. Future efforts for sustainable water resource development may need detailed information about stream-aquifer interactions for planning.

## Potential Improvements

The accuracy of the integrated hydrologic models could be improved if the input values of selected hydraulic properties, such as horizontal and vertical hydraulic conductivities and storages, could be adjusted based on additional field estimates. For example, aquifer tests combined with wellbore flow and temperature logs could be used to better assess the effects of multiple-aquifer wells on the vertical distribution of pumpage over multiple aquifers. Additional estimates of horizontal hydraulic conductivity to further constrain integrated hydrologic model properties could be obtained from aquifer tests combined with wellbore flow logs at selected supply-well sites or well specific-capacity tests at single-aquifer supply wells. In addition, there is uncertainty in the facies distributions that are based on borehole lithology, which are sparser with increasing depth. The facies subregions may need to be further subdivided using additional zones within facies and texture data estimated from lithologic data and drillers logs.

Potential future refinements and enhancements can continue to improve the level of resolution and model accuracy and reduce potential uncertainties. In general, proper design and parameter estimation of flow models is an ongoing process that, along with better spatial and temporal estimates of inflows, outflows, climate, and land use, can minimize some of the inherent model limitations. Limitations of the modeling software, assumptions made during model development, and results of model parameter estimation and sensitivity analysis all are factors that may further constrain the appropriate use of this model. In turn, these limitations can be used to identify where potential future improvements in the simulation of specific processes are needed or where new data are needed to improve the quality of the simulation.

Several of the processes within the integrated hydrologic models could also potentially allow for refined simulation of selected flow features. Improved simulation of multiple-aquifer

wells to account for partial penetration and better estimates of actual pumping capacities of all wells could increase the accuracy of simulated pumpage. Some WBSs required assumptions about well construction, so the additional location of wells or water conveyances that are used to service these properties would require additional investigation.

Future work could include data refinement and temporal updates of the integrated hydrologic models, additional calibration with additional model observations, and development of projections of alternative scenarios based on a new comprehensive basin management plan with use of the Surface-Water Operations Process in the operational model (Ferguson and Llewellyn, 2015; Ferguson and others, 2016). An expanded monitoring network would allow a better understanding of changes in surface-water flows, diversions, streamflow, and streamflow infiltration (seepage runs), which are the main sources of recharge in the valley. In particular, the monitoring of crop-specific annual land use, canal and diversion inflows, monthly well-by-well groundwater pumpage, and wellbore flow throughout the valley would help to better quantify the state of resources and provide valuable comparison to model performance.

The history matching of the historical model, based predominantly on groundwater levels and streamflows, could be supplemented with parcel-based observations of land use from remote-sensing estimates of evapotranspiration. This could improve model accuracy and embed more variability in the demand. Projections of water availability and sustainability of supply could include the analysis of alternative scenarios of land use, crops, irrigation practices, and additional capture of intermittent runoff from wet years (once climate and runoff are added to the model) for managed aquifer recharge or supplemental irrigation scenarios.

The integrated hydrologic models (SVIHM and SVOM) were developed using a “self-updating model structure,” where model data can be updated using spreadsheet software and



processing scripts. Thus, the integrated hydrologic models are readily updated and can be periodically refined, including parameter and framework adjustments as needed to keep the historical and operational models available for operational and future analysis. This structure facilitates any upgrades, updates, and additional parameter estimation that may be needed to address marginal changes in the important components of the water budget that are relevant to the operation of the SVWP and reservoir management, sustaining the groundwater resources without interfering with project deliveries, and honoring related fish passage criteria for threatened steelhead.

During model development, some potential improvements were identified that could be explored in future hydrologic models and data collection efforts.

1. Simulation of aquifer depletion and interactions among aquifers would be greatly improved with better resolution of well depths, pumping capacities, and screened intervals. These data were commonly unavailable and had to be estimated.
2. Representation of groundwater storage and levels would benefit from improved information about spatial and vertical aquifer transmissivity with facies or texture-based distributions of hydraulic properties.
3. Future evaluations of stream habitat and surface water flows would benefit from reduced overestimation bias in simulation of low flows and improved representation of the surface water drainage network, including irrigation canals.
4. Understanding of groundwater and surface water interactions gained from the model could be improved by evaluating the effects of near-river shallow well networks connected to the Salinas River and storage ponds in the Upper Valley

analysis region. Such networks are observed in aerial imagery but are not currently represented in the models or input data.

5. Estimation of agricultural demands could be enhanced using directly measured pumping data and validated field-scale land use mapping.
6. Simulation of the groundwater system could be improved with (1) additional monitoring wells in the below dam and Upper Valley regions to better characterize hydraulic gradients and groundwater use, (2) additional monitoring wells along the slopes of the Salinas Valley to provide information about lateral hydraulic gradients, and (3) additional paired monitoring wells of the shallow and deep aquifers near the coast to improve the characterization of the coastal aquifers to mitigate seawater intrusion.
7. Overall basin groundwater and surface water budgets could be refined by improving data collection and extending the model analysis into areas outside the Zone 2C Water Management Area. National-scale mapping of irrigated lands has shown that there may be substantial agricultural development outside of the Zone 2C Water Management Area (fig. 6D), where reporting of groundwater water use is not required. Agricultural pumpage was only simulated in the subareas within the Zone 2C Water Management Area where reporting of groundwater water use is required and wells have been defined.
8. Future model development could explore the influence of simulating completely unconfined conditions to understand the influence of this simplifying assumption on surface and groundwater budgets.

9. The integrated hydrologic models would benefit from comparative evaluations with higher resolution models that have been developed to evaluate aquifer storage and recovery projects in the coastal area and integration of new information gathered as part of other model development in the region.
10. Estimation of uncertainty for important model predictions, such as streamflow requirements, minimum water level thresholds, and seawater coastal inflow estimates, may help more accurately quantify the risk of management decisions.

## **Summary and Conclusions**

To evaluate the challenging water management issues in the Salinas Valley, the U.S. Geological Survey (USGS), Monterey County Water Resource Agency (MCWRA), and the Salinas Valley Basin Groundwater Sustainability Agency cooperatively developed a comprehensive suite of models that represent the Salinas Valley hydrogeologic system. The Salinas Valley surrounds the Salinas Valley groundwater basin in Monterey and San Luis Obispo Counties, California (fig. 1). The Salinas Valley study area covers about 4,200 square miles and is subdivided into five analysis regions—the Riparian, Pressure, East Side-Langley, Forebay, and Upper Valley analysis regions (fig. 15). The Riparian analysis region represents the area surrounding the Salinas River. The Pressure, East Side-Langley, Forebay, and Upper Valley analysis regions correspond to Salinas Valley groundwater subbasins defined by California Department of Water Resources (California Department of Water Resources, 2020). These groundwater subbasins are used to manage groundwater sustainability by groundwater sustainability agencies and water agencies within the Salinas Valley study area (fig. 11).

Agriculture has been a vital part of the local economy for more than a century (Manning, 1963). Increased agricultural development, which includes a shift toward more water-intensive crops (Monterey County Agricultural Commission, 2022), changes in population (U.S. Census Bureau, 2018), and climate variability have increased demand on limited water resources. Sources of surface water to meet water demands include the Salinas River and its tributaries and two reservoirs (fig. 1). Surface water in the Salinas Valley study area is managed to meet agricultural diversions at Clark Colony and the Salinas River Diversion Facility (fig. 1) and to meet minimum environmental flows to support habitat for federally listed threatened steelhead (*Oncorhynchus mykiss*). A vast network of thousands of publicly and privately owned wells (figs. 24A, 24B) is used to meet groundwater demands. Groundwater is used to meet agricultural, municipal, and industrial water demands and when surface water supplies are limited or not suitable for the intended water use.

There are substantial water management challenges that have been documented. Valley-wide groundwater storage declines have been documented for almost 80 years (California Department of Public Works, 1946) and this is well illustrated by persistent groundwater level declines, associated reductions in long-term groundwater storage observed in the Pressure and East Side-Langlely analysis regions, and seawater intrusion into the 180-Foot Aquifer and 400-Foot Aquifer hydrogeologic units along the coast, which has resulted in water quality degradation. Additionally, widespread nitrate contamination throughout the Salinas Valley has occurred (Harter and others, 2012), further limiting the available groundwater supply. Although water quality is an important management concern, it was not specifically evaluated in this study.

Managing water resources to address local shortages from spatial and temporal variability in water availability is challenging (California Department of Public Works, 1946; Leedshill-

Herkenhoff, Inc., 1985; MCWRA, 1995). Locations where water resources are needed are commonly long distances (as far as 100 miles, in some cases) from where reservoir releases or substantial recharge occur. The variation among locations of areas with substantial withdrawals and recharge require conjunctive use of groundwater and surface water to meet water demands. Surface water availability varies seasonally and year to year. Some sections of the Salinas River are intermittently dry and surface water must be conveyed to meet water demands downstream. Variability in surface water magnitude and challenges related to conveyance of surface water throughout the valley lead to substantial and primary use of groundwater to meet many water demands.

The Salinas River is a significant contributor to groundwater recharge. Additional substantial sources of recharge occur from infiltration in areas with native vegetation and agricultural areas. Surface water travels from the Upper Valley analysis region along the Salinas River to the coastal areas and infiltrates into unconfined aquifers, resulting in substantial reductions in streamflow as it moves through the valley to the ocean. This flow reduction through recharge along the Salinas River is a constraint for delivery of surface water to coastal areas to offset groundwater pumpage and for managing required minimum environmental flows. Yet, this groundwater recharge from the Salinas River also supports regional groundwater availability. This vital connection between infiltration of managed and natural surface water flows as well as the importance of riparian underflow in every analysis region and the need for concurrent delivery of surface water to the coastal regions to reduce coastal seawater intrusion underscores the importance of integrated valley-wide water management.

The evaluation of the Salinas Valley hydrologic system involves an integrated approach that combines surface and subsurface analysis to simulate both natural and managed water flows.

This is achieved through the development of a comprehensive Salinas Valley System Model, which incorporates various submodels and data related to geology, surface water, groundwater, and operational factors. All submodels of the Salinas Valley System Model and associated data can be accessed at <https://www.sciencebase.gov/catalog/item/640770fed34e76f5f75e388b>. The overarching goal of the Salinas Valley System Model is to produce a model that includes a (1) geologic framework and texture model (the Salinas Valley Geologic Framework; Sweetkind, 2023) to define aquifers as hydrogeologic units, (2) model and analysis of watershed processes (Salinas Valley Watershed Model; Hevesi and others, 2025a), (3) historical model (Salinas Valley Integrated Hydrologic Model; Henson and Culling, 2025) and analyses of historical surface and groundwater availability, and (4) operational model that simulates multi-objective reservoir operations using established operational rules or is configured to evaluate alternative rules (Salinas Valley Operational Model; Henson and Culling, 2025). The Salinas Valley System Model was developed with input and expertise from stakeholders, agriculture, surface water, groundwater, geological, reservoir management specialists, and coordination with Federal, State, and local agencies. The Salinas Valley System Model provides a comprehensive suite of tools for analysis of water resources and evaluation of reservoir operations and water use sustainability projects.

This report documents and focuses on parts 3 and 4 listed above, the development of a historical surface water and groundwater availability model integrated with an operations model. The simulation of historical conditions is accurate at scales relevant to water-supply analysis for the evaluation of water availability and sustainability, and interactions between groundwater and surface water use in analysis regions of the Salinas Valley are evaluated. Several companion

reports and data releases provide information on the input data, model representation of important processes, and connections between hydrologic models.

The integrated hydrologic models were designed to reproduce the natural and human components of the hydrologic system, including components dependent on variations in climate, permitting an accurate assessment of surface-water and groundwater conditions and processes that can inform water users and help to improve planning for future conditions. Model development included (1) a conceptual model of the flow system and the geologic framework, (2) a surface water model that provided inflows from ungaged basins that are connected to but outside of the integrated hydrologic model domain, and (3) construction of integrated hydrologic flow models with MODFLOW-One-Water Hydrologic Flow Model (MF-OWHM). The integrated hydrologic models have a uniform grid with a spatial resolution of approximately 6 acres. The historical model (SVIHM) simulates historical conditions with monthly stress periods and semi-monthly time steps. The historical model was calibrated to match observations of streamflow, groundwater levels, and groundwater pumpage and was then used to assess the use and movement of water throughout the Salinas Valley.

The operational model provides a comprehensive representation of the current reservoir operations for Lakes San Antonio and Nacimiento. The operational model can support evaluations and scenario-testing to support habitat conservation, strategies to increase surface water supply, and groundwater sustainability plans. The operational model is like the historical model but has a few differences: time steps are 5 to 6 days instead of semi-monthly, land use is assumed to be equal to 2014 for the entire simulation, all current diversions and water supply projects are implemented (Salinas Valley Water Project, including the Salinas River Diversion Facility and the Castroville Seawater Intrusion Project), and reservoir releases are computed

using operational rules instead of manually specified as they are in the historical model. The operational model uses historical information to simulate the Salinas Valley hydrologic system. Reservoir operations have changed substantially through the past 50 years. The Castroville Seawater Intrusion Project has been in operation since July 1998 and the Salinas River Diversion Facility project has been in operation since April 2010. In the operational model, these projects are implemented from the start of the simulation. Thus, the operational model is a hypothetical baseline model used to evaluate water supply project alternatives and alternate reservoir operational rules by MCWRA (MCWRA, 2005, 2018; Henson and others, 2022b). Although the intent of the operational model is not to directly represent historical conditions, there is reasonable visual correspondence in the annual time series, which shows similar wet and dry period responses among average monthly storage (fig. 42A), average annual storage (fig. 42B), and average annual releases (fig. 42C) among the SVOM and historical records.

The historical model (SVIHM) reasonably represents historical conditions for surface water, agricultural water demands, and groundwater levels. The SVIHM also provides insights into groundwater budget components such as recharge, pumping, the recharge to pumping ratio, and storage. Through model parameter estimation, the components of the historical model were calibrated to match historical observations where available using trial and error and computer assisted techniques. The observation dataset used to evaluate history matching includes more than 104,000 annual, quarterly, and monthly observations and reported data for streamflows, streamflow differences between streamgages, groundwater levels, groundwater drawdowns, groundwater contours, reported groundwater pumpage, and diversions for the period from October 1, 1967, to December 31, 2014.



## Surface Water Summary

The calibrated historical model reasonably reproduces monthly average surface water flow observations. Comparison among streamgauge data and simulated streamflows show reasonable correspondence across the observed variability in mean monthly flows throughout the Salinas River that range from 0 to 18,750 cubic feet per second (ft<sup>3</sup>/s). Simulated flows reproduce historical flows in six gages along the Salinas River and its major tributary Arroyo Seco, with a minimum Nash-Sutcliffe model efficiency (NSME) of 0.87 and maximum mean residual of 83 ft<sup>3</sup>/s. However, low flows at gages in the Forebay and Pressure analysis regions (USGS 11152300 and USGS 11152500; fig. 20) were overestimated by the historical model. This is evident in the overprediction of flows (negative residuals) at USGS 11152000, USGS 11151700, and USGS 11152500 (table 7).

Historical model results show that streamflow leakage into the groundwater system is a substantial source of recharge in all parts of the basin everywhere except for the East Side-Langley analysis region. Streamflow leakage is substantial in the Upper Valley and Forebay analysis regions, where older hydrogeologic units are present in the near surface (figs. 21, 22). The East Side-Langley analysis region has the highest inflow of subbasin underflow (table 14) into all analysis regions (tables 12, 13, 15, 16). The relatively substantial proportion of subbasin underflow to the East Side-Langley analysis region suggests that activities that alter storage or flow in upgradient basins will affect the East Side-Langley analysis region. The substantial portion of inflow represented by subbasin underflow and riparian underflow among analysis regions indicates substantial interconnectivity.

## Agricultural Demand Summary

The simulation reasonably reproduces monthly agricultural pumpage that has been regionalized to multiple water balance subregions within each of the analysis regions. The mean monthly residual between reported and simulated agricultural pumpage for the history matching period is 29 acre-feet with a root mean square error (RMSE) of 775 acre-feet. The regionalization of agricultural supply and demand calculations within water balance subregions allows for a regional assessment of agricultural water use without needing to specify what each individual grower is doing on every agricultural field. Multi-year composite land use data are available at the subbasin scale but are not available to describe all cropping patterns and agricultural management practices at a monthly time scale for each approximately 6-acre grid cell; for this reason, some model error cannot be avoided. Despite the approximations, the historical model simulates within 99 percent the total cumulative volume of reported annual agricultural pumpage in Salinas Valley from November 1994 through September 2018 and has general agreement between annual reported and simulated pumpage spatially throughout the model domain (figs. 36A–G) with all scaled RMSE less than or equal to 9 percent for among the entire domain and analysis regions.

Simulated agricultural pumpage varies from year to year with an average of approximately 481 thousand acre-feet per year (TAFY) for the period between 1970 and 1994 computed as the average of analysis periods A and B. Prior to when reliable pumpage data became available in November 1994, the annual agricultural pumpage was assumed to be variable but unknown. The average total pumpage for analysis periods A and B (1970–94; table 11), 469 TAFY and 578 TAFY, respectively, average to 524 TAFY, which is close to the previous groundwater budget tabulations of 519 TAFY for the period from 1970 to 1994

(Montgomery Watson, 1997). Agricultural pumpage was as much as 547 TAFY in 1997 and as low as 345 TAFY in 2011 (fig. 36B). Municipal and industrial pumpage ranged from 38 to 67 TAFY over the four analysis subperiods, which is approximately 10 percent of agricultural pumpage (table 11).

## **Groundwater-Level Summary**

The simulation reasonably reproduces observations of groundwater levels and drawdowns and reproduces groundwater level declines and reductions in groundwater storage over time. Groundwater levels show close correspondence with the 1:1 line with a few wells in the Upper Valley analysis region that were not well matched (fig. 33A). Drawdowns throughout the basin are simulated with a mean residual less than 1 foot (ft) with RMSE of 15 ft (table 9). The mean drawdown residuals for all observation wells show most wells have drawdown residuals within 20 ft of observed values (fig. 34). Simulated patterns of groundwater levels generally replicate the patterns and drawdowns shown in MCWRA-estimated groundwater level contours (MCWRA, 2005, 2018; Henson and others, 2023) for 1994, 2003, and 2011 (figs. 35A–C). Among all analysis regions, the absolute values of mean drawdown residuals are less than 3 ft with maximum RMSE of 18 ft (table 9).

Groundwater level changes in some analysis regions (East Side-Langley, Pressure, and Forebay analysis regions) are more sensitive to dry conditions. Groundwater levels in some areas have still not recovered from the 1984–94 dry period (East Side-Langley and Pressure analysis regions); the Upper Valley and Forebay analysis regions have had relatively more recovery of groundwater levels (figs. 13, 33). Higher sensitivity of groundwater levels to dry periods in the analysis regions close to the coast (Pressure and East Side-Langley analysis regions) indicates

that local recharge is insufficient to maintain groundwater levels with current groundwater use during these periods and indicates a dependence on regional recharge especially during dry periods.

## **Groundwater Budget Summary**

Groundwater budgets from the historical model provide valuable information about flows into and out of the Salinas Valley groundwater subbasins. Substantial inflows and outflows indicate major components of the budgets include stream leakage and recharge. In all analysis regions, subbasin underflow from adjacent groundwater subbasins is a substantial inflow. In every analysis region but the East Side-Langley analysis region, groundwater flow from the riparian area of the main Salinas River channel (riparian underflow) is a substantial inflow. Important outflows in the groundwater budgets include simulated agricultural and municipal and industrial pumpage.

The pumpage-recharge fraction is the ratio of analysis region pumping to recharge and was evaluated for each analysis region to compare the relative magnitude of analysis region (groundwater subbasin) water use and water supply. The pumpage-recharge fraction is an indicator of analysis region dependence on riparian and subbasin underflow from adjacent analysis regions. Average pumpage-recharge fractions for the integrated hydrologic model domain are on average 0.9 but are as high as 1.2 in dry analysis period B (table 11). These fractions further support that local recharge is insufficient to maintain groundwater levels with current groundwater use under all climate conditions. Except for the Riparian analysis region, the average pumpage-recharge fractions of all analysis regions are greater than 1.6 for the simulation period. Moreover, values greater than 2 commonly occur among analysis periods even outside of dry periods (tables 13–16). Fractions much greater than 1 indicate that a substantial portion of

water demands are being met by subbasin and riparian underflow, further underscoring the substantial connectivity among groundwater subbasins. These results suggest that groundwater subbasin water supply is affected by changes in groundwater availability and use in upgradient groundwater subbasins and Salinas River streamflow. This supports that groundwater sustainability efforts would be improved with regional coordination.

Storage change, the difference between inflows and outflows, provides insights into the drivers of regional changes in groundwater levels. Aquifer storage change varies considerably from year to year, depending on land use, pumpage, and climate conditions, ranging from an average of -139 TAFY (out) to 158 TAFY (in) over the four analysis subperiods (table 11). Climate-driven factors can greatly affect inflows, outflows, and water use by as much as a factor of 2 between wet and dry years. Whereas inflows during inter-decadal wet years partly replenish groundwater in the basin, the long-term water use and storage depletion from pumping diminish the effects of these wetter periods and related recharge. Substantial withdrawals from storage generally were simulated not only during drier years, but also during the increase of the practice of multi-cropping throughout the simulation period. The long-term imbalance between inflows and outflows results in simulated average annual groundwater depletion of about 15 TAFY, which is made up primarily of an average of 15 TAFY of seawater coastal inflow over the 51-year period from water year 1968 through 2018.

## **Conclusions**

The components of the Salinas Valley System Model, particularly the historical and operational model components documented in this report, allow for analysis of landscape, surface-water, and groundwater hydrologic budgets for water years 1970 through 2018. These

models support assessments of the effects of groundwater and surface water use on surface and groundwater availability, evaluation of the reservoir operating agreements used to support management of surface flows and storage, and evaluation of new and existing water supply project performance to develop groundwater sustainability plans. Overall, the historical model provides a good representation of historical conditions and hydrologic budgets for seasonal to inter-decadal time frames and subregional to valley-wide spatial scales. The integrated hydrologic models adequately represent the movement and use of all water within the regional flow system for surface water and diversions, groundwater levels, and groundwater pumpage used to meet agricultural and municipal demands. In addition to the water management challenges in the Salinas Valley with respect to water quantity, there are water quality challenges. However, these were not addressed directly in this report. Although the water supply challenges documented in the 1940s remain, improvements in efficiency, surface water supply and storage projects, and valley-wide sustainability coordination present opportunities to mitigate the undesirable effects of a variable climate on the integrated hydrologic system. Connectivity between analysis regions underscores the importance of using regional tools such as the historical and operational integrated hydrologic models. Tools that encompass the entire Salinas Valley are essential for analyses of water availability and use under changing land use, agricultural practices, climate conditions, and reservoir operations.

## References Cited

Allen, R.G., Pereira, L.S., Raes, D., and Smith, M., 1998, Crop evapotranspiration—Guidelines for computing crop water requirements: Food and Agriculture Organization of the United Nations Irrigation and Drainage Paper 56, 300 p.

Anderson, M.P., and Woessner, W.W., 1992, Applied groundwater modeling—Simulation of flow and advective transport (2nd ed.). Academic Press, 373 p.

Arcement, G.J., and Schneider, V.R., 1989, Guide for selecting Manning's roughness coefficients for natural channels and flood plains: U.S. Geological Survey Water Supply Paper 2339, 62 p.

Baillie, M., Chau, L., and Turner, J., 2015, State of the Salinas River groundwater basin: Brown and Caldwell, prepared for Monterey County Resource Management Agency, 241 p., accessed 12/30/2017, at [https://digitalcommons.csumb.edu/cgi/viewcontent.cgi?article=1020&context=hornbeck\\_cgb\\_6\\_a](https://digitalcommons.csumb.edu/cgi/viewcontent.cgi?article=1020&context=hornbeck_cgb_6_a).

Banta, E.R., 2000, MODFLOW-2000, the U.S. Geological Survey Modular Ground-Water Model—Documentation of packages for simulating Evapotranspiration with a Segmented Function (ETS1) and Drains with Return Flow (DRT1): U.S. Geological Survey Open-File Report 00-466, 127 p. [Available at <https://doi.org/10.3133/ofr00466>.]

Belitz, K., Phillips, S.P., and Gronberg, J.M., 1993, Numerical simulation of ground-water flow in the central part of the Western San Joaquin Valley, California: U.S. Geological Survey Water-Supply Paper 2396, 69 p.

Belitz, K., and Phillips, S.P., 1995, Alternative to agricultural drains in California's San Joaquin Valley—Results of a regional-scale hydrogeologic approach: *Water Resources Research*, v. 31, no. 8, p. 1845–1862. [Available at <https://doi.org/10.1029/95WR01328>.]

Bicknell, B.R., Imhoff, J.C., Kittle, J.L., Jr., Donigian, A.S., Jr., and Johanson, R.C., 1997, Hydrological simulation program—Fortran, User's manual for version 11: Athens, Ga., U.S. Environmental Protection Agency, National Exposure Research Laboratory, 755 p., EPA/600/R-97/080.

Boyce, S.E., Hanson, R.T., Ferguson, I., Schmid, W., Henson, W., Reimann, T., Mehl, S.M., and Earll, M.M., 2020, One-Water Hydrologic Flow Model—A MODFLOW based conjunctive-use simulation software: U.S. Geological Survey Techniques and Methods, book 6, chap. A60, 435 p., accessed 12/31/2021, at <https://doi.org/10.3133/tm6A60>.

Boyce, S.E., 2023, MODFLOW One-Water Hydrologic Flow Model (MF-OWHM) Conjunctive Use and Integrated Hydrologic Flow Modeling Software, version 2.3.0: U.S. Geological Survey software release, accessed 12/31/2021 12/31/2017, at <https://doi.org/10.5066/P9P8I8GS>.

Boyle Engineering Corporation, 1987, Salinas Valley ground water model, alternative analysis: Final Report prepared for the Monterey County Flood Control and Water Conservation District.

Brandt, J.T., Earll, M.M., Sneed, M., and Henson, W.R., 2021, Detection and measurement of land-surface deformation, Pajaro Valley, Santa Cruz and Monterey Counties, California, 2015–18: U.S. Geological Survey Open-File Report 2021-1101, 16 p., available at <https://doi.org/10.3133/ofr20211101>.

Brouwer, C., Goffeau, A., and Heibloem, M., 1985, Irrigation water management—Training manual no. 1—Introduction into Irrigation. Food and Agriculture Organization of the United Nations, Land and Water Development Division.

Brouwer, C., and Heibloem, M., 1986, Irrigation water management—Training manual no. 3—Irrigation water needs. Food and Agriculture Organization of the United Nations, Land and Water Development Division.

Brush, C.F., Belitz, K., and Phillips, S.P., 2004, Estimation of a water budget for 1972–2000 for the Grasslands Area, Central Part of the Western San Joaquin Valley, California: U.S. Geological Survey Scientific Investigations Report 2004–5180, 51 p. [Available at <https://doi.org/10.3133/sir20045180>.]

Burow, K.R., Shelton, J.L., Hevesi, J.A., and Weissmann, G.S., 2004, Hydrogeologic characterization of the Modesto area, San Joaquin Valley, California: U.S. Geological Survey Scientific Investigations Report 2004–5232, 54 p. [Available at <https://doi.org/10.3133/sir20045232>.]

California Department of Food and Agriculture, 2022, 2021–2022 California Agricultural Statistics Review: 159 p.

California Department of Pesticide Regulation, 2018, Pesticide use reporting—An overview of California’s unique full reporting system: California Department of Pesticide Regulation webpage, accessed January 1, 2018, at <https://www.cdpr.ca.gov/docs/pur/purovrw/tabofcon.htm#:~:text=An%20Overview%20of%20California's%20Unique%20Full>.

California Department of Public Works, 1946, Salinas Basin investigation: California Department of Water Resources Bulletin 52, 252 p.

California Department of Water Resources, 1968, Water well standards: State of California, California Department of Water Resources Bulletin 74, 248 p., accessed [12/01/2022], at [https://digitalcommons.csumb.edu/hornbeck\\_usa\\_3\\_d/52](https://digitalcommons.csumb.edu/hornbeck_usa_3_d/52).

California Department of Water Resources, 1971a, Nitrates in ground waters of the central coast area: San Joaquin District Office Memorandum Report, 16 p.

California Department of Water Resources, 1971b, Land use in California, An index to surveys conducted by the California Department of Water Resources 1950–1970: California Department of Water Resources Bulletin 176, 22 p.

California Department of Water Resources, 1973, Seawater intrusion, lower Salinas Valley, Monterey County. California Department of Water Resources, 91 p.



California Department of Water Resources, 1994, California water plan update: California Department of Water Resources Bulletin 160-93

California Department of Water Resources, 1997, Monterey County land use: California Department of Water Resources database, accessed December 1, 2016, at <https://data.cnra.ca.gov/dataset/i15-landuse-monterey1997>.

California Department of Water Resources, 2014, Statewide crop mapping GIS geodatabase, accessed January 1, 2018, at <https://data.cnra.ca.gov/dataset/statewide-crop-mapping/resource/04f89c79-59d1-4981-a3ab-853fdb79d37>.

California Department of Water Resources, 2020, California's groundwater update 2020: California Department of Water Resources Bulletin 118, accessed January 5, 2023, at [https://data.cnra.ca.gov/dataset/calgw\\_update2020](https://data.cnra.ca.gov/dataset/calgw_update2020).

California Department of Water Resources, 2023, Sustainable groundwater management act (SGMA): accessed on November 24, 2023, at <https://water.ca.gov/Programs/Groundwater-Management/SGMA-Groundwater-Management>.

California Division of Oil, Gas and Geothermal Resources, 1982, Oil and gas prospect wells drilled in California through 1980: California Division of Oil, Gas and Geothermal Resources Report TR01, 258 p.

California Irrigation Management Information System (CIMIS), 2020, Meteorological data: California Department of Water Resources and University of California at Davis, accessed 12/01/2022, at <http://www.cimis.water.ca.gov/>.

Clark, J.C., Brabb, E.E., and Rosenberg, L.I., 2000, Geologic map and map database of the Spreckels 7.5-minute quadrangle, Monterey County, California: U.S. Geological Survey Miscellaneous Field Studies Map MF-2349, scale 1:24,000.

Clark, J.C., Dupré, W.R., and Rosenberg, L.I., 1997, Geologic map of the Monterey and Seaside 7.5-minute quadrangles, Monterey County, California—A digital database: U.S. Geological Survey Open-File Report 97-30, 41 p., 2 sheets, scale 1:24,000. [Available at <https://doi.org/10.3133/ofr9730>.]

Cleath and Associates, 1991, Hydrogeologic investigation—Salinas Valley dispersed well system area: Consultants report to Monterey County Water Resources Agency, March 1991, [variously paged].

Cook, T.D., 1978, Soil survey of Monterey County, California (vol. 22): Soil Conservation Service.

Daly, C., Halbleib, M., Smith, J.I., Gibson, W.P., Doggett, M.K., Taylor, G.H., Curtis, B.J., and Pasteris, P.P., 2008, Physiographically sensitive mapping of climatological temperature and precipitation across the conterminous United States: *International Journal of Climatology*, v. 28, no. 15, p. 2031–2064. [Available at <https://doi.org/10.1002/joc.1688>.]

Dartnell, P., Maier, K.L., Erdey, M.D., Dieter, B.E., Golden, N.E., Johnson, S.Y., Hartwell, S.R., Cochrane, G.R., Ritchie, A.C., Finlayson, D.P., Kvittek, R.G., Sliter, R.W., Greene, H.G., Davenport, C.W., Endris, C.A., and Kringsman, L.M., 2016, California state waters map series—Monterey Canyon and vicinity, California: U.S. Geological Survey Open-File Report 2016–1072, 48 p., 10 sheets, scale 1:24,000, accessed 12/31/2017, at <https://doi.org/10.3133/ofr20161072>.

Desert Research Institute, 2020, Remote automatic weather stations USA climate archive: Desert Research Institute webpage, accessed December 16, 2020, at <http://www.raws.dri.edu>.

Dewitz, J., and U.S. Geological Survey, 2021, National Land Cover Database (NLCD) 2019 products: U.S. Geological Survey data release, accessed December 31, 2018, at <https://doi.org/10.5066/P9KZCM54>.

Dibblee, T.W., Jr., 1971, Geologic maps of seventeen 15-minute quadrangles (1:62,500) along the San Andreas fault in vicinity of King City, Coalinga, Panoche Valley, and Paso Robles, California, with index map (quadrangles are Adelaida, Bradley, Bryson, Coalinga, Greenfield, Hernandez Valley, Joaquin Rocks, King City, New Idria, Panoche Valley, Parkfield, Paso Robles, Polvadero Gap, Priest Valley, “Reef Ridge”, San Ardo, San Miguel): U.S. Geological Survey Open-File Report 71–87, scale 1:62,500. [Available at <https://doi.org/10.3133/ofr7187>.]

Dibblee, T.W., Jr., 1972, Geologic maps of fourteen 15-minute quadrangles along the San Andreas fault in the vicinity of Paso Robles and Cholame southeastward to Maricopa and Cuyama, California: U.S. Geological Survey Open-File Report 72–89, scale 1:62,500. [Available at <https://doi.org/10.3133/ofr7289>.]

Dimitrakopoulos, R., and Desbarats, A.J., 1993, Geostatistical modeling of grid block permeabilities for 3D reservoir simulators: *SPE Reservoir Engineering*, v. 8, no. 1, p. 13–18. [Available at <https://doi.org/10.2118/21520-PA>.]

Doherty, J., 2024, PEST-HP for Windows: Brisbane, Australia, Watermark Numerical Computing, 59 p.

Doherty, J.E., and Hunt, R.J., 2010, Approaches to highly parameterized inversion—A guide to using PEST for groundwater-model calibration: U.S. Geological Survey Scientific Investigations Report 2010–5169, 59 p. [Available at <https://doi.org/10.3133/sir20105169>.]

Durbin, T.J., Kapple, G.W., and Freckleton, J.R., 1978, Two-dimensional and three-dimensional digital flow models of the Salinas Valley ground-water basin: California, U.S. Geological Survey Water Resources Investigations, p. 78–113., 134 p.

Durham, D.L., 1974, Geology of the southern Salinas Valley area, California: U.S. Geological Survey Professional Paper 819, 111 p. [Available at <https://doi.org/10.3133/pp819>.]

Edinger-Marshall, S., and Letey, J., 1997, Irrigation shifts toward sprinklers, drip and microsprinklers: California Agriculture, v. 51, no. 3, p. 38–40. [Available at <https://doi.org/10.3733/ca.v051n03p38>.]

Faunt, C.C., Hanson, R.T., Schmid, W., Belitz, K., and Predmore, S., 2009a, Documentation of the ground-water flow model, chap. C of Faunt, C.C., ed., Ground-water availability of California's Central Valley: U.S. Geological Survey Professional Paper 1766, p. 121–212.

Faunt, C.C., Belitz, K., and Hanson, R.T., 2009b, Development of a three-dimensional model of sedimentary texture in valley-fill deposits of the Central Valley, California, USA: Hydrogeology Journal, v.18, no. 3, p. 625–649, accessed 12/31/2017, at <https://doi.org/10.1007/s10040-009-0539-7>.

Faunt, C.C., Hanson, R.T., Belitz, K., and Rogers, L., 2009c, California's Central Valley groundwater study—A powerful new tool to assess water resources in California's Central Valley: U.S. Geological Survey Fact Sheet 2009–3057, 4 p., , accessed 12/31/2017, at <https://doi.org/10.3133/fs20093057>.

Faunt, C.C., Stamos, C.L., Flint, L.E., Wright, M.T., Burgess, M.K., Sneed, M., Brandt, J., Martin, P., and Coes, A.L., 2015, Hydrogeology, hydrologic effects of development, and simulation of groundwater flow in the Borrego Valley, San Diego County, California: U.S. Geological Survey Scientific Investigations Report 2015–5150, 135 p., accessed 12/31/2017, at <https://doi.org/10.3133/sir20155150>.

Faunt, C.C., Traum, J.A., Boyce, S.E., Seymour, W.A., Jachens, E.R., Brandt, J.T., Sneed, M., Bond, S., and Marcelli, M.F., 2024, Groundwater sustainability and land subsidence in California's Central Valley: Water (Basel), v. 16, no. 8, p. 1189. [Available at <https://doi.org/10.3390/w16081189>.]

Feeney, M.B., and Rosenberg, L.I., 2003, Deep aquifer investigation—Hydrogeologic data inventory, review, interpretation and implications: Consultants technical memorandum to Monterey County Water Resources Agency, 40 p., accessed January 1, 2017, at <http://www.co.monterey.ca.us/home/showdocument?id=19614>.

Ferguson, I.A., and Llewellyn, D., 2015, Simulation of Rio Grande project operations in the Rincon and Mesilla Basins—Summary of model configuration and results: U.S. Bureau of Reclamation Technical Memorandum No. 86-68210-2015-05, 56 p.

Ferguson, I.A., Llewellyn, D., Hanson, R.T., and Boyce, S.E., 2016, User guide to the surface water operations process—Simulation of large-scale surface water management in MODFLOW-based hydrologic models: U.S. Bureau of Reclamation Technical Memorandum No. 86-68210-2015-XX, 79 p.

Ferriz, H., 2001, Groundwater resources of northern California—An overview, from engineering geology practice in Northern California: California Division of Mines and Geology Bulletin 210, 30 p.

Flint, A.L., and Flint, L.E., 2007, Application of the basin characterization model to estimate in-place recharge and runoff potential in the Basin and Range carbonate-rock aquifer system, White Pine County, Nevada, and adjacent areas in Nevada and Utah: U.S. Geological Survey Scientific Investigations Report 2007–5099, accessed 12/31/2017, at <https://doi.org/10.3133/sir20075099>.

Flint, L.E., and Flint, A.L., 2012, Downscaling future climate scenarios to fine scales for hydrologic and ecological modeling and analysis: *Ecological Processes*, v. 1, article no. 2, p. 2. [Available at <https://doi.org/10.1186/2192-1709-1-2>.]

Flint, L.E., Flint, A.L., and Stern, M.A., 2021, The basin characterization model—A regional water balance software package: U.S. Geological Survey Techniques and Methods, book 6, chap. H1, 85 p., accessed 12/31/2017, at <https://doi.org/10.3133/tm6H1>.

Fugro West, Inc. and Cleath and Associates, 2002, Final report Paso Robles groundwater basin study: Consultants report to County of San Luis Obispo Public Works Department, 396 p., accessed November 18, 2021, at [https://www.slocounty.ca.gov/Departments/Public-Works/Forms-Documents/Committees-Programs/Sustainable-Groundwater-Management-Act-\(SGMA\)/Paso-Robles-Groundwater-Basin/Archived-Documents/2002-08-PRGB-Study,-Phase-I.pdf](https://www.slocounty.ca.gov/Departments/Public-Works/Forms-Documents/Committees-Programs/Sustainable-Groundwater-Management-Act-(SGMA)/Paso-Robles-Groundwater-Basin/Archived-Documents/2002-08-PRGB-Study,-Phase-I.pdf).

GEOSCIENCE Support Services, Inc., 2013, Protective elevations to control seawater intrusion in the Salinas Valley, CA: Consultants technical memorandum to Monterey County Water Resources Agency, 36 p., accessed 12/31/2017, at <http://www.co.monterey.ca.us/home/showdocument?id=19642>.

GEOSCIENCE Support Services, Inc., 2016, Paso Robles groundwater basin model update 577: San Luis Obispo County Flood Control & Water Conservation District, 142 p.

Gibeault, V.A., Cockerham, S., Henry, J.M., and Meyer, J., 1989, California turfgrass—It's use, water requirement, and irrigation: *California Turfgrass Culture*, University of California Cooperative Extension, v. 39, no. 3–4, 14 p.

Golden, N.E., and Cochrane, G.R., eds., 2013, California State waters map series data catalog: U.S. Geological Survey Data Series 781, accessed 12/31/2017, at <https://doi.org/10.3133/ds781>.

Greene, H.G., 1970, Geology of southern Monterey Bay and its relationship to the groundwater basin and salt water intrusion: U.S. Geological Survey Open-File Report 70–141, 50 p., 5 plates.

Greene, H.G., 1977, Geology of the Monterey Bay region: U.S. Geological Survey Open-File Report 77–718, 347 p., 9 sheets, accessed 12/31/2017, at <https://doi.org/10.3133/ofr77718>.

Greene, H.G., and Clark, J.C., 1979, Neogene paleogeography of the Monterey Bay area, California, in Armentrout, J.M., Cole, M.R., and Ter Best, H., Jr., eds., Cenozoic paleogeography of the western United States: Pacific Coast Paleogeography Symposium 3, p. 277–296.

Hall, P., 1992, Selected geological cross sections in the Salinas Valley using GEOBASE: Consultants report to Monterey County Water Resources Agency, 124 p.

Hanson, B., and Bendixen, W., 2004, Drip irrigation evaluated in Santa Maria Valley strawberries: California Agriculture, University of California, v. 58, no. 1, 48 p. [Available at <https://doi.org/10.3733/ca.v058n01p48>.]

Hanson, R.T., 1988, Aquifer-system compaction, Tucson basin and Avra Valley, Arizona: U.S. Geological Survey Water-Resources Investigation Report 88–4172, 69 p.

Hanson, R.T., Anderson, S.R., and Pool, D.R., 1990, Simulation of ground-water flow and potential land subsidence, Avra Valley, Arizona: U.S. Geological Survey Water-Resources Investigation Report 90–4178, 41 p. , accessed 12/31/2017, at <https://doi.org/10.3133/wri904178>.

Hanson, R.T., and Benedict, J.F., 1994, Simulation of ground-water flow and potential land subsidence, upper Santa Cruz River Basin, Arizona: U.S. Geological Survey Water-Resources Investigation Report 93–4196, 47 p. , accessed 12/31/2017, at <https://doi.org/10.3133/wri934196>.

Hanson, R.T., Boyce, S.E., Schmid, W., Hughes, J.D., Mehl, S.M., Leake, S.A., Maddock, T., III, and Niswonger, R.G., 2014a, MODFLOW-One-Water Hydrologic Flow Model (MF-OWHM): U.S. Geological Survey Techniques and Methods, book 6, chap. A51, 122 p.

Hanson, R.T., and Leake, S.A., 1998, Documentation for HYDMOD, A program for time-series data from the U.S. Geological Survey's modular three-dimensional finite-difference ground-water flow model: U.S. Geological Survey Open-File Report 98–564, 57 p.

Hanson, R.T., Everett, R.R., Newhouse, M.W., Crawford, S.M., Pimentel, M.I., and Smith, G.A., 2002, Geohydrology of a deep-aquifer system monitoring-well site at Marina, Monterey County, California: U.S. Geological Survey Water-Resources Investigation 02–4003, 73 p., accessed 12/31/2017, at <https://doi.org/10.3133/wri024003>.

Hanson, R.T., Flint, L.E., Faunt, C.C., Gibbs, D.R., and Schmid, W., 2014b, Hydrologic models and analysis of water availability in Cuyama Valley, California: U.S. Geological Survey

Scientific Investigations Report 2014–5150, 150 p., accessed 12/31/2017, at <https://doi.org/10.3133/sir20145150>.

Hanson, R.T., Li, Z., and Faunt, C.C., 2004, Documentation of the Santa Clara Valley regional ground-water/surface-water flow model, Santa Clara County, California: U.S. Geological Survey Scientific Investigations Report 2004–5231, 75 p., accessed 12/31/2017, at <https://pubs.usgs.gov/sir/2004/5231>. <https://doi.org/10.3133/sir20045231>

Hanson, R.T., Lockwood, B., and Schmid, W., 2014c, Analysis of projected water availability with current basin management plan, Pajaro Valley, California: *Journal of Hydrology*, v. 519, p. 131–147, accessed 12/31/2017, at <https://doi.org/10.1016/j.jhydrol.2014.07.005>.

Hanson, R.T., Martin, P., and Koczot, K.M., 2003, Simulation of ground-water/surface-water flow in the Santa Clara-Calleguas basin, California: U.S. Geological Survey Water-Resources Investigation Report 02–4136, 214 p., accessed 12/31/2017, at <https://water.usgs.gov/pubs/wri/wri024136/text.html>.

Hanson, R.T., Schmid, W., Faunt, C.C., Lear, J., and Lockwood, B., 2014d, Integrated hydrologic model of Pajaro Valley, Santa Cruz and Monterey Counties, California: U.S. Geological Survey Scientific Investigations Report 2014–5111, 166 p., accessed 12/31/2017, at <https://doi.org/10.3133/sir20145111>.

Harbaugh, A.W., 2005, MODFLOW-2005, the U.S. Geological Survey modular ground-water model—the ground-water flow process: U.S. Geological Survey Techniques and Methods, book 6, chap. A16, variously paginated. [Available at <https://doi.org/10.3133/tm6A16>.]

Harding ESE, 2001, Final report—Hydrogeologic investigation of the Salinas Valley basin in the vicinity of Fort Ord and Marina, Salinas Valley, California: Consultants report to Monterey County Water Resources Agency, 41 p.

Hart, E.W., 1985, Rinconada fault (Espinosa and San Marcos segments), Monterey and San Luis Obispo Counties: California Division of Mines and Geology Fault Evaluation Report FER-175, 8 p., 2 sheets, scale 1:24,000.

Harter, T., Lund, J.R., Darby, J.L., Fogg, G.E., Howitt, R., Jessoe, K.K., Pettygrove, S.G., Quinn, J.F., Viers, J.H., Boyle, D.B., and Canada, H.E., De La Mora, N., Dzarella, K.N., Fryjoff-Hung, A., Hollander, A.D., Honeycutt, K.L., Jenkins, M.W., Jensen, V.B., King, A.M., Kourakos, G., Lopez, E.M., Mayzelle, M.M., McNally, A., Medellin-Azuara, J., and Rosenstock, T.S., 2012, Addressing nitrate in California’s drinking water with a focus on Tulare Lake Basin and Salinas Valley: Groundwater Report for the State Water Resources Control Board Report to the Legislature, 92 p. [Available at <https://ucanr.edu/sites/groundwaternitrate/files/138956.pdf>.]

Helm, D.C., 1975, One-dimensional simulation of aquifer-system compaction near Pixley, California—1, Constant parameters: American Geophysical Union, Water Resources Research, v. 11, no. 3, p. 465–478. [Available at <https://doi.org/10.1029/WR011i003p00465>.]

Henson, W., Boyce, S.E., Franklin, H., Woodrow, A., Baillie, M., and Jachens, E.R., 2022b, Salinas Valley operational model—Input operational data: U.S. Geological Survey data release, accessed 12/31/2017, at <https://doi.org/10.5066/P9CWNHN3>.

Henson, W.R., Earll, E.M., Bond, S., Jachens, E.R., and Woodrow, A., 2023, Lower Salinas Valley hydrologic models—Agricultural and municipal water supply and groundwater data: U.S. Geological Survey data release, accessed 12/31/2017, at <https://doi.org/10.5066/P9U67MIQ>.

Henson, W.R., Hevesi, J.A., Hanson, R.T., Bittner, D., Herbert, D.M., and Jachens, E.R., 2022a, Salinas Valley hydrologic models—Surface water data: U.S. Geological Survey data release, accessed 12/31/2017, at <https://doi.org/10.5066/P93COXL6>.

Henson, W.R., Hevesi, J.A., Hanson, R.T., Stern, M.A., and Jachens, E.R., 2022c, Lower Salinas Valley hydrologic models—Climate data: U.S. Geological Survey data release, accessed 12/31/2017, at <https://doi.org/10.5066/P9GTQCCF>.

Henson, W.R., and Jachens, E.R., 2022, Lower Salinas Valley hydrologic models—Discretization data: U.S. Geological Survey data release, accessed 12/31/2017, at <https://doi.org/10.5066/P9850MAK>.

Henson, W.R., Medina, R.L., Mayers, C.J., Niswonger, R.G., and Regan, R.S., 2013, CRT—Cascade Routing Tool to define and visualize flow paths for grid-based watershed models: U.S. Geological Survey Techniques and Methods, book 6, chap. D2, 28 p. [Available at <https://doi.org/10.3133/tm6D2>.]

Henson, W.R., and Voss, S.A., 2023, CalPUR land use estimation processing script, version 1.0: U.S. Geological Survey software release, accessed 12/31/2017, at <https://doi.org/10.5066/P9GUWKZZ>.

Henson, W.R., Hevesi, J.A., Hanson, R.T., Bittner, D., Herbert, D.M., and Jachens, E.R., 2022, Lower Salinas Valley Hydrologic Models: Climate Data: U.S. Geological Survey data release, <https://doi.org/10.5066/P9GTQCCF>.

Henson, W., Martin, D.J., Woodrow, A., and Jachens, E.R., 2024, Salinas Valley integrated hydrologic model and Salinas Valley operational model land use data: U.S. Geological Survey data release, accessed 12/31/2017, at <https://doi.org/10.5066/P9KSNNUD>

Henson, W., Hevesi, J.A., and Jachens, E.R., 2025, Henson, W., Hevesi, J.A., and Jachens, E.R., 2024, Lower Salinas Valley Hydrologic Models: Input Inflow Data: U.S. ScienceBase data release , <https://doi.org/10.5066/P9HAG7ZI> .

- Henson, W., and Culling, D., 2025, Salinas Valley integrated hydrologic models: U.S. Geological Survey data release, <https://doi.org/10.5066/P916YRM2>.
- Hevesi, J.A., Henson, W.R., Hanson, R.T., Earll, M.M., Herbert, D., and Jachens, E., 2025a, Application of Hydrologic Simulation Program-FORTRAN (HSPF) as part of an integrated hydrologic model for the Salinas Valley, California: U.S. Geological Survey Scientific Investigations Report 2025–5xxx, xx p., <https://doi.org/10.5066/XXXX>.
- Hevesi, J., Henson, W., Hanson, R.T., Earll, M.M., Herbert, D.M., and Jachens, E.R. (2025b). Salinas Valley Watershed Model: Application of Hydrologic Simulation Program-FORTRAN (HSPF). U.S. Geological Survey data release, <https://doi.org/10.5066/P9FJAWC4>.
- Hevesi, J.A., Wesley, H., Hanson, R.T., Stern, M.A., and Jachens, E.R., 2022, Salinas Valley hydrologic system—Regional climate data: U.S. Geological Survey data release, accessed 12/31/2017, at <https://doi.org/10.5066/P942J2BC>.
- Hill, M.C., Banta, E.R., Harbaugh, A.W., and Anderman, E.R., 2000, MODFLOW-2000, The U.S Geological Survey modular ground-water model—User guide to the observation, sensitivity, and parameter-estimation processes and three post-processing programs: U.S. Geological Survey Open-File Report 00–184, 209 p. [Available at <https://doi.org/10.3133/ofr00184>.]
- Hill, M.C., and Tiedeman, C.R., 2007, Effective groundwater model calibration—With analysis of data, sensitivities, predictions, and uncertainty: New York, Wiley and Sons, 464 p. [Available at <https://doi.org/10.1002/0470041080>.]
- Hsieh, P.A., and Freckelton, J.R., 1993, Documentation of a computer program to simulate horizontal-flow barriers using the U.S. Geological Survey’s modular three-dimensional finite-difference ground-water-flow model: U.S. Geological Survey Open-File Report 92–477, 32 p.
- Hydrometrics, 2009, Seaside groundwater basin modeling and protective groundwater elevations: Consultants report prepared for the Seaside Basin Watermaster by Hydrometrics LLC, 210 p.
- Jacob, C.E., 1940, On the flow of water in an elastic artesian aquifer: Transactions - American Geophysical Union, v. 21, no. 2, p. 574–586. [Available at <https://doi.org/10.1029/TR021i002p00574>.]
- Jennings, C.W., with modifications by Gutierrez, C., Bryant, W., Saucedo, G., and Wills, C., 2010, Geologic map of California: California Geological Survey Geologic Data Map No. 2, scale 1:750,000, accessed 12/31/2017, at <https://maps.conservation.ca.gov/cgs/gmc>.
- Johnson, S.Y., Dartnell, P., Hartwell, S.R., Cochrane, G.R., Golden, N.E., Watt, J.T., Davenport, C.W., Kvitek, R.G., Erdey, M.D., Kringsman, L.M., Sliter, R.W., and Maier, K.L., (Johnson, S.Y., and S.A., eds.), 2016, California State waters map series—Offshore of Monterey, California:



U.S. Geological Survey Open-File Report 2016–1110, pamphlet 44 p., 10 sheets, scale 1:24,000, accessed 12/31/2017, at <https://doi.org/10.3133/ofr20161110>.

Kennedy/Jenks, 2004a, Final report—Hydrostratigraphic analysis of the northern Salinas Valley: Consultants report to Monterey County Water Resources Agency, [variously paged].

Kennedy/Jenks, 2004b, Hydrogeologic analysis of the northern Salinas Valley: Consultants report prepared for Monterey County Water Resources Agency, 98 p.

Konikow, L.F., Hornberger, G.Z., Halford, K.J., and Hanson, R.T., 2009, Revised Multi-Node Well (MNW2) package for MODFLOW groundwater flow model: U.S. Geological Survey Techniques, book 6, chap. A30, 67 p.

Krause, P., Boyle, D.P., and Bäse, F., 2005, Comparison of different efficiency criteria for hydrological model assessment: *Advances in Geosciences*, v. 5, p. 89–97. [Available at <https://doi.org/10.5194/adgeo-5-89-2005>.]

Kulongoski, J.T., and Belitz, K., 2007, Ground-water quality data in the Monterey Bay and Salinas Valley Basins, California, 2005—Results from the California GAMA Program: U.S. Geological Survey Data Series 258, 84 p. [Available at <https://doi.org/10.3133/ds258>.]

Lapham, M.H., and Heileman, W.H., 1901, Soil survey of the lower Salinas Valley: California, U.S. Department of Agriculture, Bureau of Soils.

Laudon, J., and Belitz, K., 1991, Texture and depositional history of late Pleistocene-Holocene alluvium in the central part of the western San Joaquin Valley, California: *Environmental & Engineering Geoscience*, v. xxviii, no. 1, p. 73–88. [Available at <https://doi.org/10.2113/gsegeosci.xxviii.1.73>.]

Leedshill-Herkenhoff, Inc., 1985, Salinas Valley seawater intrusion study: Prepared for the Monterey County Flood Control and Water Conservation District.

Leighton, D.A., Fio, J.L., and Metzger, L.F., 1995, Database of well and areal data, South San Francisco Bay and Peninsula area, California: U.S. Geological Survey Water-Resources Investigations Report 94–4151, 47 p., accessed 12/31/2017, at <https://pubs.er.usgs.gov/publication/wri944151>.

Manning, J.C., 1963, Resume of ground water hydrology in Salinas Valley, California: HydroDevelopment, Inc., Bakersfield, California, 5 p.

Markstrom, S.L., Niswonger, R.G., Regan, R.S., Prudic, D.E., and Barlow, P.M., 2008, GSFLOW—Coupled ground-water and surface-water flow model based on the integration of the Precipitation-Runoff Modeling System (PRMS) and the Modular Ground-Water Flow Model

(MODFLOW-2005): U.S. Geological Survey Techniques and Methods, book 6, chap. D1, 240 p., accessed 12/31/2017, at <https://doi.org/10.3133/tm6D1>.

Monterey County Agricultural Commission, 2022, Annual crop reports: Monterey County Agricultural Commission webpage, accessed December 31, 2022, at [www.co.monterey.ca.us/government/departments-a-h/agricultural-commissioner/forms-publications/crop-reports-economic-contributions](http://www.co.monterey.ca.us/government/departments-a-h/agricultural-commissioner/forms-publications/crop-reports-economic-contributions).

Monterey County Water Resources Agency (MCWRA), 1995, 1995—Hydrogeology and water supply of Salinas Valley, White paper by Salinas Valley Ground Water Basin Hydrology Conference: Monterey County Water Resources Agency Water Reports. 21 p., accessed 12/31/2017, at [https://digitalcommons.csumb.edu/hornbeck\\_cgb\\_6\\_a/25](https://digitalcommons.csumb.edu/hornbeck_cgb_6_a/25).

Monterey County Water Resources Agency (MCWRA), 1996, Summary report—1995 groundwater extraction data and agricultural water conservation practices: Monterey County Water Resources Agency, 8 p.

Monterey County Water Resources Agency (MCWRA), 2001, Draft environmental impact report/environmental impact statement for the Salinas Valley water project. Monterey County Water Resources Agency, 21 p.

Monterey County Water Resources Agency (MCWRA), 2005, Salinas Valley water project flow prescription for Steelhead trout in the Salinas River: Salinas, California, October 2005, 140 p. accessed 12/31/2017, at <http://www.co.monterey.ca.us/home/showdocument?id=23311>.

Monterey County Water Resources Agency (MCWRA), 2018, Nacimiento Dam operation policy: Monterey County Water Resources Agency, 31 p. plus appendixes, accessed December 31, 2018, at <https://www.co.monterey.ca.us/Home/ShowDocument?id=63151>.

Monterey County Water Resources Agency (MCWRA), 2020, Recommendations to address the expansion of seawater intrusion in the Salinas Valley groundwater basin—2020 Update. Monterey County Water Resources Agency, 96 p.

Monterey County Water Resources Agency (MCWRA), 2023, Groundwater elevation contour and 500 milligram per liter chloride isocontour data: Monterey County Water Resources Agency data, accessed March 26, 2023, at <https://www.co.monterey.ca.us/government/government-links/water-resources-agency/documents/groundwater-elevation-contours>.

Montgomery Watson, 1997, Salinas River Basin water resources management plan task 1.09, 1994, Salinas Valley groundwater flow and quality model report: prepared for Monterey County Water Resources Agency by Montgomery Watson, 189 p.

Moran, J.E., Esser, B.K., Hillemonds, D., Holtz, M., Roberts, S.K., Singleton, M.J., and Visser, A., 2011, California GAMA special study—Nitrate fate and transport in the Salinas Valley:

Lawrence Livermore National Lab Report No. LLNL-TR-484186, 52 p. [Available at <https://doi.org/10.2172/1122241>.]

Motz, L.H., and Sedighi, A., 2009, Representing the coastal boundary condition in regional groundwater flow models: *Journal of Hydrologic Engineering*, v. 14, no. 8, p. 821–831. [Available at [https://doi.org/10.1061/\(ASCE\)HE.1943-5584.0000049](https://doi.org/10.1061/(ASCE)HE.1943-5584.0000049).]

Nalder, I.A., and Wein, R.W., 1998, Spatial interpolation of climatic normal—Test of a new method in the Canadian boreal forest: *Agricultural and Forest Meteorology*, v. 92, no. 4, p. 211–225. [Available at [https://doi.org/10.1016/S0168-1923\(98\)00102-6](https://doi.org/10.1016/S0168-1923(98)00102-6).]

Nash, J.E., and Sutcliffe, J.V., 1970, River flow forecasting through conceptual models part I—A discussion of principles: *Journal of Hydrology*, v. 10, no. 3, p. 282–290. [Available at [https://doi.org/10.1016/0022-1694\(70\)90255-6](https://doi.org/10.1016/0022-1694(70)90255-6)].

National Marine Fisheries Service, 2007, Biological opinion of the Salinas Valley water project—National Oceanic and Atmospheric Administration: Southwest Region, 123 p.

National Oceanic and Atmospheric Administration, 2019, Tides and currents—Datums for 9413450 and 9414290, Monterey CA: National Oceanic and Atmospheric Administration data, accessed December 16, 2019, at <https://www.tidesandcurrents.noaa.gov>.

National Oceanic and Atmospheric Administration, 2020, Cooperative observer network climate data for sites within Monterey County: National Oceanic and Atmospheric Administration database, accessed December 16, 2020, at <http://www.ncdc.noaa.gov>.

Niswonger, R.G., and Prudic, D.E., 2005, Documentation of the Streamflow-Routing (SFR2) Package to include unsaturated flow beneath streams—A modification to SFR1: *U.S. Geological Survey Techniques and Methods*, book 6, chap. A13, 50 p. [Available at <https://doi.org/10.3133/tm6A13>.]

Nutter, E.H., 1901, Sketch of the geology of the Salinas Valley, California: *The Journal of Geology*, v. 9, no. 4, p. 330–336. [Available at <https://doi.org/10.1086/620913>.]

Orang, M.N., Scott Matyac, J., and Snyder, R.L., 2008, Survey of irrigation methods in California in 2001: *Journal of Irrigation and Drainage Engineering*, v. 134, no. 1, p. 96–100. [Available at [https://doi.org/10.1061/\(ASCE\)0733-9437\(2008\)134:1\(96\)](https://doi.org/10.1061/(ASCE)0733-9437(2008)134:1(96)).]

Orgaz, F., Fernández, M.D., Bonachela, S., Gallardo, M., and Fereres, E., 2005, Evapotranspiration of horticultural crops in an unheated plastic greenhouse: *Agricultural Water Management*, v. 72, no. 2, p. 81–96. [Available at <https://doi.org/10.1016/j.agwat.2004.09.010>.]

Phillips, S.P., and Belitz, K., 1991, Calibration of a textured-based model of a ground-water flow system, western San Joaquin Valley, California: *Ground Water*, v. 29, no. 5, p. 702–715. [Available at <https://doi.org/10.1111/j.1745-6584.1991.tb00562.x>.]

Phillips, S.P., Green, C.T., Burow, K.R., Shelton, J.L., and Rewis, D.L., 2007, Simulation of multiscale ground-water flow in part of the northeastern San Joaquin Valley, California: U.S. Geological Survey Scientific Investigations Report 2007–5009, 43 p. [Available at <https://doi.org/10.3133/sir20075009>.]

PRISM Climate Group, 2020 Parameter-elevation Relationships on Independent Slopes Model (PRISM): Climate Group, Oregon State University, accessed December 16, 2020, at <https://prism.oregonstate.edu>.

Sandoval-Solis, S., Orang, M., Snyder, R.L., Orloff, S., Williams, K.E., and Rodriguez, J.M., 2013, Spatial analysis of application efficiencies in irrigation for the State of California—Final report—Water Management Research Group. University of California Davis, 115 p.

Schmid, W., and Hanson, R.T., 2009, The farm process version 2 (FMP2) for MODFLOW-2005—Modifications and upgrades to FMP1: U.S. Geological Survey Techniques in Water Resources Investigations, book 6, chap. A32, 102 p. [Available at <https://doi.org/10.3133/tm6A32>.]

Schmid, W., Hanson, R.T., Maddock, T.M., III, and Leake, S.A., 2006, User's guide for the Farm Package (FMP1) for the U.S. Geological Survey's modular three-dimensional finite-difference ground-water flow model, MODFLOW-2000: U.S. Geological Survey Techniques and Methods, book 6, chap. A17, 127 p., accessed 12/31/2017, at <https://pubs.usgs.gov/tm/2006/tm6A17>.

Showalter, P., Akers, J.P., and Swain, L.A., 1983, Design of a ground-water quality monitoring network for the Salinas River Basin, California: U.S. Geological Survey Water Resources Investigation Report 83–4049, 74 p.

Smukler, S.M., Jackson, L.E., Murphree, L., Yokota, R., Koike, S.T., and Smith, R.F., 2008, Transition to large-scale organic vegetable production in the Salinas Valley, California: *Agriculture, Ecosystems & Environment*, v. 126, no. 3–4, p. 168–188. [Available at <https://doi.org/10.1016/j.agee.2008.01.028>.]

Snyder, R.L., Lamina, B.J., Shaw, D.A., and Pruitt, W.O., 1987a, Using reference evapotranspiration (E<sub>Th</sub>) and crop coefficients to estimate crop evapotranspiration (E<sub>tc</sub>) for agronomic crops, grasses, and vegetable crops: Cooperative Extension of the University of California Division of Agriculture and Natural Resources, Leaflet 21427, 12 p.

Snyder, R.L., Lamina, B.J., Shaw, D.A., and Pruitt, W.O., 1987b, Using reference evapotranspiration (E<sub>Th</sub>) and crop coefficients to estimate crop evapotranspiration (E<sub>tc</sub>) for

trees and vines: Cooperative Extension of the University of California, Division of Agriculture and Natural Resources, Leaflet 21428, 8 p.

Snyder, R.L., and Schullbach, K.F., 1992, Central coast crop coefficients for field and vegetable crops: California Department of Water Resources, Water Conservation Office, Drought Tips No. 92-45, 12 p.

Staal, Gardner, and Dunne, Inc., 1993, Hydrogeologic study—Salinas Valley groundwater basin seawater intrusion delineation/monitoring well construction program—180-Foot Aquifer, Salinas area, California: Consultants report to Monterey County Water Resources Agency, 41 p.

Sweetkind, D.S., 2017, Three-dimensional hydrogeologic framework model of the Rio Grande transboundary region of New Mexico and Texas, USA, and northern Chihuahua, Mexico: U.S. Geological Survey Scientific Investigations Report 2017–5060, 49 p. [Available at <https://doi.org/10.3133/sir20175060>.]

Sweetkind, D.S., 2023, Digital data for the Salinas Valley Geologic framework, California: U.S. Geological Survey data release, accessed 12/31/2017, at <https://doi.org/10.5066/P9IL8VBD>.

Sweetkind, D.S., Faunt, C.C., and Hanson, R.T., 2013, Construction of 3-D geologic framework and textural models for Cuyama Valley groundwater basin, California: U.S. Geological Survey Scientific Investigations Report 2013–5127, 46 p. [Available at <https://doi.org/10.3133/sir20135127>.]

Thorup, R.R., 1983, Hydrogeologic report on the deep aquifer, Salinas Valley, Monterey County, California: Consultants report to Monterey County Board of Supervisors, 40 p.

Thorup, R.R., 1985, Summary hydrogeological report on the relationship of the 4 recently completed water wells on Fort Ord military reservation to the Salinas Valley 180 and 400 foot aquifers: Consultants report to Monterey County Board of Supervisors, [variously paged].

Tindula, G.N., Orang, M.N., and Snyder, R.L., 2013, Survey of irrigation methods in California in 2010: *Journal of Irrigation and Drainage Engineering*, v. 139, no. 3, p. 233–238. [Available at [https://doi.org/10.1061/\(ASCE\)IR.1943-4774.0000538](https://doi.org/10.1061/(ASCE)IR.1943-4774.0000538).]

Tinsley, J.C., III, 1975, Quaternary geology of northern Salinas Valley, Monterey County, California: Dissertation, Stanford University, 213 p.

U.S. Census Bureau, 2018, Published population estimates for Monterey County: U.S. Department of Commerce data, accessed November 2018, at [www.data.census.gov](http://www.data.census.gov).

U.S. Department of Agriculture, 2016, USGS EROS archive-aerial photography-national agriculture imagery program: U.S. Geological Survey database, accessed December 16, 2016, at <https://doi.org/10.5066/F7QN651G>.

U.S. Geological Survey, 2000, National Land Cover Database (NLCD) 1992 land cover conterminous United States: U.S. Geological Survey data release, accessed December 31, 2018, at <https://doi.org/10.5066/P92G34R9>.

U.S. Geological Survey, 2003, National Land Cover Database (NLCD) 2001 land cover conterminous United States: U.S. Geological Survey data release, accessed December 31, 2018, at <https://doi.org/10.5066/P9MZGHLF>.

U.S. Geological Survey, 2011, National Land Cover Database (NLCD) 2006 land cover conterminous United States: U.S. Geological Survey data release, accessed December 31, 2018, at <https://doi.org/10.5066/P9HBR9V3>.

U.S. Geological Survey, 2013, National Elevation Dataset (USGS NED n35w121 1/3 arc-second 2013 1 x 1 degree ArcGrid: U.S. Geological Survey dataset, accessed March 8, 2016, at <https://www.usgs.gov/core-science-systems/nationalgeospatial-program/national-map>.

U.S. Geological Survey, 2014, National Land Cover Database (NLCD) 2011 land cover conterminous United States: U.S. Geological Survey data release, accessed December 31, 2018, at <https://doi.org/10.5066/P97S2IID>.

U.S. Geological Survey, 2018, USGS water data for the Nation: U.S. Geological Survey National Water Information System, accessed December 23, 2018, at <https://doi.org/10.5066/F7P55KJN>.

U.S. Geological Survey, 2019a, 3D elevation program 1-meter resolution digital elevation model: U.S. Geological Survey dataset, accessed October 23, 2019, at <https://www.usgs.gov/the-national-map-data-delivery>.

U.S. Geological Survey, 2019b, National hydrography dataset: U.S. Geological Survey web page, accessed January 3, 2020, at <https://www.usgs.gov/national-hydrography/national-hydrography-dataset>.

U.S. Geological Survey, [2024], USGS water data for the Nation: U.S. Geological Survey National Water Information System database, accessed [10/1/2023], at <https://doi.org/10.5066/F7P55KJN>.

U.S. Geological Survey and California Geological Survey, 2021, Quaternary fault and fold database for the United States: U.S. Geological Survey database, accessed November 19, 2021, at <https://www.usgs.gov/natural-hazards/earthquake-hazards/faults>.

Wagner, D.L., Greene, H.G., Saucedo, G.J., and Pridmore, C.L., 2002, Geologic map of the Monterey 30' x 60' quadrangle and adjacent areas, California: California Geological Survey Regional Geologic Map Series, scale 1:100,000, accessed 12/31/2017, at [http://ngmdb.usgs.gov/Prodesc/proddesc\\_63084.htm](http://ngmdb.usgs.gov/Prodesc/proddesc_63084.htm).

Watt, J.M., Morin, R.L., and Langenheim, V.E., 2010, Using potential fields to refine basin and fault geometry in Salinas Valley, California: Geological Society of America Abstracts with Programs, v. 42, no. 4, 78 p.

White, J.T., Hemmings, B., Fienen, M.N., and Knowling, M.J., 2021, Towards improved environmental modeling outcomes—Enabling low-cost access to high-dimensional, geostatistical-based decision-support analyses: Environmental Modelling & Software, v. 139, p. 105022. [Available at <https://doi.org/10.1016/j.envsoft.2021.105022>.]

Williamson, A.K., Prudic, D.E., and Swain, L.A., 1989, Ground-water flow in the Central Valley, California: U.S. Geological Survey Professional Paper 1401–D, 127 p. [Available at <https://doi.org/10.3133/pp1401D>.]

Xie, Y., Lark, T.J., Brown, J.F., and Gibbs, H.K., 2022, Mapping irrigated cropland extent across the conterminous United States at 30m resolution using a semi-automatic training approach on Google Earth Engine: ISPRS Journal of Photogrammetry and Remote Sensing, v. 1, no. 155, p. 136–149.

Yates, E.B., 1988, Simulated effects of ground-water management alternatives for the Salinas Valley, California: U.S. Geological Survey Water-Resources Investigations Report 87–4066, 86 p.

**Table 1.** Summary of MODFLOW-One Water Hydrologic Model (MF-OWHM) packages and processes used in the Salinas Valley Integrated Hydrologic Model and Salinas Valley Operational Model.

Computer program (packages, processes, parameter estimation)	Function	Reference
<b>Processes and Solvers</b>		
Farm process (FMP)	Setup and solve equations simulating use and movement of water on the landscape as irrigated agriculture, urban landscape, and natural vegetation.	Schmid and Hanson (2009) Boyce and others (2020)
Surface Water Operations (SWO)	Subpackage of FMP that simulates the reservoir storage, releases and operations for the operational model.	Henson and others (2023)
Groundwater Flow (GWF) processes of MODFLOW model	Setup and solve equations simulating a basic groundwater flow model.	Harbaugh (2005)
Preconditioned Conjugate-Gradient with improved Nonlinear control (PCGN)	Solves groundwater flow equations; requires convergence of heads and (or) flow rates.	Harbaugh (2005)
<b>Discretization</b>		
Basic Package (BAS6)	Defines the initial conditions and some of the boundary conditions of the model.	Harbaugh (2005)
Discretization Package (DIS)	Space and time information.	Harbaugh (2005)
<b>Boundary Conditions</b>		
Streamflow Routing (SFR2)	Simulates the routed streamflow, infiltration, exfiltration, runoff, and return-flows from FMP.	Niswonger and Prudic (2005)
General Head Boundaries (GHB)	Head-dependent boundary condition used along the edge of the model to allow groundwater to flow into or out of the model under a regional gradient.	Harbaugh (2005)
Multi-node Wells (MNW2)	Simulates pumpage from wells with screens that span multiple layers.	Konikow and others (2009)
Drain Return Package (DRT)	Simulates drain boundary condition and routes drain flows to streams.	Harbaugh (2005)
<b>Aquifer Parameters</b>		
Layer Property Flow Package (LPF)	Calculates the hydraulic conductance between cell centers.	Harbaugh (2005)
Hydrologic Flow Barriers (HFB6)	Simulates a groundwater barrier by defining a hydraulic conductance between two adjacent cells in the same layer.	Hsieh and Freekelton (1993)
Multiplier Package (MULT)	Defines multiplier arrays for calculation of model-layer characteristics from parameter values.	Harbaugh (2005)
Zones (ZONE)	Defines arrays of different zones. Parameters may be composed of one or many zones.	Harbaugh (2005)
<b>Output and Observations</b>		
Head Observation (HOB)	Defines the head observation and weight by layer(s), row, column, and time and generates simulated values for comparison with observed values.	Hill and others (2000) Harbaugh (2005)
Hydmod (HYD)	Generates simulated values for specified locations at each time step for groundwater levels and streamflow attributes.	Hanson and Leake (1998)



---

Files

Name File (Name)	Controls the capabilities of MODFLOW One Water Hydrologic Model used during a simulation. Lists most of the files used in the model, observations, and Farm Package (FMP) Processes.	Harbaugh (2005)
Output Control Option (OC)	Used in conjunction with flags in other packages to output head, drawdown, and budget information for specified time periods into separate files.	Harbaugh (2005)
List File	Output file for allocation information, values used by the GWF, and calculated results such as head, drawdown, and the water budget.	Harbaugh (2005)

**Table 2.** Summary of analysis regions, Salinas Valley groundwater subbasins, named subareas, water-balance subregions, and their available water sources to meet demands.

[—, no data]

Analysis region	Salinas Valley groundwater subbasin	Water balance subregion	Water balance subregion identifier	Region description	Simulated water supply
Riparian Pressure	—	Riparian Corridor	1	Monterey and San Luis Obispo Counties	Root zone
	180-Foot/400-Foot Aquifer	Castroville Seawater Intrusion Project Area	2	Area receiving water from Castroville Seawater Intrusion Project	Root zone, surface water, groundwater, recycled water
Pressure Forebay	180-Foot/400-Foot Aquifer	Coastal Urban areas	3	Areas containing cities of Salinas, Castroville, Marina, Seaside, Sand City, Monterey, Del Rey Oaks	Root zone, municipal groundwater
		Inland Urban areas	4	Areas containing cities of Chualar, Gonzales, Soledad, Greenfield, King City, & San Ardo	Root zone, municipal groundwater
Outside	180-Foot/400-Foot Aquifer	Highlands South	5	Northwest of East Side analysis region outside of Zone 2C	Root zone, groundwater
East Side	Langley Area	Granite Ridge	6	Northwest of East Side analysis region outside of Zone 2C	Root zone, groundwater
Outside	Monterey	Corral De Tierra	7	South of Pressure part within Zone 2C	Root zone, groundwater
Pressure	180-Foot/400-Foot Aquifer	Blanco Drain Area	8	Drain subarea within Pressure subarea of Zone2C	Root zone, groundwater
East Side	East Side Aquifer	East Side	9	Remainder of East Side subarea in Zone2C	Root zone, groundwater
Pressure	180-Foot/400-Foot Aquifer	Pressure Northeast	10	Pressure subarea northeast of Salinas River in Zone 2C	Root zone, groundwater
Pressure	180-Foot/400-Foot Aquifer	Pressure Southwest	11	Pressure subarea southwest of Salinas River in Zone 2C	Root zone, groundwater
Forebay	Forebay Aquifer	Forebay Northeast	12	Forebay subarea northeast of Salinas River in Zone 2C	Root zone, groundwater
Forebay	Forebay Aquifer	Forebay Southwest	13	Forebay subarea southwest of Salinas River in Zone 2C	Root zone, groundwater
Forebay	Forebay Aquifer	Arroyo Seco	14	Subarea southwest of Salinas River outside of Zone 2C	Root zone, groundwater
Forebay	Forebay Aquifer	Clark Colony	15	Subarea southwest of Salinas River partly outside of Zone 2C	Root zone, surface water, groundwater

Upper Valley	Upper Valley Aquifer	Upper Valley Northeast	16	Upper Valley subarea northeast of Salinas River and northeast of King City in Zone 2C	Root zone, groundwater
Upper Valley	Upper Valley Aquifer	Upper Valley Northwest	17	Upper Valley subarea northwest of Salinas River and west of King City in Zone 2C	Root zone, groundwater
Upper Valley	Upper Valley Aquifer	Upper Valley Southeast	18	Upper Valley subarea southeast of Salinas River and east of King City in Zone 2C	Root zone, groundwater
Upper Valley	Upper Valley Aquifer	Upper Valley Southwest	19	Upper Valley subarea southwest of Salinas River and west of King City in Zone 2C	Root zone, groundwater
Below Dam	Upper Valley Aquifer	Below Dam	20	Subregion below Nacimiento Dam and within Zone 2C	Root zone
Outside	Forebay Aquifer	Westside Region	21	Westside Regions of model domain outside of Zone 2C boundary in Monterey County Inland Southwest of Arroyo Seco and Clark Colony subregion	Root zone, groundwater
Outside	Upper Valley Aquifer	Hames Valley	22	Outside Zone 2C but in Monterey County	Root zone
Outside	East Side Aquifer	Northeast Quarries	23	Outside Zone 2C but in Monterey County	Root zone
Outside	—	Northeast Region	24	Northeast Regions of model domain outside of Zone 2C on the Northeast side of the East Side, Granite Ridge, and Highlands South subregions	Root zone
Outside	—	Southwest Region	25	Southwest regions of model domain outside of Coastal Pressure subregion Zone 2C boundary in Monterey County	Root zone
Outside	—	Northeast Region	26	Northeast Region of model domain outside of Zone 2C Forebay subregion in Monterey County	Root zone
Outside	—	Southwest Region	27	Southwest regions of model domain outside of the Upper Valley and Forebay regions subregions of Zone 2C in Monterey County plus outside of Arroyo Seco, Hames Valley, and San Luis Obispo County active subregions	Root zone
Outside	—	Southeast Region	28	Southeast Region of model domain outside of Below Dam and Upper Valley subregions of Zone 2C boundary in Monterey County	Root zone
Outside	Paso Robles Area	Paso Robles	29	Portion of active model grid in located San Luis Obispo County	Root zone
Seaside	—	Seaside Basin	30	Seaside Adjudicated Basin not included in analysis due to adjudication	Root zone
Offshore	—	Offshore	31	Offshore region used to support analysis of seawater-aquifer exchanges	None

**Table 3.** Summary of geologic formations and hydrogeologic units in the Salinas Valley Geologic Framework (Sweetkind, 2023).

Hydrogeologic unit name	Model layer	Geologic material	Age	Description
Shallow aquifer	1	Sand and gravel of unspecified origin	Quaternary	The Shallow aquifer is a shallow surficial aquifer in the Salinas Valley basin north of the Salinas River consisting of unconfined sands and gravels.
Upper confining unit	2	Alluvial sediment, mostly fine-grained	Quaternary	The Upper confining unit is a laterally extensive series of blue or yellow sandy clay layers, with minor sand layers covering much of the Salinas Valley basin, east of Fort Ord, and from the Monterey Bay south past Salinas. This aquitard ranges in thickness from 25 feet near Salinas to more than 100 feet near Monterey Bay.
The 180-foot aquifer	3	Alluvial sediment, mostly coarse-grained	Quaternary	The 180-Foot aquifer is the uppermost laterally extensive aquifer in the northern Salinas Valley. The 180-Foot aquifer name is based on the depth where it is typically encountered in the subsurface. This unit consists of a complex zone of interconnected sands and gravels with intervening clay layers. The thickness of the 180-Foot aquifer varies from 50 to 150 feet, with an average of about 100 feet. The 180-Foot aquifer may be in part correlative to older portions of Quaternary terrace deposits or the upper Aromas Sand.
Middle confining unit	4	Alluvial sediment, mostly fine-grained	Quaternary	The Middle confining unit separates the 180-Foot aquifer from the underlying 400-Foot aquifer. It is a zone of variably thick layers of blue clay to thin layers of brown clay. This aquitard is widespread in the Salinas Valley basin and varies in thickness and quality. The Middle confining unit is commonly 50 to 100 feet thick and rarely as much as 200 to 250 feet thick; local variations in thickness produces local areas where the 180-Foot and 400-Foot aquifers are connected.
400-foot aquifer	5	Alluvial sediment, mostly coarse-grained	Quaternary	The 400-Foot aquifer is areally extensive and consists of sands, gravels, and clay lenses; it is typically encountered between 270 and 470 feet below ground surface. The 400-Foot aquifer has an average thickness of 200 feet, although the depth to the top of the aquifer, the thickness of the aquifer, and the degree of complex interbedding with clay layers is quite variable between wells. The thickness of this aquifer is variable but typical sand beds are 50 to 100 feet thick and can be more than 200 feet-thick. The upper portion of this aquifer may be correlative with the Aromas Sand and the lower portion with the upper part of the Paso Robles Formation.
Lower confining unit	6	Alluvial sediment, mostly coarse-grained	Pleistocene	Interval of blue marine clay that separates the 400-Foot aquifer from the deeper Paso Robles, Purisima, and basement aquifers. The Lower confining unit thickness is highly variable, from as thin as 50 feet to as much as 750 feet.

<p>Paso Robles aquifer</p>	<p>7</p>	<p>Clastic sedimentary rock</p>	<p>upper Pliocene to middle to lower Pleistocene</p>	<p>Paso Robles aquifer sediments consists of lenticular beds of sand, gravel, silt, and clay. Beds are laterally discontinuous and may indicate an alluvial fan or braided stream depositional environment, likely deposited in part by an ancestral Salinas River. In places, the unit forms a part of the "deep aquifer" system of Monterey County, which in general terms includes all sediments below the 400-Foot aquifer without respect to geology. Together the Paso Robles, Purisima, and Basement aquifers are referred to in general terms as the "deep aquifer".</p>
<p>Purisima aquifer</p>	<p>8</p>	<p>Clastic sedimentary rock</p>	<p>Pliocene</p>	<p>Purisima aquifer sediments are the Pliocene Purisima Formation that is a shallow marine unit composed of intercalated siltstone, sandstone, conglomerate, clay, and shale. In places, the unit forms a part of the "deep aquifer" system of Monterey County, which in general terms includes all sediments below the 400-Foot aquifer without respect to geology</p>
<p>Basement</p>	<p>9</p>	<p>Rock</p>	<p>Miocene and older</p>	<p>The rocks that form the basement aquifer are the Santa Margarita Formation, Monterey Formation and older consolidated-rock units. The upper 500 feet of this hydrogeologic unit is considered the base of the hydrologic system.</p>

**Table 4.** Summary of hydrogeologic units, model layers, and aquifer properties in the Salinas Valley Integrated Hydrologic Model and Salinas Valley Operational Model with corresponding layers and properties from the previously developed Salinas Valley Integrated Groundwater and Surface Model (SVIGSM; Montgomery Watson, 1997).

[ft/day, foot per day; —, no data]

Hydrogeologic unit	Model layer	Statistic	Salinas Valley Integrated Hydrologic Model (SVIHM)			
			Horizontal hydraulic conductivity (ft/day)	Vertical hydraulic conductivity (ft/day)	Specific yield for composite upper layer (dimensionless)	Specific storage (per foot)
Shallow aquifer	1	max	139	14	0.14	—
		mean	55	2	0.12	—
		min	0.02	2.88E-04	0.05	—
Upper confining unit	2	max	0.58	0.07	—	5.00E-05
		mean	0.04	2.63E-03	—	4.95E-05
		min	7.98E-04	9.58E-05	—	4.88E-05
180-Ft aquifer	3	max	230	15	—	3.09E-05
		mean	94	6	—	1.83E-05
		min	1.98E-01	2.49E-03	—	7.21E-06
Middle confining unit	4	max	7.71E-03	6.72E-03	—	2.76E-05
		mean	4.33E-03	2.35E-03	—	1.99E-05
		min	1.46E-03	1.36E-03	—	1.09E-05
400-Ft aquifer	5	max	242	16	—	7.21E-05
		mean	70	6	—	3.88E-05
		min	0.40	2.30E-03	—	6.34E-06
Deep confining unit	6	max	0.04	4.35E-03	—	8.86E-05
		mean	0.02	1.85E-03	—	5.76E-05
		min	1.21E-03	1.21E-04	—	1.26E-05
Paso Robles aquifer	7	max	87	9	—	1.21E-05
		mean	28	0.5	—	8.17E-05
		min	0.02	2.84E-06	—	1.07E-06
Purisima aquifer	8	max	9	0.36	—	—
		mean	1.2	0.05	—	—
		min	8.47E-03	3.53E-05	—	—
		constant				1.49E-05
Bedrock aquifer	9	max	3.66	6.80E-03	—	—
		Mean	2.35	4.46E-03	—	—
		Min	0.09	6.80E-04	—	—
		constant				1.62E-06

**Table 5.** Summary of IBOUND parameter and zone codes used to represent the hydrogeologic properties used in the integrated hydrologic models.

[—, no data]

Codes	Hydrogeologic units								
	Shallow aquifer	Upper confining unit	180-foot aquifer	Middle confining unit	400-foot aquifer	Deep confining unit	Paso Robles aquifer	Purisima aquifer	Bedrock aquifer
Offshore codes									
Pinched	None	91	92	93	94	95	96	97	—
Active	10	11	12	13	14	15	16	17	18
Onshore codes									
Pinched	None	81	82	83	84	85	86	87	—
Pinched with nearby well	69	69	69	69	69	69	69	69	69
Active main zone	1	2	3	4	5	6	7	8	9
Riparian	101	201	—	—	—	—	—	—	—
Riparian Upper Valley	—	—	—	—	—	—	701	—	—
Granite Ridge	102	—	302	—	502	—	702	—	—
Highlands South	103	—	303	—	503	—	703	—	—
East Side	104	—	304	—	504	—	—	—	—
Pressure	105	—	305	—	505	—	—	—	—
Forebay	106	—	306	—	506	—	—	430	—
Arroyo Seco	107	—	307	—	507	—	—	—	—
Coastal Region	—	—	—	—	—	—	708	420	—
Upper Valley	—	—	—	—	—	—	709	440	—
Central	—	—	—	—	—	—	—	460	—
Uplands	—	—	—	—	—	—	—	470	530
Seaside	—	—	—	—	—	—	—	450	510
Southern side	—	—	—	—	—	—	—	—	520
Northern side	—	—	—	—	—	—	—	—	540

**Table 6.** Summary of sensitive calibration parameters from composite scaled sensitivity analyses for the Salinas Valley Integrated Hydrologic Model.

Parameter type	Parameter name	Parameter description	Conductance (ft/day)	Rank	Composite scaled sensitivity <sup>1</sup>
Stream conductance	salriv_lcr	Salinas River stream segments near the coast.	4.15	14	0.5
Stream conductance	salriv_lv	Salinas River stream segments in the lower central valley.	8.08	12	0.6
Stream conductance	salriv_cv	Salinas River stream segments located near the center of the valley.	2.66	15	0.5
Stream conductance	salriv_cv1	Salinas River stream segments located near the center of the valley.	5.36	8	0.8
Stream conductance	wch_as	Arroyo Seco stream segments.	6.93	11	0.6
Stream conductance	cst_ditch	Central coastal region ditch.	12.96	29	0.3
Multiplier					
Aquifer conductivity	11hkpressure	Layer 1 Pressure lateral hydraulic conductivity.	0.75	17	0.4
Aquifer conductivity	17hkrip	Layer 7 riparian lateral hydraulic conductivity.	1	33	0.3
Aquifer conductivity	12vk	Layer 2 Vertical hydraulic conductivity.	0.1	38	0.3
Conductance (ft/day)					
Aquifer conductivity	kc_ly1	Hydraulic conductivity-end member for 100 percent coarse.	141	10	0.7
Aquifer conductivity	kf_ly2	Hydraulic conductivity end member for 0 percent coarse.	0.01	37	0.3
Aquifer conductivity	kc_ly3	Hydraulic conductivity end member for 100 percent coarse.	160	20	0.4
Aquifer conductivity	kc_ly5	Hydraulic conductivity end member for 100 percent coarse.	161	22	0.4
Aquifer conductivity	kc_ly7	Hydraulic conductivity end member for 100 percent coarse.	90.4	21	0.4
Value (unitless)					
Aquifer conductivity	p17	Power law exponent layer 7 where aquifer is confined.	0	1	2.7
Aquifer conductivity	p17u	Power law exponent layer 7 where aquifer is closer to surface in upper valley.	0.1	16	0.4
Scaling factor (ft/day)					
Aquifer storage	sy_ly1c	Specific yield of aquifer materials for 100 percent coarse.	0.14	31	0.3
Aquifer storage	sy_ly1f	Specific yield of aquifer materials for 0 percent coarse.	0.13	39	0.3
Multiplier (fraction)					
Aquifer storage	11ss	Specific storage scaling factor layer 1 in upland areas of the valley.	10	27	0.3
Multiplier (fraction)					
Climate-stress scale factor	kc_norm_sum	Crop coefficient climate scale factor normal year before 1995.	0.75	40	0.3



Climate-stress scale factor	kc_dry_win2	Crop coefficient climate scale factor dry year after 1995.	1	18	0.4
Climate-stress scale factor	kc_dry_spr2	Crop coefficient climate scale factor dry year after 1995.	1.11	7	0.9
Climate-stress scale factor	kc_dry_sum2	Crop coefficient climate scale factor dry year after 1995.	0.94	6	1.1
Climate-stress scale factor	kc_dry_fal2	Crop coefficient climate scale factor dry year after 1995.	1.55	32	0.3
Climate-stress scale factor	kc_norm_win2	Crop coefficient climate scale factor normal year after 1995.	1	9	0.7
Climate-stress scale factor	kc_norm_spr2	Crop coefficient climate scale factor normal year after 1995.	1.08	3	1.9
Climate-stress scale factor	kc_norm_sum2	Crop coefficient climate scale factor normal year after 1995.	0.96	2	2.3
Climate-stress scale factor	kc_norm_fal2	Crop coefficient climate scale factor normal year after 1995.	1.27	13	0.5
Climate-stress scale factor	kc_wet_win2	Crop coefficient climate scale factor wet year after 1995.	0.95	24	0.4
Climate-stress scale factor	kc_wet_spr2	Crop coefficient climate scale factor wet year after 1995.	1.01	5	1.4
Climate-stress scale factor	kc_wet_sum2	Crop coefficient climate scale factor wet year after 1995.	0.95	4	1.7
Climate-stress scale factor	kc_wet_fal2	Crop coefficient climate scale factor wet year after 1995.	1.1	19	0.4
Conductance (ft/day)					
Drain conductance	drt_rip	drain conductance in model cells adjacent to Salinas River.	1,180	30	0.3
Multiplier (fraction)					
Runoff parameter	ag_popc	Inefficient loss from precipitation factor for agricultural land uses.	0.05	28	0.3
Runoff parameter	ag_popc2	Inefficient loss from precipitation factor for agricultural land uses.	0.05	34	0.3
Runoff parameter	ag_pcpj	Inefficient loss from precipitation factor for agricultural land uses.	0.07	35	0.3
Runoff parameter	ag_irrc	Inefficient loss from irrigation factor for agricultural land uses.	0.05	25	0.4
Runoff parameter	ag_irrc2	Inefficient loss from irrigation factor for agricultural land uses.	0.07	23	0.4
Runoff parameter	ag_irri	Inefficient loss from irrigation factor for agricultural land uses.	0.05	26	0.3
Runoff parameter	semi_nati	Inefficient loss from precipitation factor for semi-agricultural land uses.	0	35	0.3

<sup>1</sup>Composite scaled sensitivity computed using PEST-HP for Highly Parallelized Computing Environments (Doherty, 2024).

**Table 7.** Summary of streamflow history matching showing streamflow statistics for the period from 1970 to 2018, mean residual streamflow

computed as observed minus the simulated equivalent value, root mean squared error, scaled root mean square error, and Nash-Sutcliffe model efficiency for U.S. Geological Survey gages and diversions in the Salinas Valley Integrated Hydrologic Model.

[ft<sup>3</sup>/s, cubic foot per second; —, no data; <, less than]

Gage identifiers	Observation group	Number of observations	Streamflow			Mean residual (ft <sup>3</sup> /s)	Root mean square error (ft <sup>3</sup> /s)	Scaled root mean square error (percent)	Nash Sutcliffe model efficiency (unitless)
			Minimum observed value (ft <sup>3</sup> /s)	Mean observed value (ft <sup>3</sup> /s)	Maximum observed value (ft <sup>3</sup> /s)				
USGS 11150500	SANT_BR	566	0	519	10,185	-83	333	3	0.89
USGS 11152050	ARS_REL	243	0	117	2,801	-9	116	4	0.87
USGS 11152000	ARS_SOL	567	0	175	2,697	8	125	5	0.88
USGS 11151700	SAL_SOL	495	0	371	11,169	-38	343	3	0.89
USGS 11152300	SAL_CHU	459	0	414	14,352	19	388	3	0.91
USGS 11152500	SAL_SPR	567	0	402	16,204	-11	437	3	0.90
Streamflow difference									
USGS 11150500- USGS 11151700	BR_SOL	494	-1,655	117	860	-45	210	8	0.14
USGS 11151700- USGS 11152300	SOL_CHU	399	-3,183	3	729	-30	197	5	0.52
USGS 11152300- USGS 11152500	CHU_SPR	459	-2,153	18	1,331	24	238	7	0.00
USGS 11152000- USGS 11152050	ARR_SEC	243	-537	52	323	5	64	7	0.17
Diversion									
CLARK_DIV		139	0	—	—	3	8	13	0.52
SRDF_DIV		23	0	—	—	<1	<1	2	1.00

**Table 8.** Summary of selected observation wells used to illustrate Salinas Valley Integrated Hydrologic Model history matching, indicating the number of observations, representative model layers, hydrogeologic units, mean residual computed as observed minus the simulated equivalent value, and root mean square error.

[<, less than]

Well name	Construction date	Number of observations	Model layers	Hydrogeologic units	Mean residual (feet)	Root mean square error (feet)
Pressure						
CSI239	12/22/1961	639	5	400-foot aquifer	6	11
BDA331	01/25/1964	84	3	180-foot aquifer	-19	20
ZPN1529	04/01/1954	53	3	180-foot aquifer	-21	23
ZPN441	08/01/1941	40	5	400-foot aquifer	<1	4
East Side						
ZES1572	12/18/1946	608	3,5,7	180-foot, 400-foot, and Paso Robles aquifers	-5	8
ZES871	08/10/1950	534	3,5,7	180-foot, 400-foot, and Paso Robles aquifers	-2	11
Forebay						
ZFS1001	11/01/1938	44	5	400-foot aquifer	1	4
ZNE1267	01/01/1900	40	7,8	Paso Robles and Purisima aquifers	-5	6
Upper Valley						
ZSE355	06/06/1951	597	8	Purisima aquifer	1	9
ZSE733	04/17/1952	41	8	Purisima aquifer	1	3

**Table 9.** Summary of groundwater level history matching showing drawdown mean residual (computed as observed minus the simulated equivalent value), root mean square error, and scaled root mean square error for the integrated hydrologic model domain and analysis regions.

Analysis Region	Number of observations	Number of wells	Minimum observed water level (feet)	Maximum observed water level (feet)	Mean drawdown residual (feet)	Drawdown root mean square error (feet)	Scaled root mean square error (percent)
Entire domain	3,805	439	-168	472	<1	14	6
Pressure	779	171	-103	113	1	14	8
East Side-Langley	1,144	119	-168	472	-1	18	7
Forebay	1,196	100	-10	282	-3	10	9
Upper Valley	686	39	201	447	2	8	14

**Table 10.** Summary of monthly agricultural pumpage history matching by analysis region showing mean residual computed as observed minus the simulated equivalent value, root mean square error, and scaled root mean square error for the integrated hydrologic model domain.

Analysis region	Number of monthly observations	Mean residual (acre-feet)	Root mean square error (acre-feet)	Scaled root mean square error (percent)
Entire domain	3,630	39	774	5
Pressure	968	107	727	5
East Side	242	-53	1,346	8
Forebay	968	183	784	8
Upper Valley	968	-119	804	9

**Table 11.** Summary of groundwater budget data for the entire Salinas Valley integrated hydrologic model domain for the simulation period 1970–2018, analysis periods A–D and high and low precipitation years representing conditions before and after the Salinas River Diversion Facility was implemented.

[Average flows in thousands of acre-feet per year rounded to the nearest thousand. The calendar year is January through December. Abbreviations: GW, groundwater; —, no data]

GW-flow components	Entire simulation 1970–2018	Analysis period				Analysis period D 2010–18		1983		1989		2010		2013	
		1970–83	1984–94	1995–2004	2010–18	High precipitation	Low precipitation	High precipitation	Low precipitation	High precipitation	Low precipitation	High precipitation	Low precipitation		
Net average GW inflows and outflows															
Recharge	93	159	79	80	28	168	55	58	2						
Stream leakage	683	790	575	757	527	1113	271	748	386						
Riparian drainage	-171	-208	-147	-190	-112	-350	-74	-181	-90						
Tributary drainage	-8	-9	-6	-11	-6	-18	-2	-10	-3						
Surface drainage	-89	-116	-73	-99	-47	-238	-30	-88	-35						
Inter-basin underflow	-5	-5	-5	-5	-5	-5	-5	-5	-5						
Municipal & industrial pumpage	-53	-38	-48	-67	-57	-44	-49	-66	-62						
Agricultural pumpage	-457	-431	-530	-447	-423	-426	-635	-356	-481						
Seawater coastal inflow	15	16	16	14	12	14	18	12	13						
Aquifer storage change	8	158	-139	32	-83	214	-451	112	-275						
Summarized quantities of interest															
Stream recharge <sup>5</sup>	504	573	422	556	409	745	195	557	258						
Total recharge <sup>6</sup>	597	732	501	636	437	913	250	615	260						
Total pumpage <sup>7</sup>	510	469	578	514	480	470	684	422	543						
Pumpage-recharge fraction <sup>8</sup>	0.9	0.6	1.2	0.8	1.1	0.5	2.7	0.7	2.1						
Storage loss <sup>9</sup>	—	—	139	—	83	—	451	—	275						
Groundwater depletion <sup>10</sup>	15	16	155	14	95	14	469	12	288						

<sup>1</sup>Highest total precipitation for the entire active model domain before the implementation of the Salinas Valley Water Project.  
<sup>2</sup>Lowest total precipitation for the entire active model domain was before the implementation of the Salinas Valley Water Project.  
<sup>3</sup>Highest total precipitation for the entire active model domain after Salinas Valley Water Project implementation.  
<sup>4</sup>Lowest total precipitation for the entire active model domain after Salinas Valley Water Project implementation.  
<sup>5</sup>Stream Leakage + Riparian Drainage + Tributary Drainage.

<sup>6</sup>Recharge + Stream Recharge.

<sup>7</sup>Agricultural Pumpage + Municipal & Industrial Pumpage.

<sup>8</sup>Absolute value of Total Pumpage/Total Recharge.

<sup>9</sup>Aquifer Storage Change < 0.

<sup>10</sup>Storage Loss + Seawater Intrusion.

**Table 12.** Summary of groundwater budget data for the Riparian analysis region for the simulation period 1970–2018, analysis periods A–D and high and low precipitation years representing conditions before and after the Salinas River Diversion Facility was implemented.

[Average flows in thousands of acre-feet per year rounded to the nearest thousand. The calendar year is January through December. Abbreviations: GW, groundwater; —, no data]

GW-flow components	Entire simulation 1970–2018	Analysis period A 1970–83		Analysis period B 1984–94		Analysis period C 1995–2004		Analysis period D 2010–18		1983 High precipitation		1989 Low precipitation		2010 High precipitation		2013 Low precipitation	
		1970–83	1984–94	1995–2004	2010–18	1983 High precipitation	1989 Low precipitation	2010 High precipitation	2013 Low precipitation								
Net average GW inflows and outflows																	
Recharge	-101	-98	-100	-104	-100	-100	-106	-96	-106	-106	-96	-106	-96	-106	-96	-106	-106
Stream leakage	569	662	478	629	436	948	212	622	436	948	212	622	436	948	212	622	436
Riparian drainage	-171	-208	-147	-190	-112	-350	-74	-181	-112	-350	-74	-181	-112	-350	-74	-181	-112
Tributary drainage	—	—	—	—	—	—	—	—	—	—	—	—	—	—	—	—	—
Surface drainage	—	—	—	—	—	—	—	—	—	—	—	—	—	—	—	—	—
Riparian underflow	-291	-339	-243	-325	-221	-530	-114	-321	-221	-530	-114	-321	-221	-530	-114	-321	-221
Inter-basin underflow	-1	-1	-1	-1	-1	-1	-1	-1	-1	-1	-1	-1	-1	-1	-1	-1	-1
Municipal & industrial pumpage	—	—	—	-1	—	—	—	—	—	—	—	—	—	—	—	—	—
Agricultural pumpage	-12	-10	-13	-13	-12	-10	-16	-10	-12	-10	-16	-10	-12	-10	-16	-10	-12
Seawater coastal inflow	2	2	2	2	2	2	2	2	2	2	2	2	2	2	2	2	2
Aquifer storage change	-5	8	-24	-3	-8	-41	-97	14	-8	-41	-97	14	-8	-41	-97	14	-8
Summarized quantities of interest																	
Local stream recharge <sup>5</sup>	297	356	231	335	224	498	32	345	224	498	32	345	224	498	32	345	224
Total recharge <sup>6</sup>	297	356	231	335	224	498	32	345	224	498	32	345	224	498	32	345	224
Total pumpage <sup>7</sup>	12	10	13	14	12	10	16	10	12	10	16	10	12	10	16	10	12
Pumpage-recharge fraction <sup>8</sup>	—	—	0.1	—	0.1	—	0.5	—	0.1	—	0.5	—	0.1	—	0.5	—	0.1
Storage loss <sup>9</sup>	5	—	24	3	8	41	97	—	8	41	97	—	8	41	97	—	8
Groundwater depletion <sup>10</sup>	7	2	26	5	10	43	99	1	10	43	99	1	10	43	99	1	10

<sup>1</sup>Highest total precipitation for the entire active model domain before the implementation of the Salinas Valley Water Project.

<sup>2</sup>Lowest total precipitation for the entire active model domain was before the implementation of the Salinas Valley Water Project.

<sup>3</sup>Highest total precipitation for the entire active model domain after the implementation of the Salinas Valley Water Project.

<sup>4</sup>Lowest total precipitation for the entire active model domain after Salinas Valley Water Project implementation.

<sup>5</sup>Recharge + Stream Leakage + Riparian Drainage + Tributary Drainage.

<sup>6</sup>Local stream recharge.



<sup>7</sup>Agricultural Pumpage + Municipal & Industrial Pumpage.

<sup>8</sup>Absolute value of Total Pumpage/Total Recharge.

<sup>9</sup>Aquifer Storage Change < 0.

<sup>10</sup>Storage Loss + Seawater Intrusion.

**Table 13.** Summary of groundwater budget data for the Pressure analysis region for the simulation period 1970–2018, analysis periods A–D and high and low precipitation years representing conditions before and after the Salinas River Diversion Facility was implemented.

[Average flows in thousands of acre-feet per year rounded to the nearest thousand. The calendar year is January through December. Abbreviations: GW, groundwater; —, no data]

GW-flow components	Entire simulation 1970–2018		Analysis period A 1970–83		Analysis period B 1984–94		Analysis period C 1995–2004		Analysis period D 2010–18		21989 Low precipitation		32010 High precipitation		42013 Low precipitation	
Net average GW inflows and outflows																
Recharge	46	64	47	37	32	32	64	48	32	32	48	32	32	30	32	27
Stream leakage	29	32	24	32	23	23	43	14	30	14	30	30	30	30	16	16
Riparian drainage	—	—	—	—	—	—	—	—	—	—	—	—	—	—	—	—
Tributary drainage	-2	-2	-1	-3	-1	-1	-6	—	-2	—	—	-2	—	—	—	—
Surface drainage	-22	-29	-18	-26	-11	-11	-65	-6	-22	-6	-22	-22	-22	-22	-8	-8
Riparian underflow	105	122	88	118	76	76	186	45	113	45	113	113	113	113	56	56
Subbasin underflow	-11	-11	-8	-14	-11	-11	-14	-3	-14	-3	-14	-14	-14	-14	-10	-10
Inter-basin underflow	—	—	—	—	—	—	—	—	—	—	—	—	—	—	—	—
Municipal & industrial pumpage	-32	-22	-28	-40	-38	-38	-26	-28	-42	-28	-42	-42	-42	-42	-43	-43
Agricultural pumpage	-118	-119	-148	-108	-96	-96	-118	-180	-78	-180	-78	-78	-78	-78	-110	-110
Seawater coastal inflow	11	10	11	11	10	10	9	14	10	14	10	10	10	10	10	10
Aquifer storage change	6	45	-33	7	-16	-16	73	-96	27	-96	27	27	27	27	-62	-62
Summarized quantities of interest																
Local stream recharge <sup>5</sup>	27	30	23	29	22	22	37	14	28	14	28	28	28	28	16	16
Total recharge <sup>6</sup>	73	94	70	66	54	54	101	62	60	62	60	60	60	60	35	35
Total pumpage <sup>7</sup>	150	141	176	148	134	134	144	208	120	208	120	120	120	120	153	153
Pumpage-recharge fraction <sup>8</sup>	2.1	1.5	2.5	2.2	2.5	2.5	1.4	3.4	2.0	3.4	2.0	2.0	2.0	2.0	4.4	4.4
Storage loss <sup>9</sup>	—	—	33	—	16	16	—	96	—	96	—	—	—	—	62	62
Groundwater depletion <sup>10</sup>	11	10	44	11	26	26	9	110	10	110	10	10	10	10	72	72

<sup>1</sup>Highest total precipitation for the entire active model domain before the implementation of the Salinas Valley Water Project.

<sup>2</sup>Lowest total precipitation for the entire active model domain was before the implementation of the Salinas Valley Water Project.

<sup>3</sup>Highest total precipitation for the entire active model domain after the implementation of the Salinas Valley Water Project.

<sup>4</sup>Lowest total precipitation for the entire active model domain after the implementation of the Salinas Valley Water Project.

<sup>5</sup>Analysis region Stream Leakage + Riparian Drainage + Tributary Drainage.

<sup>6</sup>Recharge + Local stream recharge.

<sup>7</sup>Agricultural Pumpage + Municipal & Industrial Pumpage.

<sup>8</sup>Aquifer Storage Change < 0.

<sup>9</sup>Absolute value of Total Pumpage/Total Recharge.

<sup>10</sup>Storage Loss + Seawater Intrusion.

**Table 14.** Summary of groundwater budget data for the East Side-Langley analysis region for the simulation period 1970–2018, analysis period A–D, and high and low precipitation years representing conditions before and after the Salinas River Diversion Facility was implemented.

[Average flows in thousands of acre-feet per year rounded to the nearest thousand. The calendar year is January through December. Abbreviations: GW, groundwater; —, no data]

GW-flow components	Entire simulation 1970–2018	Analysis period A 1970–83	Analysis period B 1984–94	Analysis period C 1995–2004	Analysis period D 2010–18	1983 High precipitation	1989 Low precipitation	2010 High precipitation	2013 Low precipitation
	Net average GW inflows and outflows								
Recharge	40	58	40	32	25	62	36	27	20
Stream leakage	12	14	11	13	9	18	8	12	8
Riparian drainage	—	—	—	—	—	—	—	—	—
Tributary drainage	—	—	—	—	—	—	—	—	—
Surface drainage	—	—	—	—	—	—	—	—	—
Riparian underflow	—	—	—	—	—	—	—	—	—
Subbasin underflow	22	22	22	23	22	24	19	22	22
Inter-basin underflow	—	—	—	—	—	—	—	—	—
Municipal & industrial pumpage	-2	-2	-3	-2	-2	-3	-3	-3	-1
Agricultural pumpage	-81	-83	-96	-74	-71	-84	-104	-59	-80
Seawater coastal inflow	—	—	—	—	—	—	—	—	—
Aquifer storage change	-9	9	-26	-8	-17	17	-44	-1	-31
Summarized quantities of interest									
Local stream recharge <sup>5</sup>	12	14	11	13	9	18	8	12	8
Total recharge <sup>6</sup>	52	72	51	45	34	80	44	39	28
Total pumpage <sup>7</sup>	83	85	99	76	73	87	107	62	81
Pumpage-recharge fraction <sup>8</sup>	1.6	1.2	1.9	1.7	2.1	1.1	2.4	1.6	2.9
Storage loss <sup>9</sup>	9	—	26	8	17	—	44	1	31
Groundwater depletion <sup>10</sup>	9	—	26	8	17	—	44	1	31

<sup>1</sup>Highest total precipitation for the entire active model domain before the implementation of the Salinas Valley Water Project.

<sup>2</sup>Lowest total precipitation for the entire active model domain was before the implementation of the Salinas Valley Water Project.

<sup>3</sup>Highest total precipitation for the entire active model domain after Salinas Valley Water Project implementation.

<sup>4</sup>Lowest total precipitation for the entire active model domain after Salinas Valley Water Project implementation.

<sup>5</sup>Analysis region Stream Leakage + Riparian Drainage + Tributary Drainage.

<sup>6</sup>Recharge + Local stream recharge.

<sup>7</sup>Agricultural Pumpage + Municipal & Industrial Pumpage.

<sup>8</sup>Aquifer Storage Change < 0.

<sup>9</sup>Absolute value of Total Pumpage/Total Recharge.

<sup>10</sup>Storage Loss + Seawater Intrusion.

**Table 15.** Summary of groundwater budget data for the Forebay analysis region for 1970–2018, analysis period A–D, and high and low precipitation years representing conditions before and after the Salinas River Diversion Facility was implemented.

[Average flows in thousands of acre-feet per year rounded to the nearest thousand. The calendar year is January through December. Abbreviations: GW, groundwater; —, no data]

GW-flow components	Entire simulation 1970–2018	Analysis period A 1970–83		Analysis period B 1984–94		Analysis period C 1995–2004		Analysis period D 2010–18		1983 High precipitation		21989 Low precipitation		32010 High precipitation		42013 Low precipitation	
		47	59	44	47	47	29	29	39	39	53	48	23	56	32	28	
Recharge	46	59	44	47	29	29	39	39	53	48	23	56	32	28			
Stream leakage	48	53	39	55	39	39	68	68	53	23	56	32	23				
Riparian drainage	—	—	—	—	—	—	—	—	—	—	—	—	—				
Tributary drainage	-6	-6	-4	-7	-4	-4	-10	-7	-10	-2	-7	-7	-2				
Surface drainage	-36	-48	-29	-42	-18	-18	-102	-38	-102	-10	-38	-38	-13				
Riparian underflow	110	128	93	122	82	82	194	120	194	48	120	120	62				
Subbasin underflow	-5	-4	-6	-4	-4	-4	-4	-6	-4	-6	-5	-5	-4				
Inter-basin underflow	—	—	—	—	—	—	—	—	—	—	—	—	—				
Municipal & industrial pumpage	-9	-4	-7	-15	-10	-10	-5	-7	-5	-7	-10	-10	-11				
Agricultural pumpage	-146	-135	-163	-147	-141	-141	-130	-202	-130	-202	-118	-118	-161				
Seawater coastal inflow	—	—	—	—	—	—	—	—	—	—	—	—	—				
Aquifer storage change	2	43	-33	9	-27	-27	64	-108	64	-108	30	-108	-78				
Net average GW inflows and outflows																	
Summarized quantities of interest																	
Local stream recharge <sup>5</sup>	42	47	35	48	35	35	58	21	58	21	49	49	21				
Total recharge <sup>6</sup>	88	106	79	95	64	64	111	69	111	69	81	81	36				
Total pumpage <sup>7</sup>	155	139	170	162	151	151	135	209	135	209	128	128	172				
Pumpage-recharge fraction <sup>8</sup>	1.8	1.3	2.2	1.7	2.4	2.4	1.2	3.0	1.2	3.0	1.6	1.6	4.8				
Storage loss <sup>9</sup>	—	—	33	—	27	27	—	108	—	108	—	—	78				
Groundwater depletion <sup>10</sup>	—	—	33	—	27	27	—	108	—	108	—	—	78				

<sup>1</sup>Highest total precipitation for the entire active model domain before the implementation of the Salinas Valley Water Project.

<sup>2</sup>Lowest total precipitation for the entire active model domain was before the implementation of the Salinas Valley Water Project.

<sup>3</sup>Highest total precipitation for the entire active model domain after Salinas Valley Water Project implementation.

<sup>4</sup>Lowest total precipitation for the entire active model domain after Salinas Valley Water Project implementation.

<sup>5</sup>Analysis region Stream Leakage + Riparian Drainage + Tributary Drainage.

<sup>6</sup>Recharge + Local stream recharge.

<sup>7</sup>Agricultural Pumpage + Municipal & Industrial Pumpage,

<sup>8</sup>Aquifer Storage Change < 0,

<sup>9</sup>Absolute value of Total Pumpage/Total Recharge.

<sup>10</sup>Storage Loss + Seawater Intrusion.

**Table 16.** Summary of groundwater budget data for the Upper Valley analysis region for the simulation period 1970–2018, analysis period A–D, and high and low precipitation years representing conditions before and after the Salinas River Diversion Facility was implemented.

[Average flows in thousands of acre-feet per year rounded to the nearest thousand. The calendar year is January through December. Abbreviations: GW, groundwater; —, no data]

GW-flow components	Entire simulation 1970–2018		Analysis period A 1970–83		Analysis period B 1984–94		Analysis period C 1995–2004		Analysis period D 2010–18		1983 High precipitation		21989 Low precipitation		32010 High precipitation		42013 Low precipitation		
Net average GW inflows and outflows																			
Recharge	33	41	29	34	24	42	25	33	22	42	25	33	33	22	42	25	33	22	42
Stream leakage	11	12	10	12	8	16	7	12	8	16	7	12	12	8	16	7	12	8	16
Riparian drainage	—	—	—	—	—	—	—	—	—	—	—	—	—	—	—	—	—	—	—
Tributary drainage	-1	-1	—	-1	—	-2	—	—	—	-2	—	-1	—	-1	—	—	—	—	—
Surface drainage	-28	-38	-24	-29	-16	-69	-12	-26	-14	-69	-12	-26	-26	-14	-69	-12	-26	-14	-69
Riparian underflow	74	83	61	82	61	132	27	85	48	132	27	85	90	48	132	27	85	48	132
Subbasin underflow	4	4	4	4	4	5	4	4	3	5	4	4	4	3	5	4	4	3	5
Inter-basin underflow	—	—	—	—	—	—	—	—	—	—	—	—	—	—	—	—	—	—	—
Municipal & industrial pumpage	-3	-3	-3	-2	-3	-3	-3	-3	-3	-3	-3	-4	-3	-3	-3	-4	-3	-3	-3
Agricultural pumpage	-94	-78	-103	-99	-98	-80	-124	-86	-111	-80	-124	-86	-111	-86	-124	-86	-111	-111	-86
Seawater coastal inflow	—	—	—	—	—	—	—	—	—	—	—	—	—	—	—	—	—	—	—
Aquifer storage change	-4	20	-26	1	-20	41	-76	17	-47	41	-76	17	-47	41	-76	17	-47	-47	41
Summarized quantities of interest																			
Local stream recharge <sup>5</sup>	10	11	10	11	8	14	7	11	8	14	7	11	11	8	14	7	11	8	14
Total recharge <sup>6</sup>	43	52	39	45	32	56	32	44	16	56	32	44	44	16	56	32	44	16	56
Total pumpage <sup>7</sup>	97	81	106	101	101	83	127	90	114	83	127	90	90	114	83	127	90	114	83
Pumpage-recharge fraction <sup>8</sup>	2.3	1.6	2.7	2.2	3.2	1.5	4.0	2.0	7.1	1.5	4.0	2.0	2.0	7.1	1.5	4.0	2.0	7.1	1.5
Storage loss <sup>9</sup>	4	—	26	—	20	—	76	—	47	—	76	—	—	47	—	76	—	—	47
Groundwater depletion <sup>10</sup>	4	—	26	—	20	—	76	—	47	—	76	—	—	47	—	76	—	—	47

<sup>1</sup>Highest total precipitation for the entire active model domain before the implementation of the Salinas Valley Water Project.

<sup>2</sup>Lowest total precipitation for the entire active model domain was before the implementation of the Salinas Valley Water Project.

<sup>3</sup>Highest total precipitation for the entire active model domain after Salinas Valley Water Project implementation.

<sup>4</sup>Lowest total precipitation for the entire active model domain after Salinas Valley Water Project implementation.

<sup>5</sup>Analysis region Stream Leakage + Riparian Drainage + Tributary Drainage.



<sup>6</sup>Recharge + Local stream recharge.

<sup>7</sup>Agricultural Pumpage + Municipal & Industrial Pumpage.

<sup>8</sup>Aquifer Storage Change < 0.

<sup>9</sup>Absolute value of Total Pumpage/Total Recharge.

<sup>10</sup>Storage Loss + Seawater Intrusion.

**Table 17.** Description of Salinas Valley Operational Model (SVOM) operational rules that define reservoir releases triggered based on flow conditions and downstream water demands.

<b>Ruleset</b>	<b>Description</b>
Fish passage	Flow requirements for managing steelhead trout in the Salinas River follow the National Marine Fisheries Service Requirements across the lifecycle including the adult steelhead upstream migration, downstream migration of smolt steelhead, downstream migration of juvenile and post-spawn adult steelhead, and spawning and rearing habitat.
Water Rights	The flow requirements related to water rights evaluate the storage for each reservoir for accumulation and release to comply with water rights in the basin and deliver water to coastal communities to mitigate sea water intrusion.
Flood Release	The flow requirements related to flood release evaluate the downstream streamflow and the reservoir release to minimize high streamflow and mitigate flood threats.
Reservoir release fraction	The relative fraction of water that is released from each of the reservoirs. The reservoir release fraction rules verify the storage in each of the reservoirs and evaluate the release demand to determine which reservoir the water should be released from. One of the reservoir release fraction rules checks the logic at each iteration before convergence and the other checks the logic at each iteration after convergence.
Spillway release thresholds	Reservoir operation thresholds determine the spill calculation and maximum release changes based on the reservoir stage.
Salinas River diversion facility	Conveyance and flow requirements to compute reservoir releases to meet diversion targets at the diversion facility.

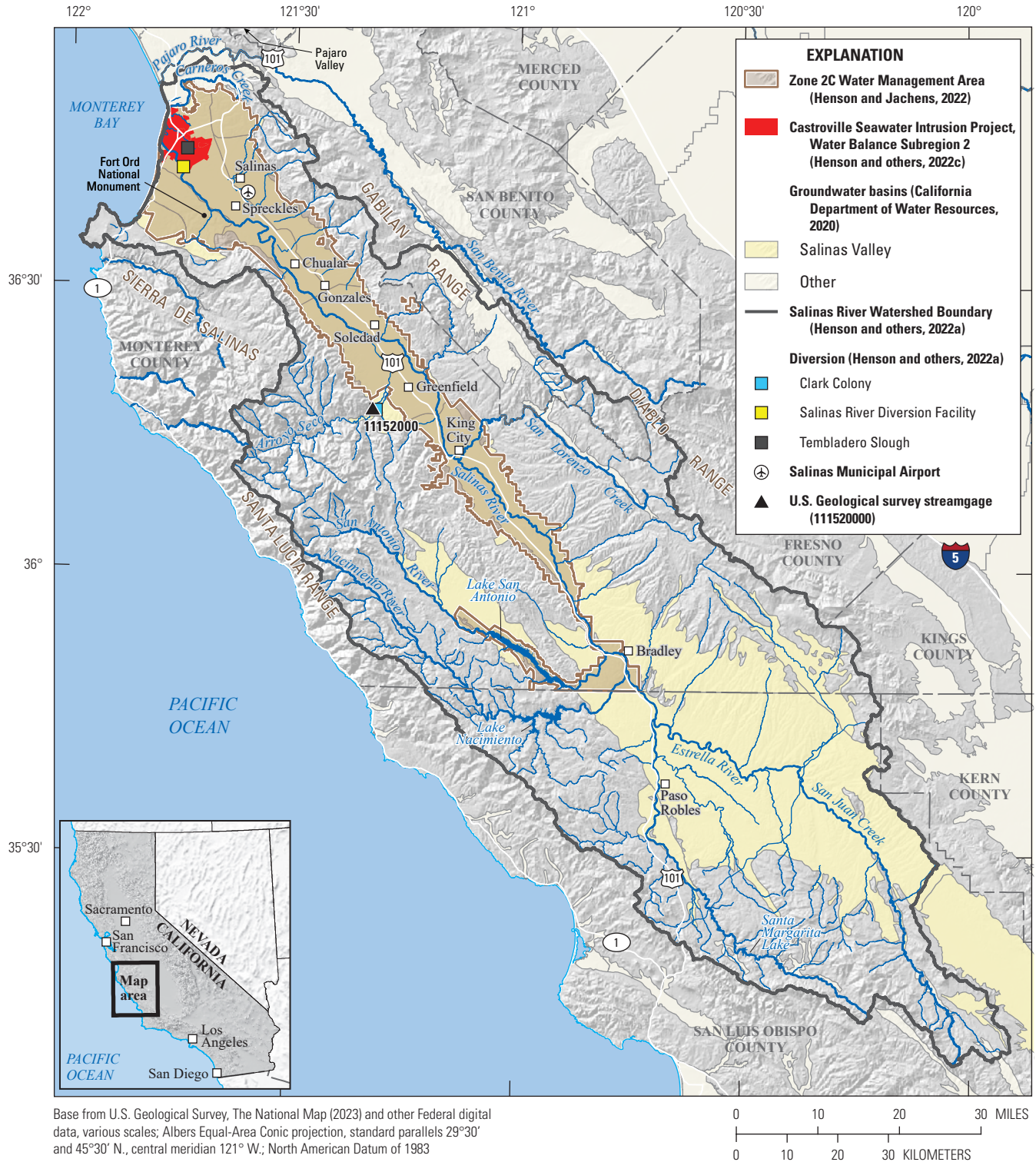
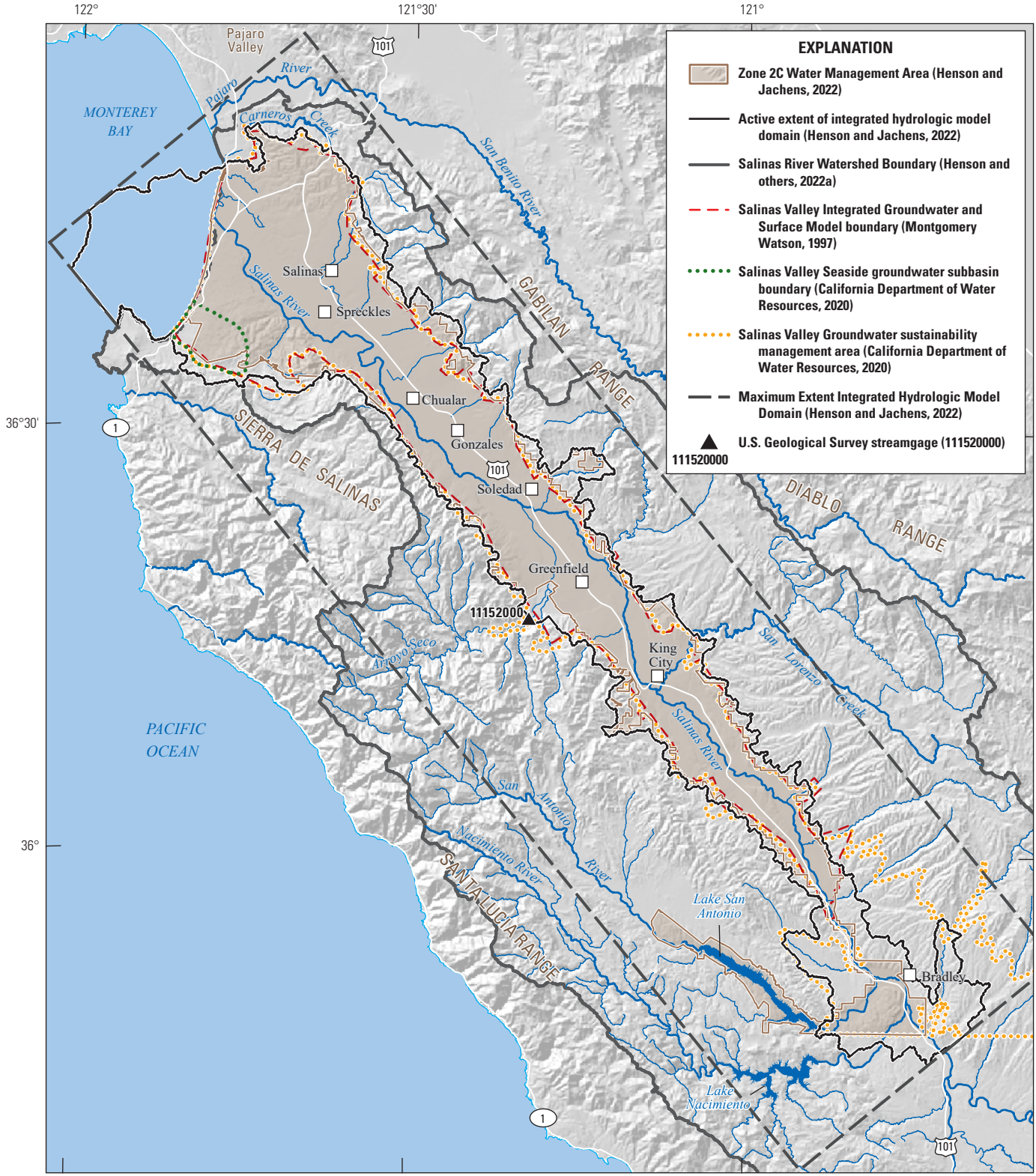


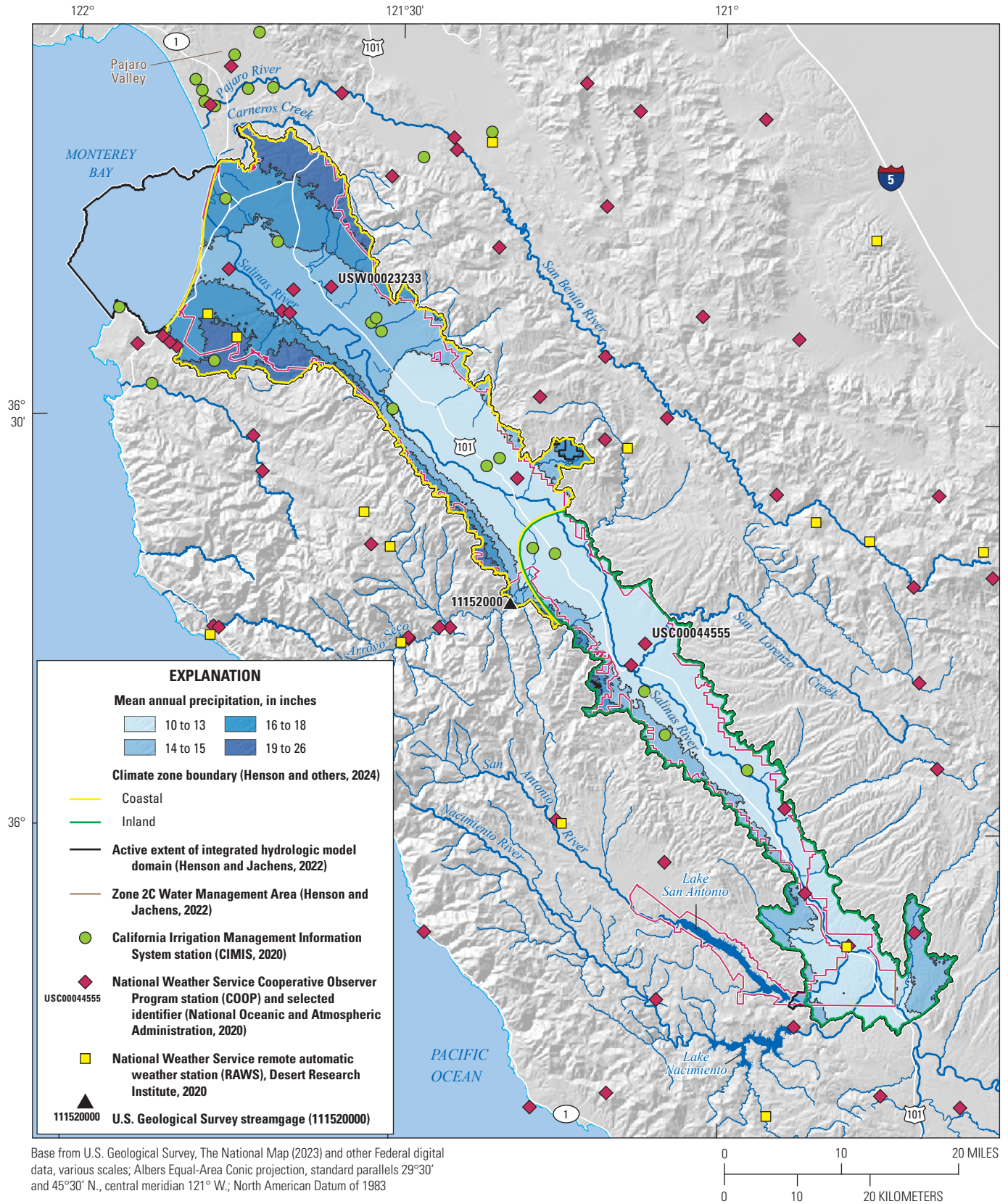
Figure 1. Map of Salinas River watershed in Monterey and San Luis Obispo counties, showing the Salinas Valley Groundwater Basin (California Department of Water Resources, 2020), Zone 2C water management area (Henson and Jachens, 2022), Salinas, Nacimiento and San Antonio Reservoirs, Castroville Seawater Intrusion Project (CSIP)(Henson and Jachens, 2022), Salinas River Diversion Facility (SRDF), Clark Colony, and Tembladero Slough diversions (Henson and others, 2023).



Base from U.S. Geological Survey, The National Map (2023) and other Federal digital data, various scales; Albers Equal-Area Conic projection, standard parallels 29°30' and 45°30' N., central meridian 121° W.; North American Datum of 1983



Figure 2. Salinas Valley showing the Monterey County groundwater sustainability management area, Zone 2C Water Management Area, integrated hydrologic model domain, Salinas Valley Integrated Groundwater Model domain, and Seaside adjudicated groundwater subbasin.



Base from U.S. Geological Survey, The National Map (2023) and other Federal digital data, various scales; Albers Equal-Area Conic projection, standard parallels 29°30' and 45°30' N., central meridian 121° W.; North American Datum of 1983

Figure 3. Integrated hydrologic model domain annual average gridded precipitation at 530-foot resolution for water years 1968 through 2018, coastal and inland climate zones based on aggregation of California Irrigation Management Information System (CIMIS) climate zones, CIMIS stations, selected climate stations, Remote Automatic Weather Stations (RAWS), Cooperative Observer Network (COOP) stations, and two analysis COOP stations: Salinas Airport (USW00023233) and King City (USC00044555).

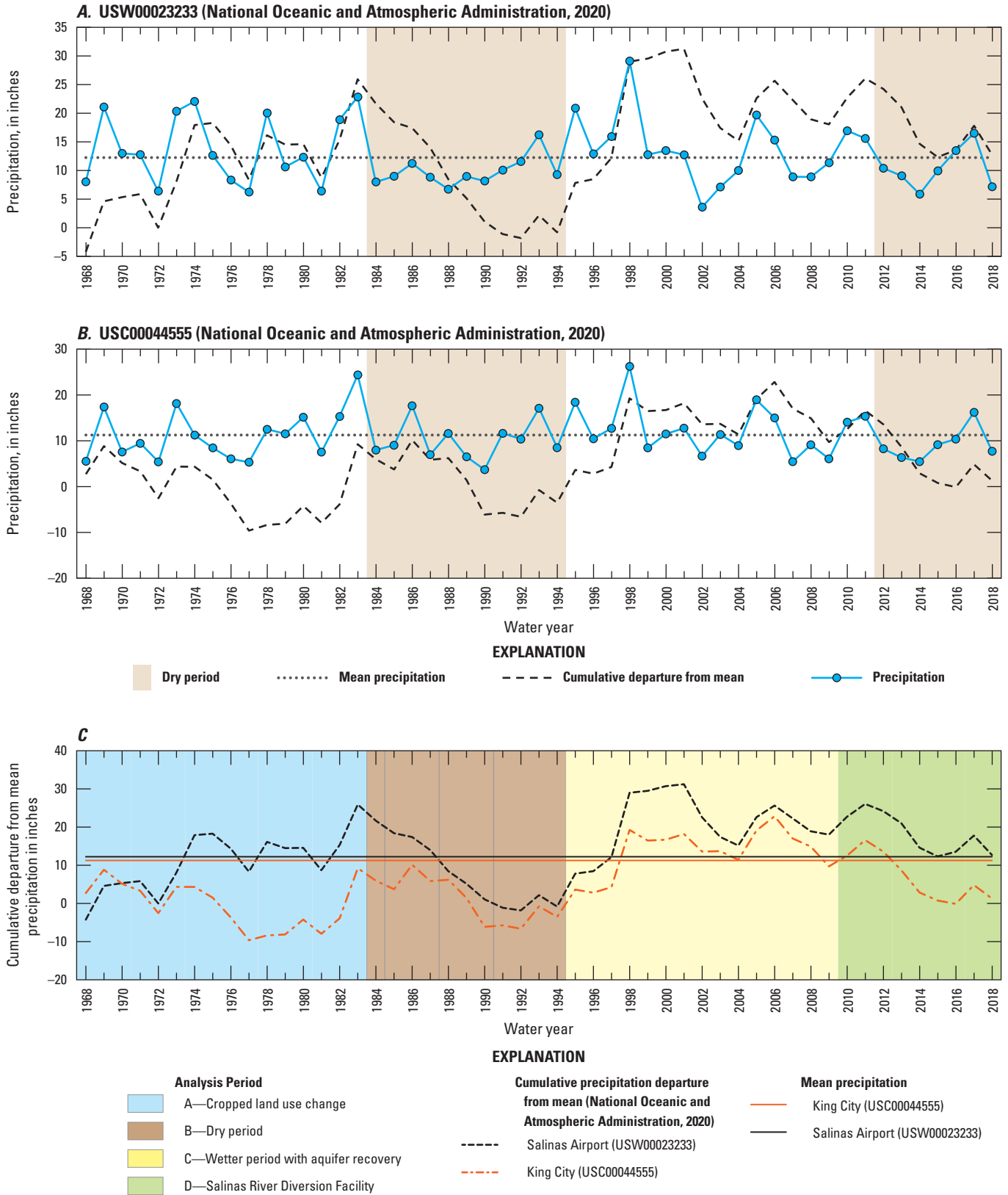


Figure 4. Annual precipitation at selected Cooperative Observer Network stations (COOP; National Oceanic and Atmospheric Administration, 2020) for water years 1968 through 2018 for A) Salinas Airport (USW00023233) and B) King City (USC00044555). Shaded regions illustrate two relatively dry periods in the Salinas Valley defined based on generally decreasing or flat cumulative precipitation departure from the mean and annual precipitation less than mean precipitation from water years 1968 through 2018. C) Cumulative precipitation departure from the mean at Salinas Airport (USW00023233) and King City (USC00044555) showing delineation of analysis periods A, B, C, and D for the study.

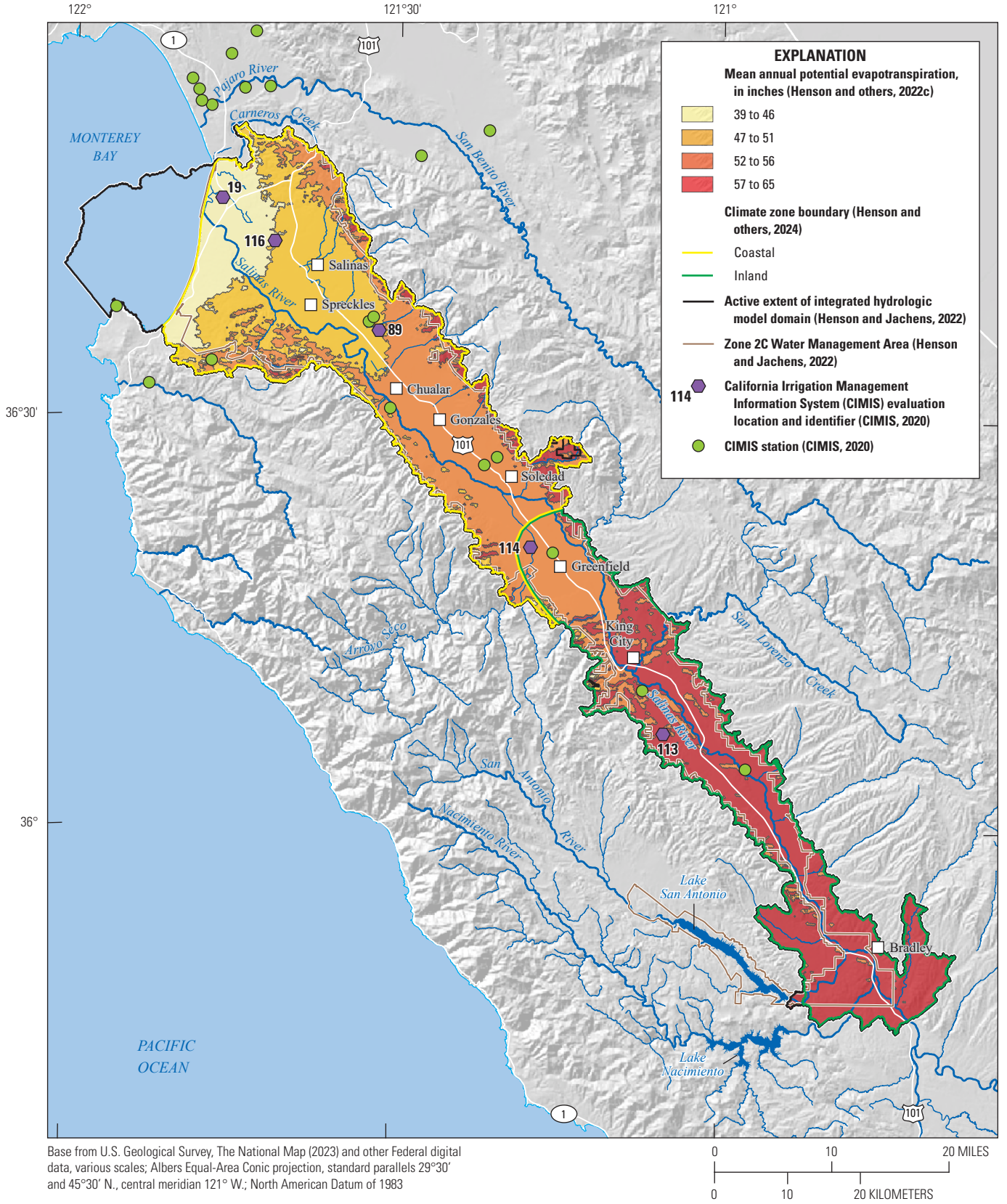
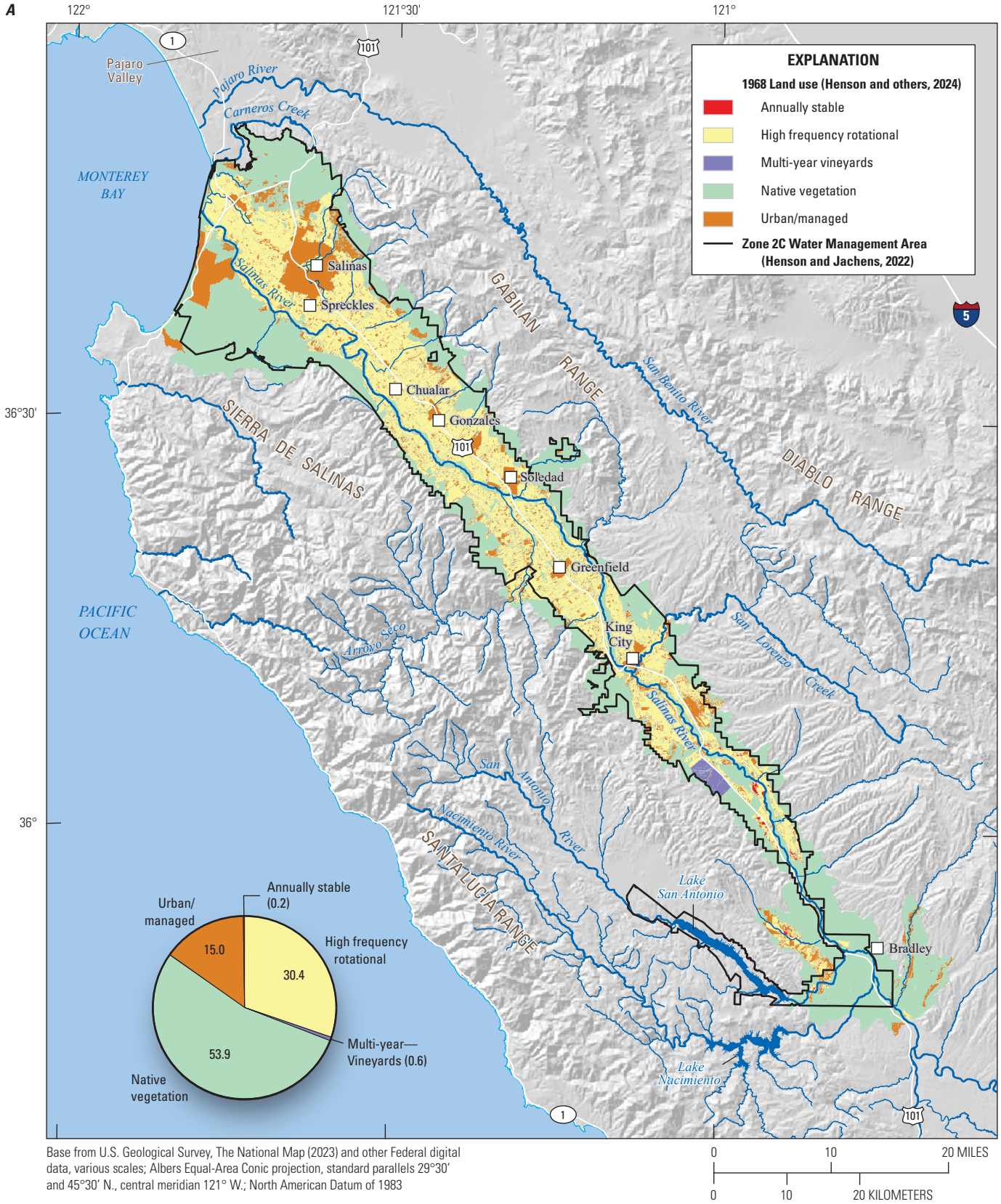


Figure 5. Integrated hydrologic model domain annual average gridded potential evapotranspiration at 530-foot resolution for water years 1968 to 2018, coastal and inland climate zones based on aggregation of California Irrigation Management Information System (CIMIS) climate zones, CIMIS evaluation locations, Remote Automatic Weather Stations (RAWS), and Cooperative Observer Network (COOP) stations.

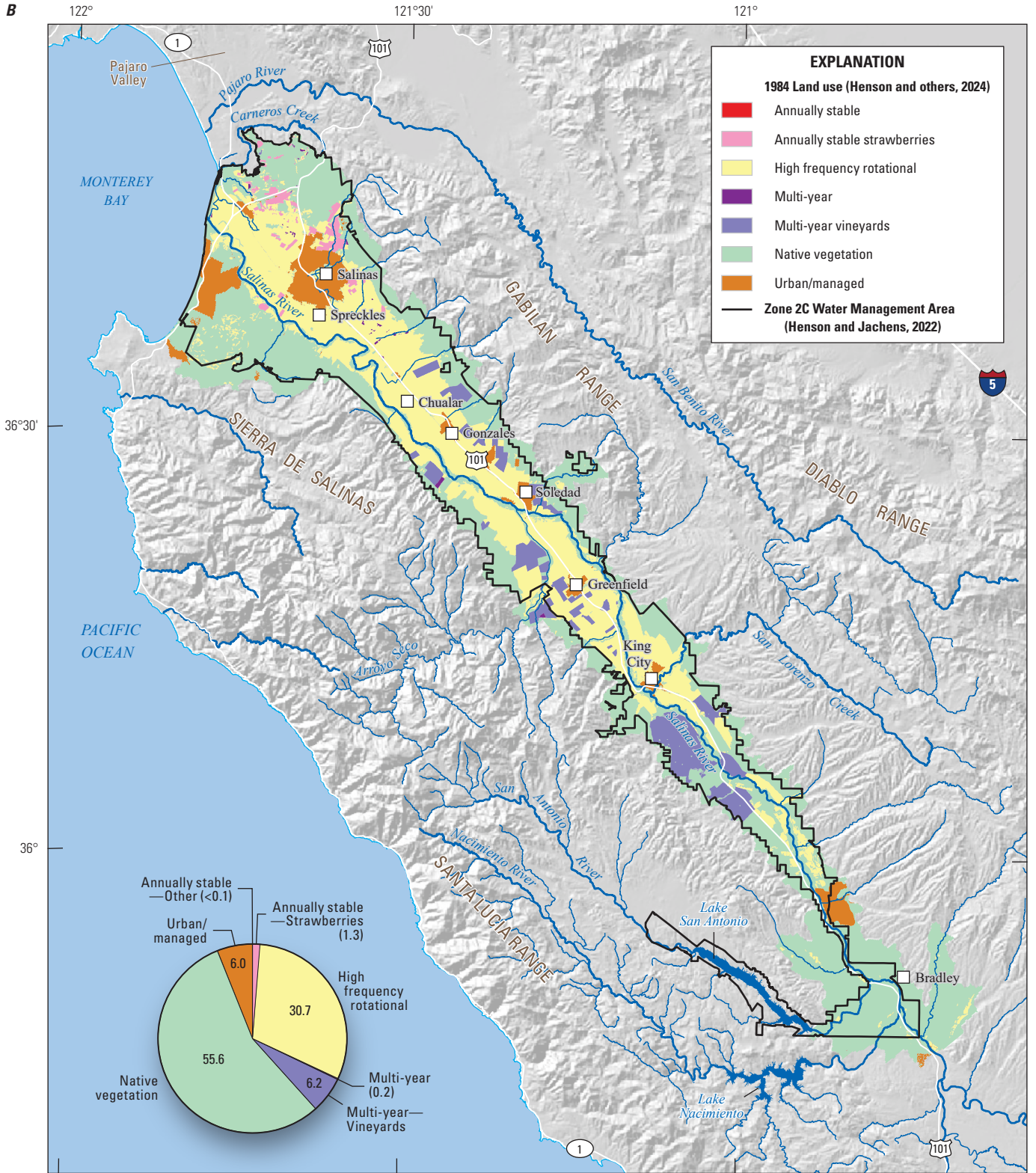


Base from U.S. Geological Survey, The National Map (2023) and other Federal digital data, various scales; Albers Equal-Area Conic projection, standard parallels 29°30' and 45°30' N., central meridian 121° W.; North American Datum of 1983

Figure 6. Integrated hydrologic model domain land use (Henson and others, 2024) for calendar years A) 1968, B) 1984, C) 1998, and D) 2014 that includes additional remotely sensed irrigated areas within the study area and outside of Zone 2C Water Management Area.



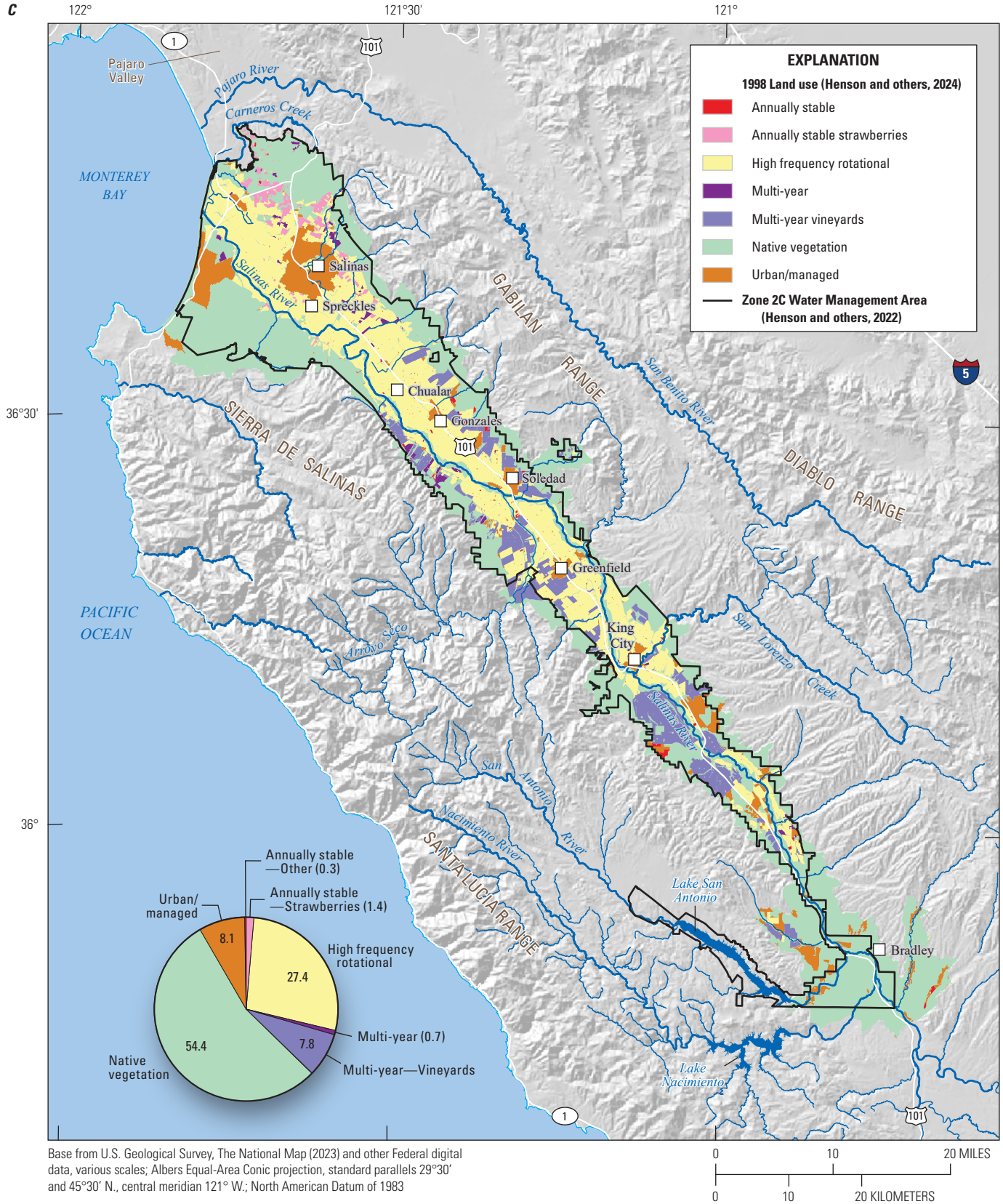
B



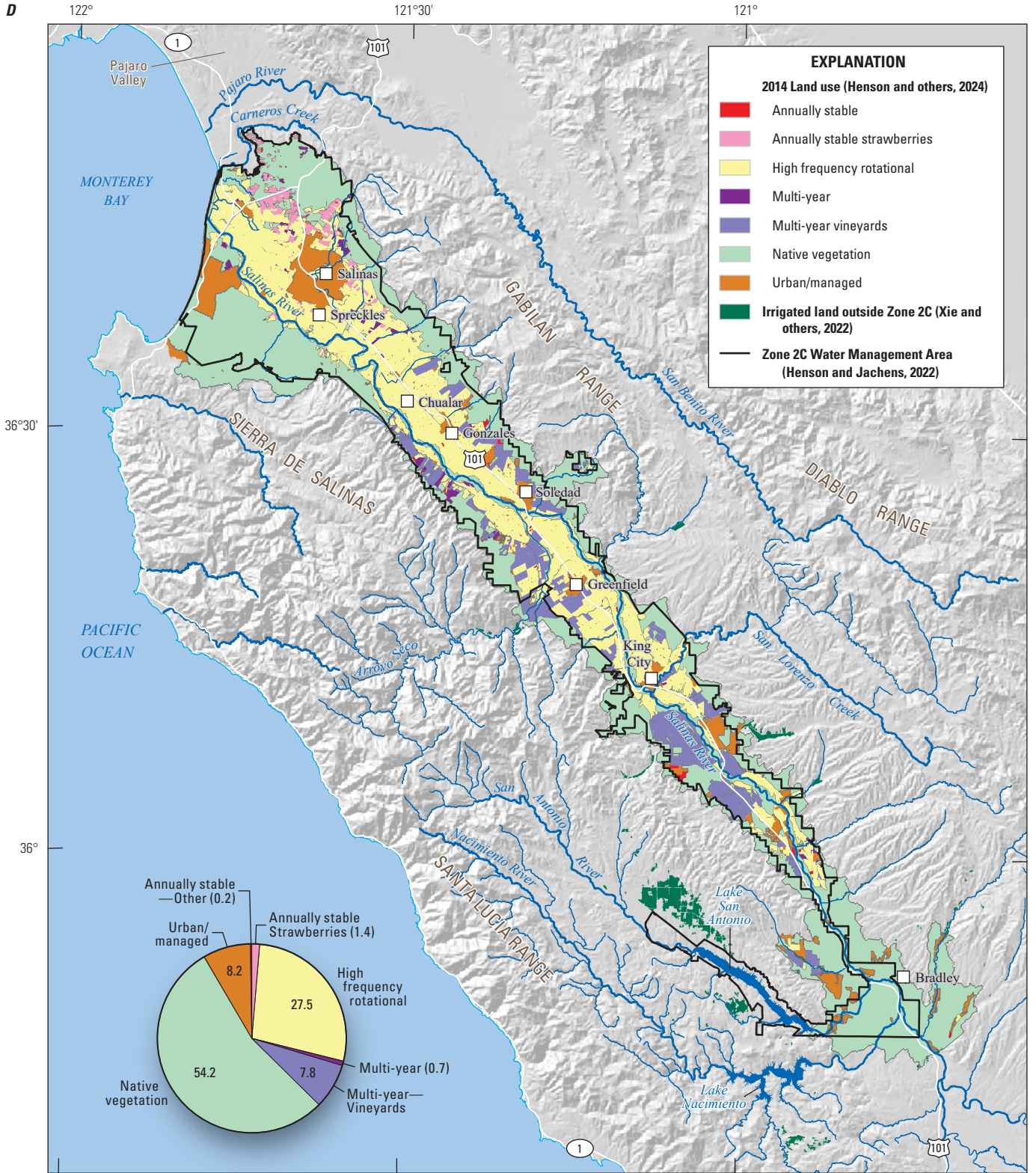
Base from U.S. Geological Survey, The National Map (2023) and other Federal digital data, various scales; Albers Equal-Area Conic projection, standard parallels 29°30' and 45°30' N., central meridian 121° W.; North American Datum of 1983



C



D



Base from U.S. Geological Survey, The National Map (2023) and other Federal digital data, various scales; Albers Equal-Area Conic projection, standard parallels 29°30' and 45°30' N., central meridian 121° W.; North American Datum of 1983



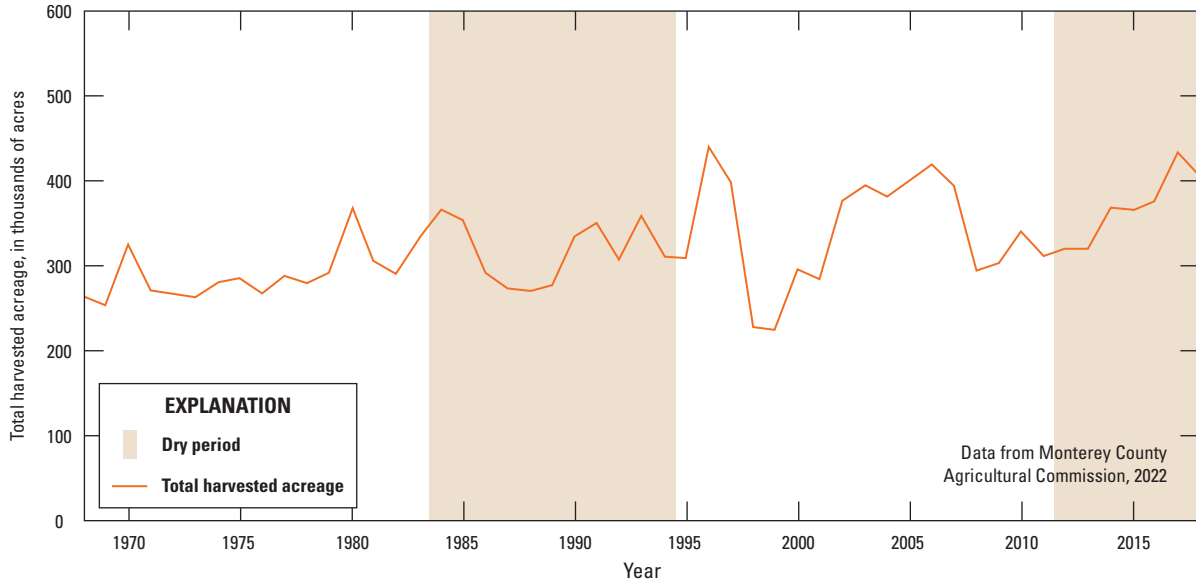


Figure 7. Cropped acreage estimates in the integrated hydrologic model domain showing total harvested acres in Monterey County during the study period.

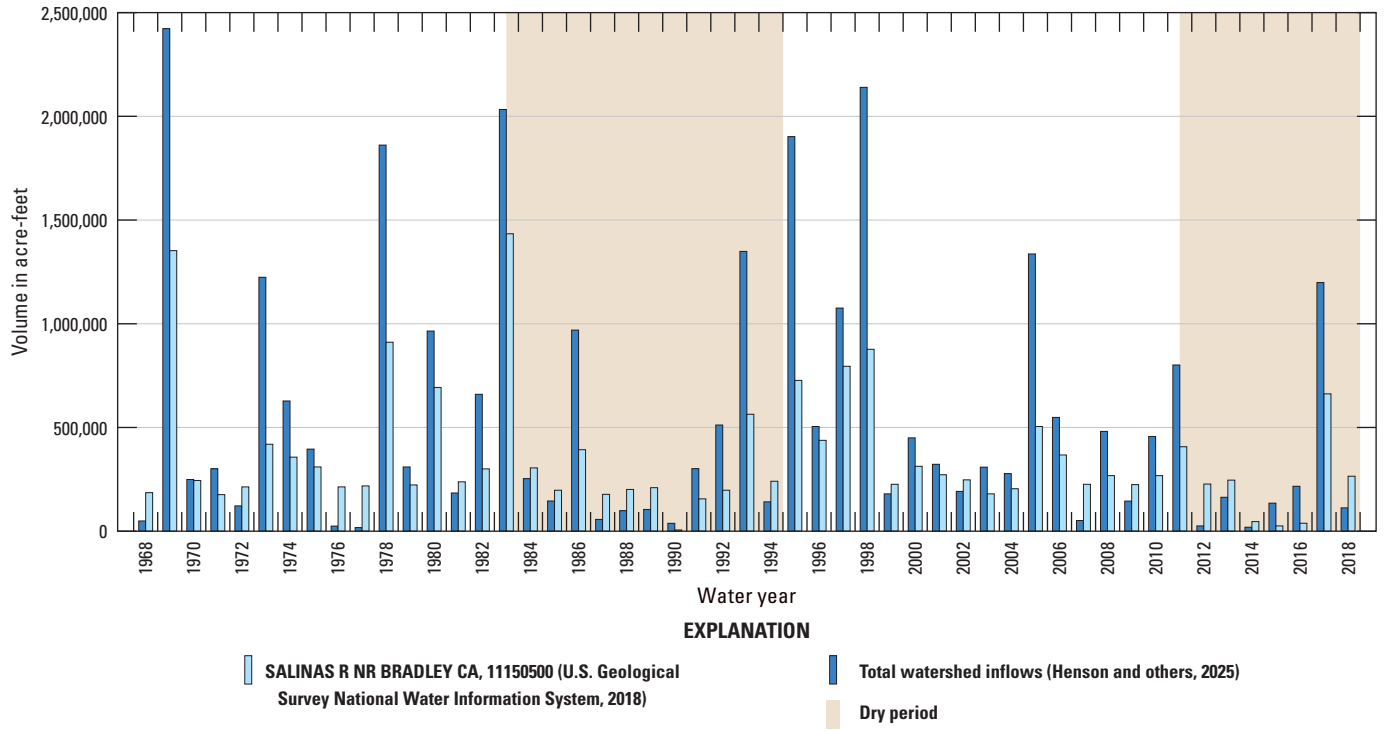


Figure 8. Comparison of total annual watershed inflows into the integrated hydrologic model domain from the Salinas Valley Watershed Model and observed Salinas River flows at the first gage on Salinas River in the study area (USGS 11150500 Salinas River near Bradley, California) (USGS, 2018) to show the relative contribution of surface water from adjacent watershed inflows and inflows from the upper watershed outside of the study area for water years 1968 through 2018.

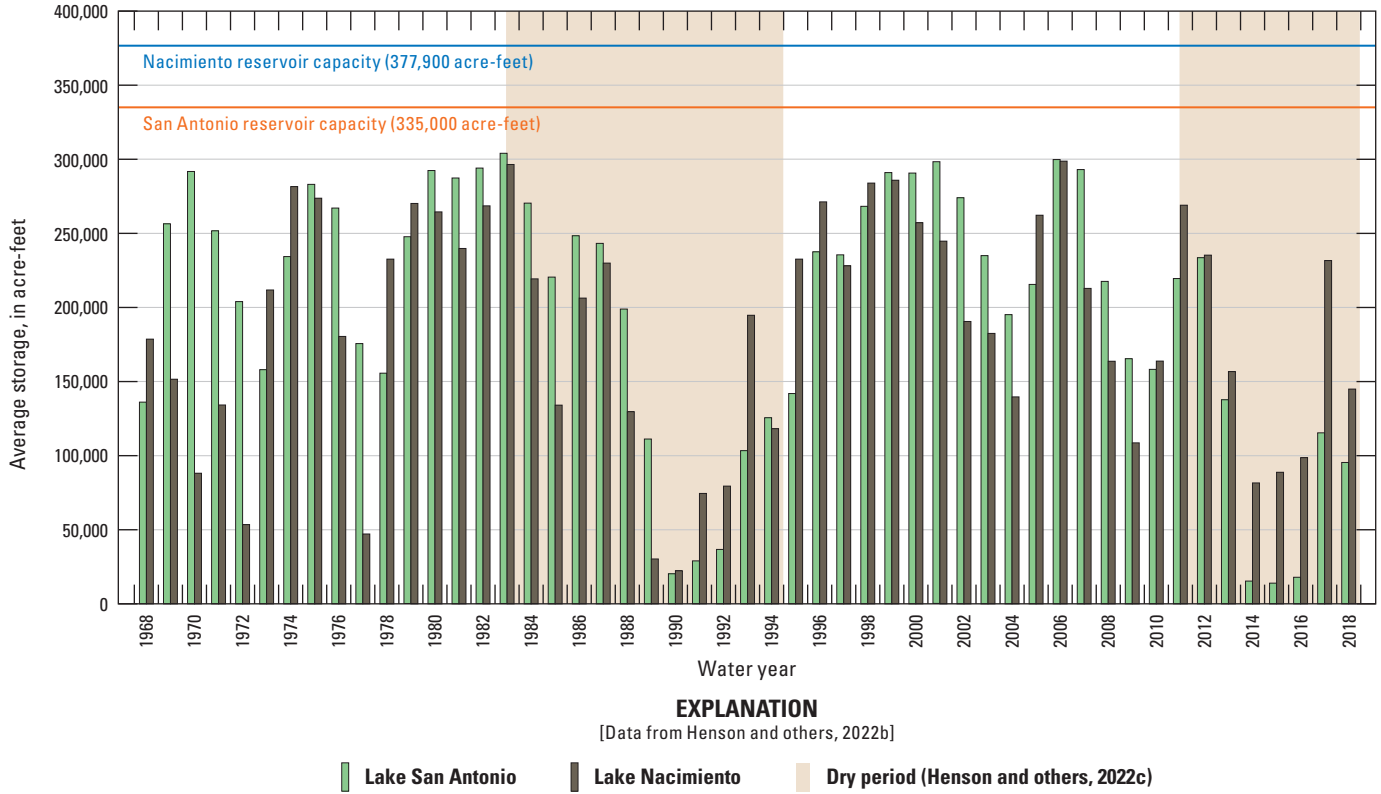


Figure 9. Comparison of annual mean storage in Lakes San Antonio and Nacimiento for water years 1968 through 2018.

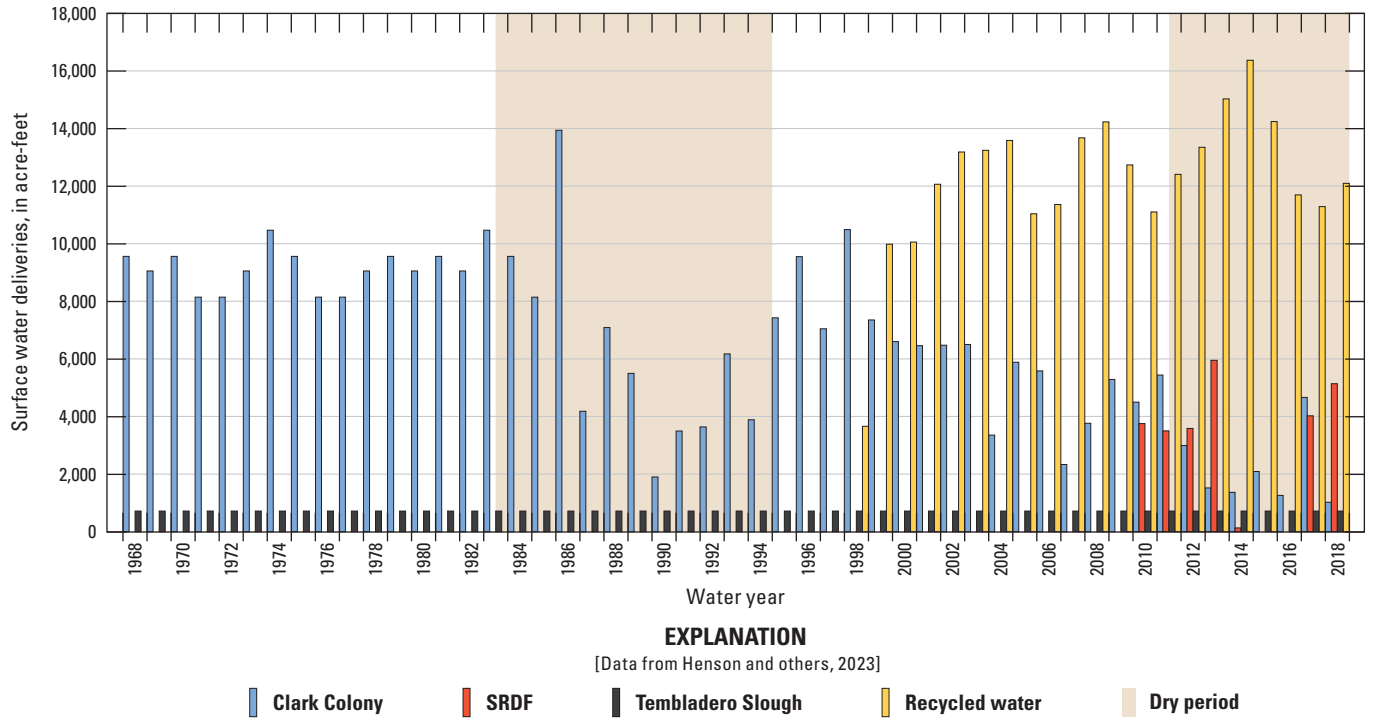


Figure 10. Surface water deliveries from agricultural diversions for Clark Colony and Salinas River Diversion Facility (SRDF), channel wetting diversions for Tembladero Slough, and recycled water deliveries for the Castroville Seawater Intrusion Project (CSIP) from water year 1968 to 2018 (Henson and others, 2023).

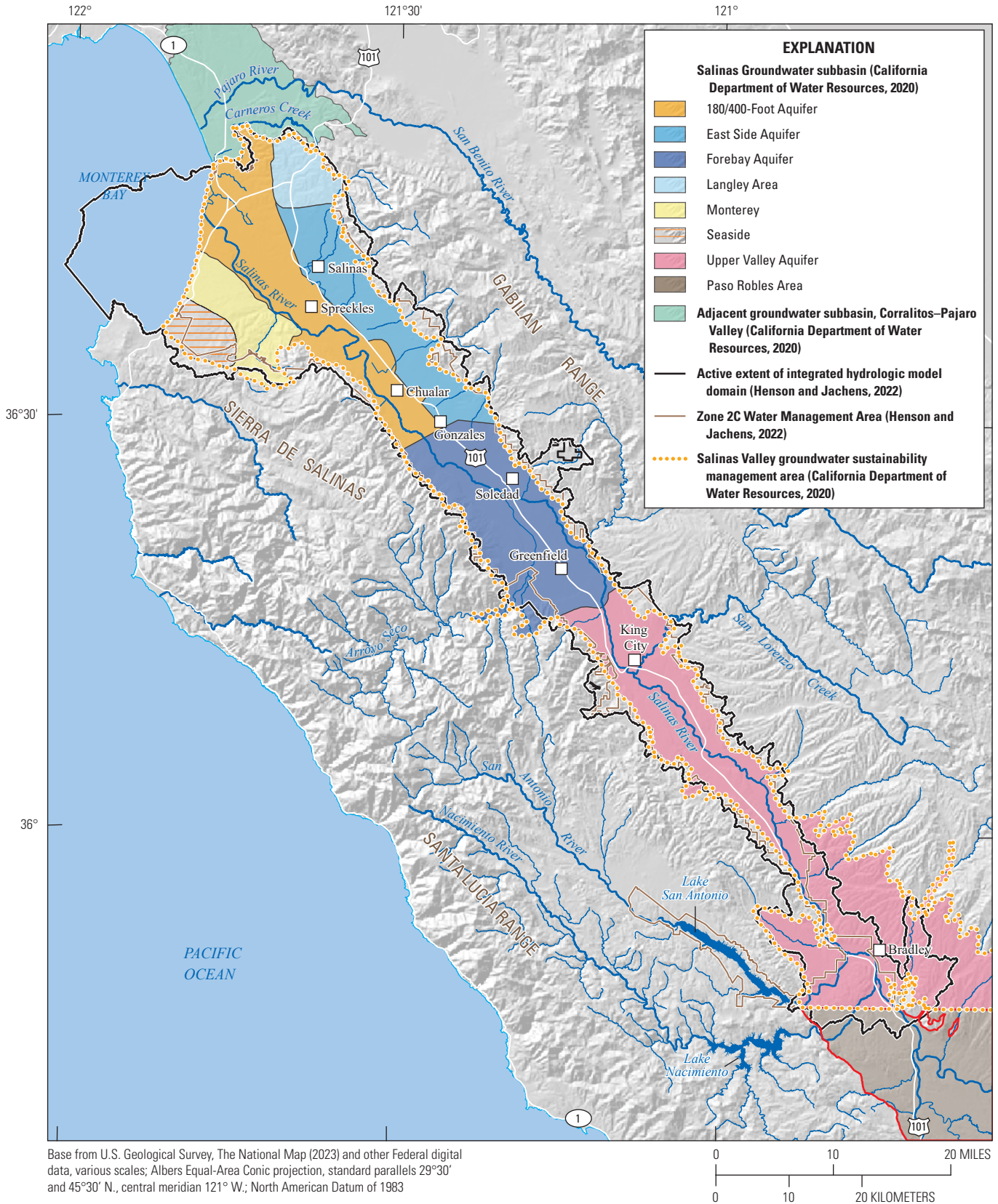


Figure 11. Groundwater basins and subbasins within and adjacent to the Salinas Valley.



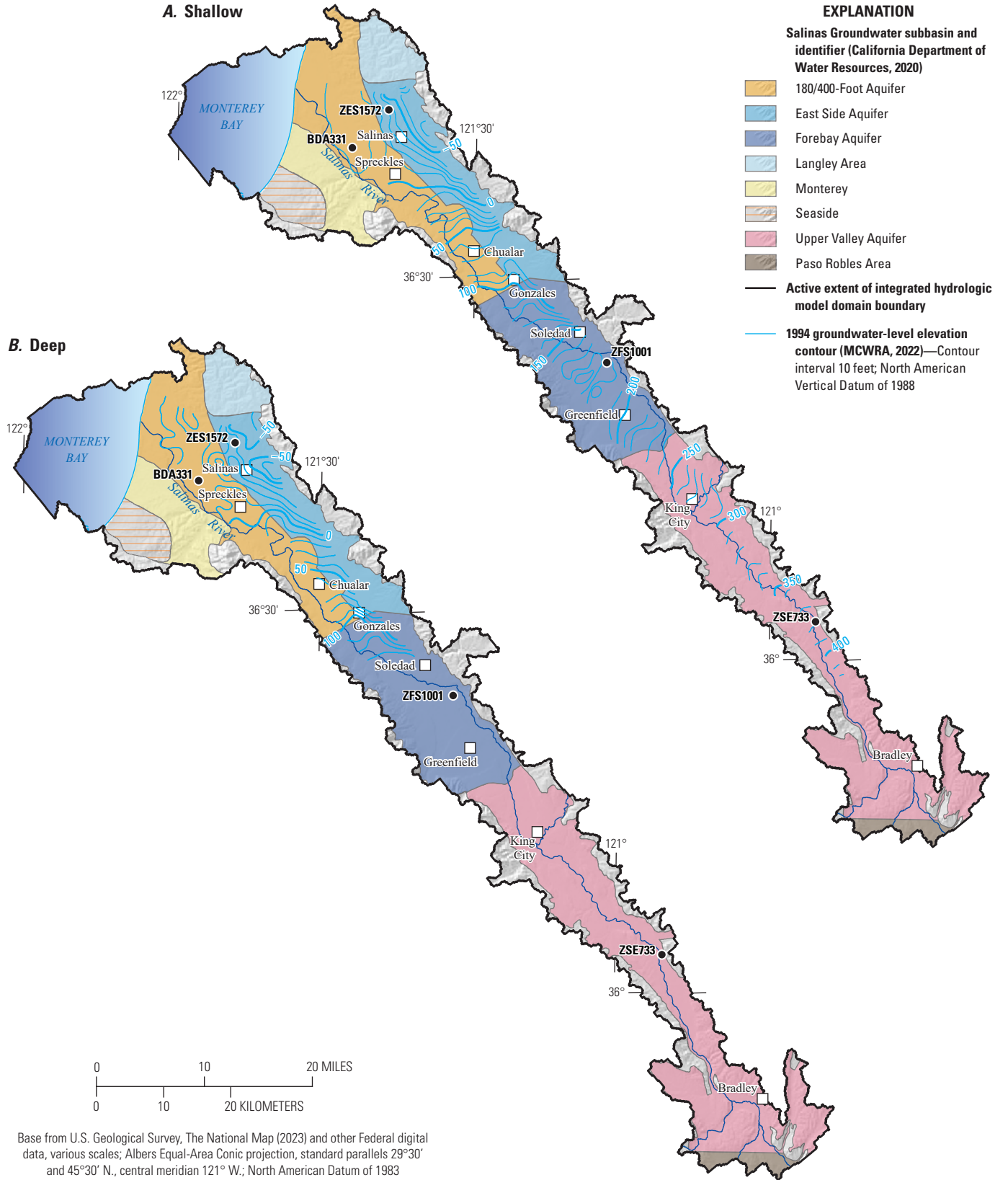


Figure 12. Estimated groundwater level contours in the integrated hydrologic model domain for A) shallow aquifers (less than 200 feet deep) and B) deep aquifers (greater than 200 feet deep) in fall 1994. The Salinas River, Salinas Valley groundwater subbasins, and selected observation wells are also shown.

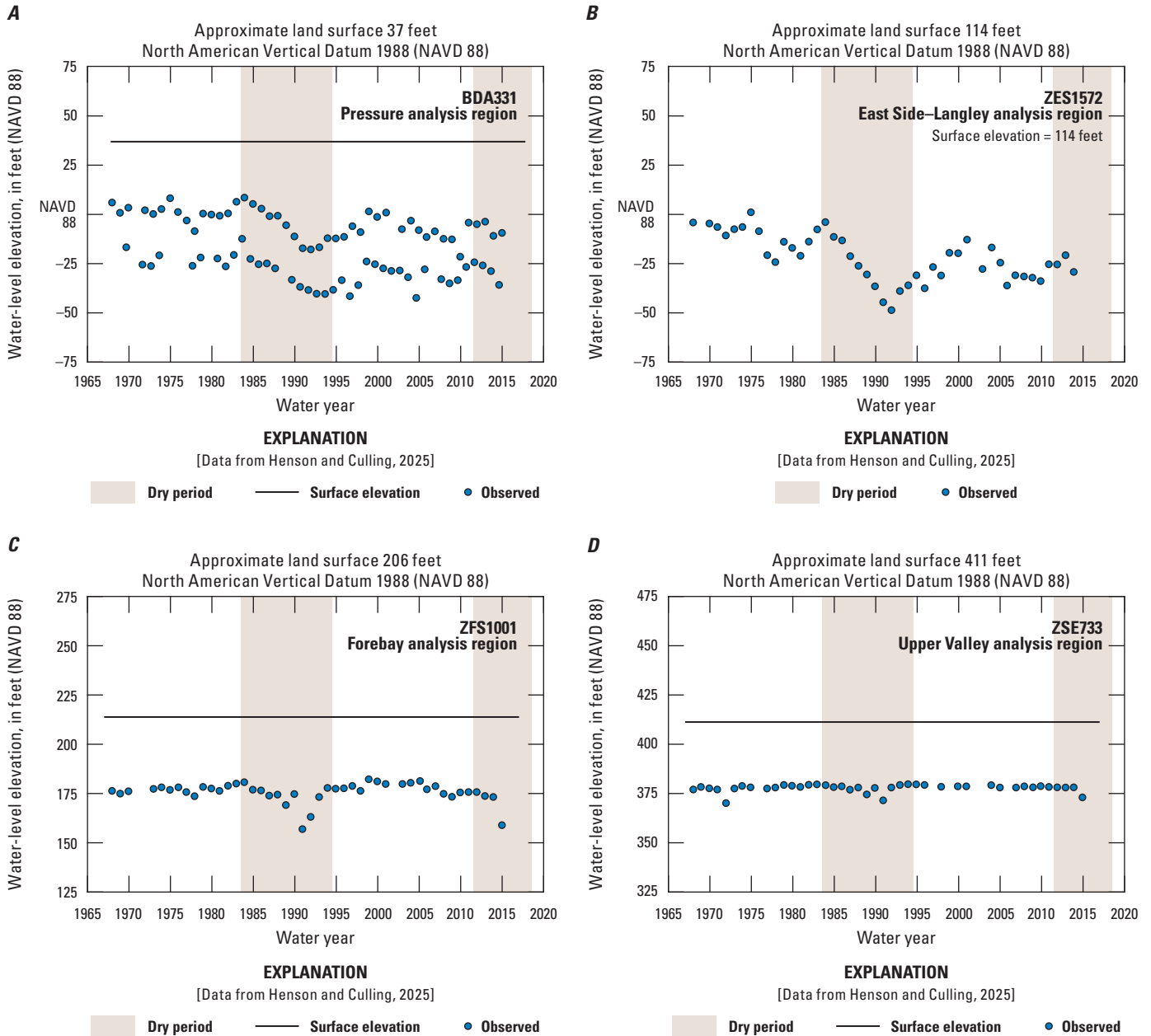


Figure 13. Observed water levels during the study period for A) well BDA331 in the 180-Foot/400-Foot Aquifer groundwater subbasin, B) well ZES1572 in the East Side Aquifer groundwater subbasin, C) ZFS1001 in the Forebay Aquifer groundwater subbasin, and D) well ZSE733 in the Upper Valley Aquifer groundwater subbasin.

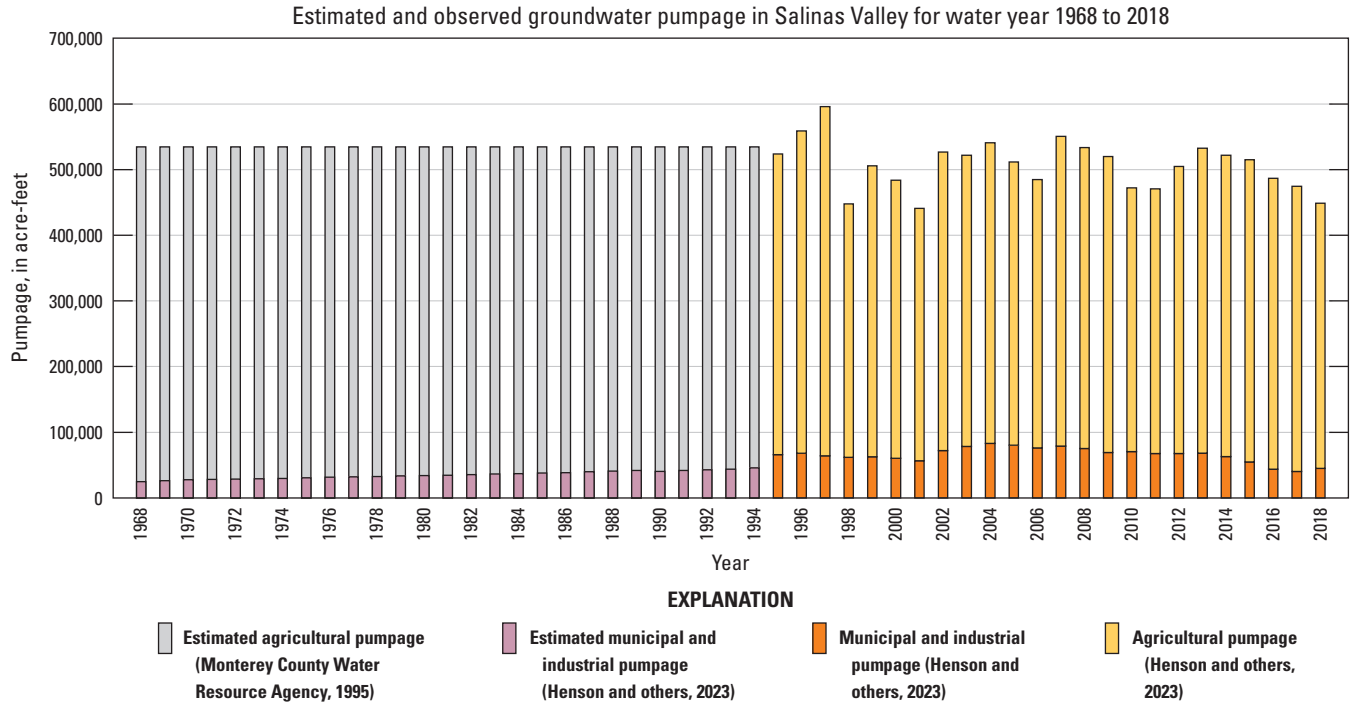


Figure 14. Annual total municipal, industrial, and agricultural pumpage in Zone 2C Water Management Area from water year 1970 through 2018. Pumpage is estimated before 1994 and reported for water years 1995 to 2018.

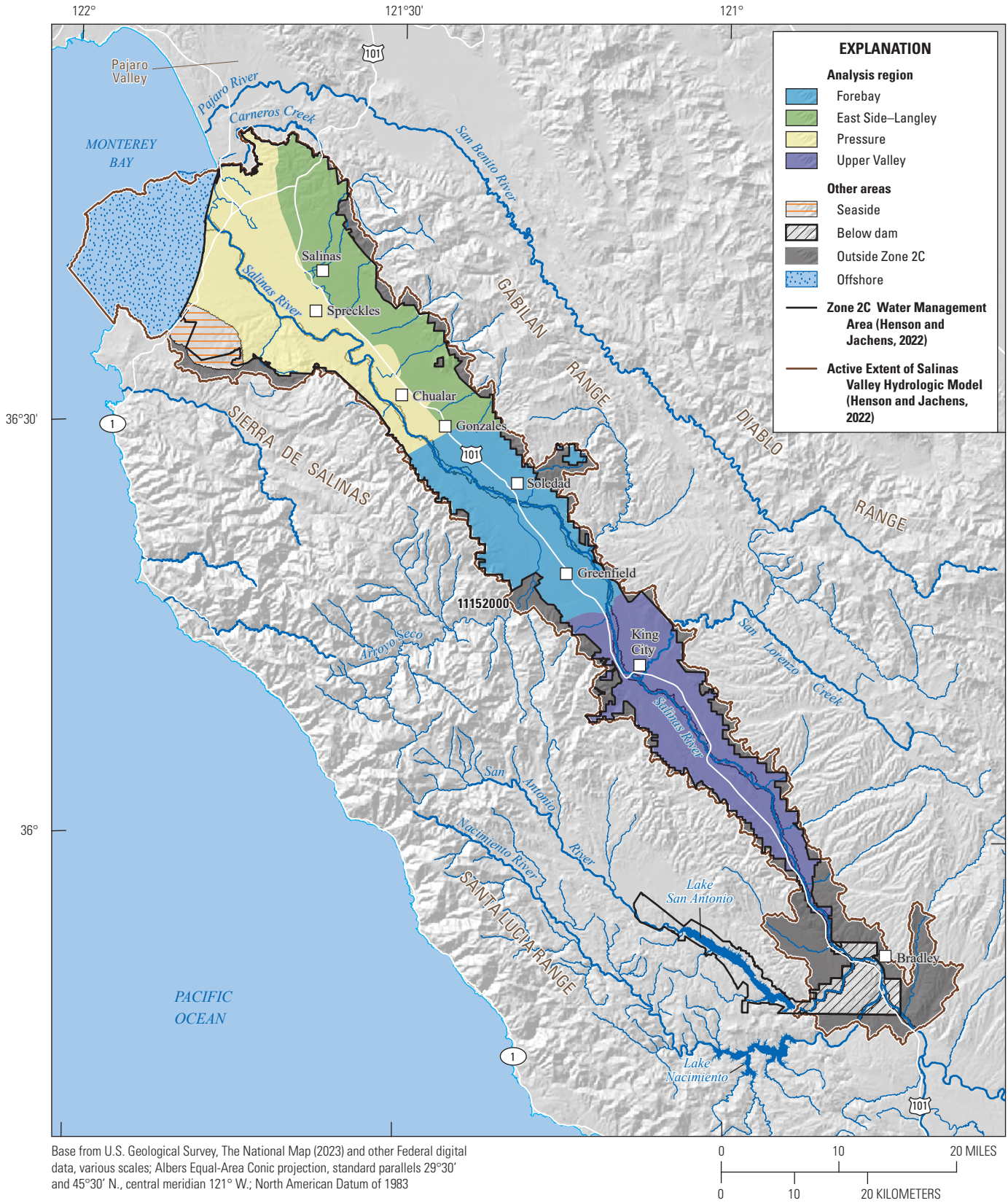


Figure 15. Analysis regions and other areas that are simulated within the integrated hydrologic model domain.

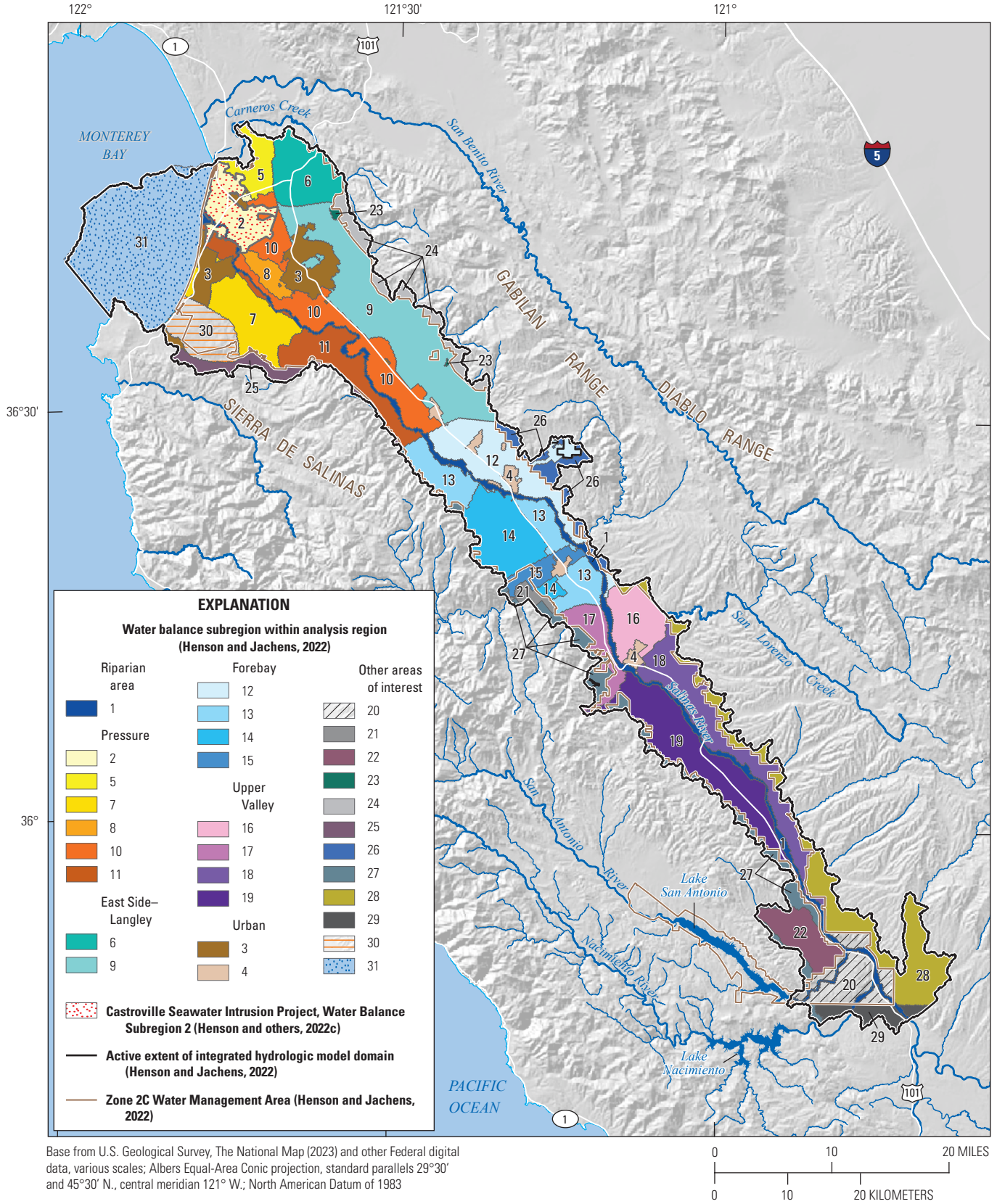


Figure 16. Thirty-one (31) water balance subregions of the integrated hydrologic model domain.

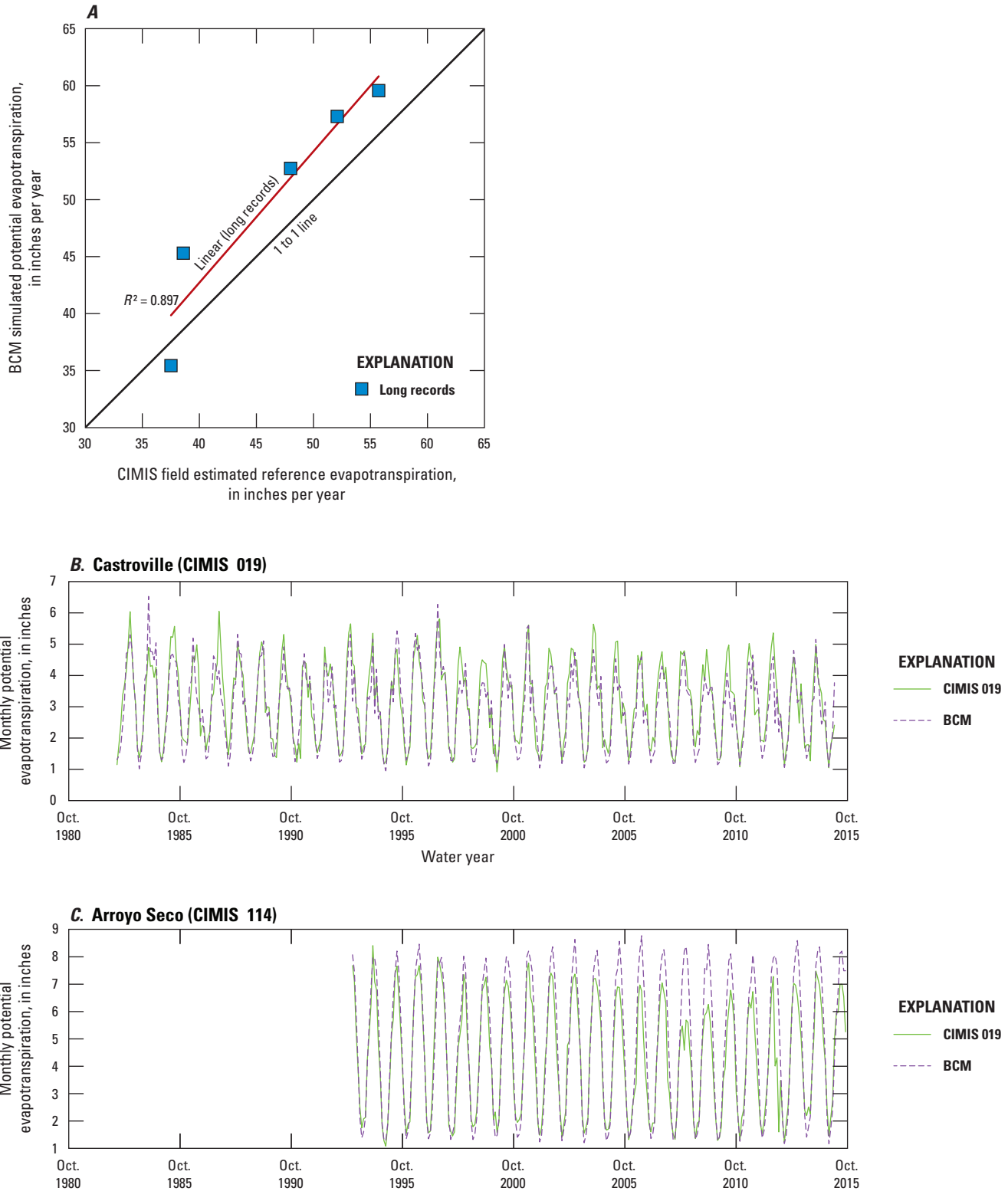
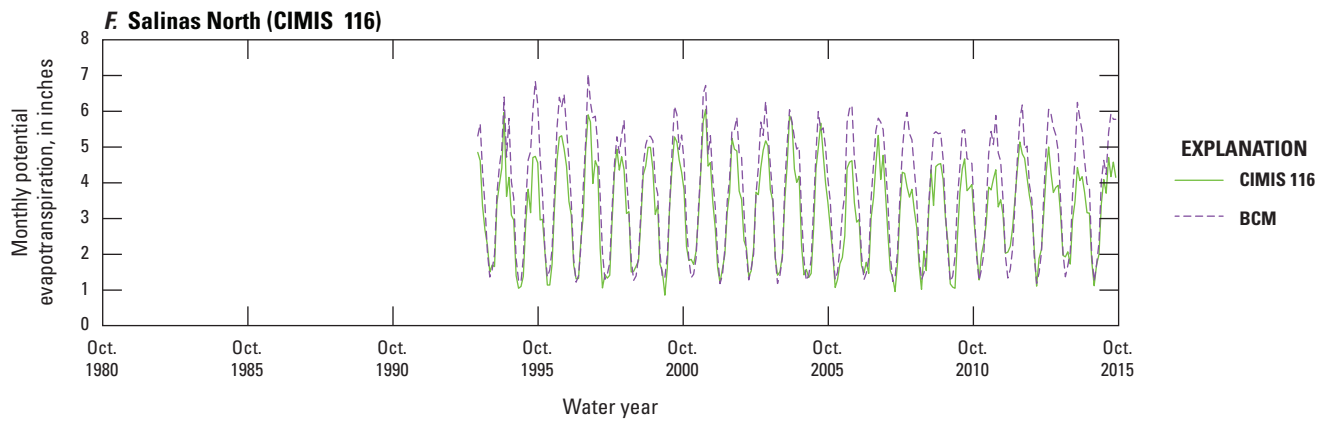
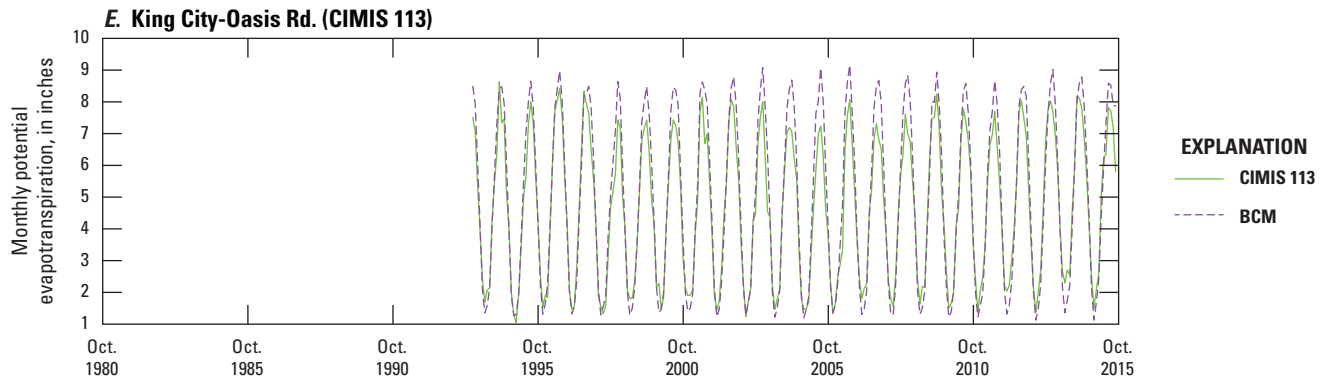
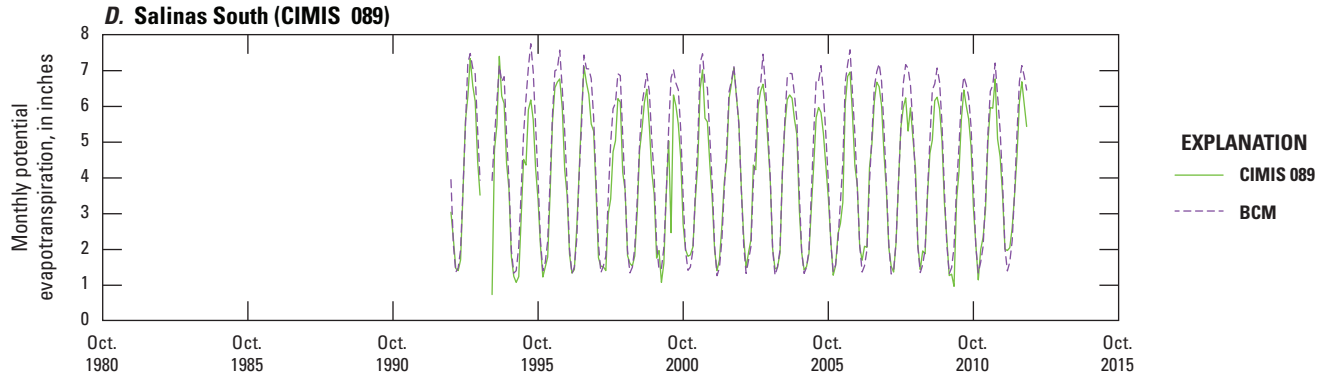


Figure 17. California Irrigation Management Information System (CIMIS, 2020) field-scale reference evapotranspiration (ET<sub>ref</sub>) and potential evapotranspiration (PET) estimated using the 270-meter-resolution Basin Characterization Model (BCM; Hevesi and others, 2022) at the same location. A) Correlation and comparison of stations with long-term records used for more detailed comparisons. Comparisons of time series are shown for B) Castroville (CIMIS 019), C) Arroyo Seco (CIMIS 114), D) Salinas South (CIMIS 089), E) King City-Oasis Rd. (CIMIS 113), and F) Salinas North (CIMIS 116).



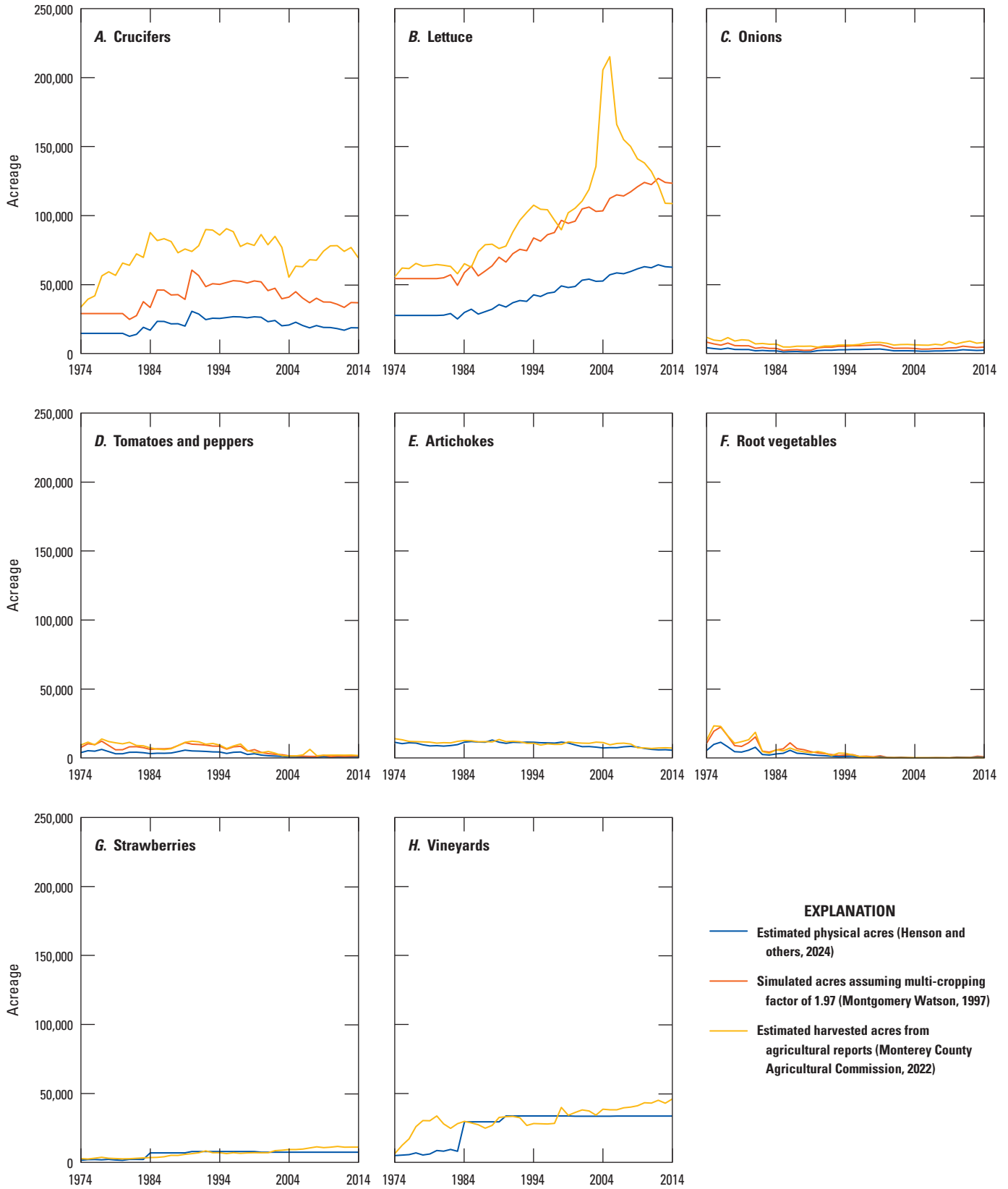
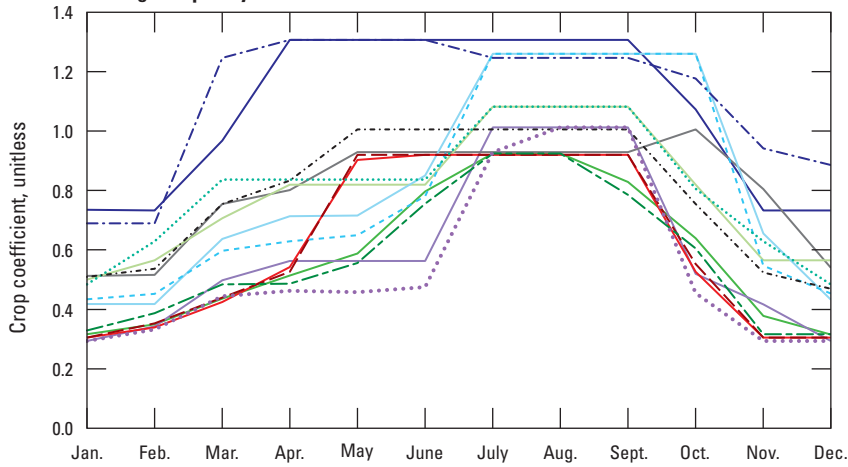


Figure 18. Comparison of time series of physical acreage, simulated acreage assuming a multi-cropping factor of 1.97, and harvested acreage for selected land use types in the Salinas Valley for water years 1968 through 2014.

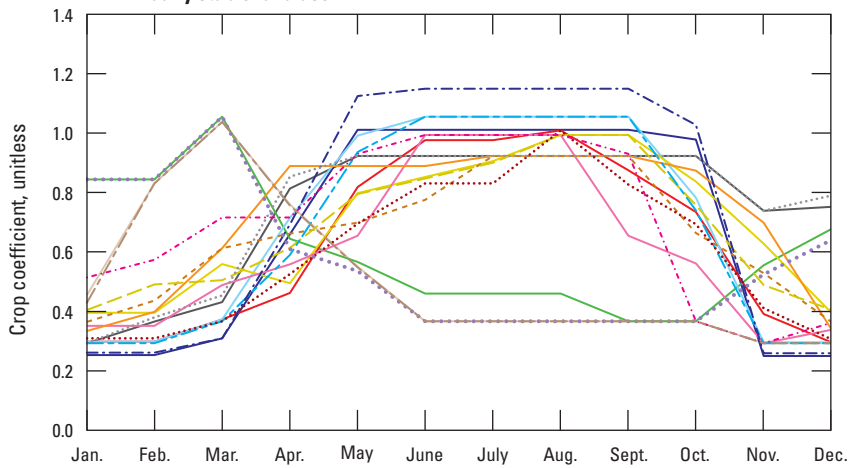


**A. High frequency land use**



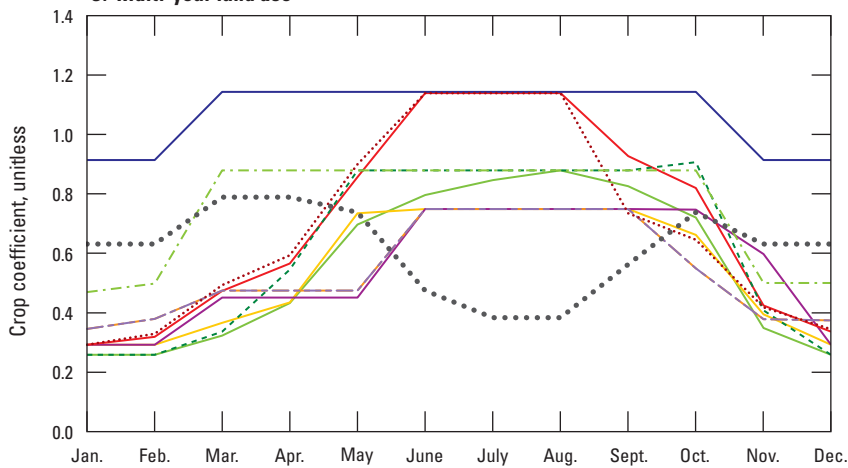
EXPLANATION	
Coastal	Inland
Celery	Celery
Cucumber/melons/squash	Cucumber/melons/squash
Legumes	Legumes
Lettuce	Lettuce
Rotational 30-day	Rotational 30-day
Crucifers-cabbages	Crucifers-cabbages
Unspecified irrigated row crops	Unspecified irrigated row crops

**B. Annually stable land use**



EXPLANATION	
Coastal	Inland
Carrots	Carrots
Onions/garlic	Onions/garlic
Root vegetables	Root vegetables
Tomato/peppers	Tomato/peppers
Strawberries	Strawberries
Corn	Corn
Field crops	Field crops
Grain crops	Grain crops
Cane/bush berries	Cane/bush berries

**C. Multi-year land use**



EXPLANATION	
Coastal	Inland
Deciduous fruits and nuts	Deciduous fruits and nuts
Citrus and subtropical	Citrus and subtropical
Vineyards	Vineyards
Nurseries, outdoor	Nurseries, outdoor
Nurseries, indoor	
Artichokes	
Pasture	

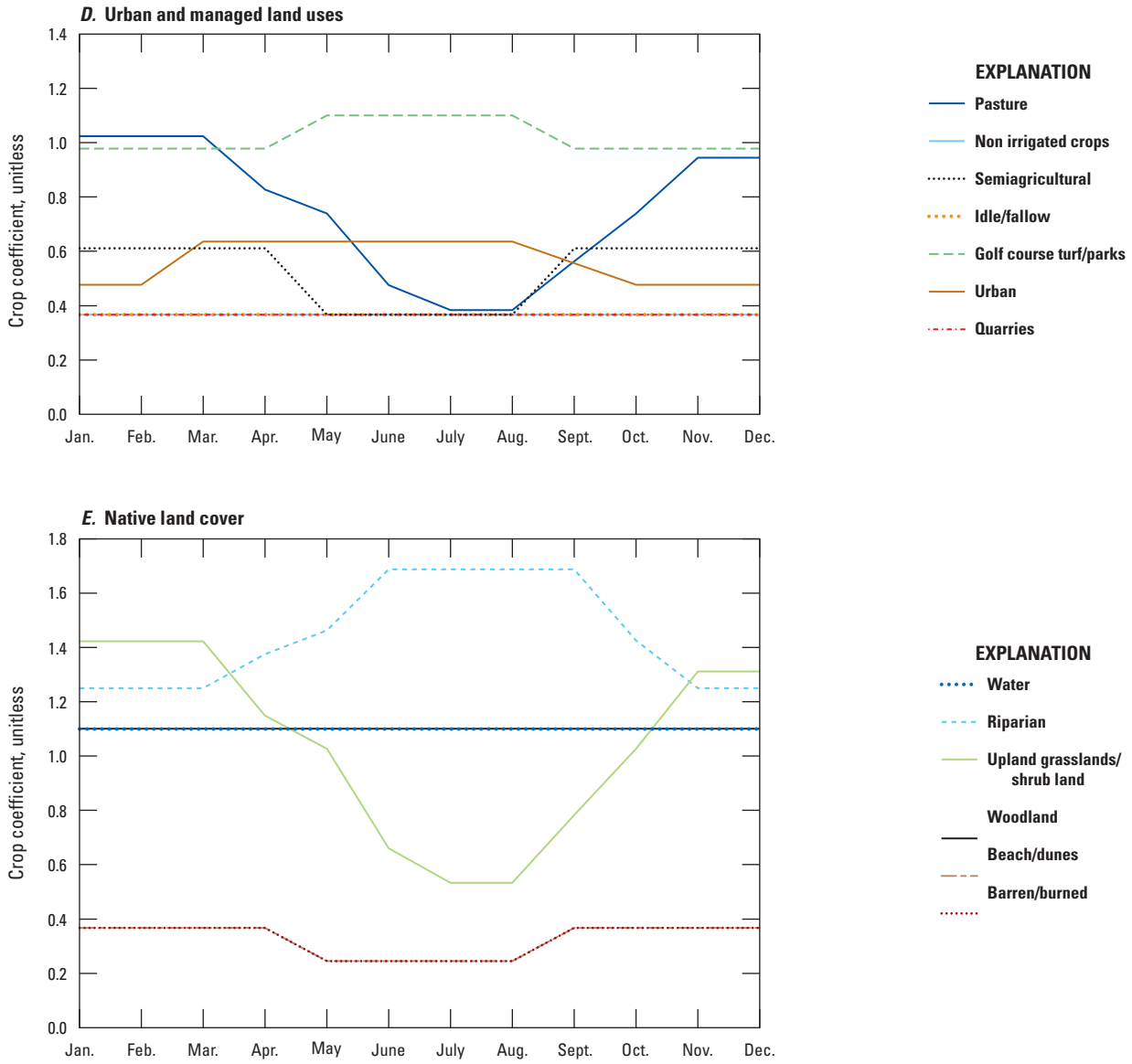


Figure 19. Crop coefficients by land use type for A) high frequency land use, B) annually stable land use, C) multi-year land use, D) urban and managed land use, and E) native land cover in Salinas Valley, California.

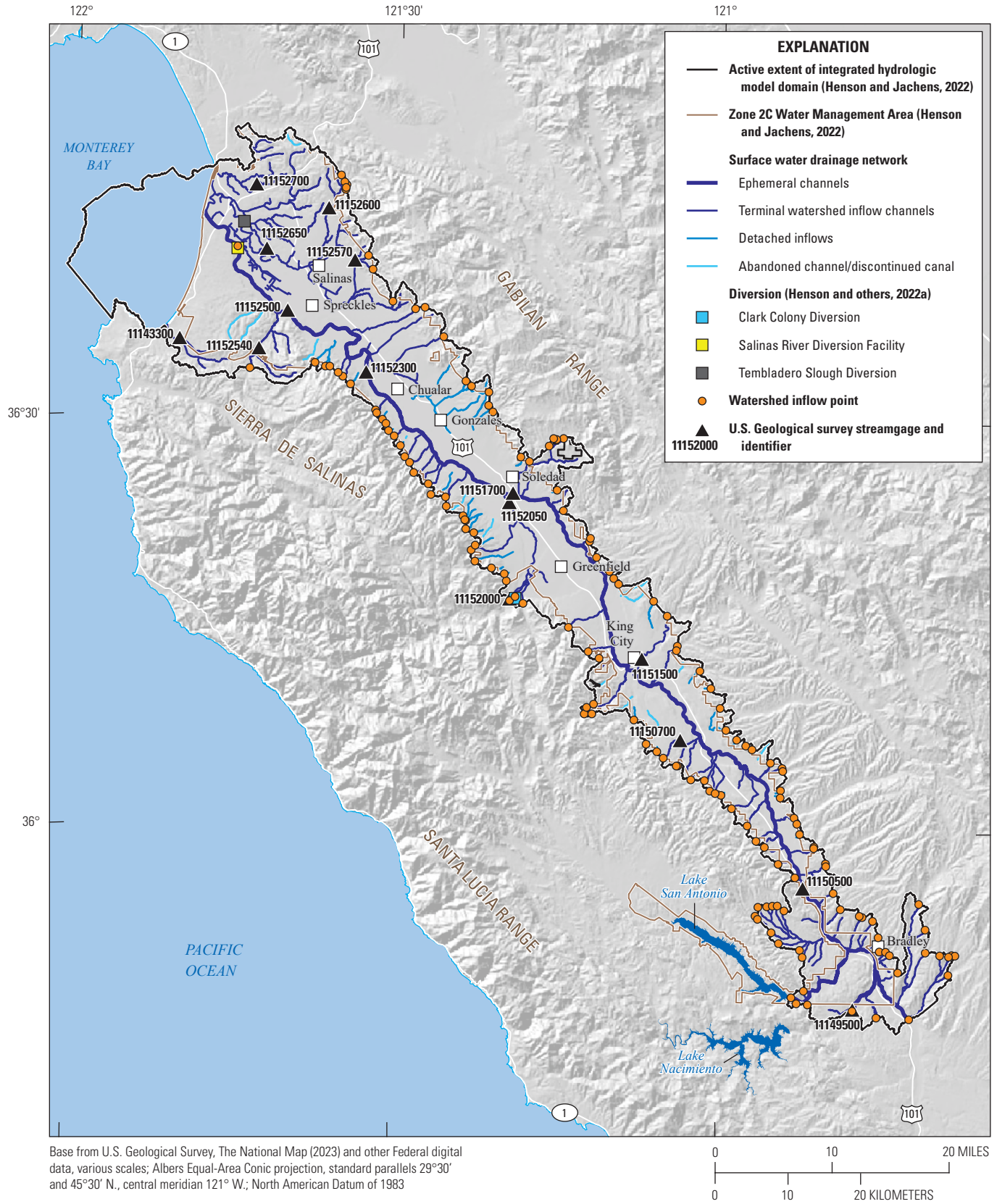
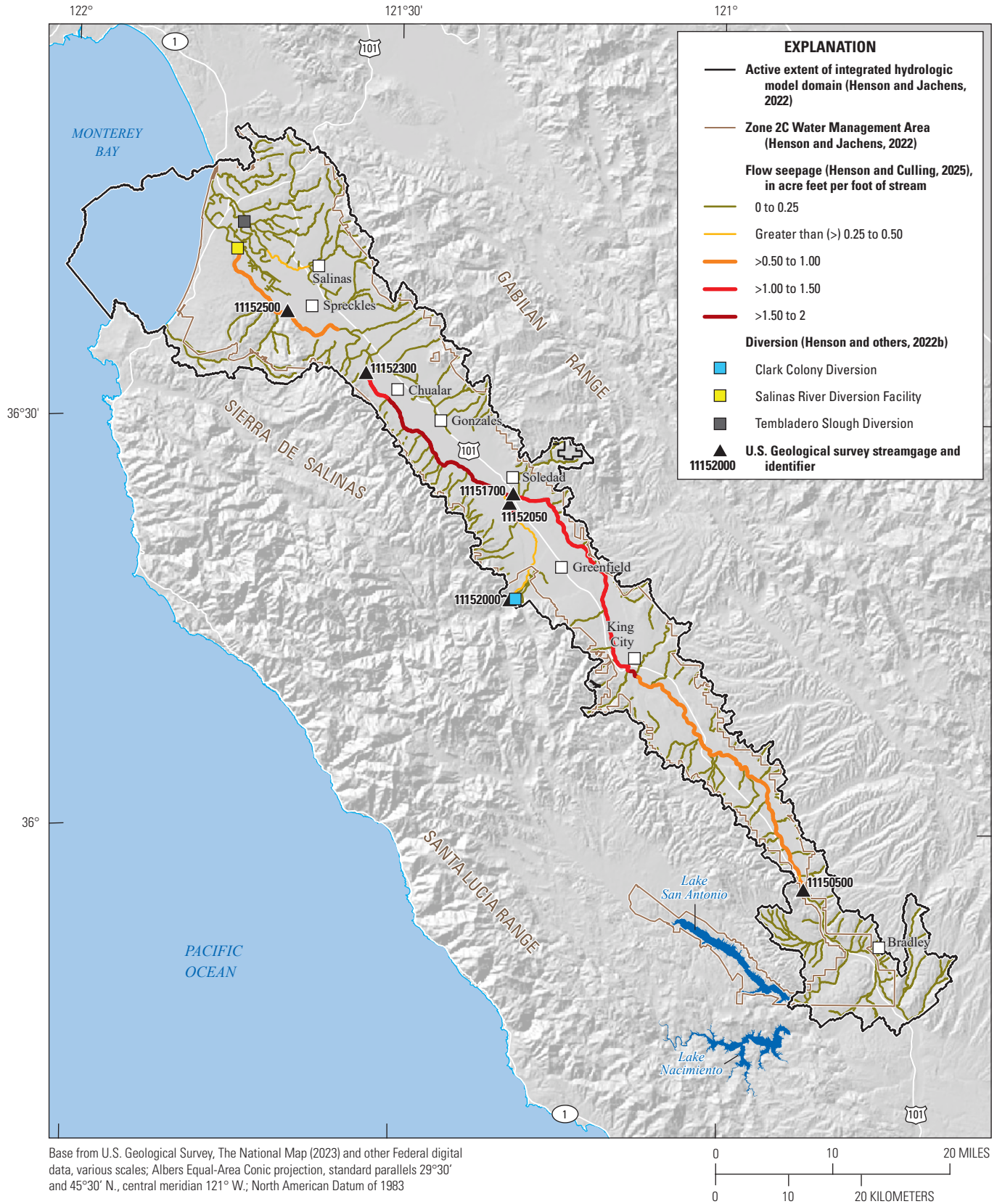
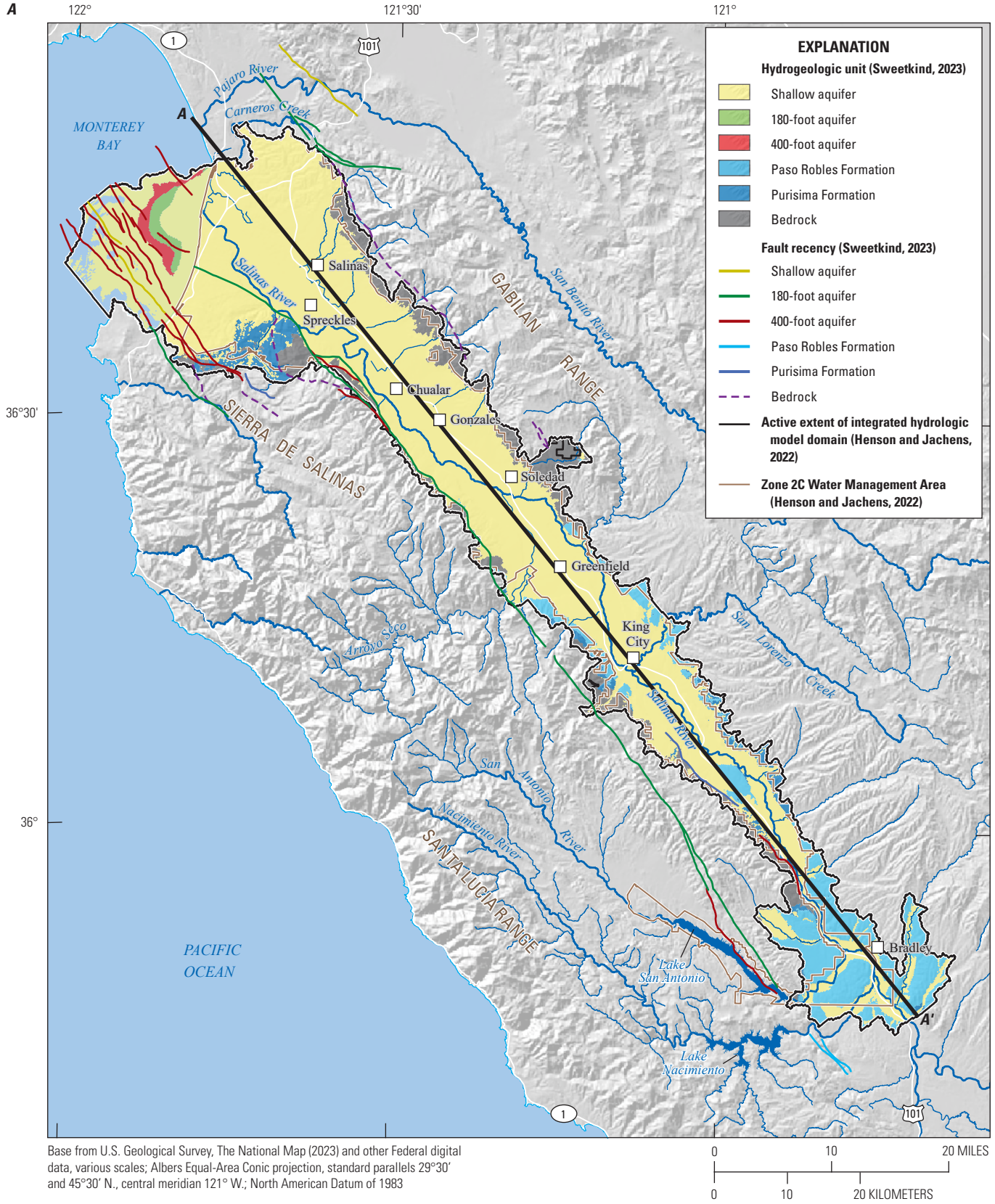


Figure 20. Surface water drainage network channel types within the Salinas Valley study area, USGS National Water Information System streamgages, stream diversion locations, and point locations of watershed inflows from outside the active model domain.



Base from U.S. Geological Survey, The National Map (2023) and other Federal digital data, various scales; Albers Equal-Area Conic projection, standard parallels 29°30' and 45°30' N., central meridian 121° W.; North American Datum of 1983

Figure 21. Annual average net stream leakage normalized by segment length in the surface water drainage network in acre-feet per year per foot (af/f), diversion locations, and selected streamgages used for analysis.



Base from U.S. Geological Survey, The National Map (2023) and other Federal digital data, various scales; Albers Equal-Area Conic projection, standard parallels 29°30' and 45°30' N., central meridian 121° W.; North American Datum of 1983

Figure 22. A) surface extent of hydrogeologic units and fault traces of the Salinas Valley study area in Monterey and San Luis Obispo Counties, California, adapted from the Salinas Valley Geologic Framework (Sweetkind, 2023) and B) conceptual cross section through hydrogeologic units of the Salinas Valley Geologic Framework along the central axis of the Salinas Valley. Vertical exaggeration is approximately 100 times.

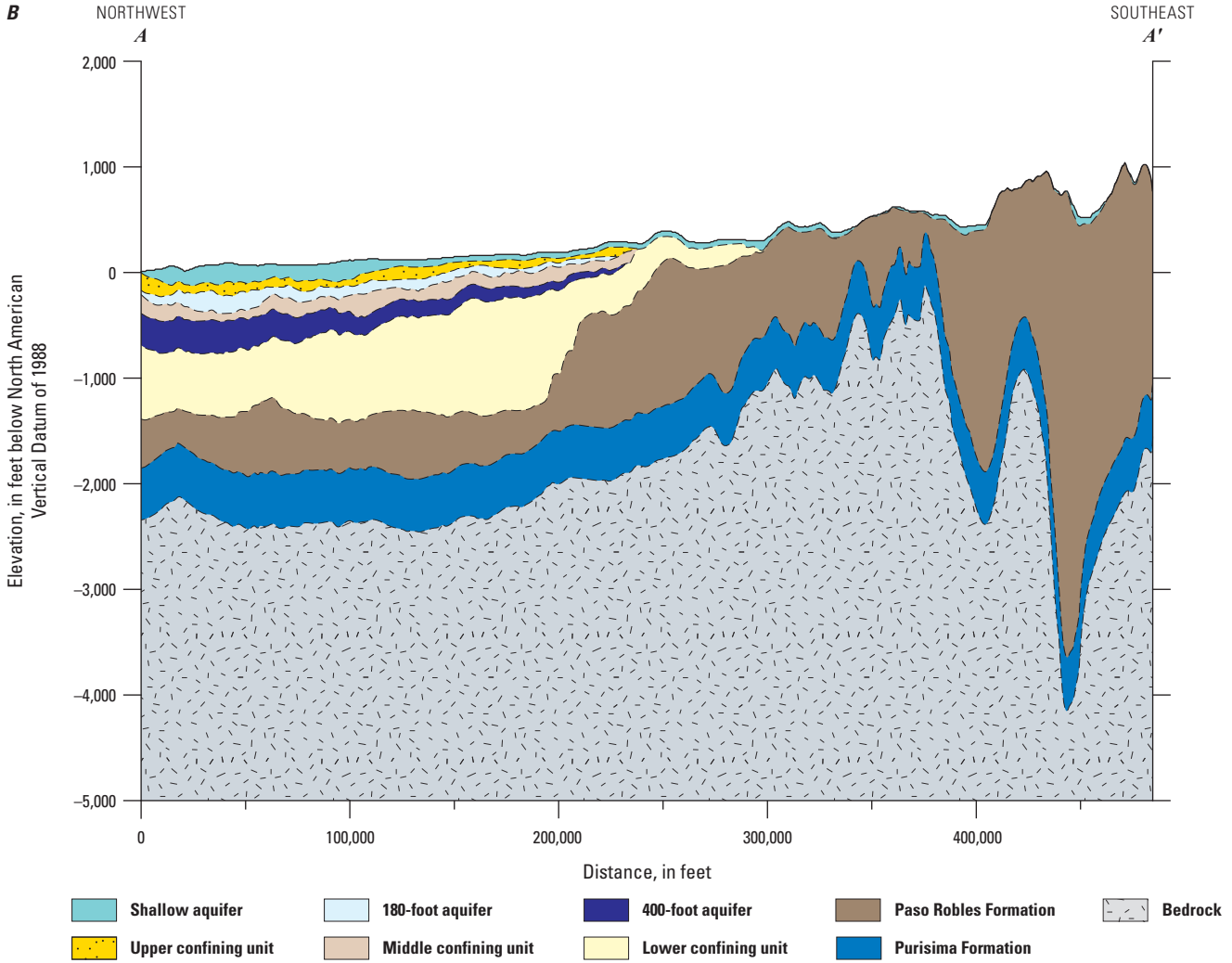
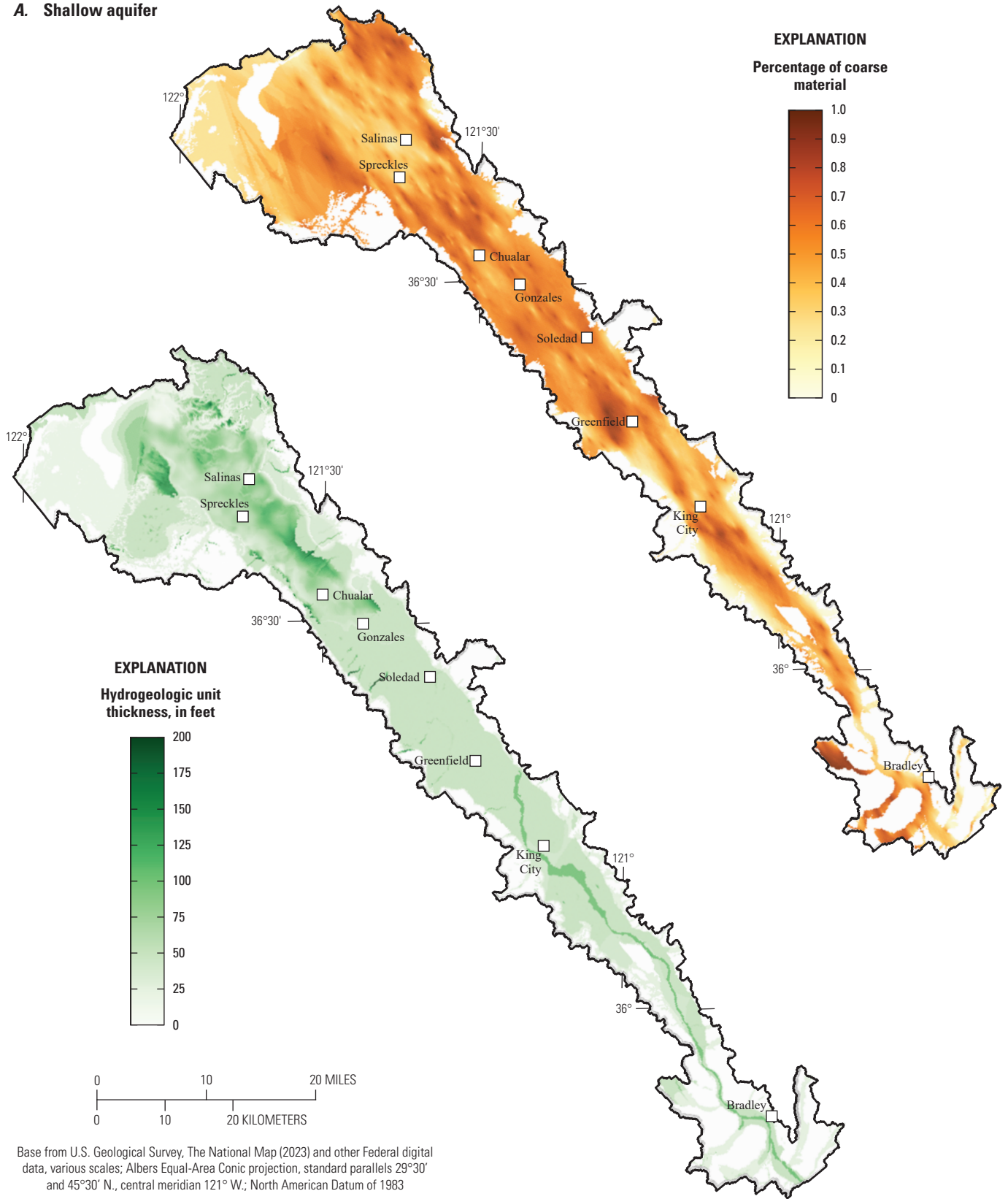


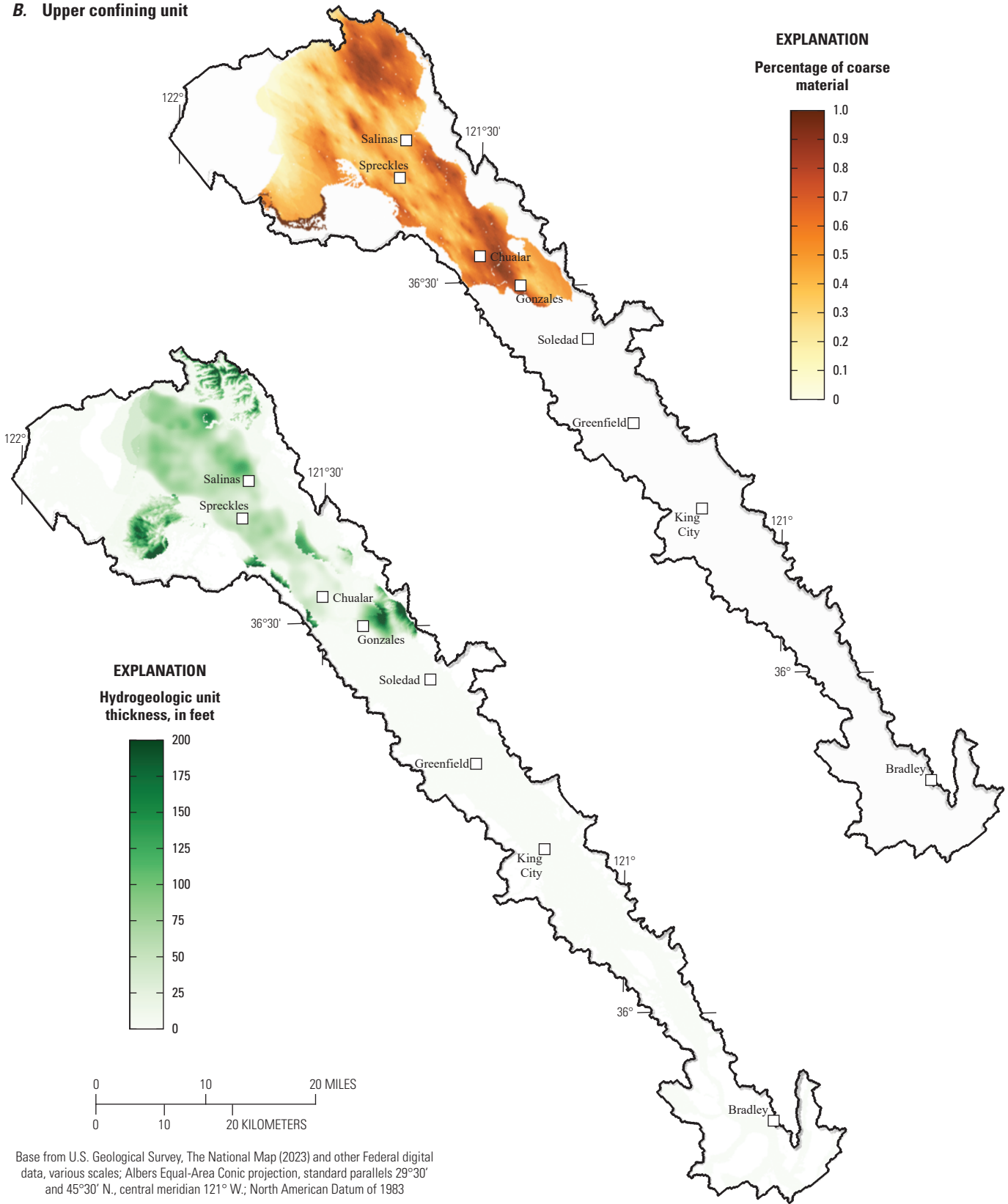
Figure 23. Hydrogeologic unit thickness and percentage of coarse material for hydrogeologic units in the Salinas Valley, California that are not fully consolidated (Sweetkind, 2023): A) shallow aquifer, B) upper confining unit, C) 180-Foot Aquifer, D) middle confining unit, E) 400-Foot Aquifer, F) lower confining unit, and G) Paso Robles Formation; and H) maps showing hydrogeologic unit thickness for Purisima Formation and bedrock hydrogeologic units. The Purisima Formation and bedrock hydrogeologic units represent composite rock aquifers without a textural classification so the percentage of coarse materials is not shown.

**A. Shallow aquifer**



Base from U.S. Geological Survey, The National Map (2023) and other Federal digital data, various scales; Albers Equal-Area Conic projection, standard parallels 29°30' and 45°30' N., central meridian 121° W.; North American Datum of 1983

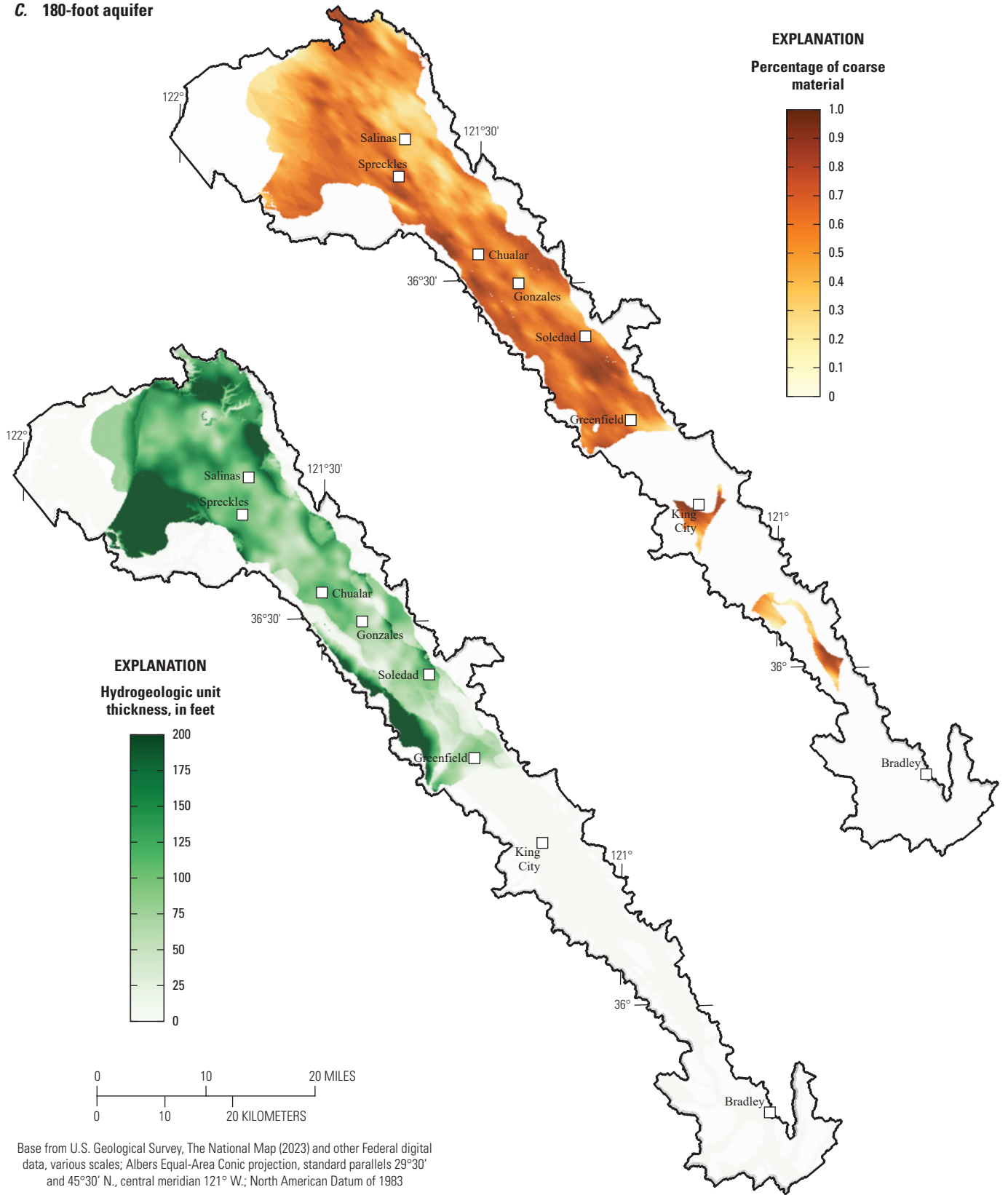
**B. Upper confining unit**



Base from U.S. Geological Survey, The National Map (2023) and other Federal digital data, various scales; Albers Equal-Area Conic projection, standard parallels 29°30' and 45°30' N., central meridian 121° W.; North American Datum of 1983

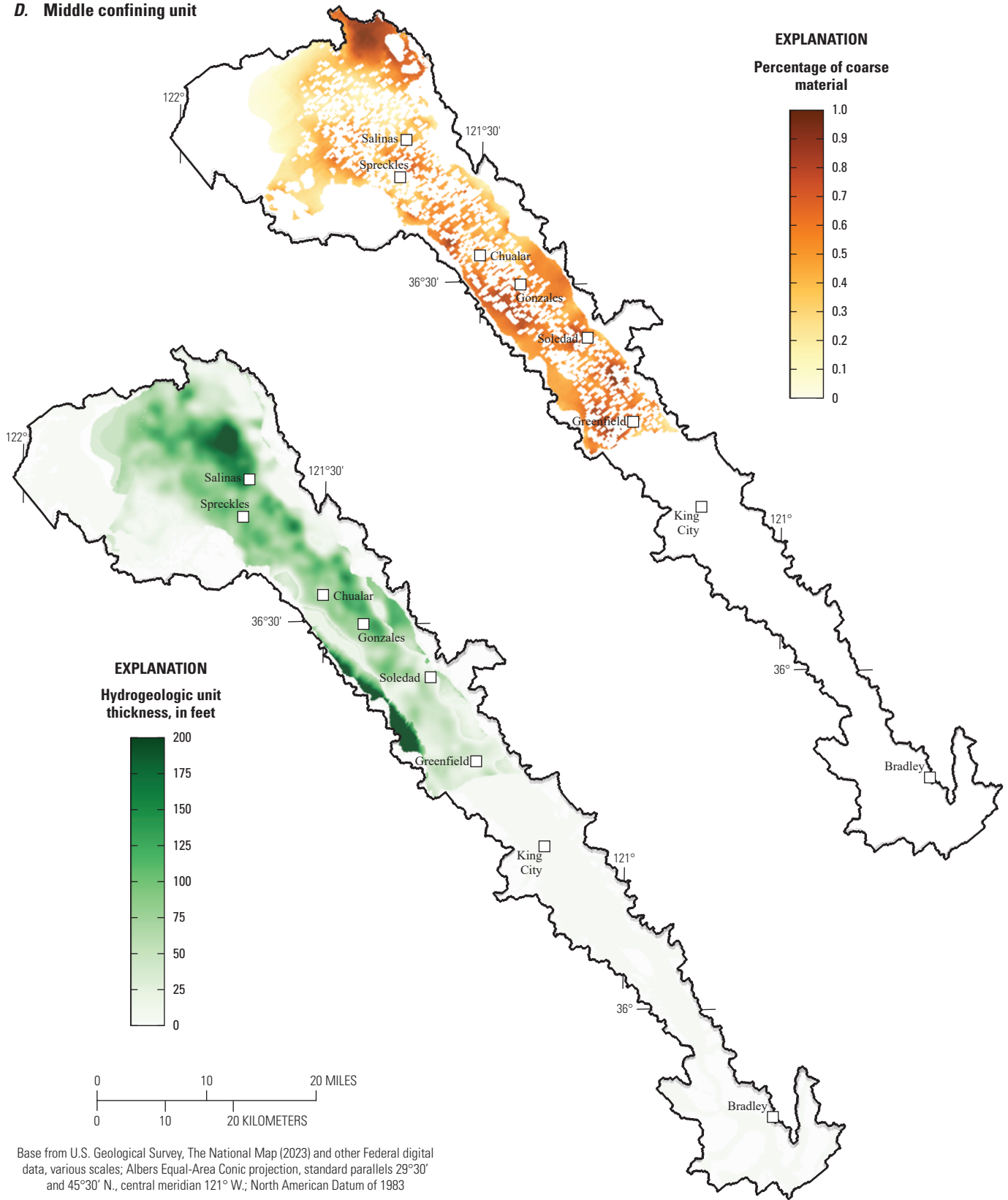


C. 180-foot aquifer

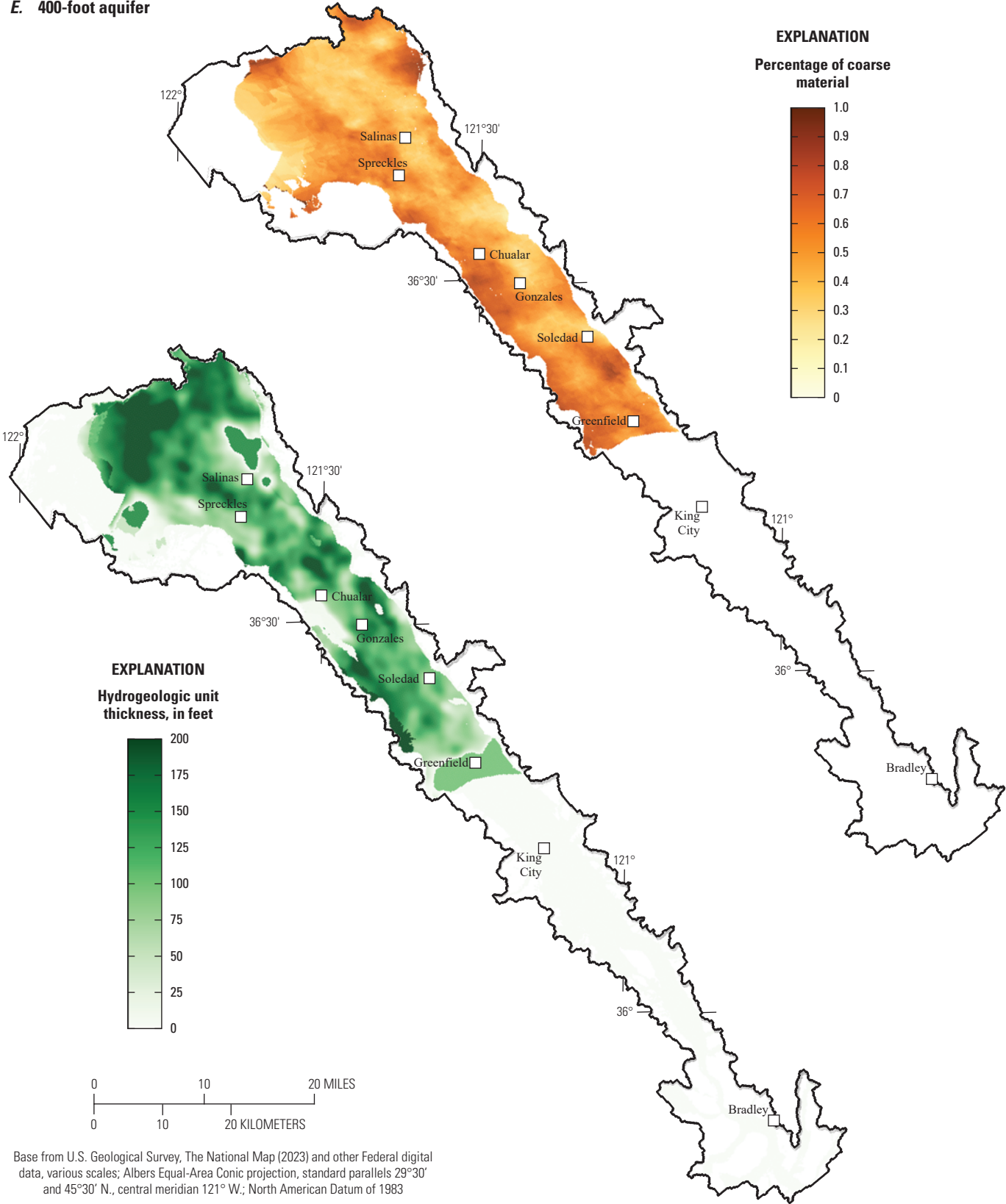


Base from U.S. Geological Survey, The National Map (2023) and other Federal digital data, various scales; Albers Equal-Area Conic projection, standard parallels 29°30' and 45°30' N., central meridian 121° W.; North American Datum of 1983

**D. Middle confining unit**

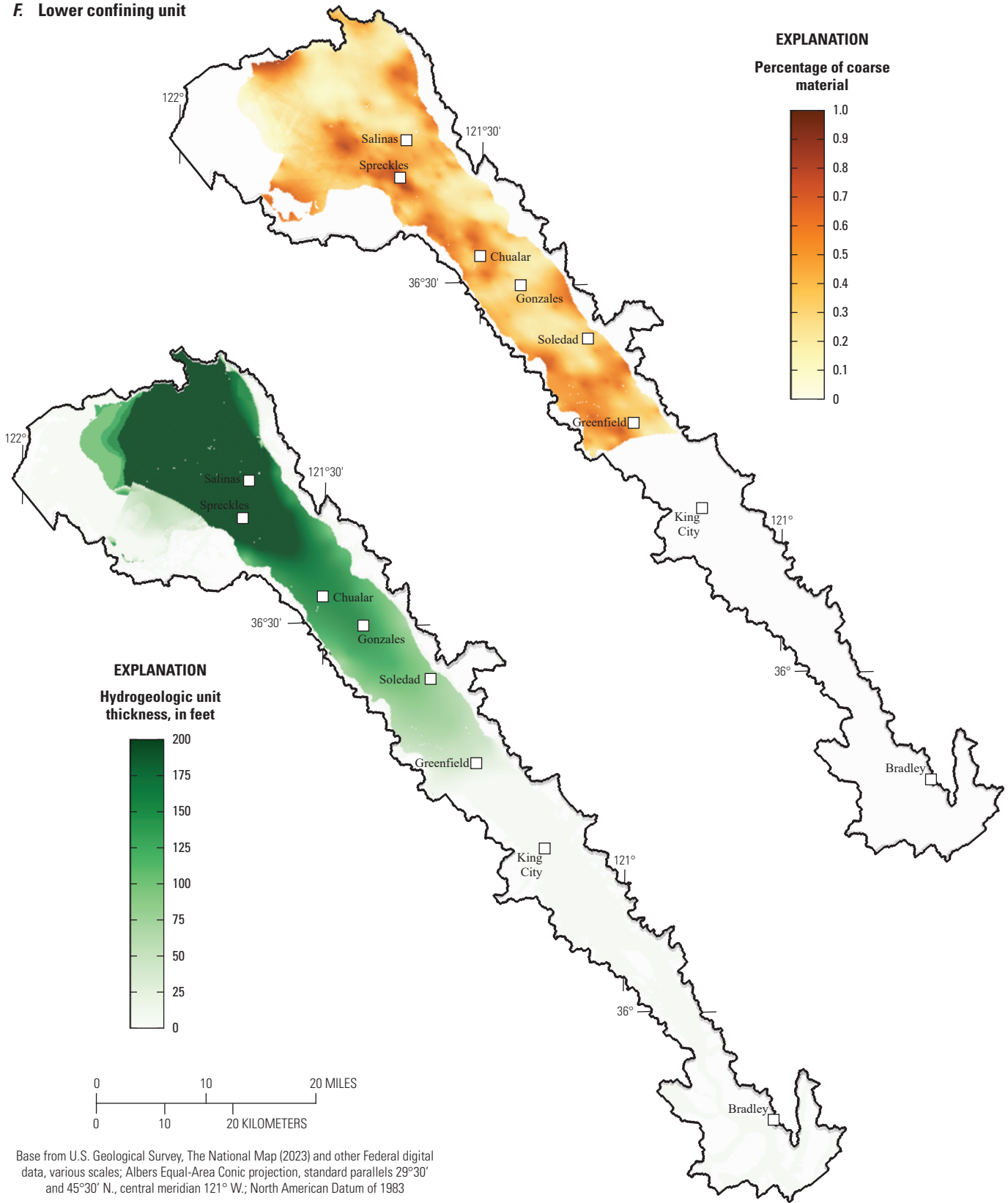


E. 400-foot aquifer

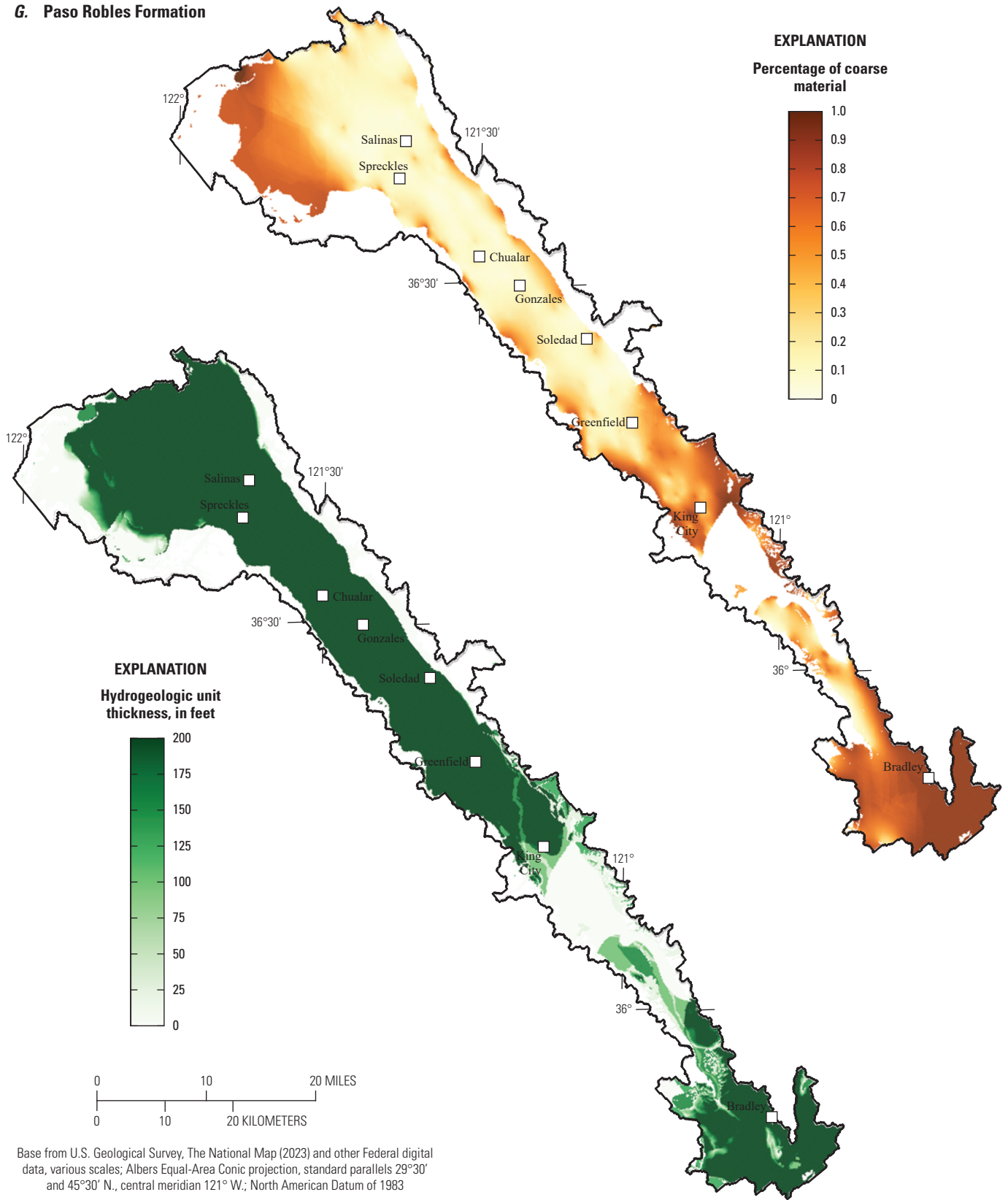


Base from U.S. Geological Survey, The National Map (2023) and other Federal digital data, various scales; Albers Equal-Area Conic projection, standard parallels 29°30' and 45°30' N., central meridian 121° W.; North American Datum of 1983

F Lower confining unit

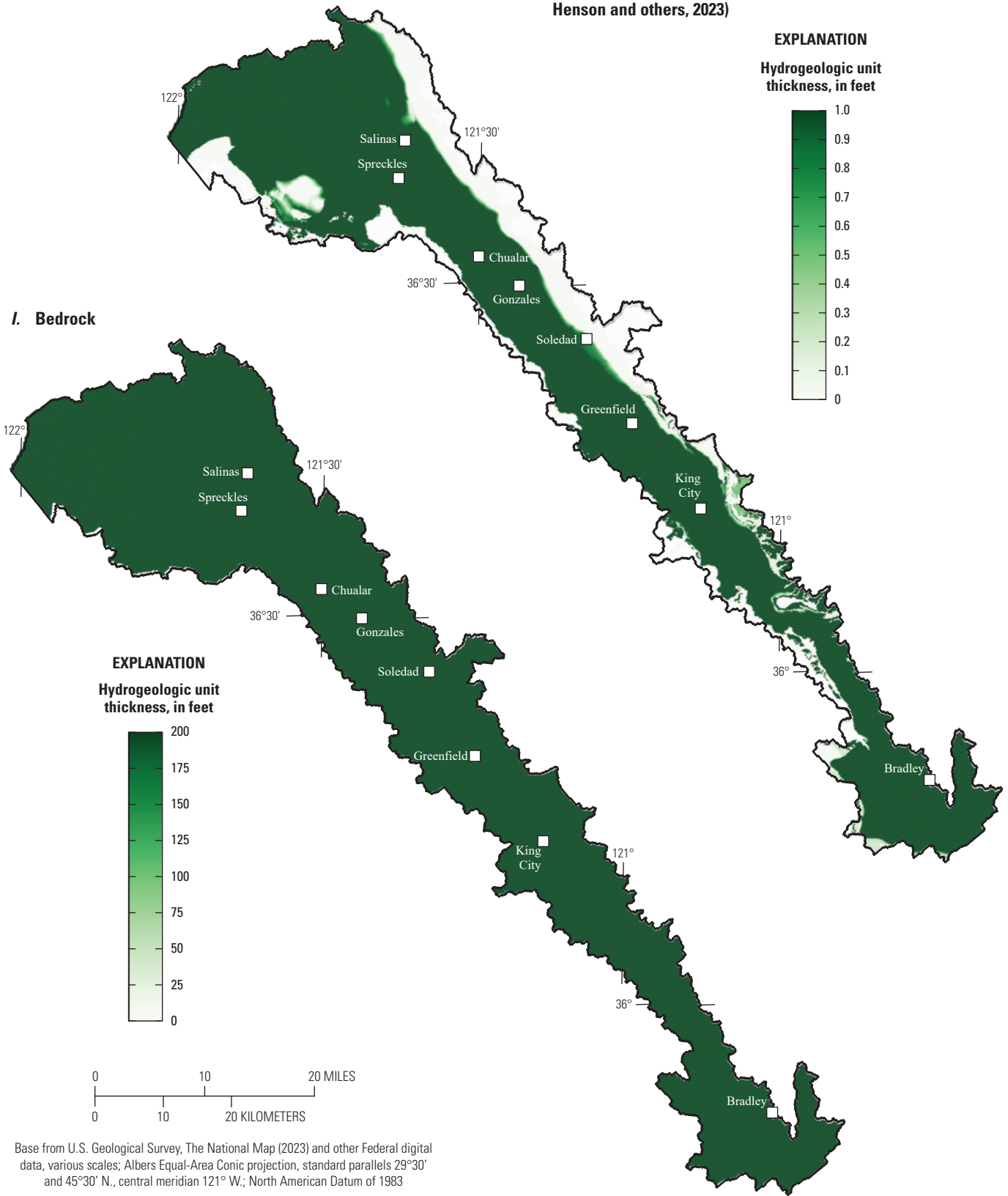


### G. Paso Robles Formation

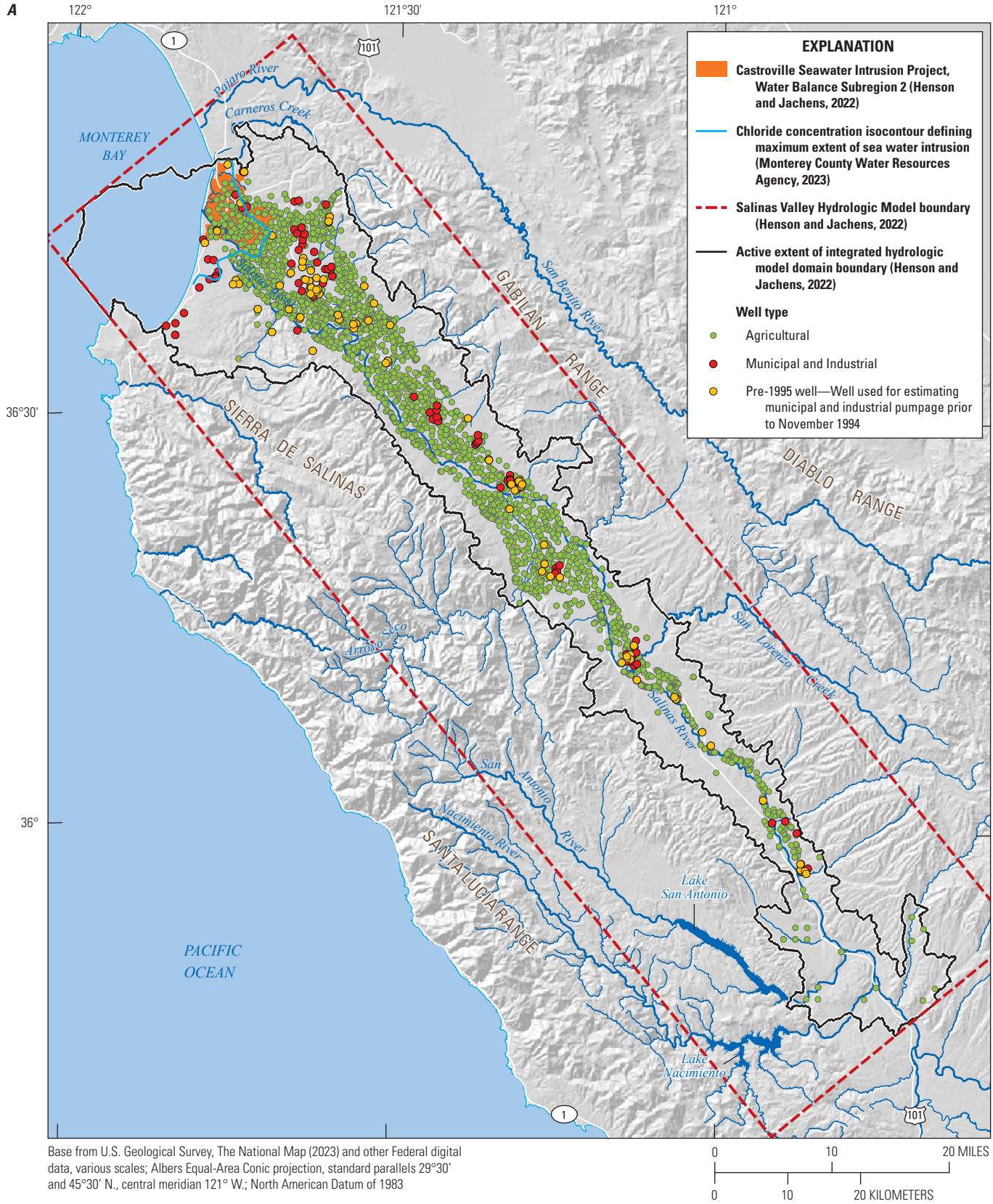


Base from U.S. Geological Survey, The National Map (2023) and other Federal digital data, various scales; Albers Equal-Area Conic projection, standard parallels 29°30' and 45°30' N., central meridian 121° W.; North American Datum of 1983

H. Purisima Formation (Sweetkind, 2023; Henson and others, 2023)



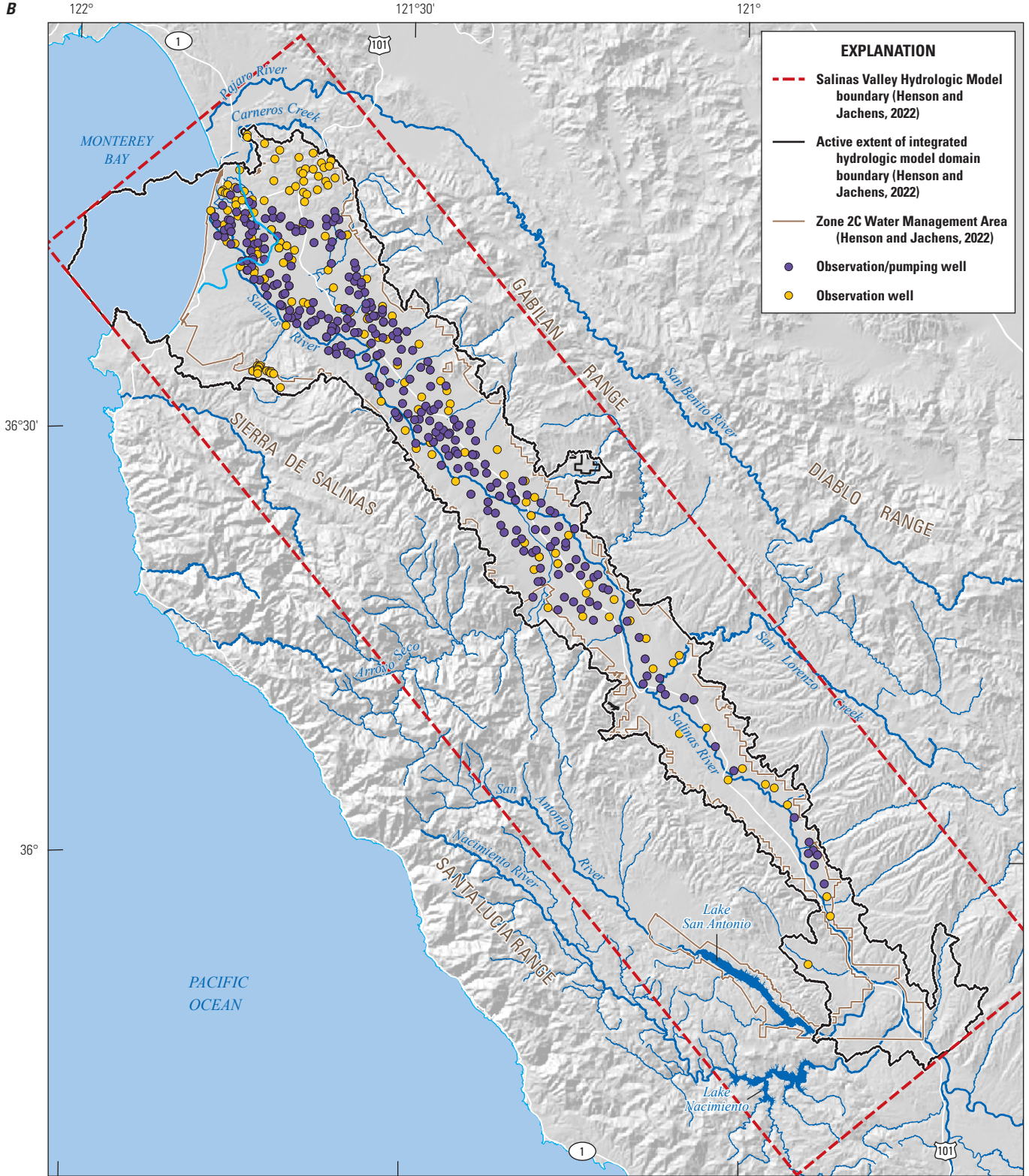
Base from U.S. Geological Survey, The National Map (2023) and other Federal digital data, various scales; Albers Equal-Area Conic projection, standard parallels 29°30' and 45°30' N., central meridian 121° W.; North American Datum of 1983



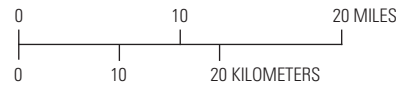
Base from U.S. Geological Survey, The National Map (2023) and other Federal digital data, various scales; Albers Equal-Area Conic projection, standard parallels 29°30' and 45°30' N., central meridian 121° W.; North American Datum of 1983

Figure 24. Wells within the integrated hydrologic model domain for A) municipal, industrial, and agricultural wells, and a subset of wells used to estimate municipal and industrial pumpage from water year 1968 to 1994 (pre-1995 wells); and B) location of observation wells.

B



Base from U.S. Geological Survey, The National Map (2023) and other Federal digital data, various scales; Albers Equal-Area Conic projection, standard parallels 29°30' and 45°30' N., central meridian 121° W.; North American Datum of 1983





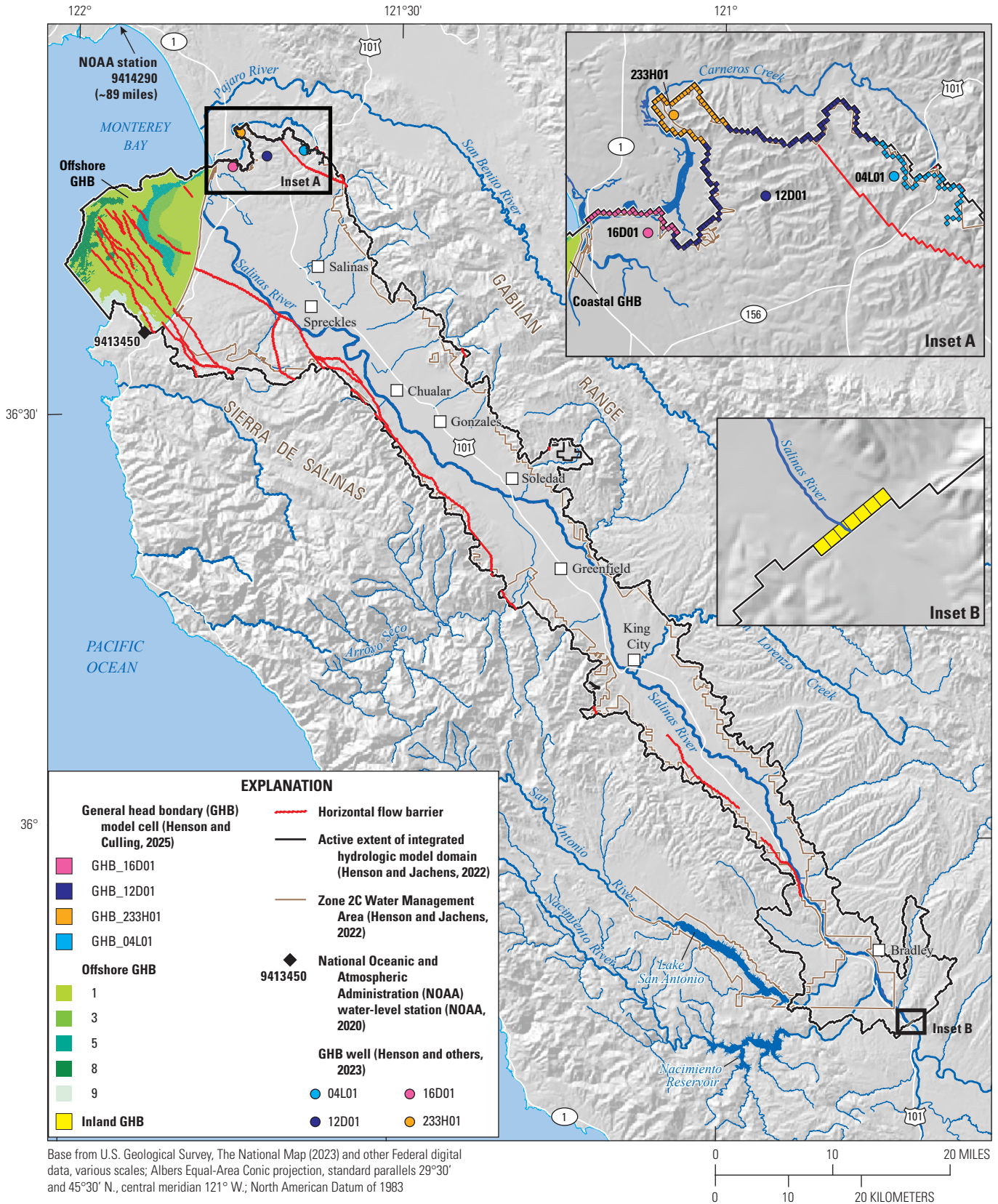
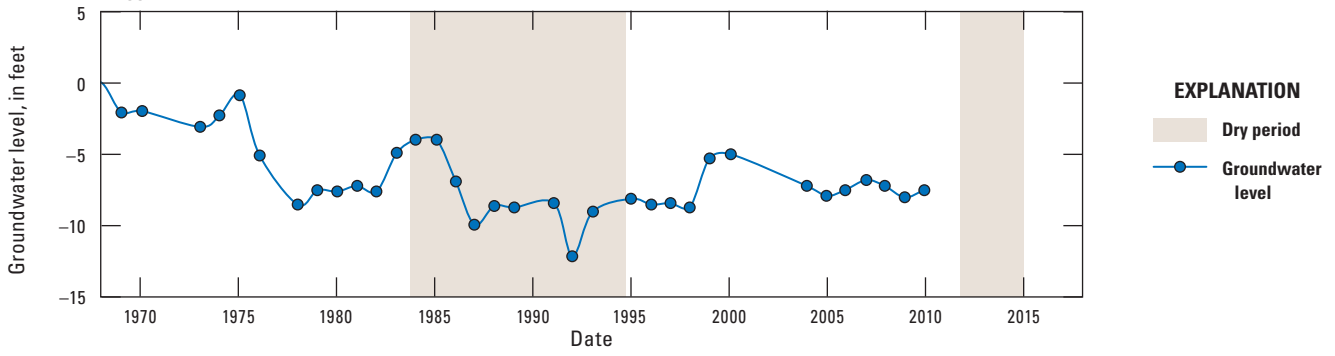
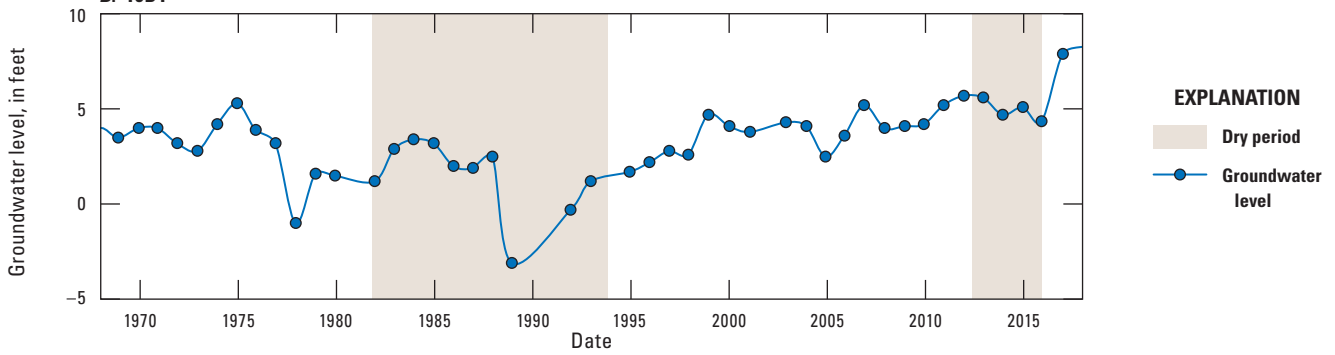


Figure 25. Specification of general head boundaries (GHB) in the integrated hydrologic model domain. The location of GHB wells and the cells used to define the offshore GHB, coastal GHB, and inland GHB in the Salinas Valley Integrated Hydrologic Model domain are shown.

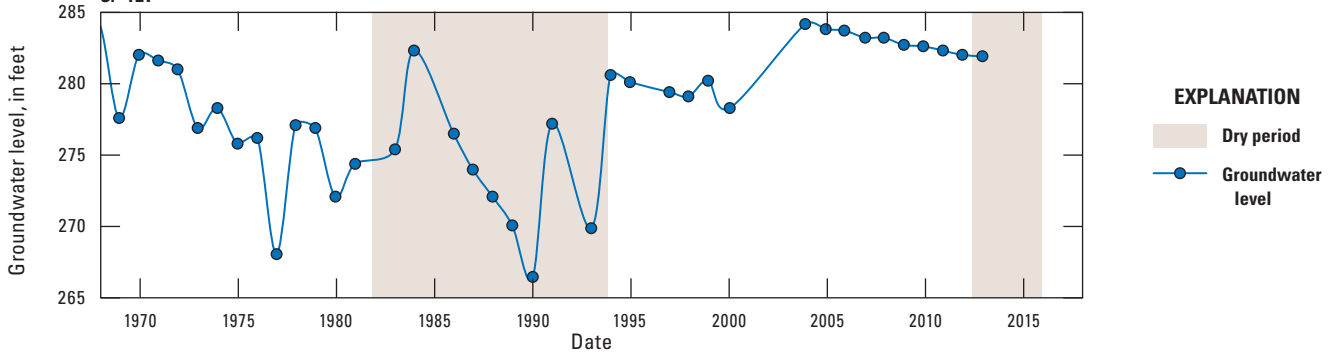
**A. 33H1**



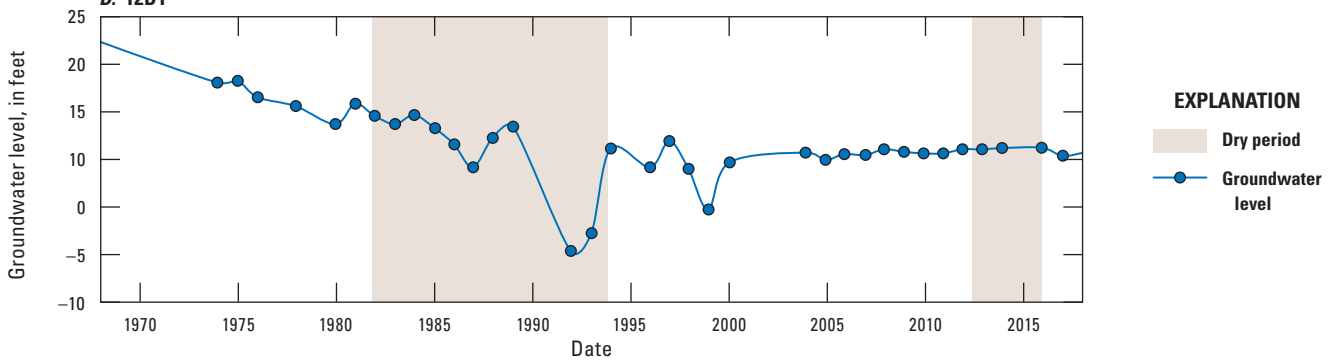
**B. 16D1**



**C. 4L1**



**D. 12D1**



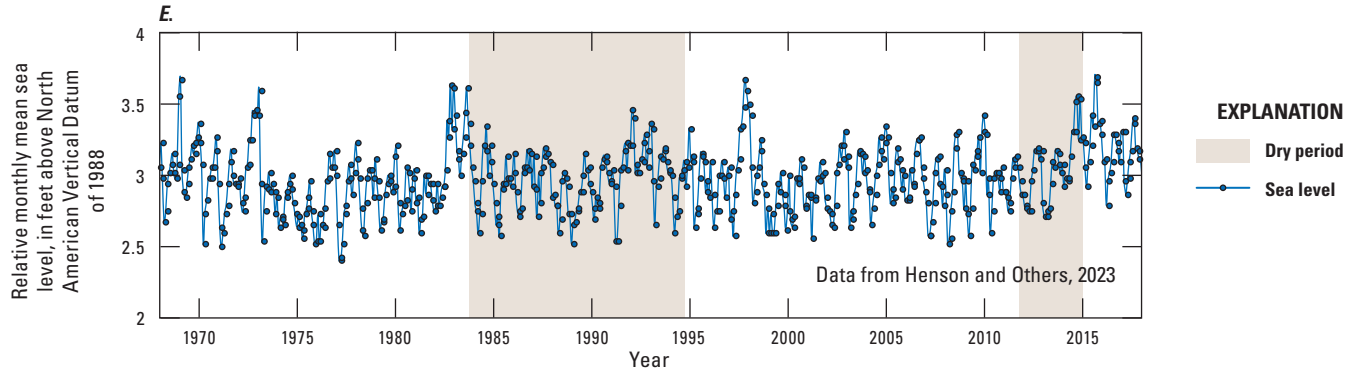


Figure 26. General head boundary (GHB) time series in the Salinas Valley, California for A) coastal GHB boundary well 33H1, B) coastal GHB boundary well 16D1, C) coastal GHB boundary well 4L1, D) coastal GHB boundary well 12D1 (Henson and others, 2023), and E) mean monthly sea level (National Oceanic and Atmospheric Administration, 2019).

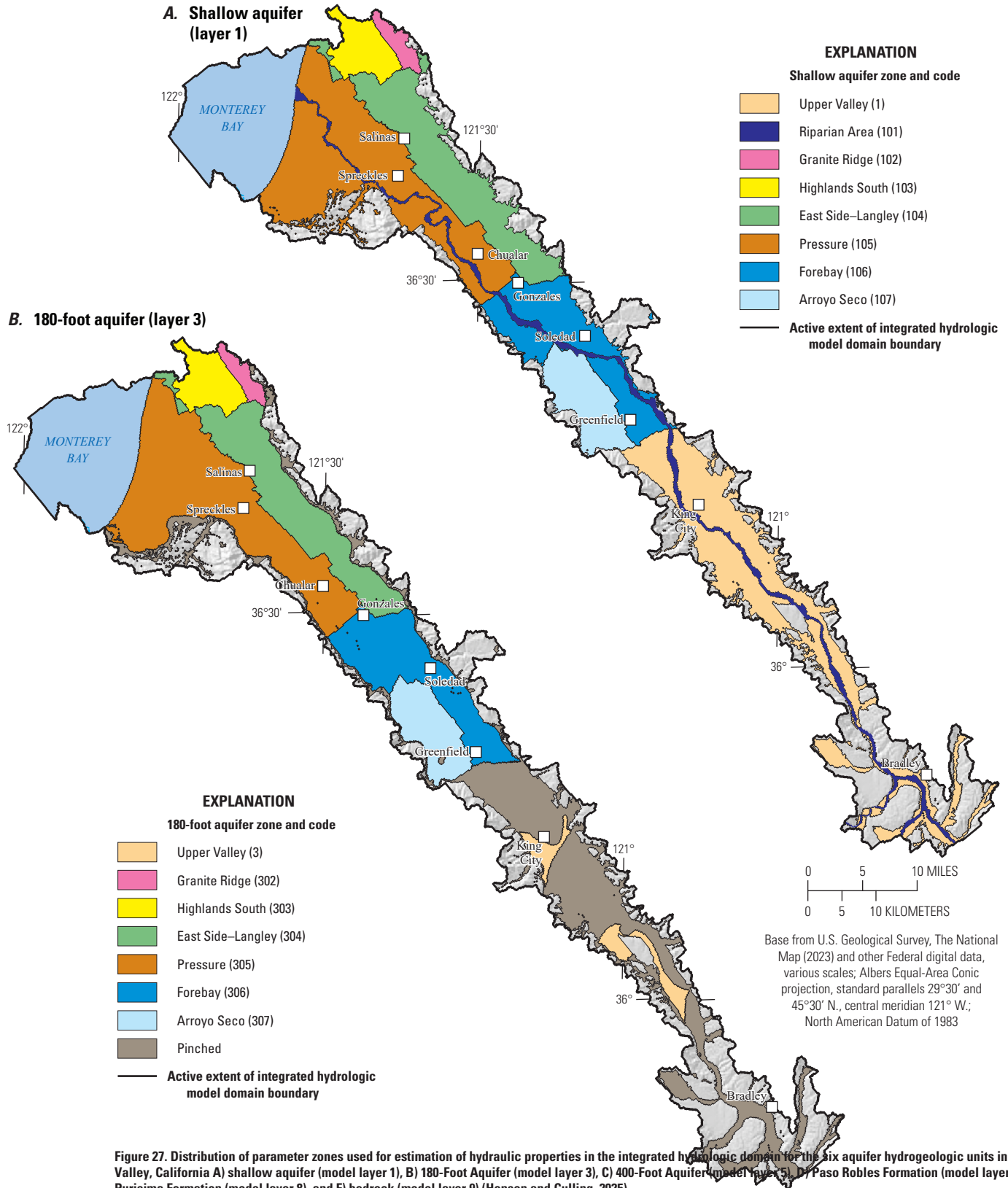
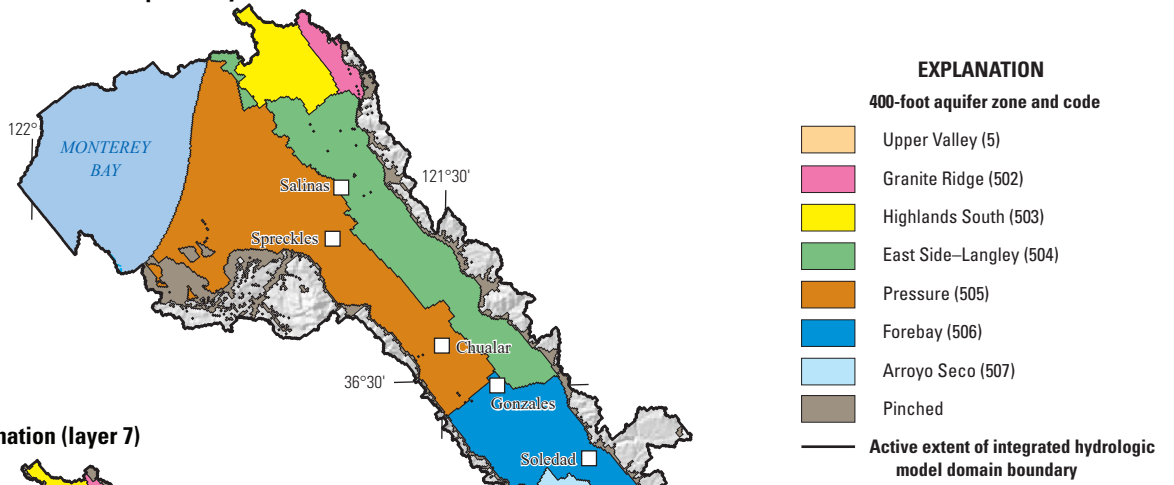
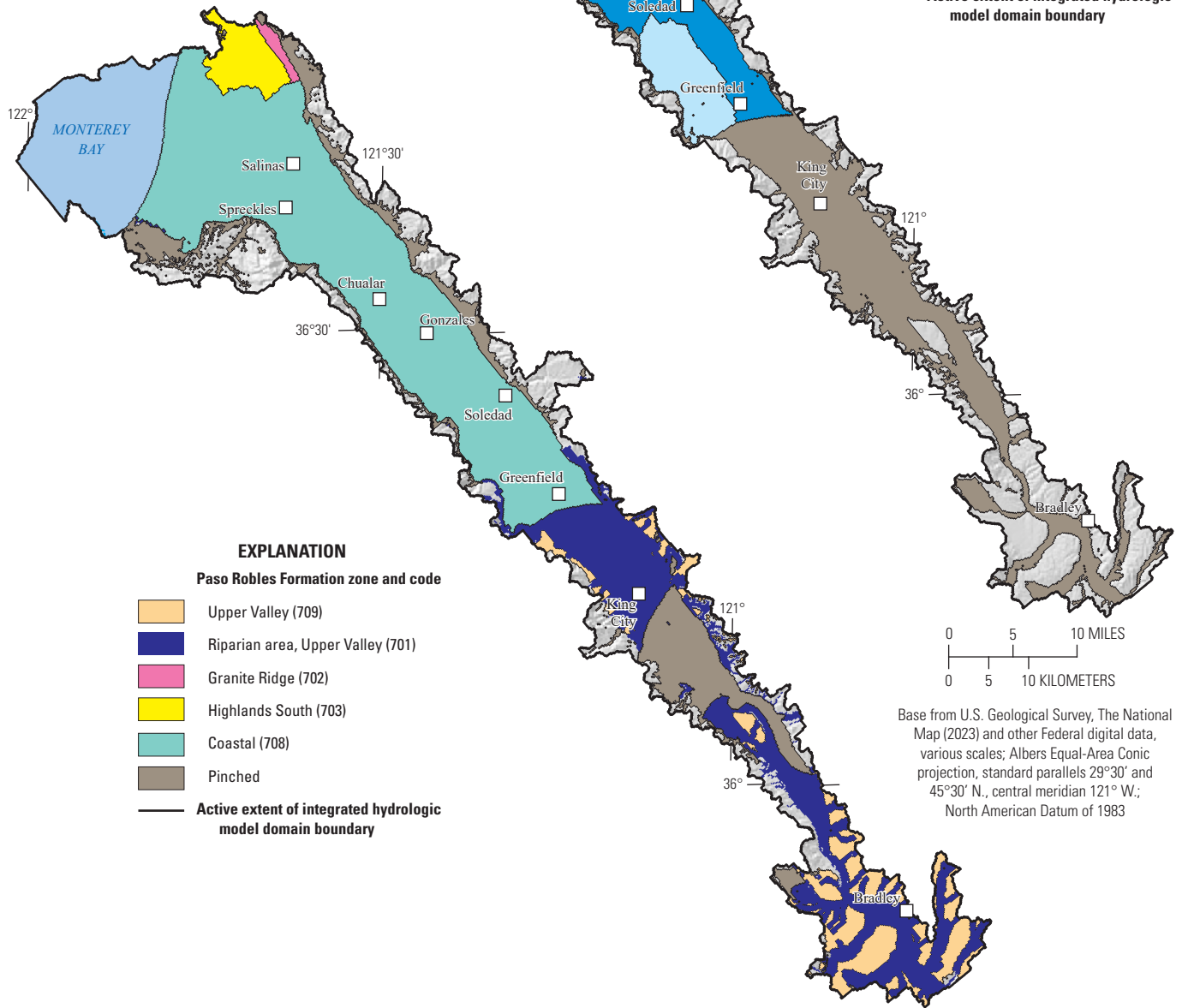


Figure 27. Distribution of parameter zones used for estimation of hydraulic properties in the integrated hydrologic domain for the six aquifer hydrogeologic units in the Salinas Valley, California A) shallow aquifer (model layer 1), B) 180-Foot Aquifer (model layer 3), C) 400-Foot Aquifer (model layer 5), D) Paso Robles Formation (model layer 7), E) Purisima Formation (model layer 8), and F) bedrock (model layer 9) (Henson and Culling, 2025).

**C. 400-foot aquifer (layer 5)**

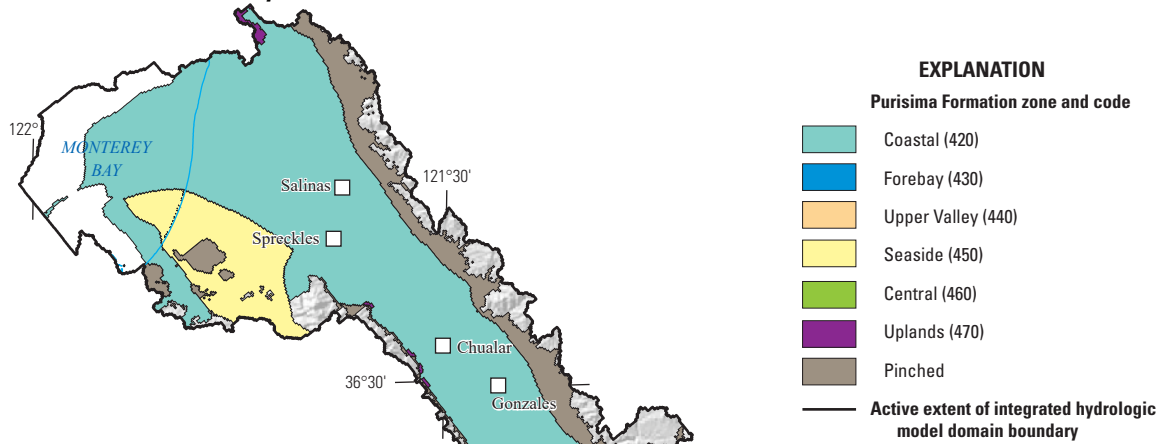


**D. Paso Robles Formation (layer 7)**

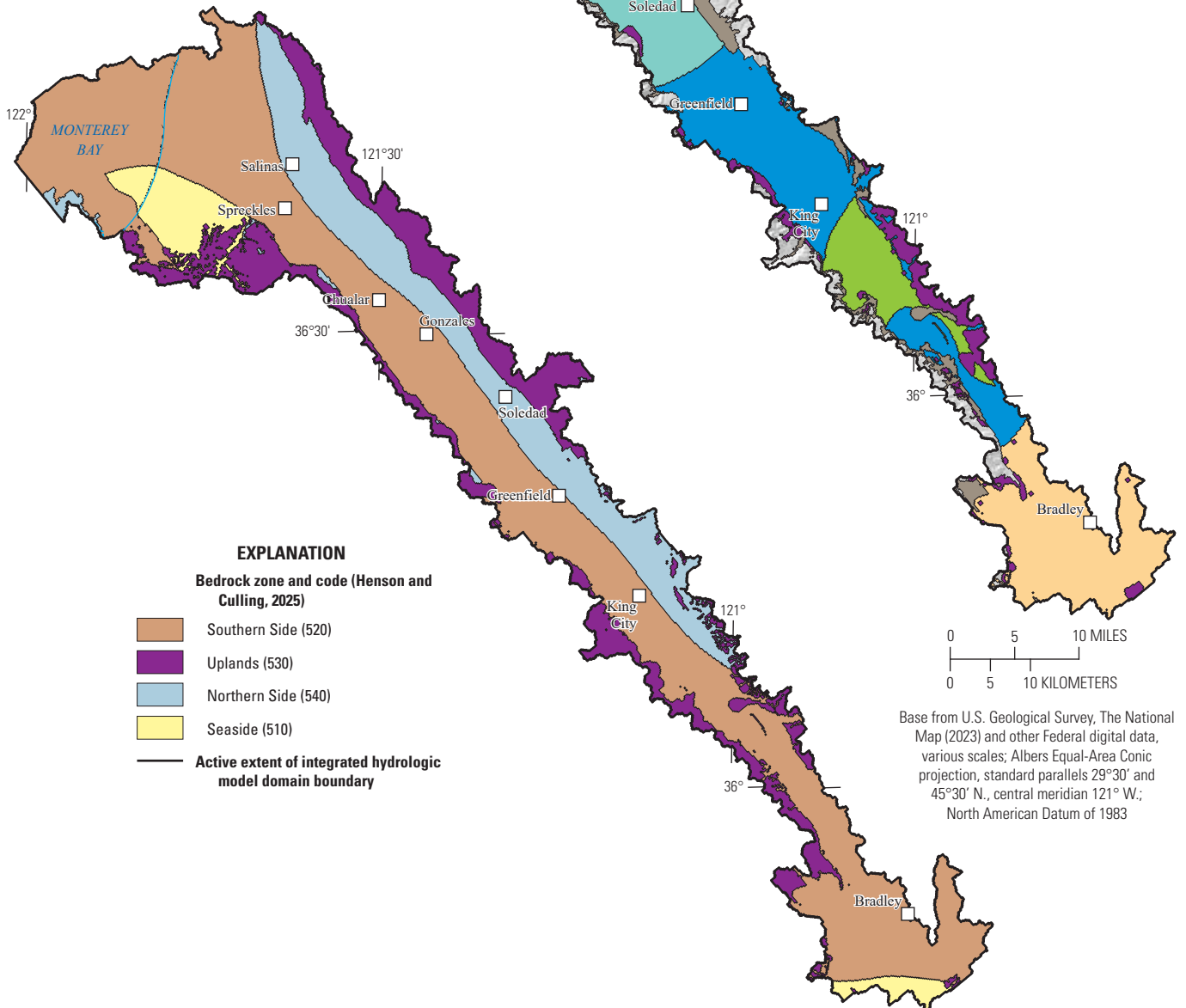


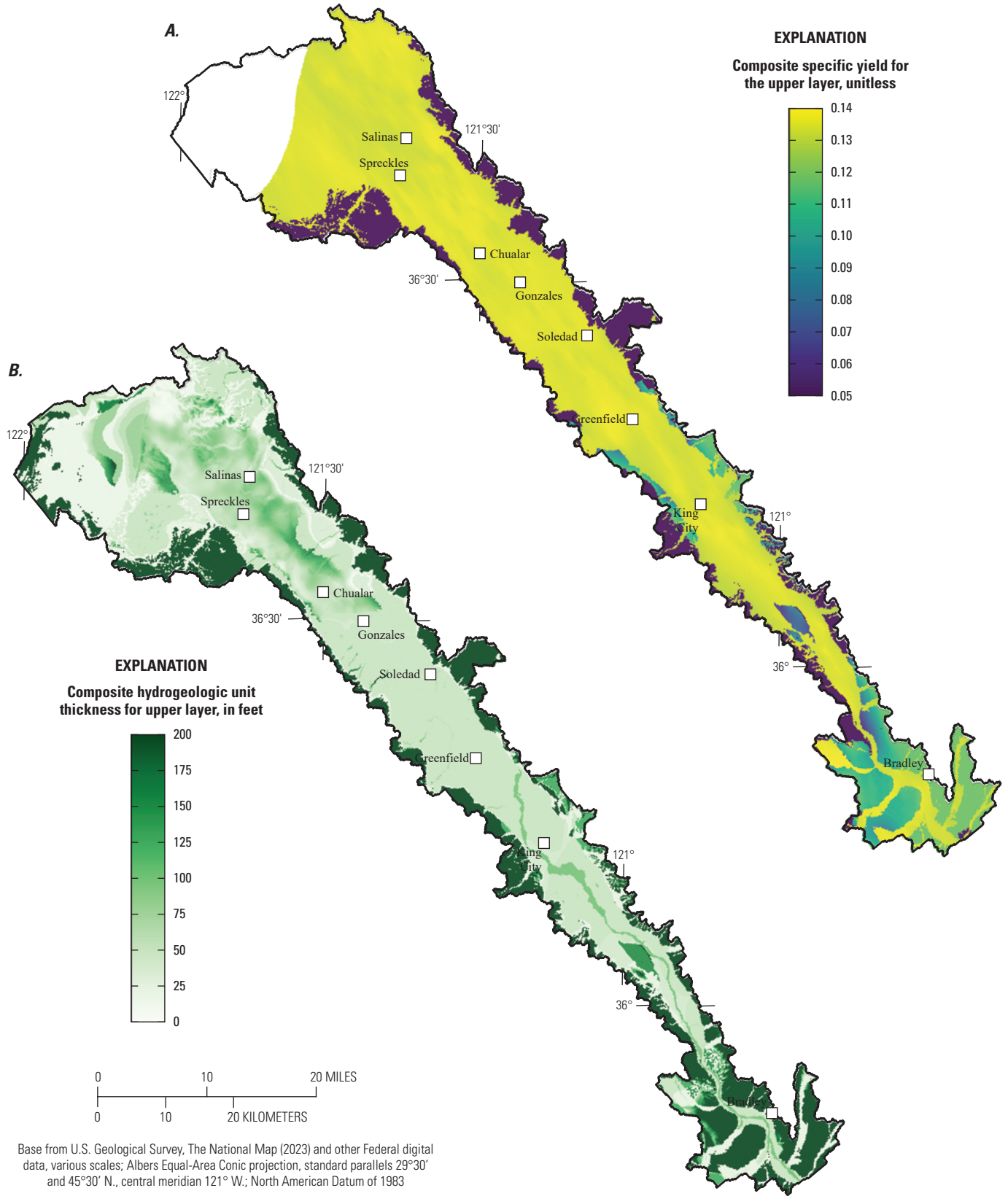
Base from U.S. Geological Survey, The National Map (2023) and other Federal digital data, various scales; Albers Equal-Area Conic projection, standard parallels 29°30' and 45°30' N., central meridian 121° W.; North American Datum of 1983

**E. Purisima Formation (layer 8)**



**F. Bedrock (layer 9)**

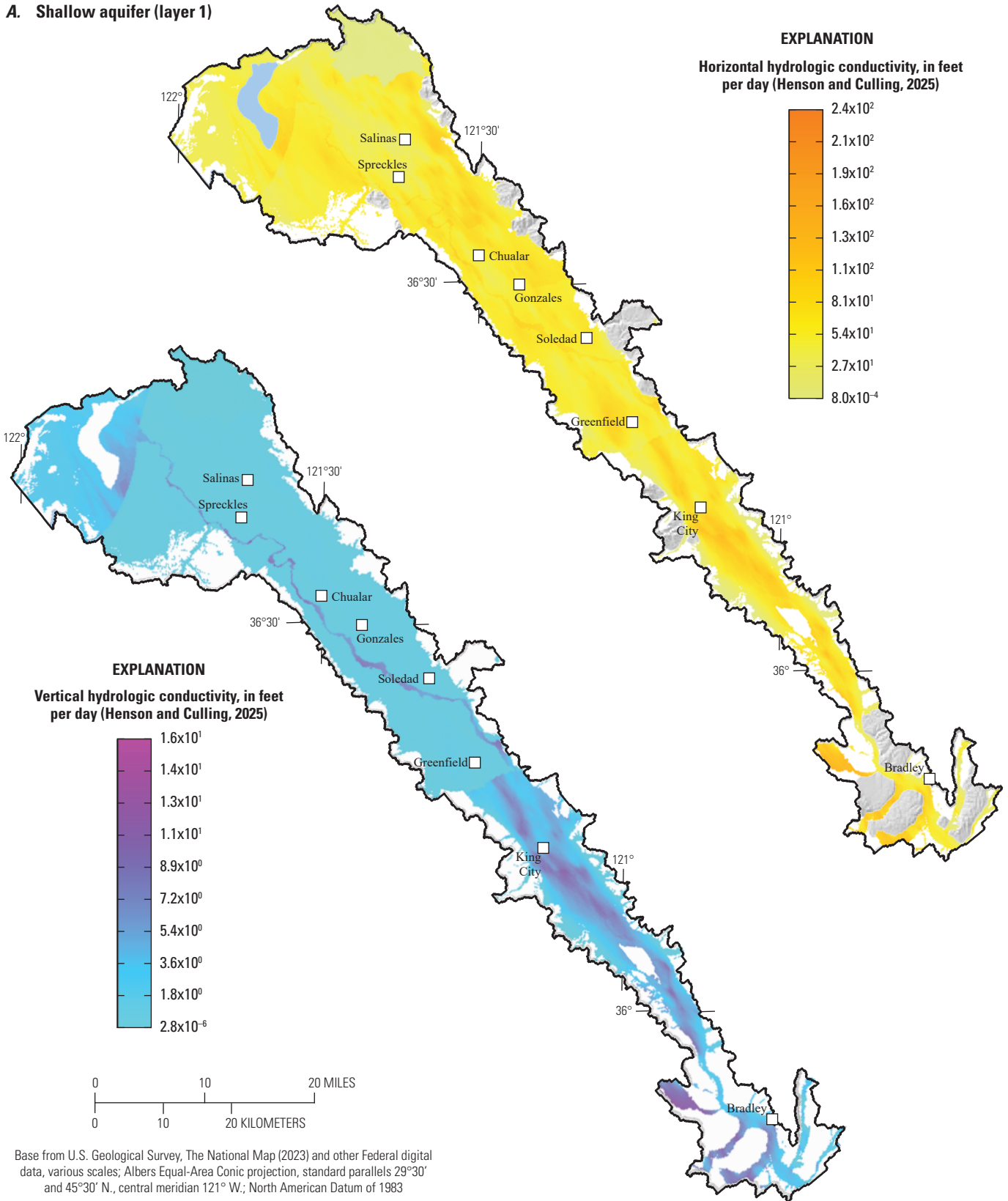




Base from U.S. Geological Survey, The National Map (2023) and other Federal digital data, various scales; Albers Equal-Area Conic projection, standard parallels 29°30' and 45°30' N., central meridian 121° W.; North American Datum of 1983

Figure 28. Hydrogeologic unit A) specific yield and B) thickness for the uppermost layer of each model cell in the integrated hydrologic model domain for the Salinas Valley, California. The uppermost layer is a composite of hydrogeologic units in the uppermost cell in layers 1, 3, 5, 7, 8, or 9 (Henson and Culling, 2025).

A. Shallow aquifer (layer 1)

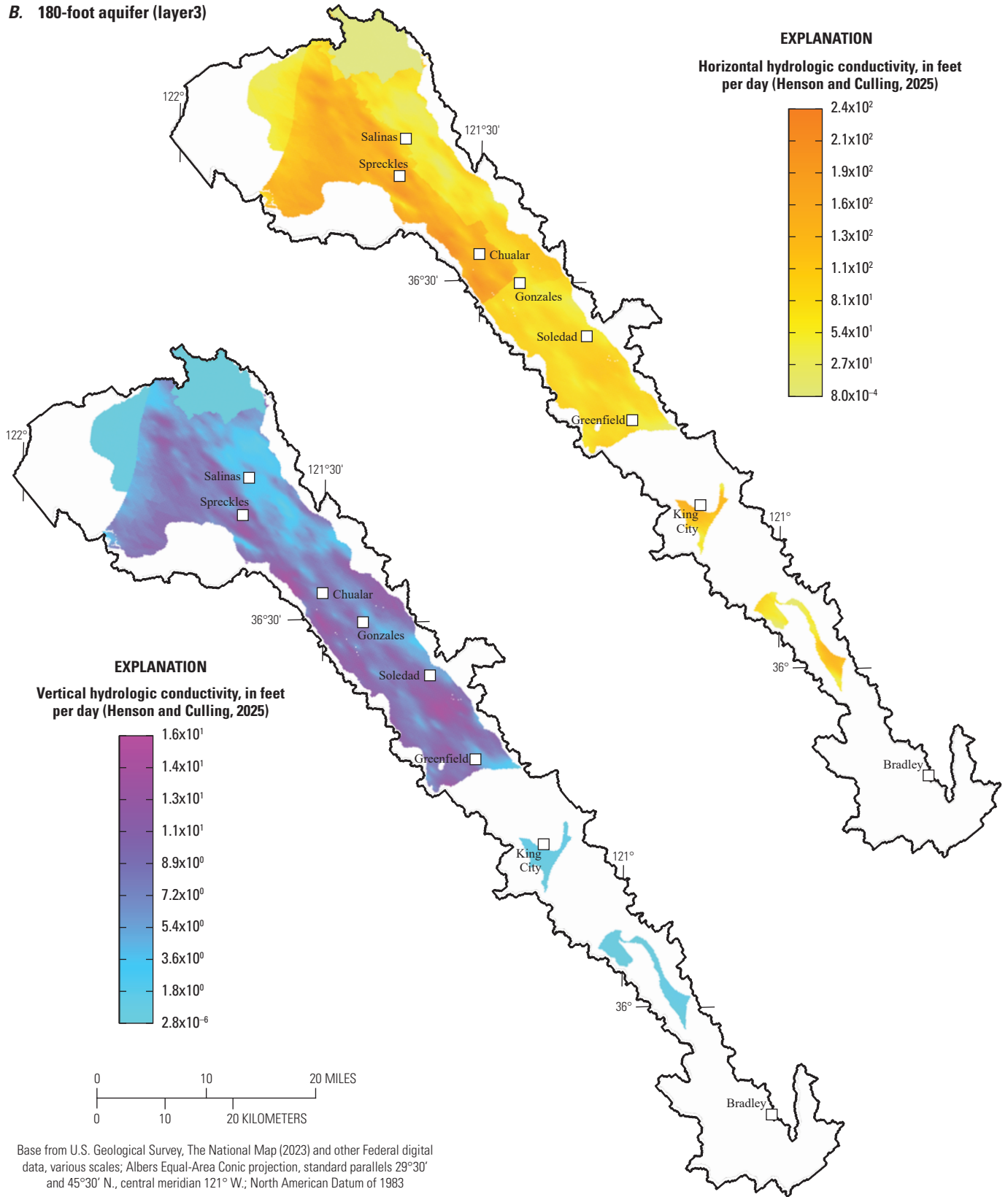


Base from U.S. Geological Survey, The National Map (2023) and other Federal digital data, various scales; Albers Equal-Area Conic projection, standard parallels 29°30' and 45°30' N., central meridian 121° W.; North American Datum of 1983

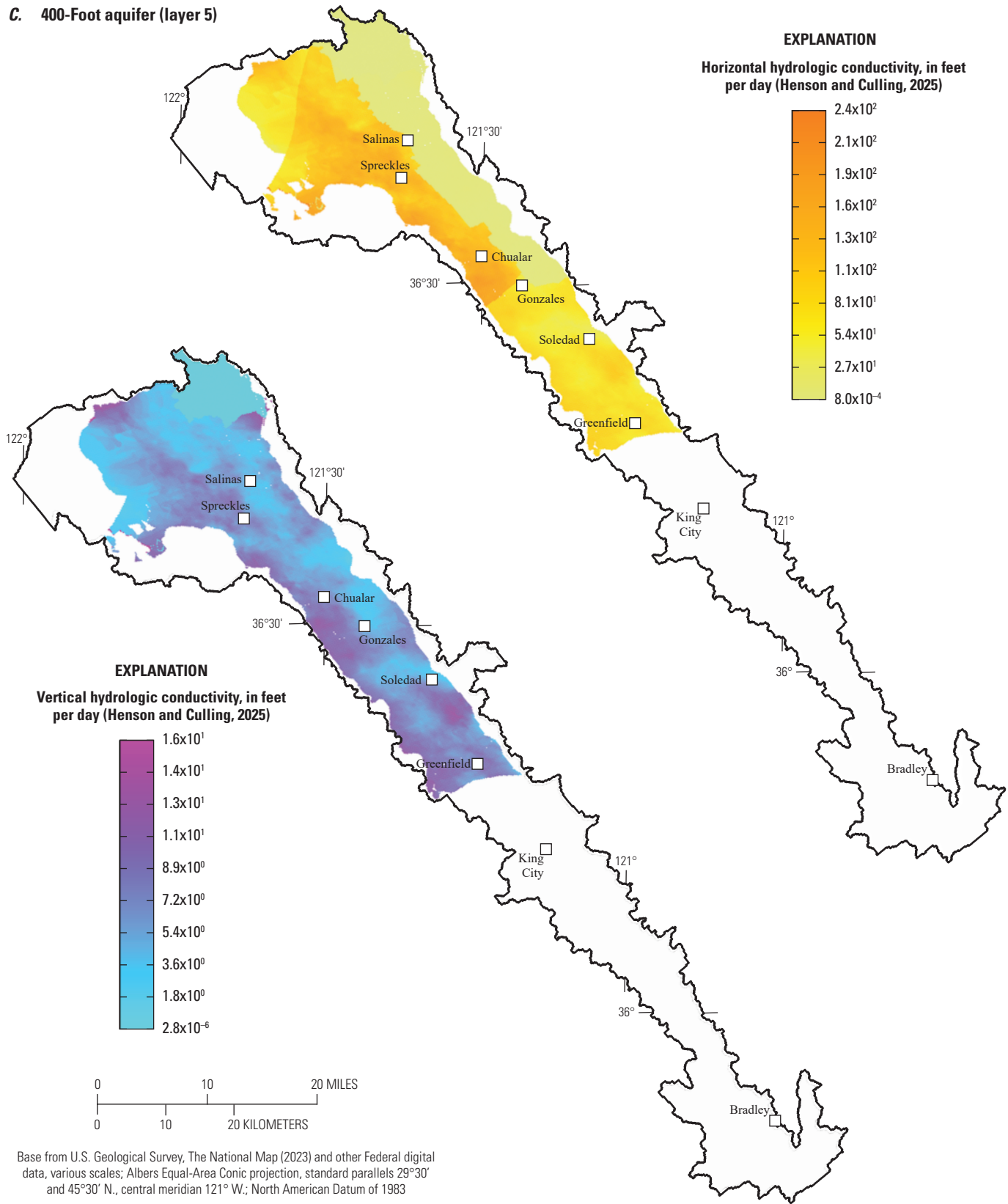
Figure 29. Horizontal and vertical hydraulic conductivity in six aquifer hydrogeologic units in the Salinas Valley, California A) shallow aquifer, B) 180-Foot Aquifer, C) 400-Foot Aquifer, D) Paso Robles Formation, E) Purisima Formation, and F) bedrock (Henson and Culling, 2025).



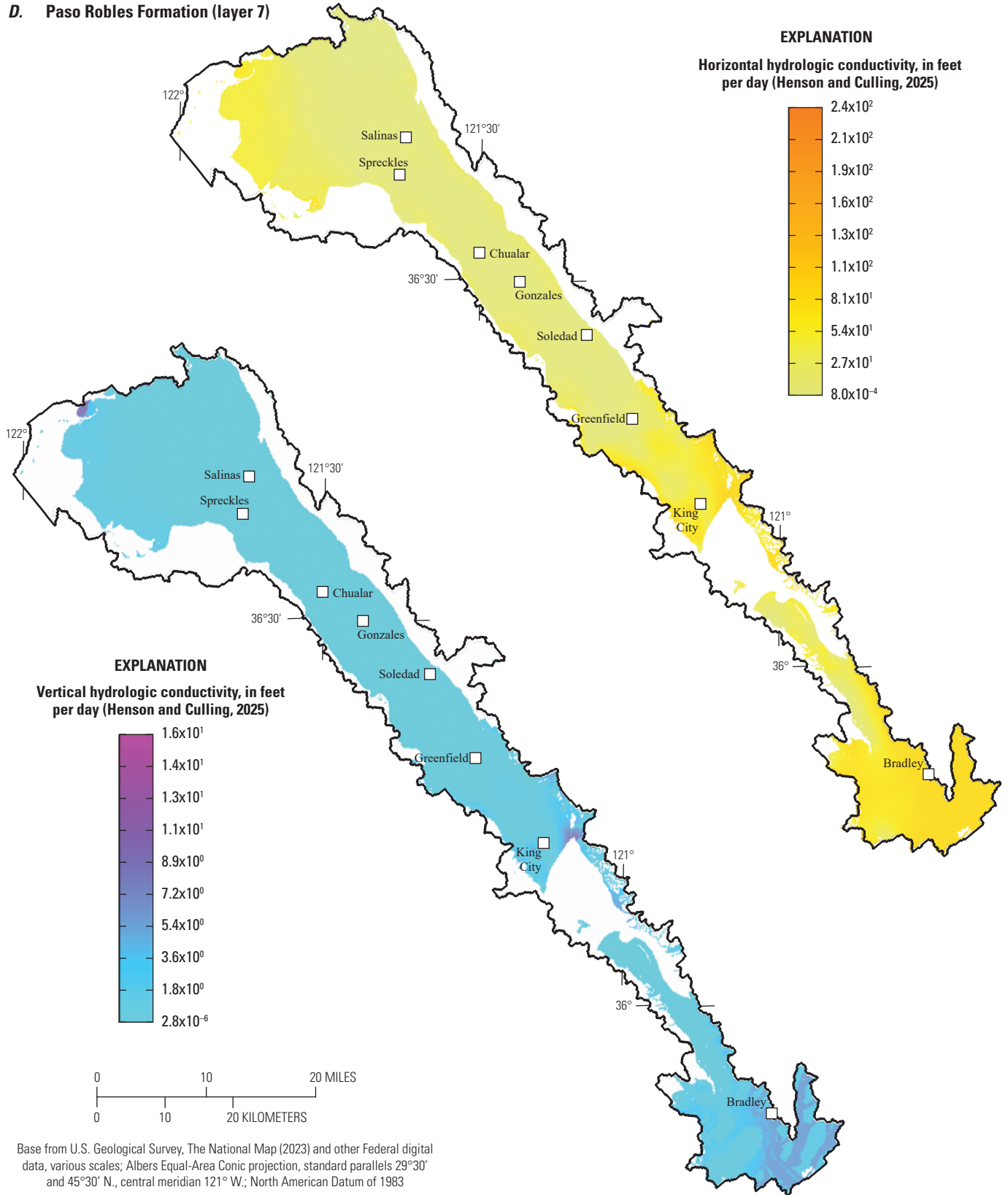
**B. 180-foot aquifer (layer3)**



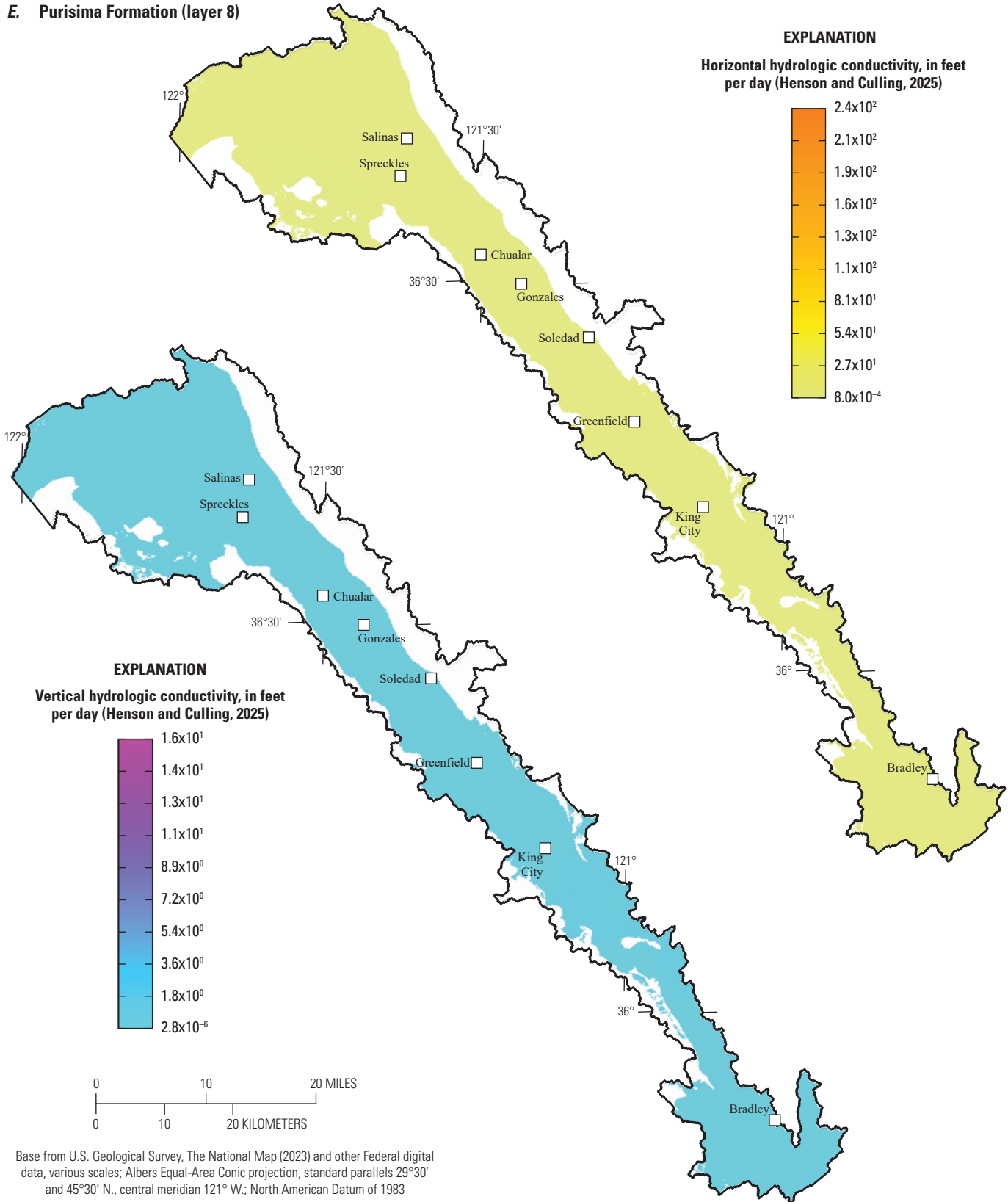
C. 400-Foot aquifer (layer 5)



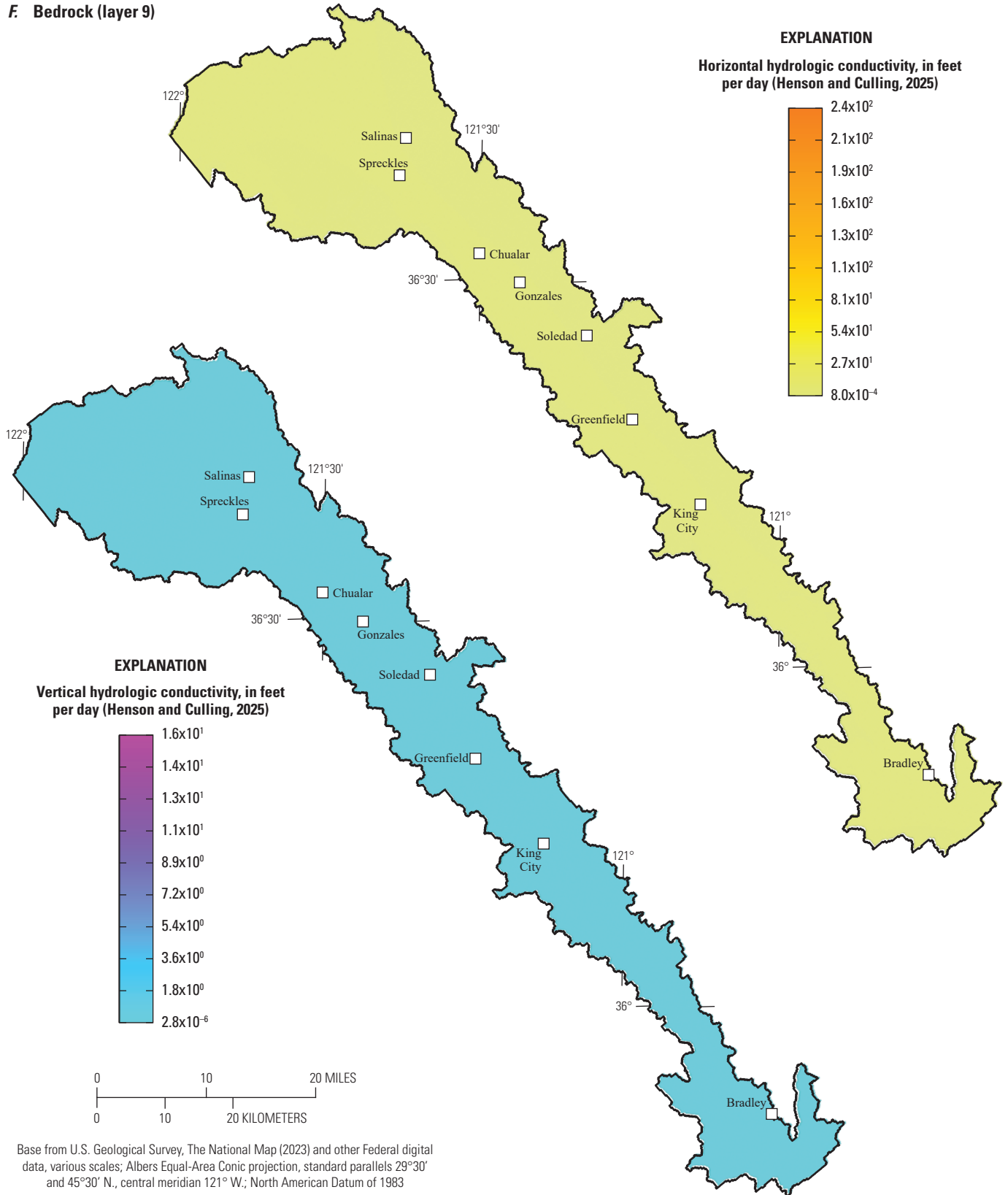
D. Paso Robles Formation (layer 7)



**E. Purisima Formation (layer 8)**



**F. Bedrock (layer 9)**



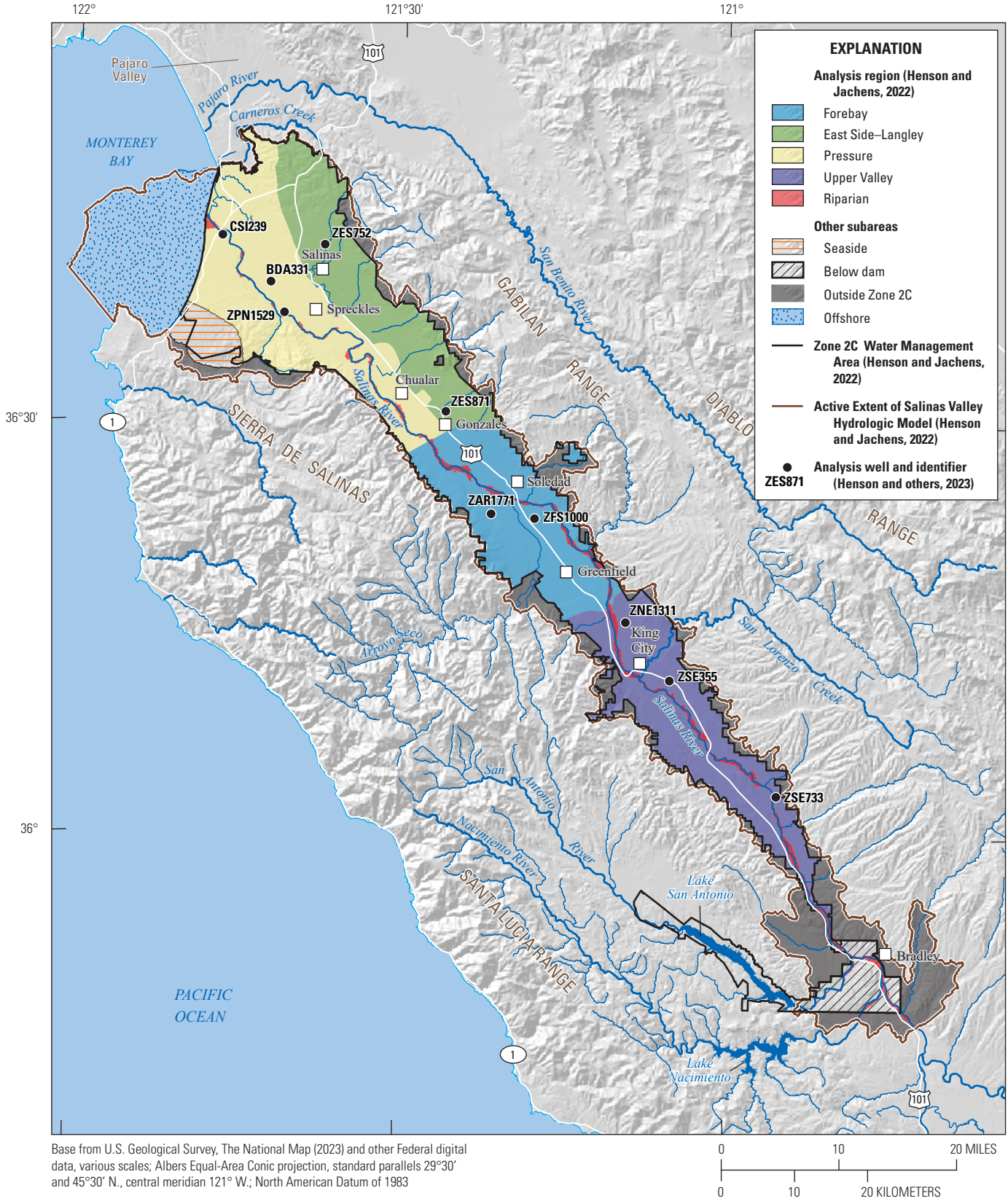


Figure 30. Analysis regions with locations of selected observation wells in Salinas Valley, California.

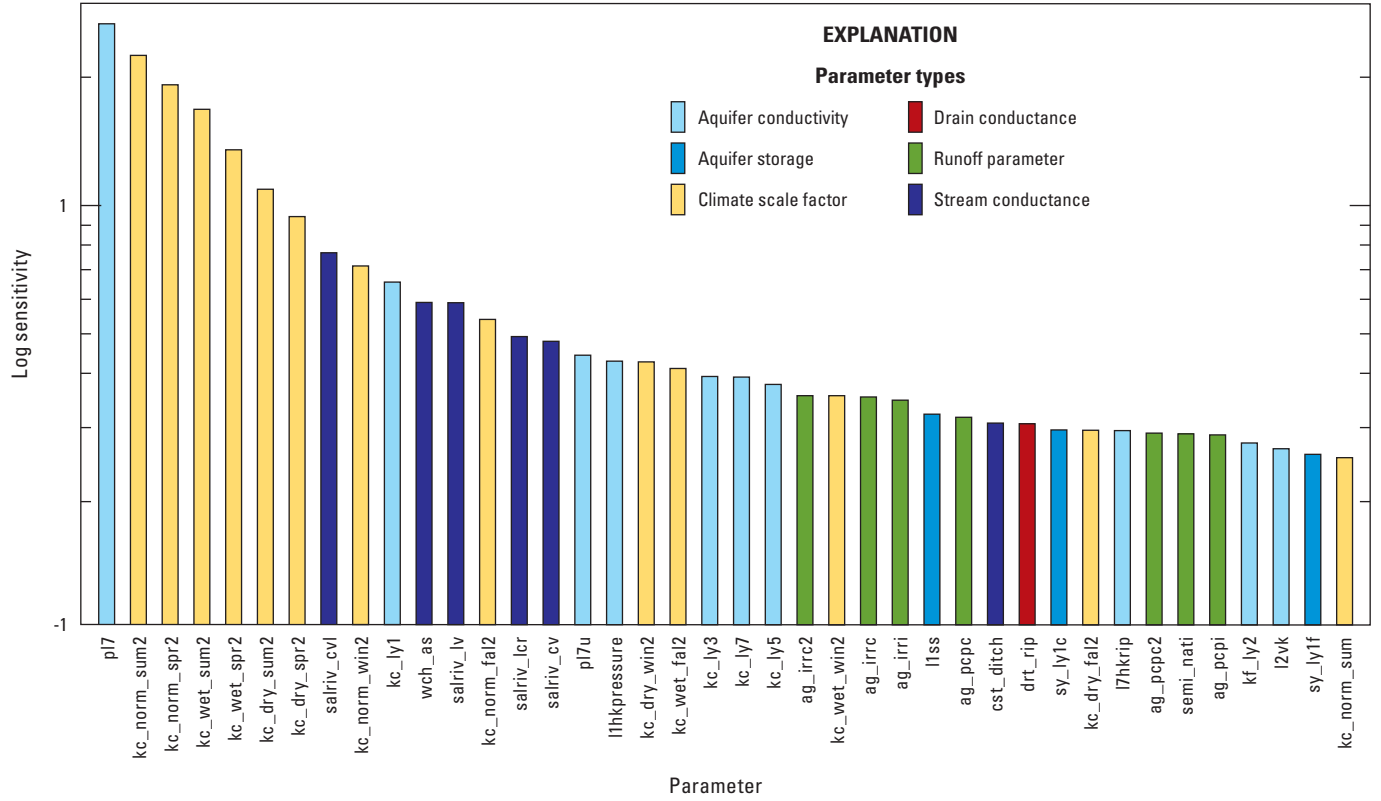
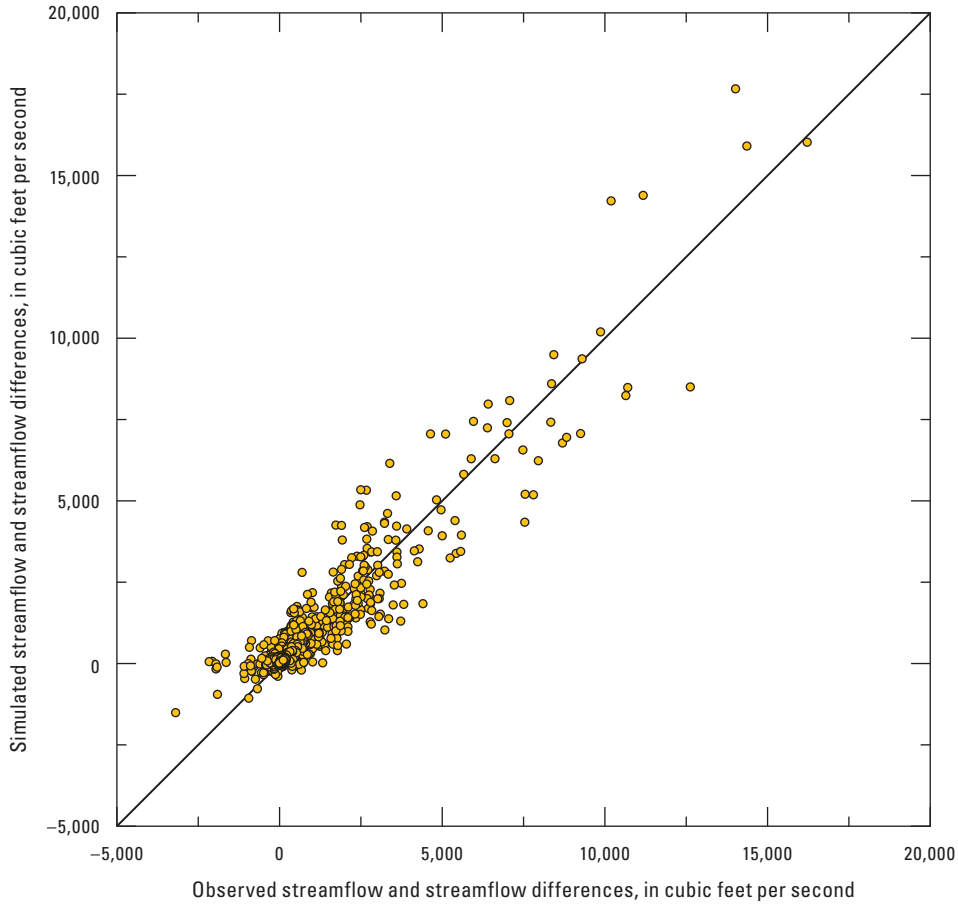
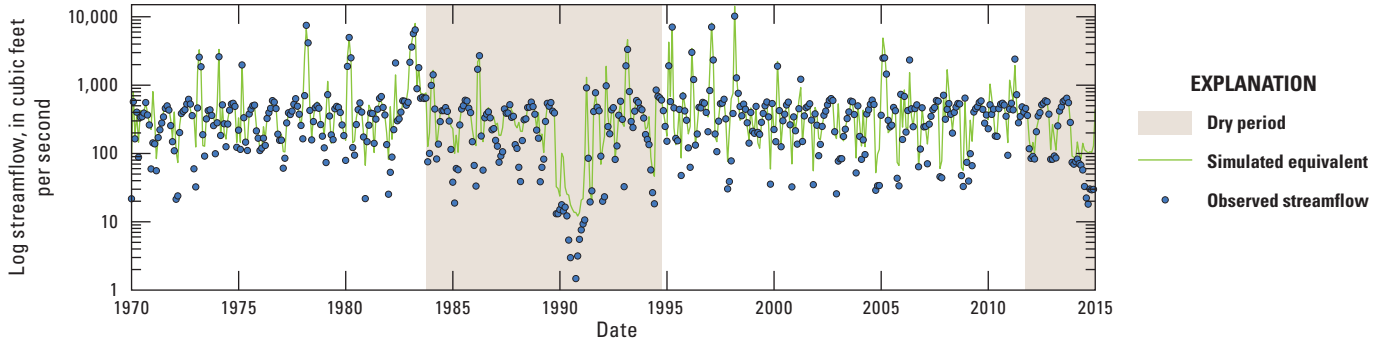


Figure 31. Magnitudes of the relative composite scaled sensitivity for selected parameters used in Salinas Valley integrated and reservoir operations models for Monterey and San Luis Obispo Counties, California. Refer to table 6 for a full description of the sensitive parameter names and values. All model parameters described by Henson and Culling (2025).

A

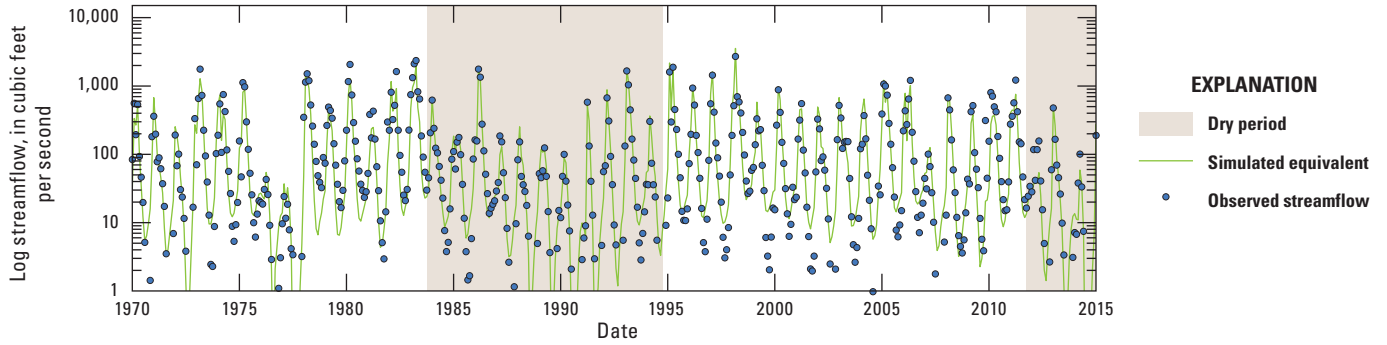


B. Upper Valley analysis region: USGS 11150500 SALINAS R NR BRADLEY CA

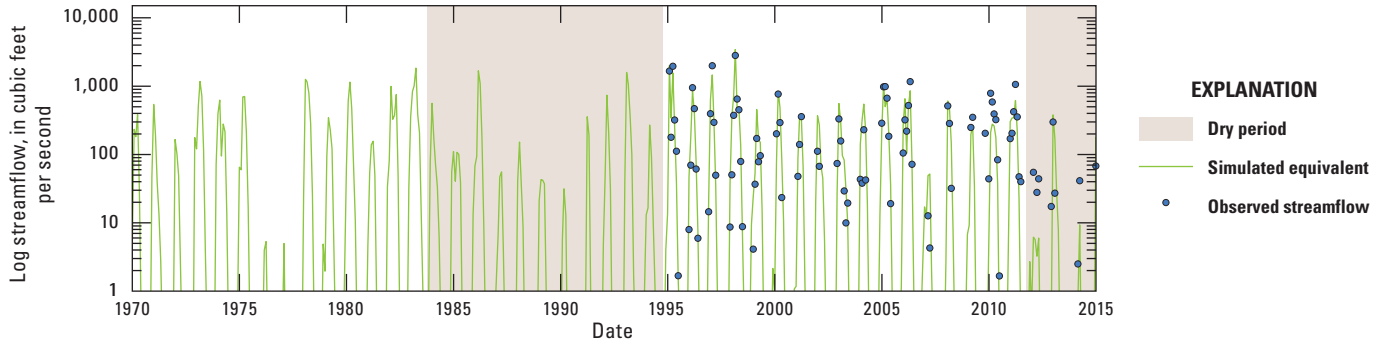




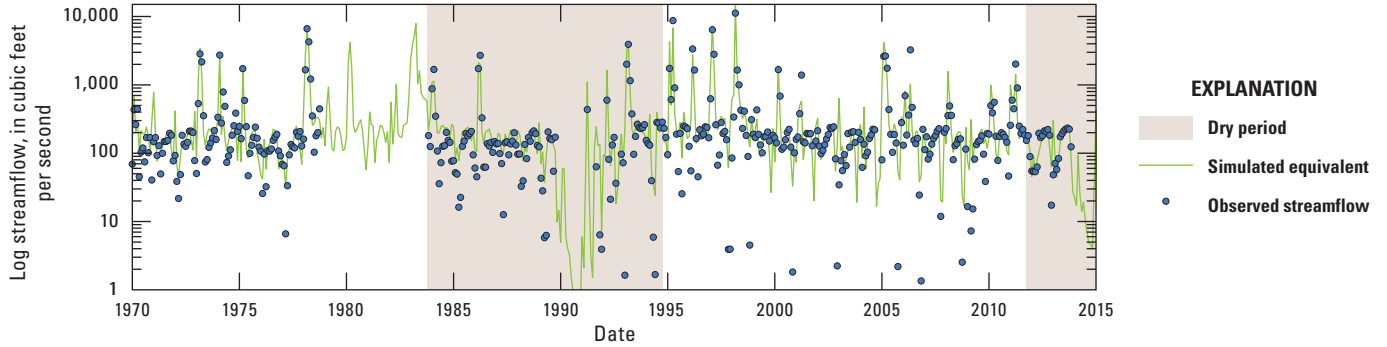
**C. Forebay analysis region: USGS 11152000 ARROYO SECO NR SOLEDAD CA**



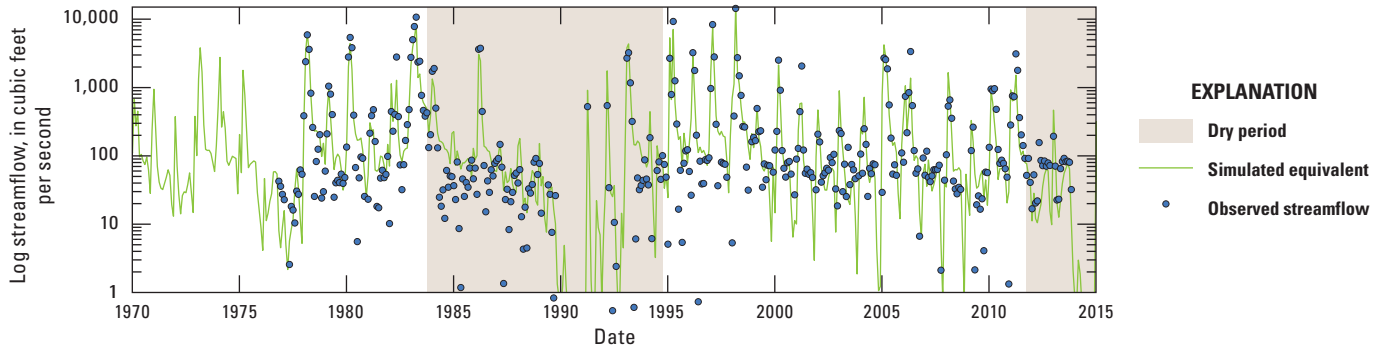
**D. Forebay analysis region: USGS 11152000 ARROYO SECO BL RELIZ C NR SOLEDAD CA**



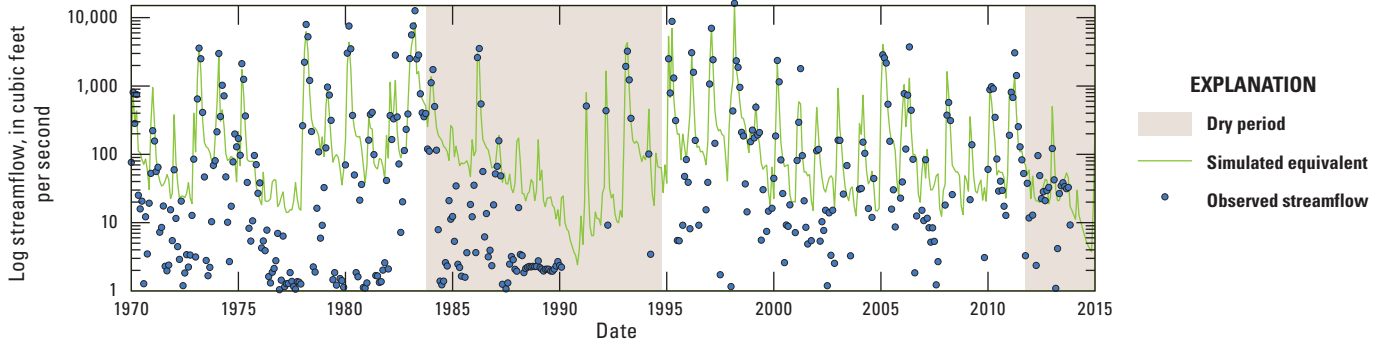
**E. Forebay analysis region: USGS 11151700 SALINAS R A SOLEDAD CA**



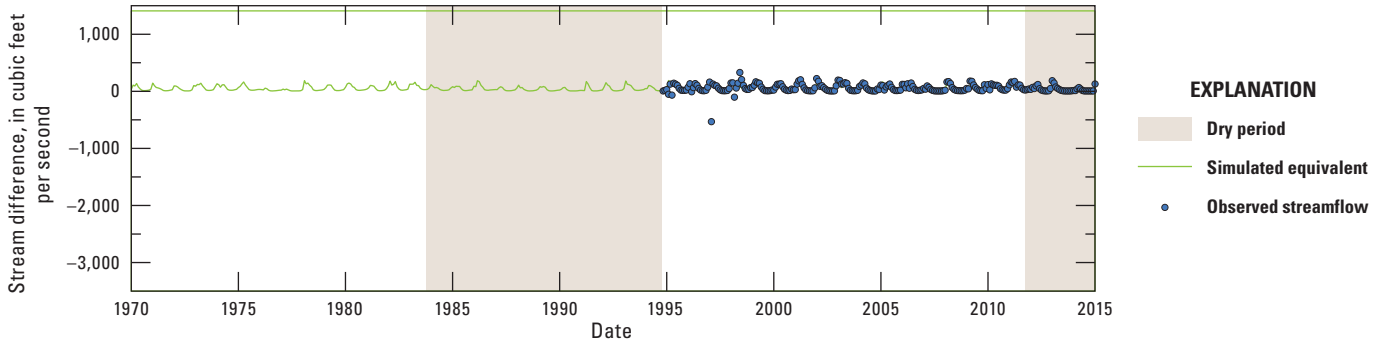
**F. Forebay analysis region: USGS 11152000 SALINAS R NR CHUALAR CA SOLEDAD CA**



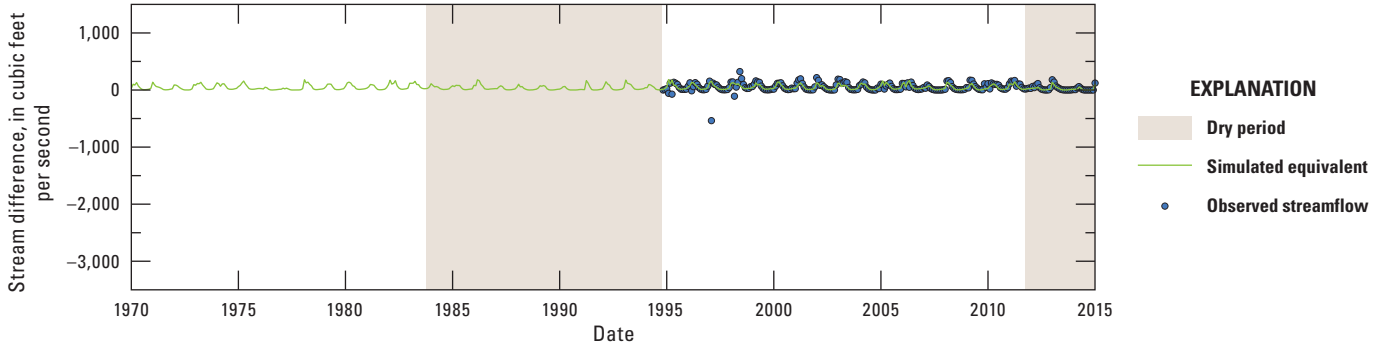
**G. Pressure analysis region: USGS 11152500 SALINAS R NR SPRECKELS CA**



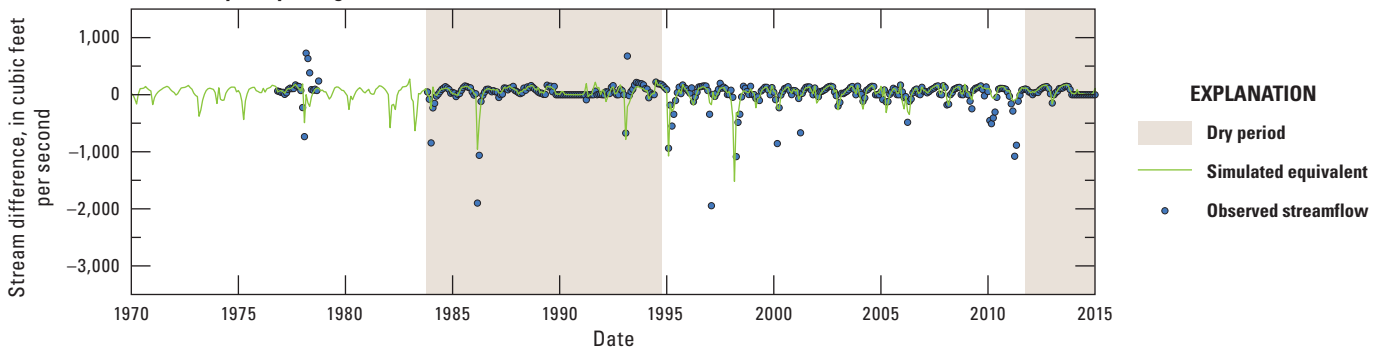
**H. Upper Valley analysis region: Stream difference USGS 11150500 - USGS 11151700**



**I. Forebay analysis region: Stream difference USGS 11152000 - USGS 11152050**



**J. Forebay analysis region: Stream difference USGS 11151700 - USGS 11152300**



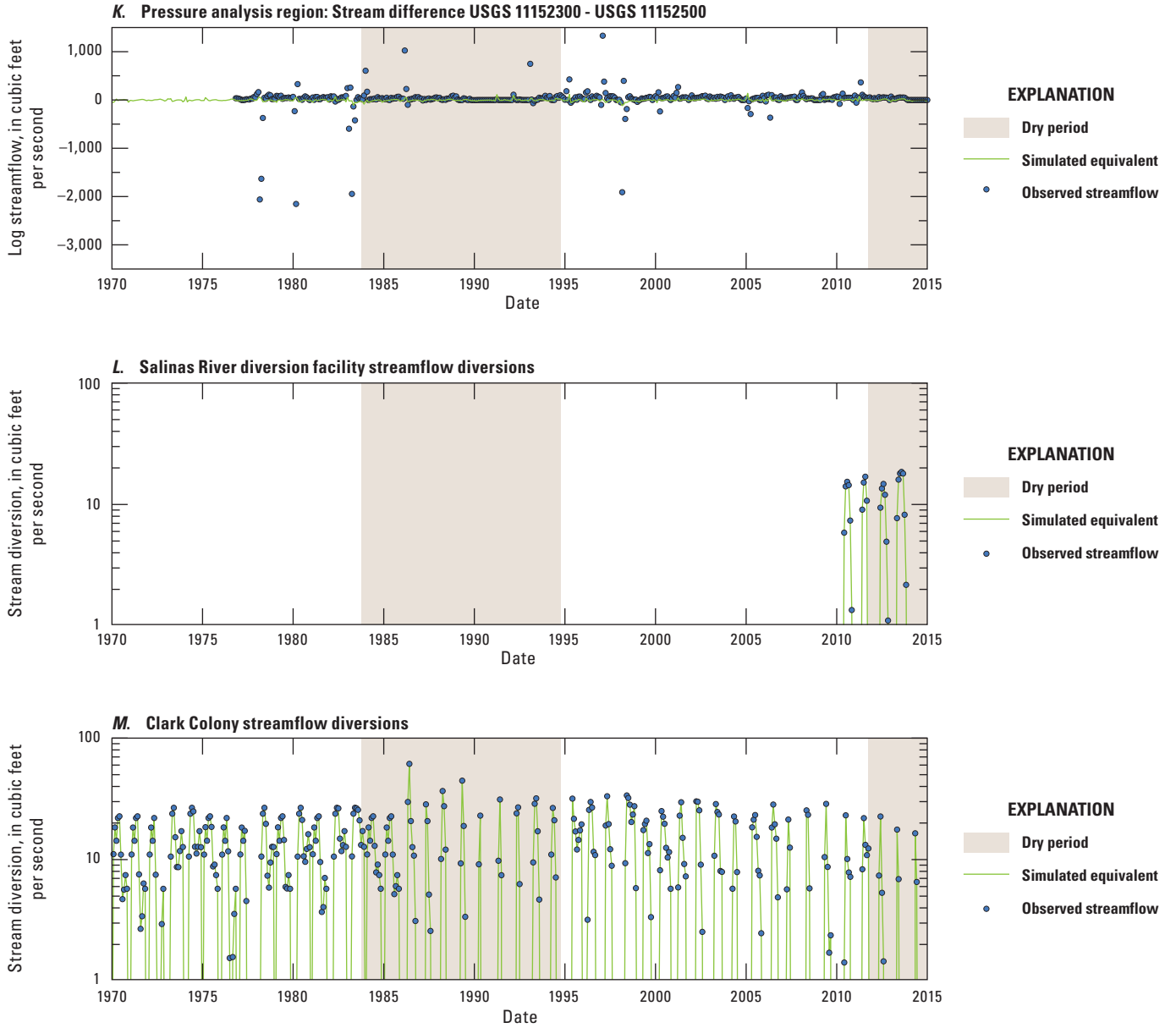
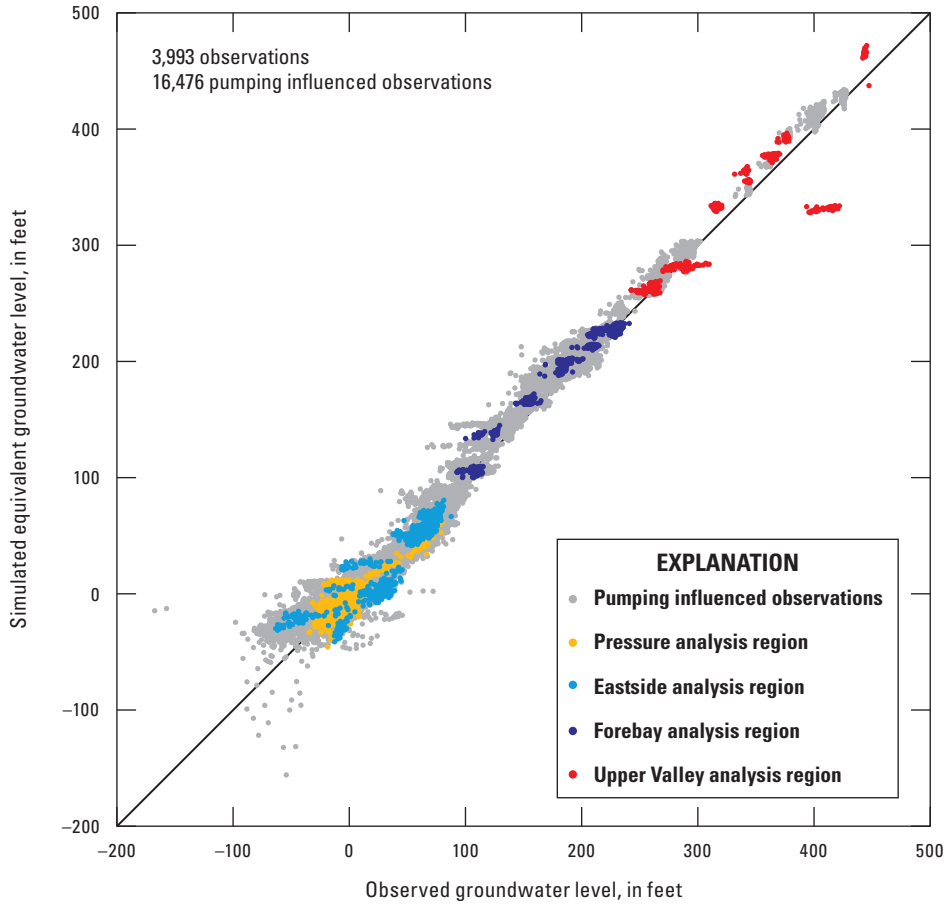
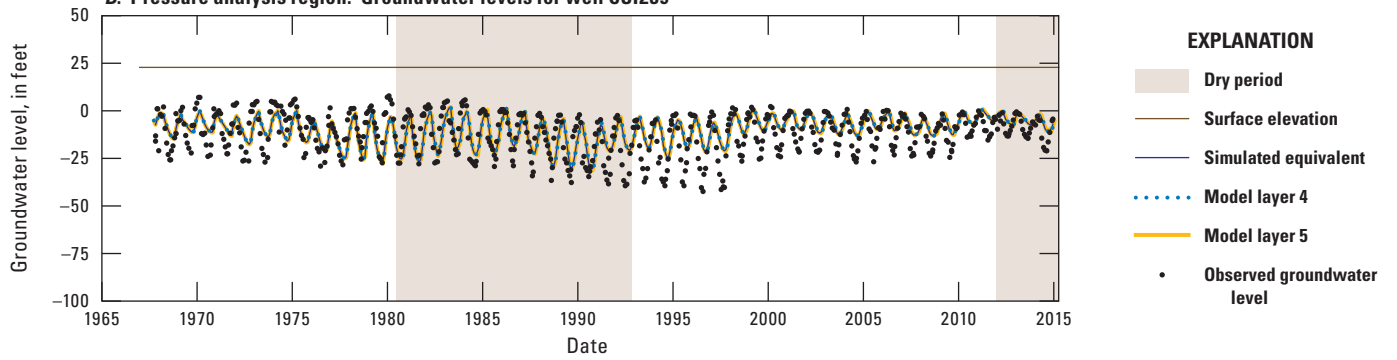


Figure 32. Observed and simulated equivalent streamflow hydrographs for selected river gages and diversions within the Salinas Valley Integrated Hydrologic Model domain for water years 1968 to 2018. A) Correlation among simulated and observed streamflows for all stream observations. Simulated and observed streamflow at B) USGS 11150500, C) USGS 11151700, D) USGS 11152300, E) USGS 11152500, F) USGS 11152000, and G) USGS 11152050 gages. Simulated and observed stream difference for H) USGS 11150500 – USGS 11151700, I) USGS 11151700 – USGS 11152300, J) USGS 11152300 – USGS 11152500, and K) USGS 11152000 – USGS 11152050. Simulated and observed diversions from L) Arroyo Seco for Clark Colony and M) Salinas River at the Salinas River Diversion Facility (Henson and Culling, 2025).

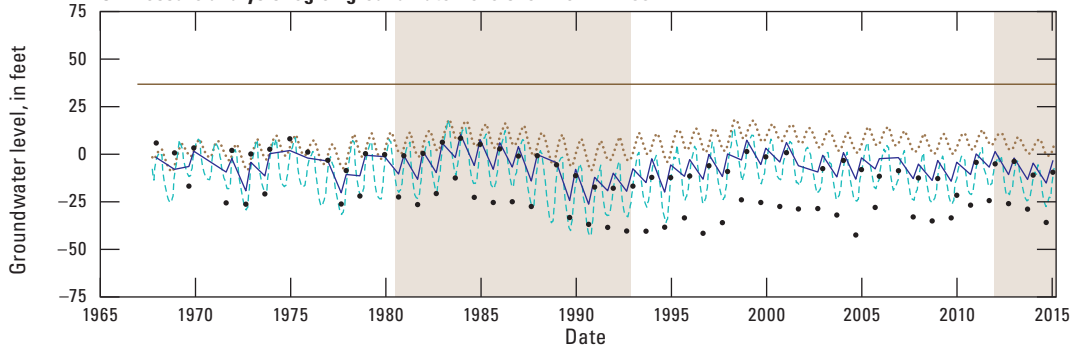
A



B. Pressure analysis region: Groundwater levels for well CS1239

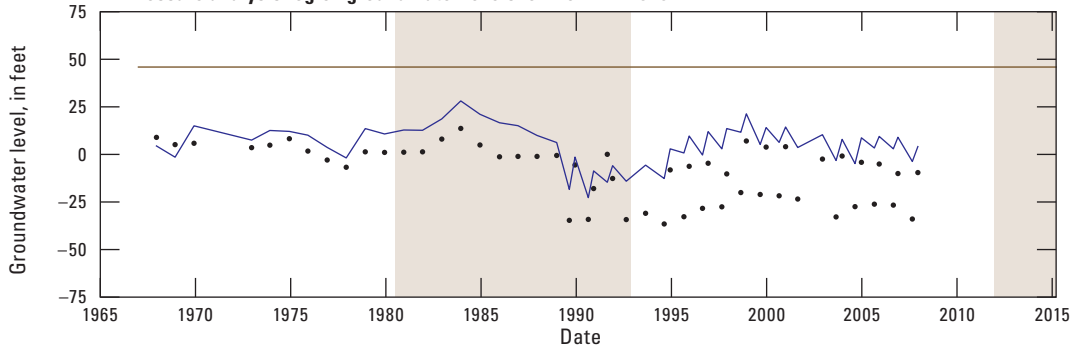


C. Pressure analysis region groundwater levels for well BDA331



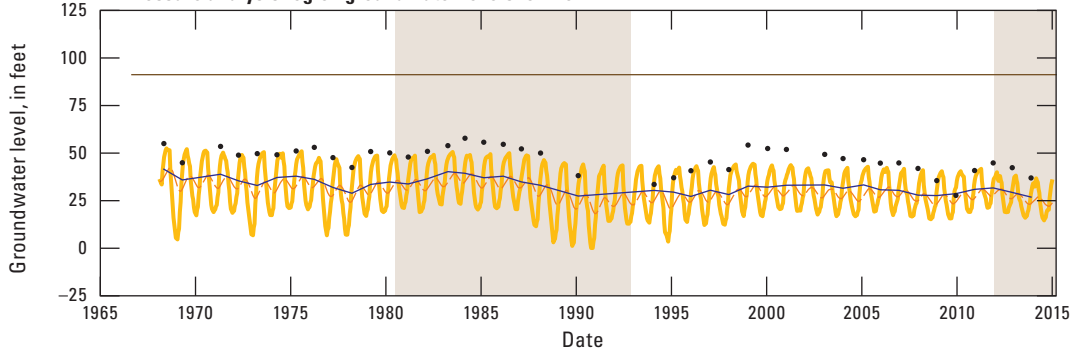
- EXPLANATION**
- Dry period
  - Surface elevation
  - Simulated equivalent
  - Model layer 2
  - Model layer 3
  - Observed groundwater level

D. Pressure analysis region groundwater levels for well ZPN1529



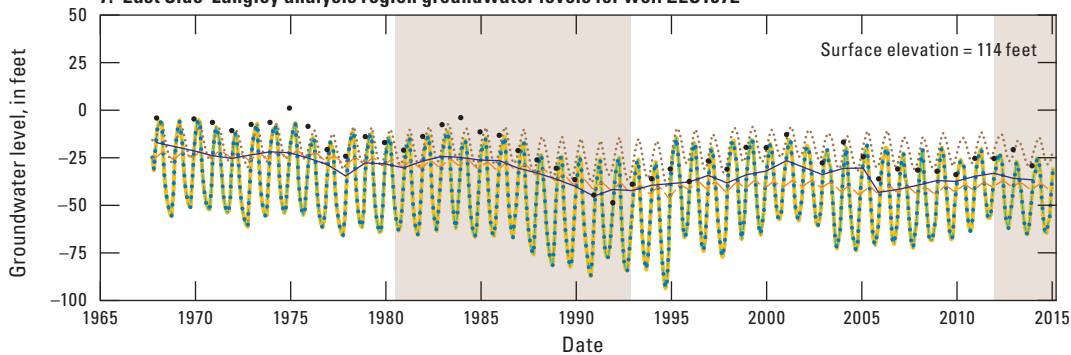
- EXPLANATION**
- Dry period
  - Surface elevation
  - Simulated equivalent
  - Observed groundwater level

E. Pressure analysis region groundwater levels for well ZPN441



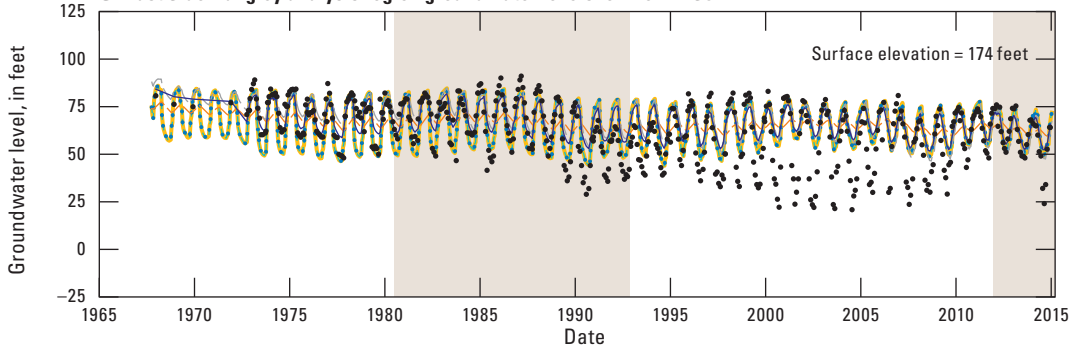
- EXPLANATION**
- Dry period
  - Surface elevation
  - Simulated equivalent
  - Model layer 5
  - Model layer 6
  - Observed groundwater level

F. East Side-Langley analysis region groundwater levels for well ZES1572



- EXPLANATION**
- Dry period
  - Simulated equivalent
  - Model layer 2
  - Model layer 3
  - Model layer 4
  - Model layer 5
  - Model layer 6
  - Observed groundwater level

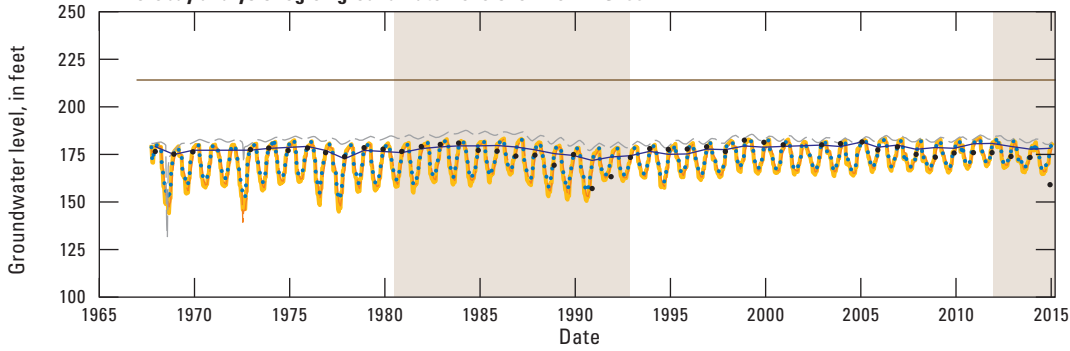
**G. East Side-Langley analysis region groundwater levels for well ZES871**



**EXPLANATION**

- Dry period
- Surface elevation
- Simulated equivalent
- Model layer 3
- Model layer 4
- Model layer 5
- Model layer 6
- Model layer 7
- Observed groundwater level

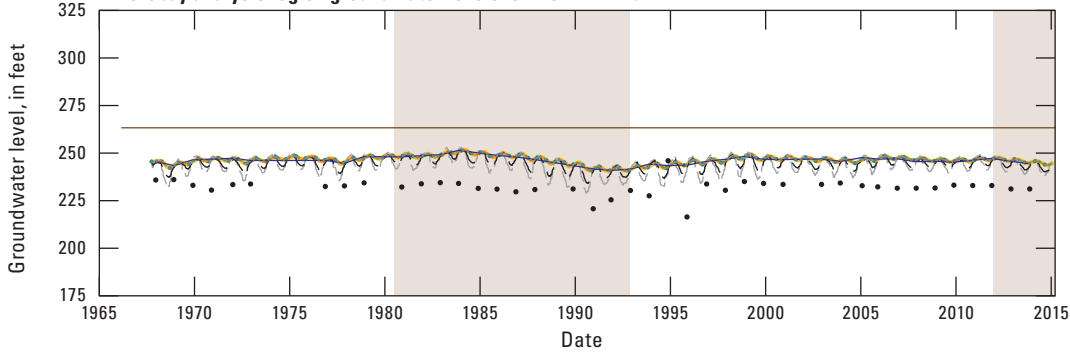
**H. Forebay analysis region groundwater levels for well ZFS1001**



**EXPLANATION**

- Dry period
- Surface elevation
- Simulated equivalent
- Model layer 4
- Model layer 5
- Model layer 6
- Model layer 7
- Observed groundwater level

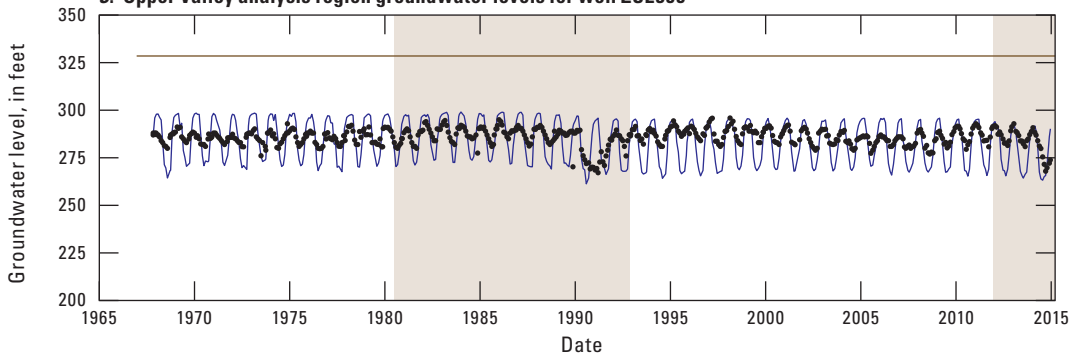
**I. Forebay analysis region groundwater levels for well ZNE1267**



**EXPLANATION**

- Dry period
- Surface elevation
- Simulated equivalent
- Model layer 2
- Model layer 3
- Model layer 4
- Model layer 5
- Model layer 6
- Model layer 7
- Model layer 8
- Observed groundwater level

**J. Upper Valley analysis region groundwater levels for well ZSE355**



**EXPLANATION**

- Dry period
- Surface elevation
- Simulated equivalent
- Observed groundwater level

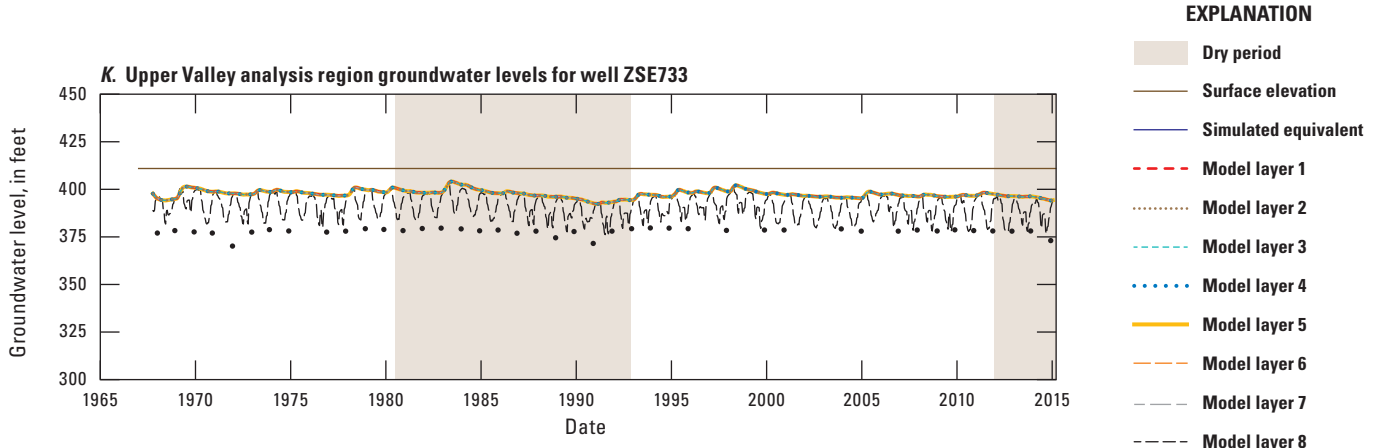


Figure 33. Groundwater observations and simulated equivalent values from the Salinas Valley Integrated Hydrologic Model. A) Graph of correlation among groundwater level measurements and simulated equivalent groundwater-level hydrographs for selected wells. Hydrographs are shown for wells B) CS1239, C) BDA331, D) ZPN1529, and E) ZPN441 in the Pressure analysis region; wells F) ZES1572 and G) ZES871 in the East Side-Langley analysis region; wells H) ZNE1267 and I) ZSE355 in the Forebay analysis region; and wells J) ZSE355 and K) ZSE733 in the Upper Valley analysis region (Henson and Culling, 2025).

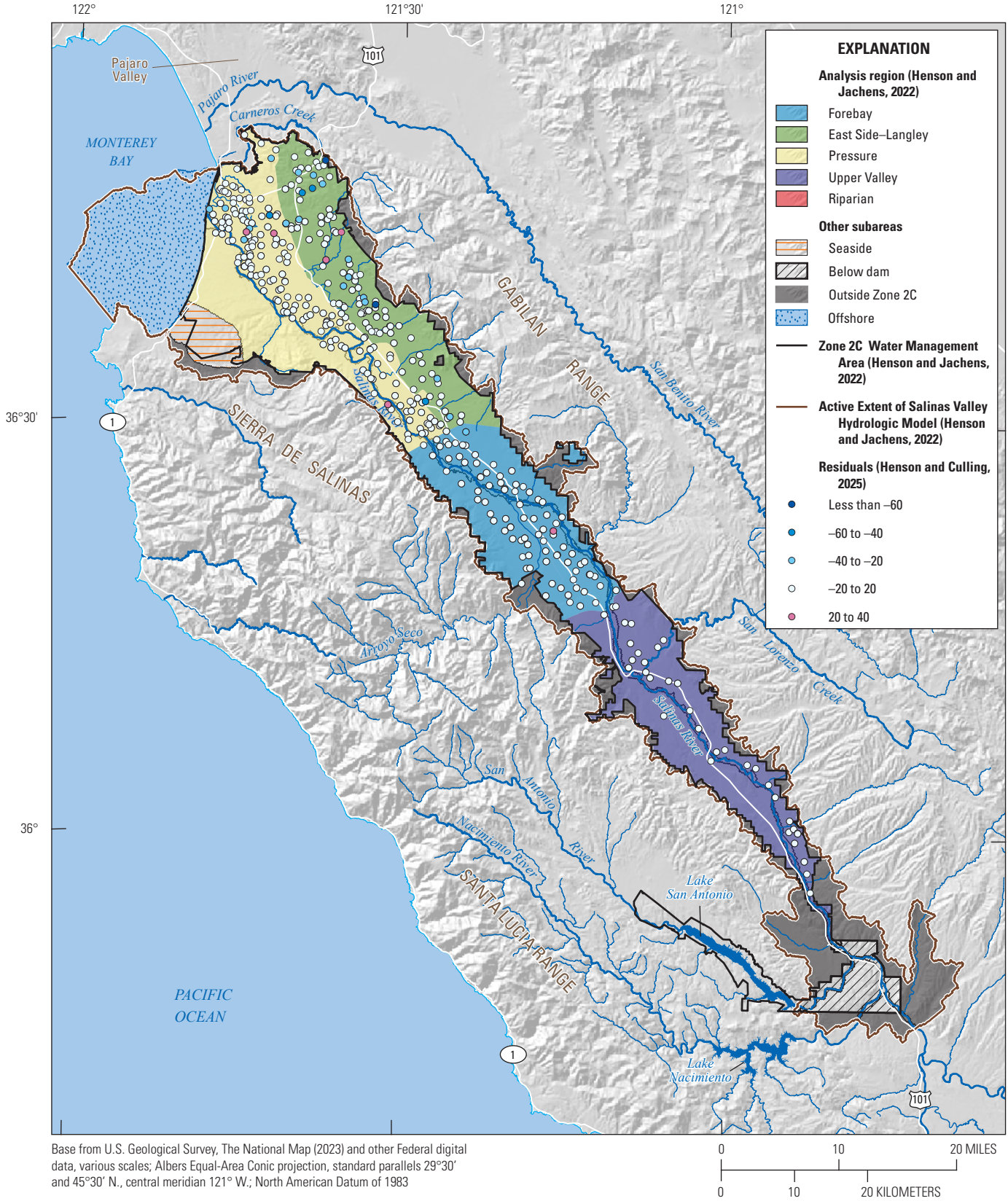


Figure 34. Mean residuals computed as the difference between observed and simulated equivalent values in the Salinas Valley Integrated Hydrologic Model for all observation wells for the parameter estimation period from water year 1968 through 2014 (Henson and Culling, 2025).



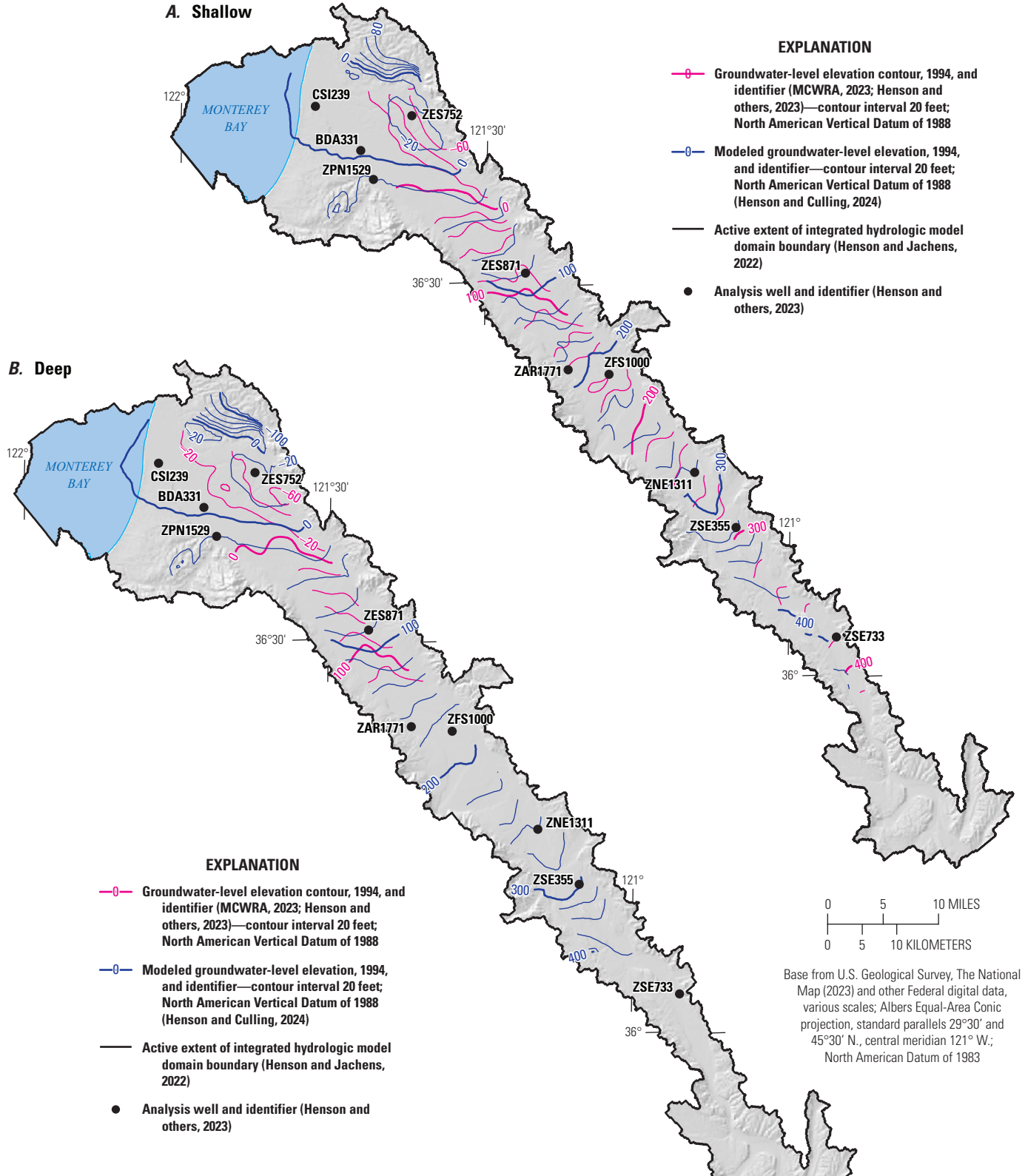
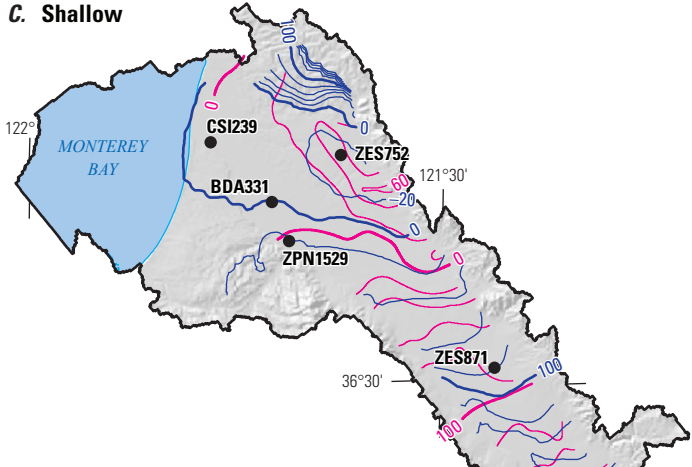


Figure 35. Historical model groundwater contours in Salinas Valley, California developed from simulated equivalent December groundwater levels to Monterey County Water Resource Agency (MCWRA) fall composite contoured groundwater levels. The shallow aquifer composite contour map was computed by MCWRA using measurements in aquifers that are less than 200 feet deep. The shallow contours are compared to groundwater level contours from model cells within the 180-Foot Aquifer hydrogeologic unit (layer 3). The deep aquifer composite contour map was computed by MCWRA using measurements greater than 200 but less than 420 feet deep. The deep contours are compared to groundwater level contours from model cells within the 400-Foot Aquifer hydrogeologic unit (layer 5). These maps show A) shallow aquifer composite contours and simulated equivalent contours in fall of 1994, B) deep aquifer composite contours and simulated equivalent contours in fall 1994, C) shallow aquifer composite contours and simulated equivalent contours in fall of 2003, D) deep aquifer composite contours and simulated equivalent contours in fall 2003, and E) shallow aquifer composite contours and simulated equivalent contours in fall 2011, and F) deep aquifer composite contours and simulated equivalent contours in fall 2011.

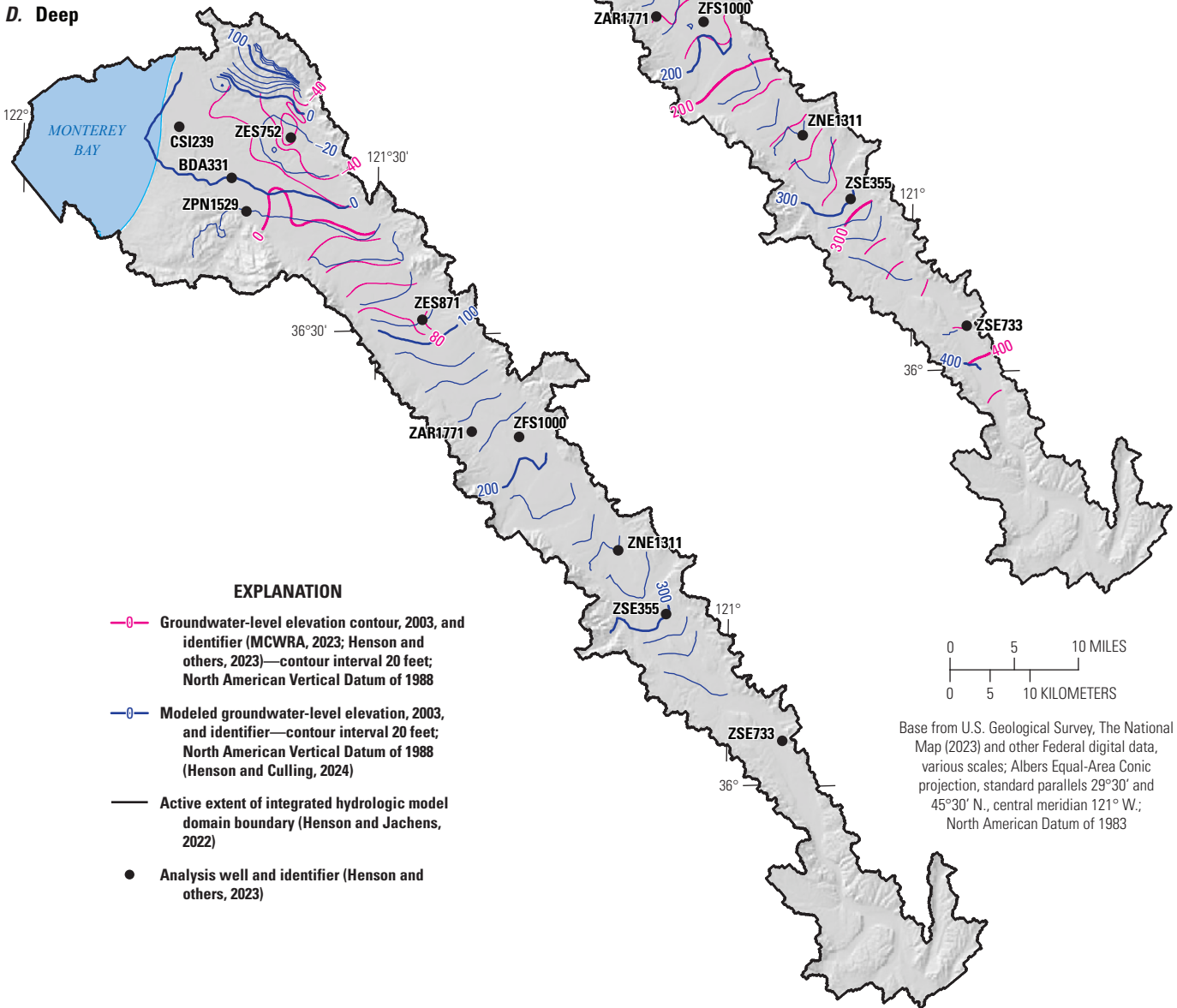
**C. Shallow**



**EXPLANATION**

- Groundwater-level elevation contour, 2003, and identifier (MCWRA, 2023; Henson and others, 2023)—contour interval 20 feet; North American Vertical Datum of 1988
- Modeled groundwater-level elevation, 2003, and identifier—contour interval 20 feet; North American Vertical Datum of 1988 (Henson and Culling, 2024)
- Active extent of integrated hydrologic model domain boundary (Henson and Jachens, 2022)
- Analysis well and identifier (Henson and others, 2023)

**D. Deep**



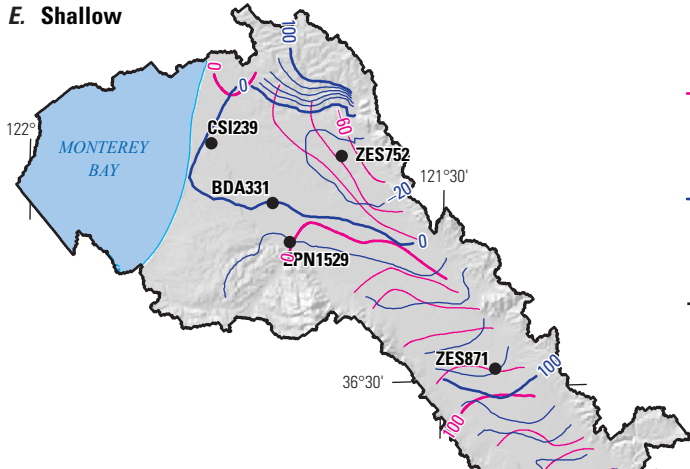
**EXPLANATION**

- Groundwater-level elevation contour, 2003, and identifier (MCWRA, 2023; Henson and others, 2023)—contour interval 20 feet; North American Vertical Datum of 1988
- Modeled groundwater-level elevation, 2003, and identifier—contour interval 20 feet; North American Vertical Datum of 1988 (Henson and Culling, 2024)
- Active extent of integrated hydrologic model domain boundary (Henson and Jachens, 2022)
- Analysis well and identifier (Henson and others, 2023)



Base from U.S. Geological Survey, The National Map (2023) and other Federal digital data, various scales; Albers Equal-Area Conic projection, standard parallels 29°30' and 45°30' N., central meridian 121° W.; North American Datum of 1983

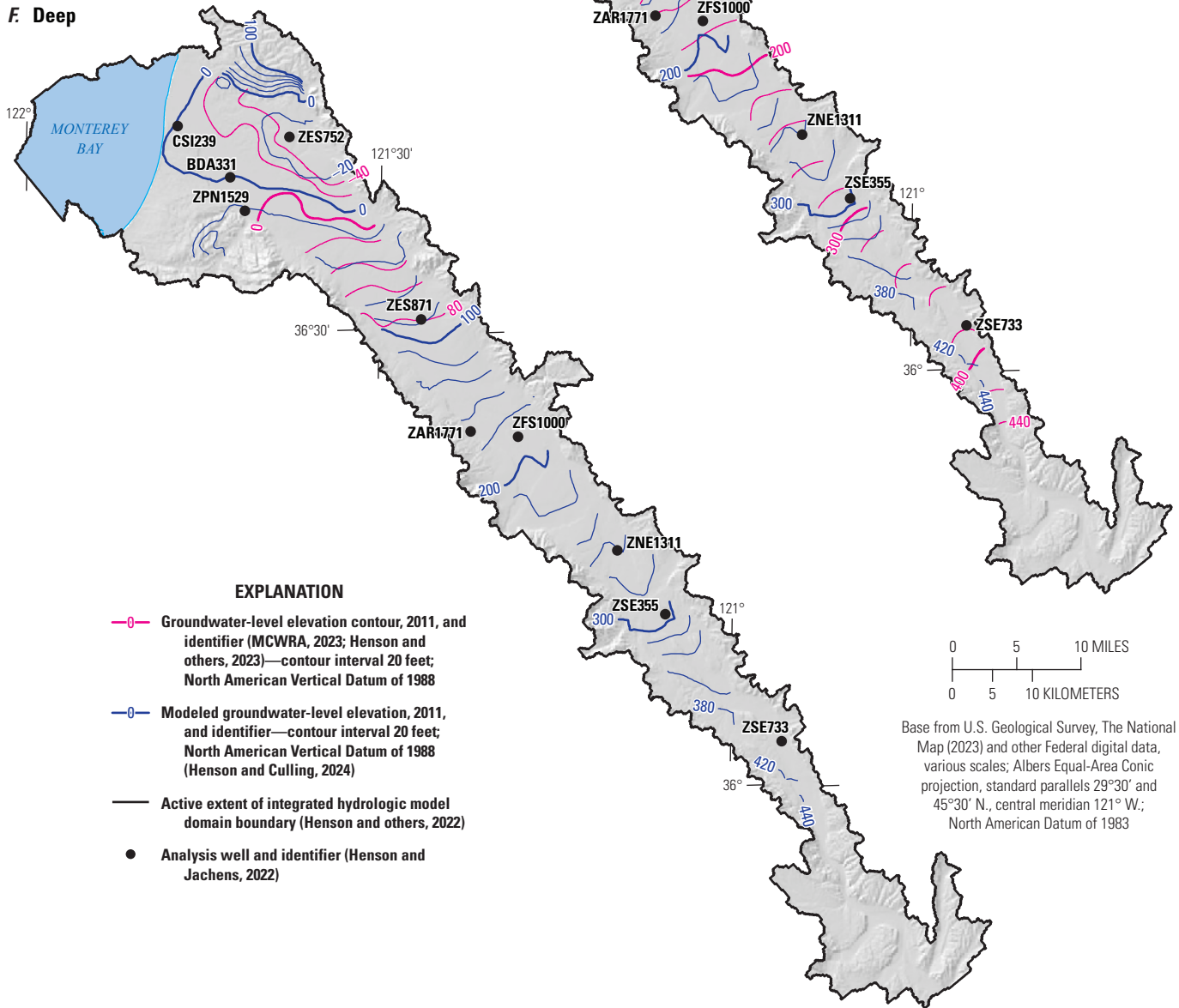
**E. Shallow**



**EXPLANATION**

- Groundwater-level elevation contour, 2011, and identifier (MCWRA, 2023; Henson and others, 2023)—contour interval 20 feet; North American Vertical Datum of 1988
- Modeled groundwater-level elevation, 2011, and identifier—contour interval 20 feet; North American Vertical Datum of 1988 (Henson and Culling, 2024)
- Active extent of integrated hydrologic model domain boundary (Henson and Jachens, 2022)
- Analysis well and identifier (Henson and others, 2023)

**F. Deep**



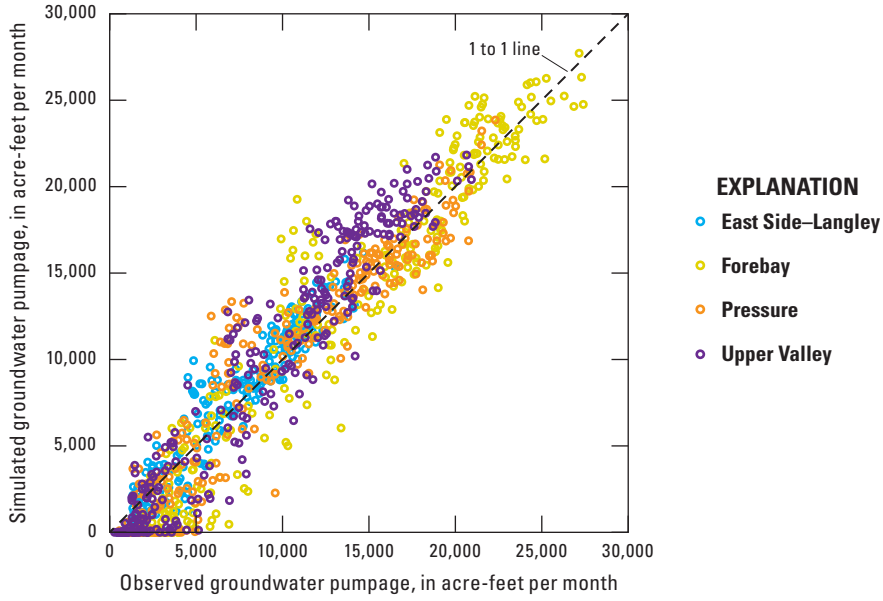
**EXPLANATION**

- Groundwater-level elevation contour, 2011, and identifier (MCWRA, 2023; Henson and others, 2023)—contour interval 20 feet; North American Vertical Datum of 1988
- Modeled groundwater-level elevation, 2011, and identifier—contour interval 20 feet; North American Vertical Datum of 1988 (Henson and Culling, 2024)
- Active extent of integrated hydrologic model domain boundary (Henson and others, 2022)
- Analysis well and identifier (Henson and Jachens, 2022)

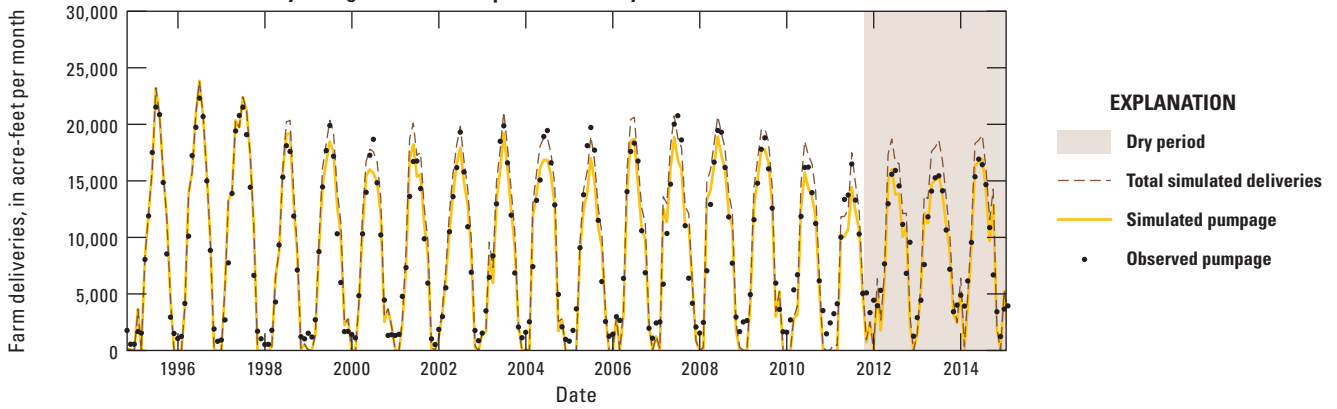


Base from U.S. Geological Survey, The National Map (2023) and other Federal digital data, various scales; Albers Equal-Area Conic projection, standard parallels 29°30' and 45°30' N., central meridian 121° W.; North American Datum of 1983

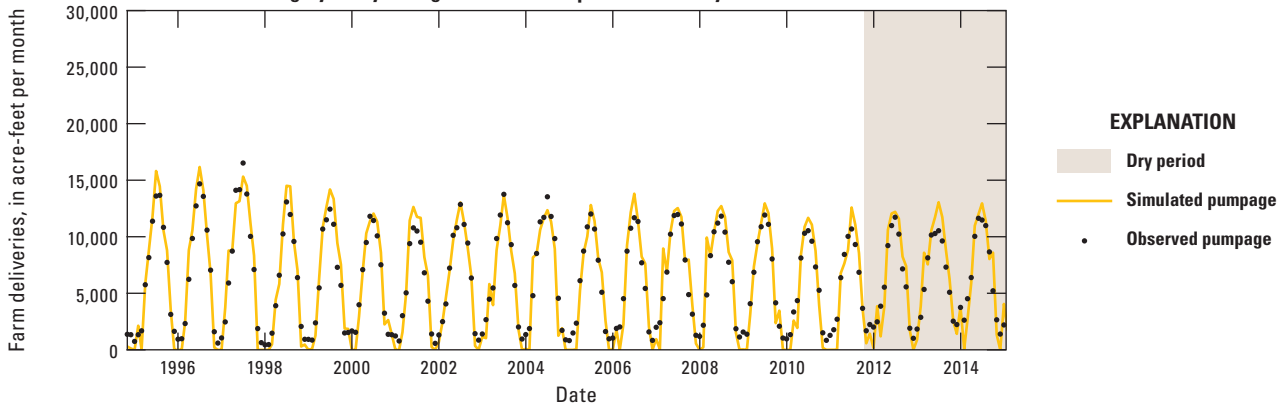
A



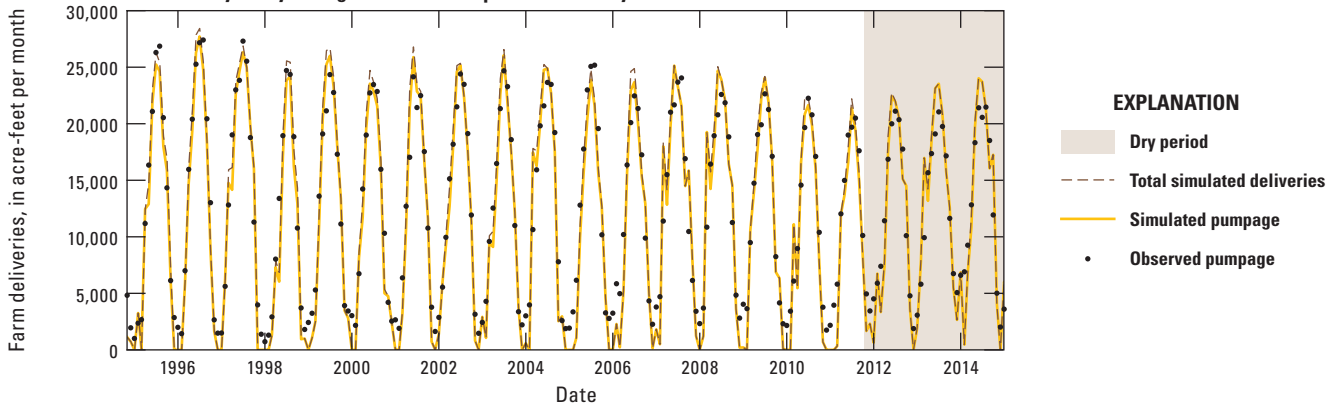
**B. Pressure analysis region calibration period: Monthly farm deliveries**



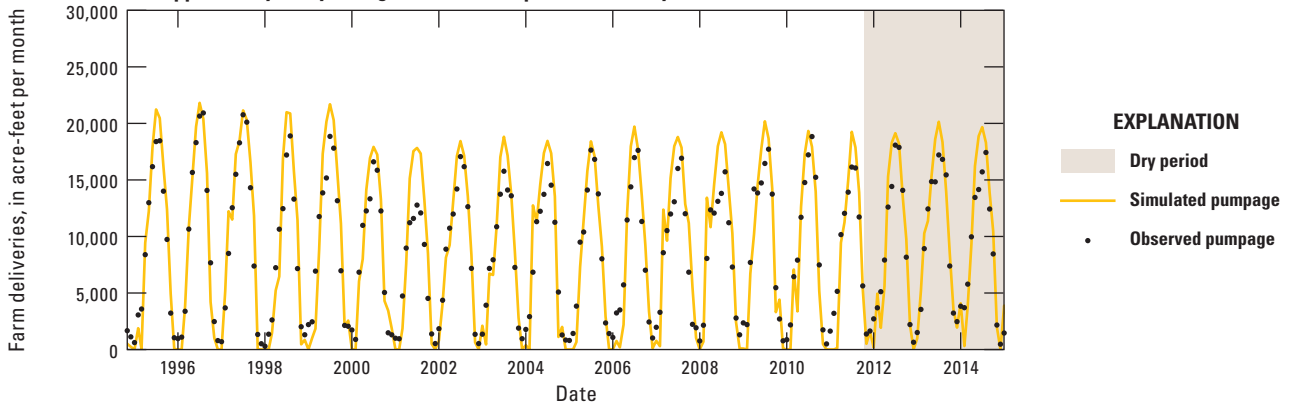
**C. East Side-Langley analysis region calibration period: Monthly farm deliveries**



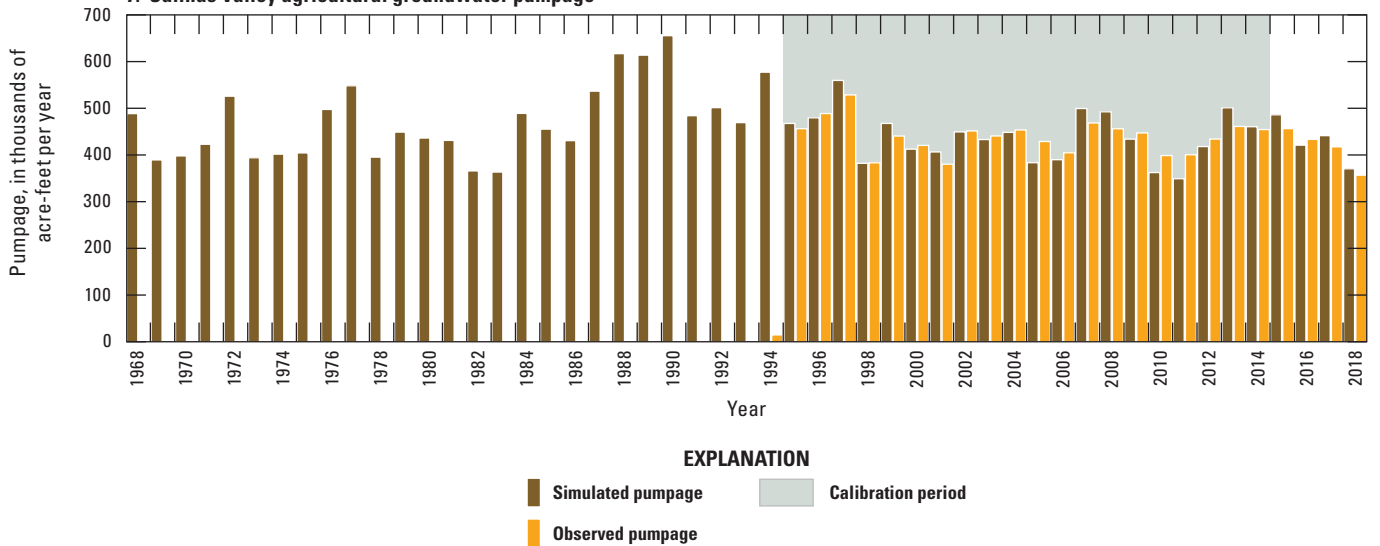
**D. Forebay analysis region calibration period: Monthly farm deliveries**



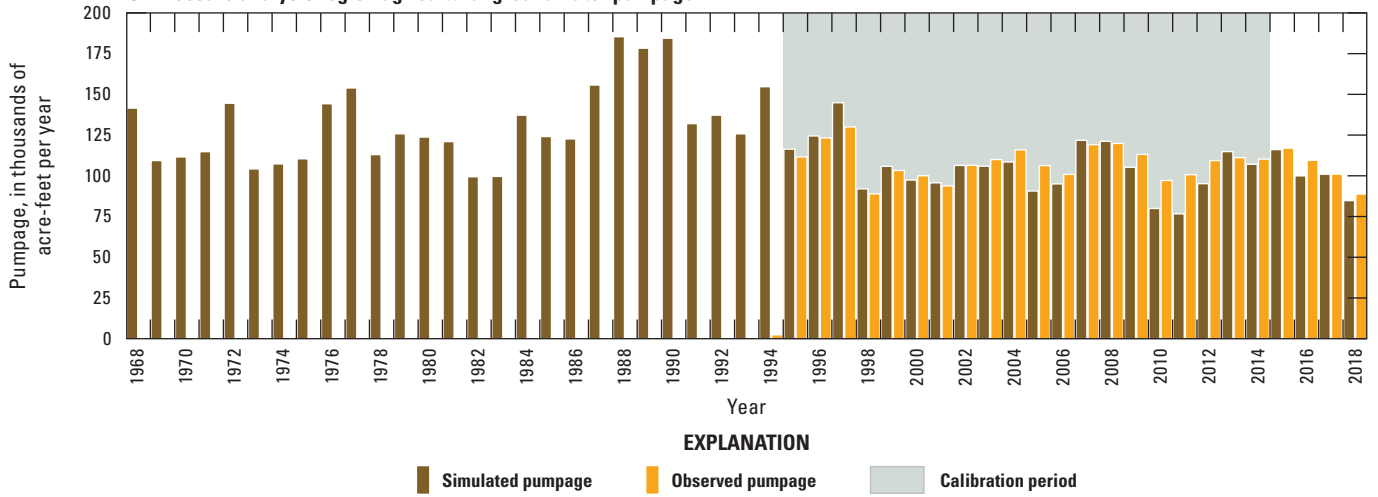
**E. Upper Valley analysis region calibration period: Monthly farm deliveries**



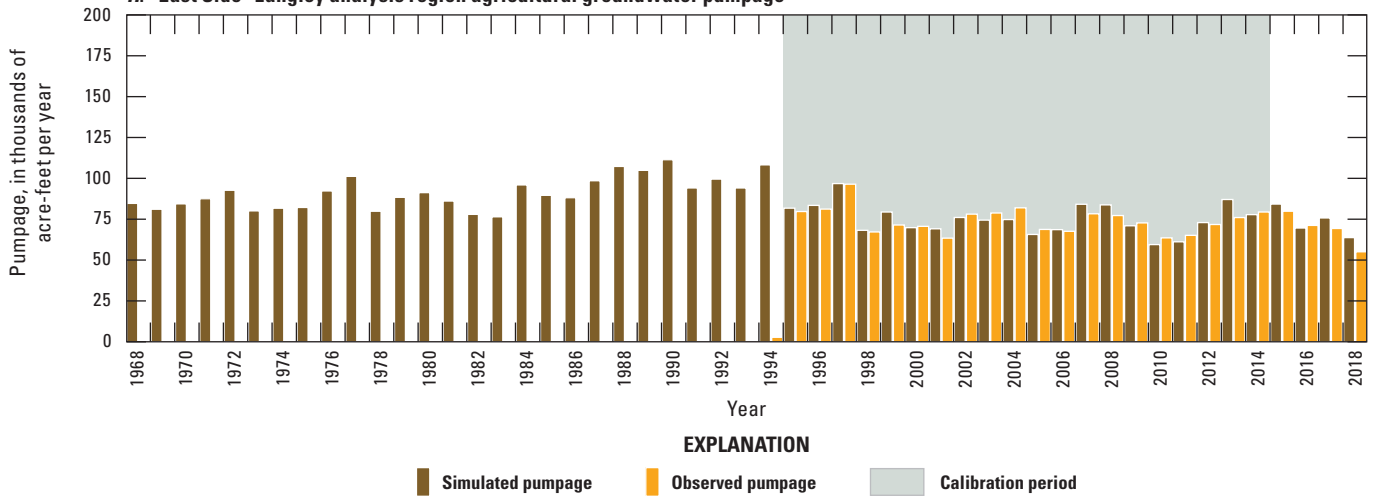
**F. Salinas Valley agricultural groundwater pumpage**



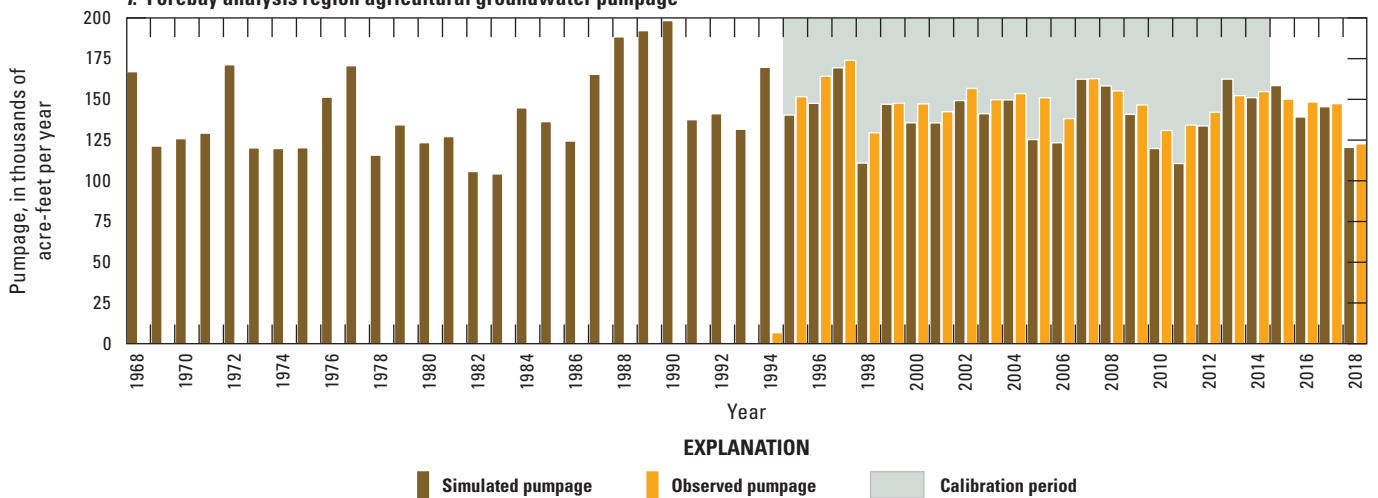
**G. Pressure analysis region agricultural groundwater pumpage**



**H. East Side–Langley analysis region agricultural groundwater pumpage**



**I. Forebay analysis region agricultural groundwater pumpage**



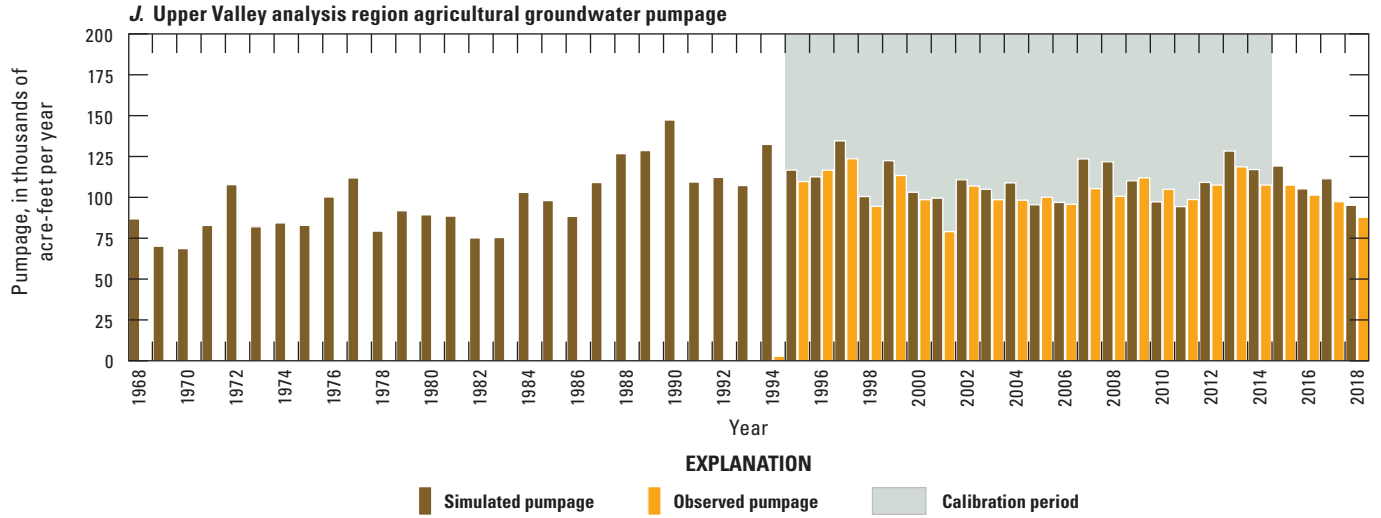


Figure 36. Reported and simulated equivalent agricultural pumpage within the Salinas Valley Integrated Hydrologic Model. A) Correlation among monthly reported and simulated equivalent groundwater pumpage. Time series of monthly observed and simulated equivalent farm deliveries for the B) Pressure analysis region, C) East Side-Langley analysis region, D) Forebay analysis region, and E) Upper Valley analysis region. Times series of annual observed and simulated equivalent pumpage for F) entire integrated hydrologic model domain, G) Pressure analysis region, H) East Side-Langley analysis region, I) Forebay analysis region, and J) Upper Valley analysis region (Henson and others, 2023; Henson and Culling, 2025).

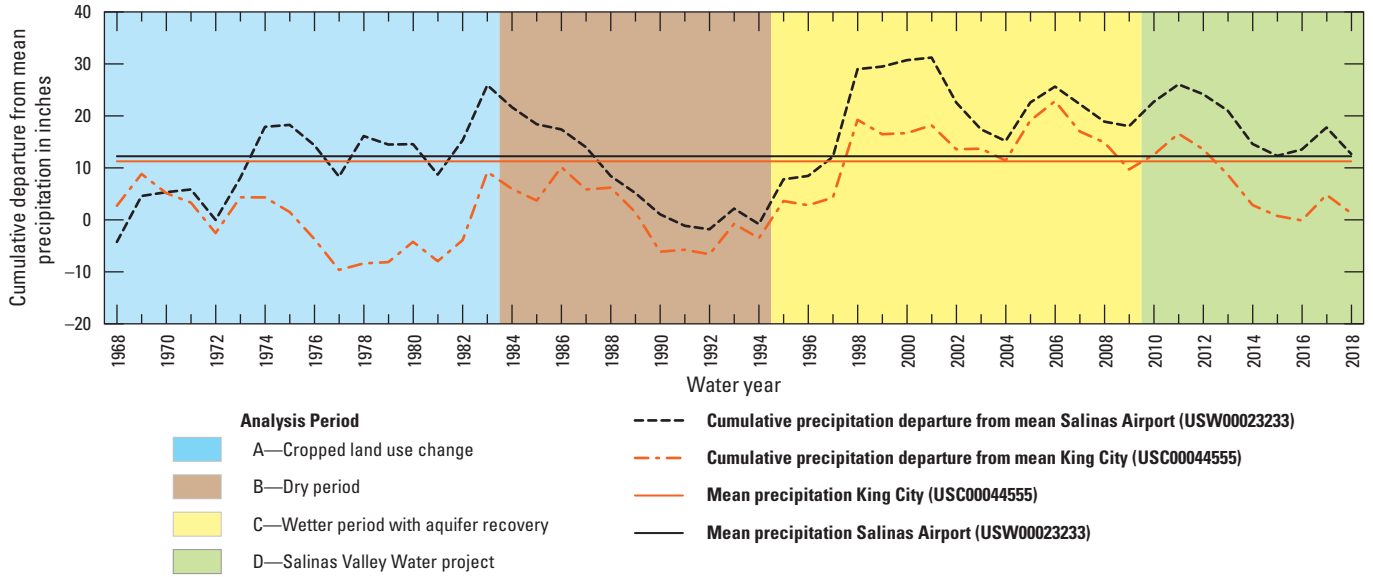
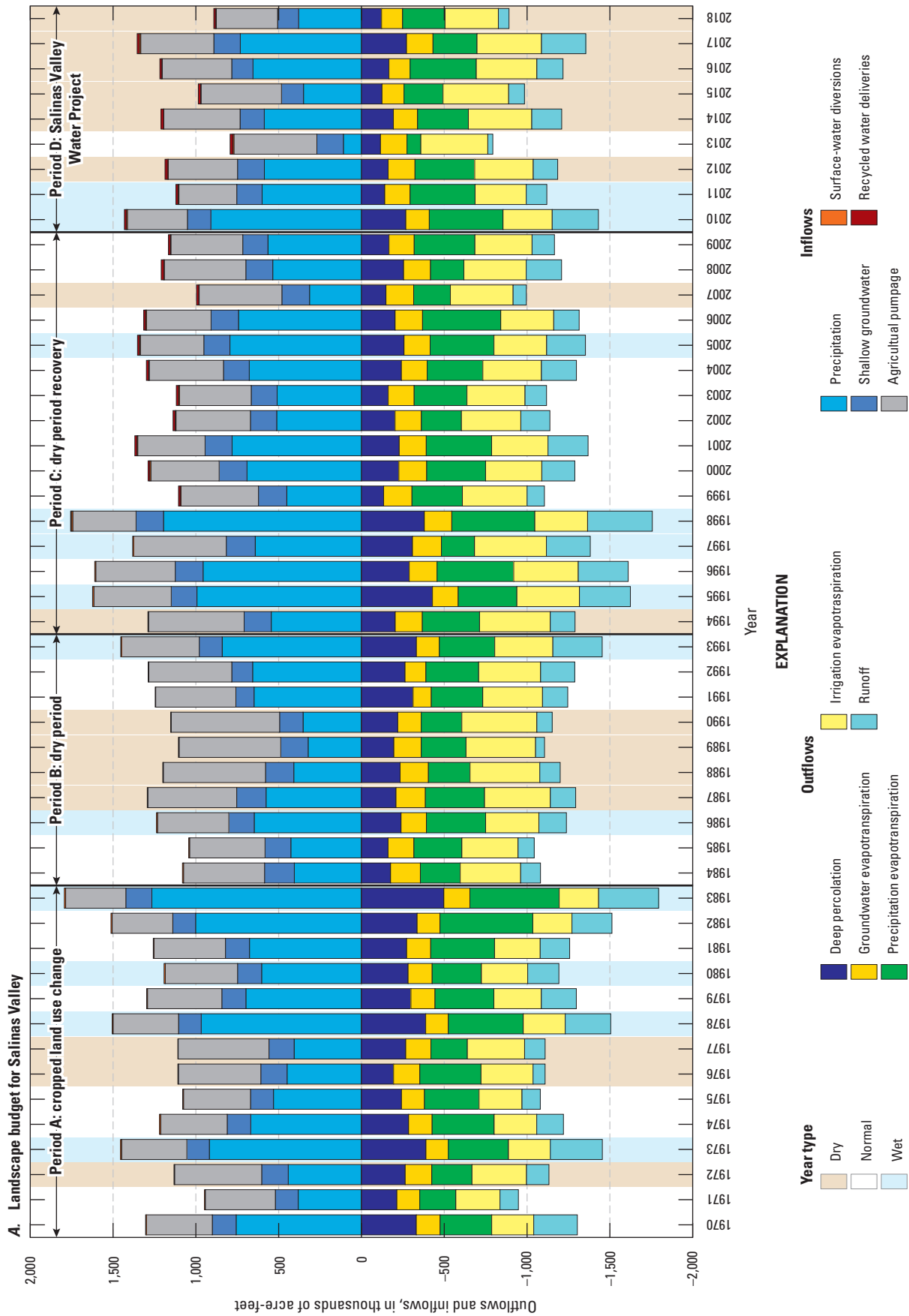
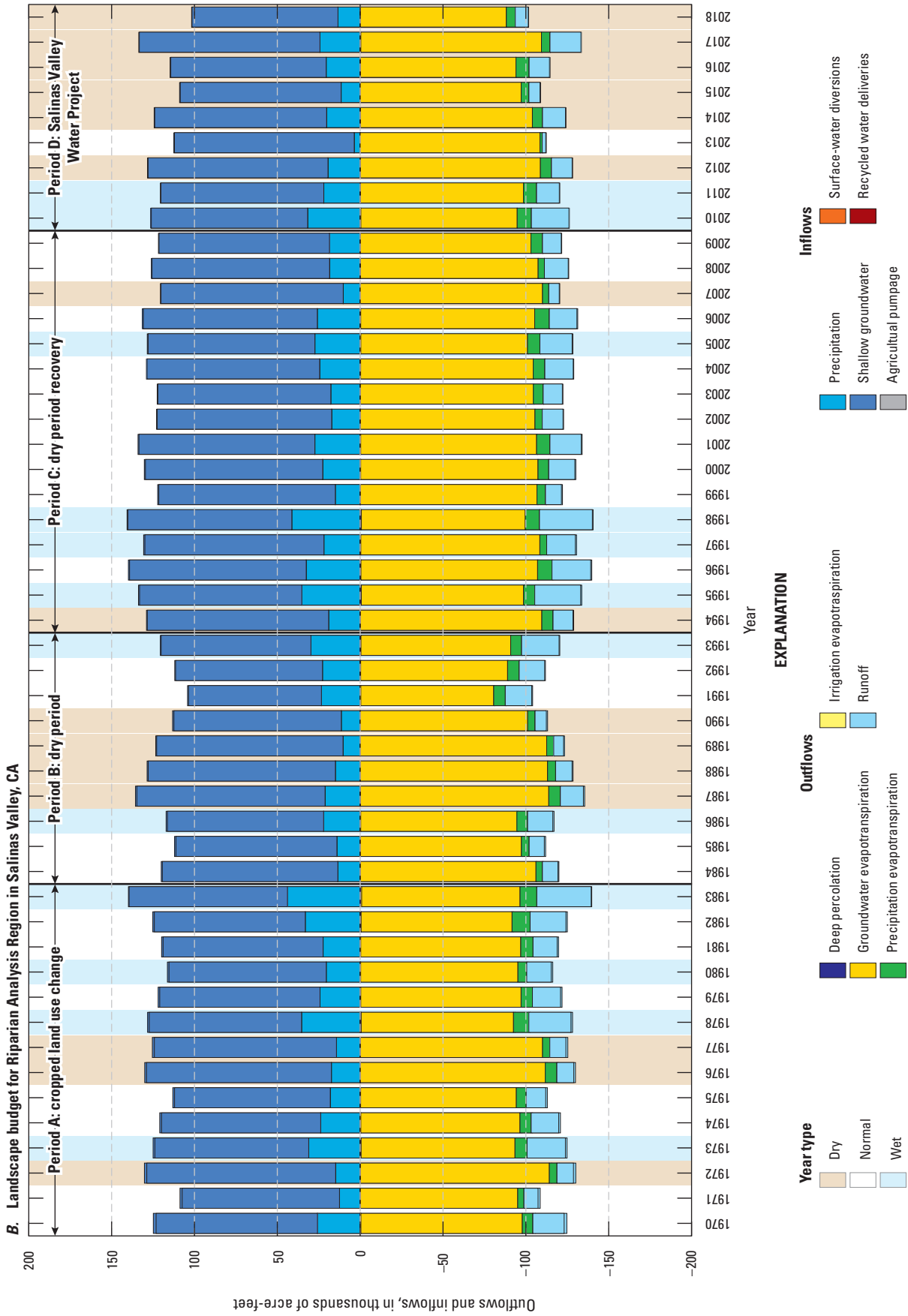


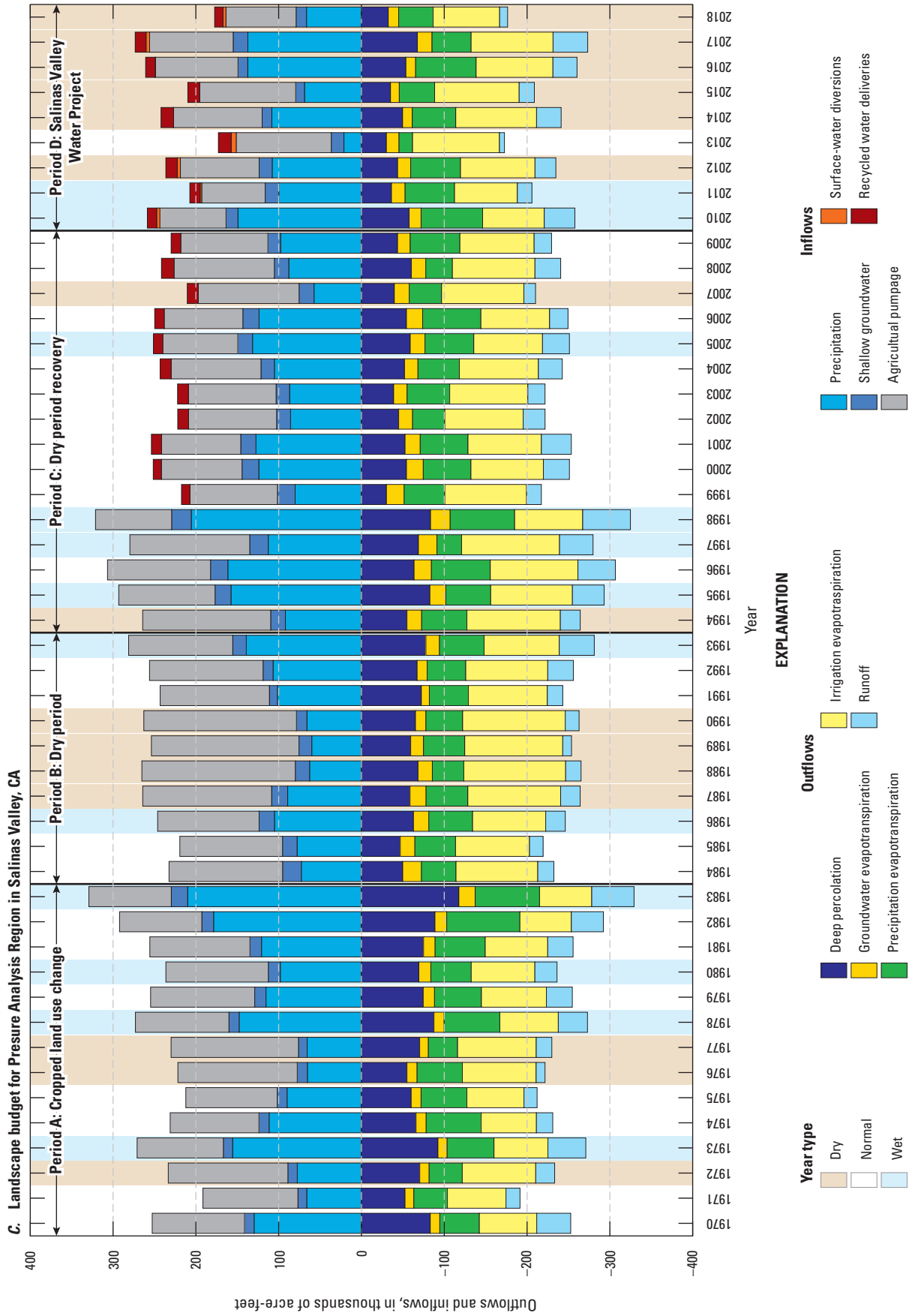
Figure 37. Four hydrologic budget analysis subperiods in the study that is informed by the cumulative departure of precipitation at Cooperative Observer Network stations for the Salinas Airport (USW00023233) and King City (USC00044555), California. The subperiods represent A) the start of land use conversion to more multi-cropping, 1970–1983; B) historical dry period, 1984–1994; C) start of reported withdrawal data collection with relatively wetter conditions, 1995–2009; and D) initiation and operation of the Salinas River Diversion Facility and recent recycled water deliveries, 2010–2018.

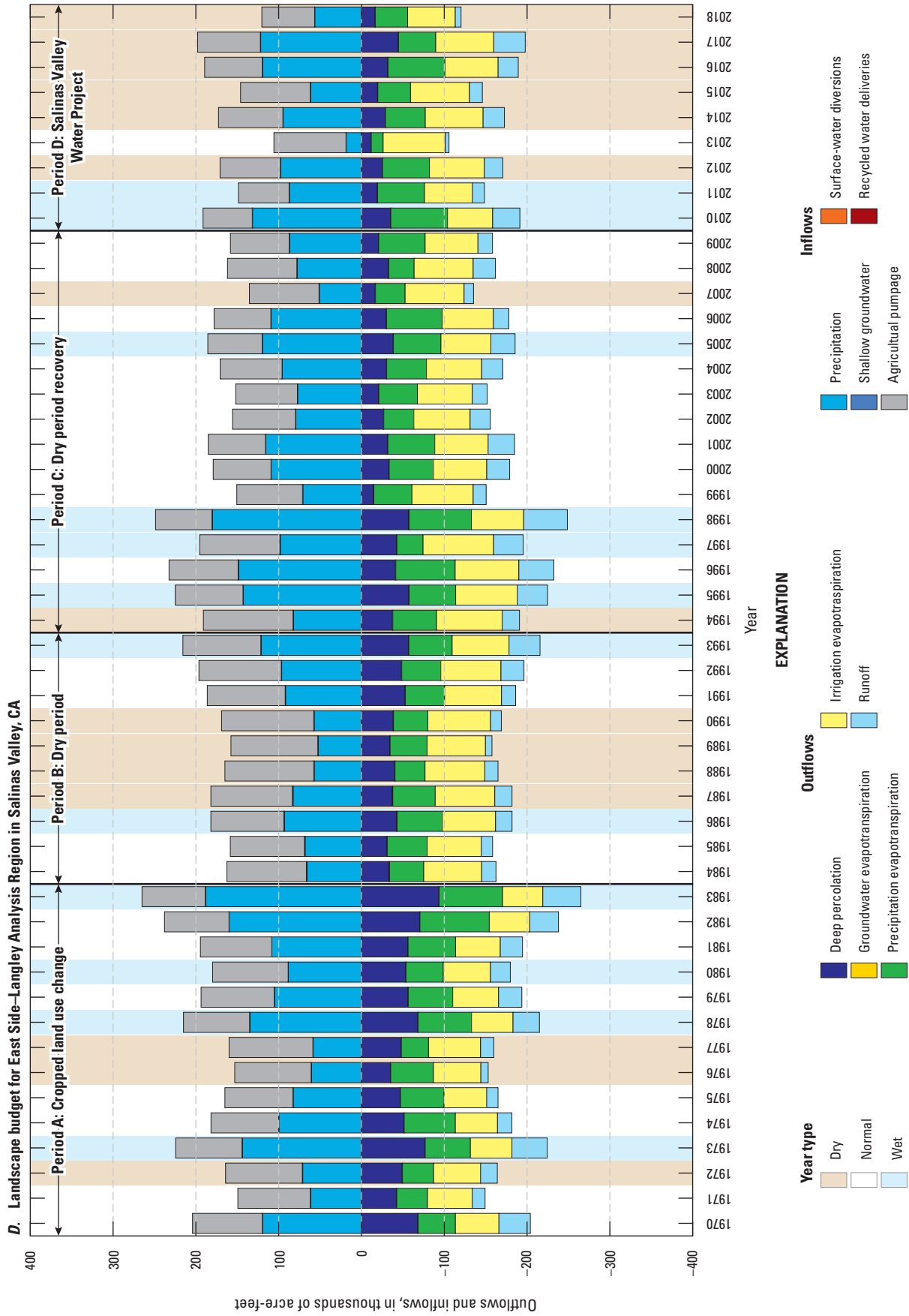


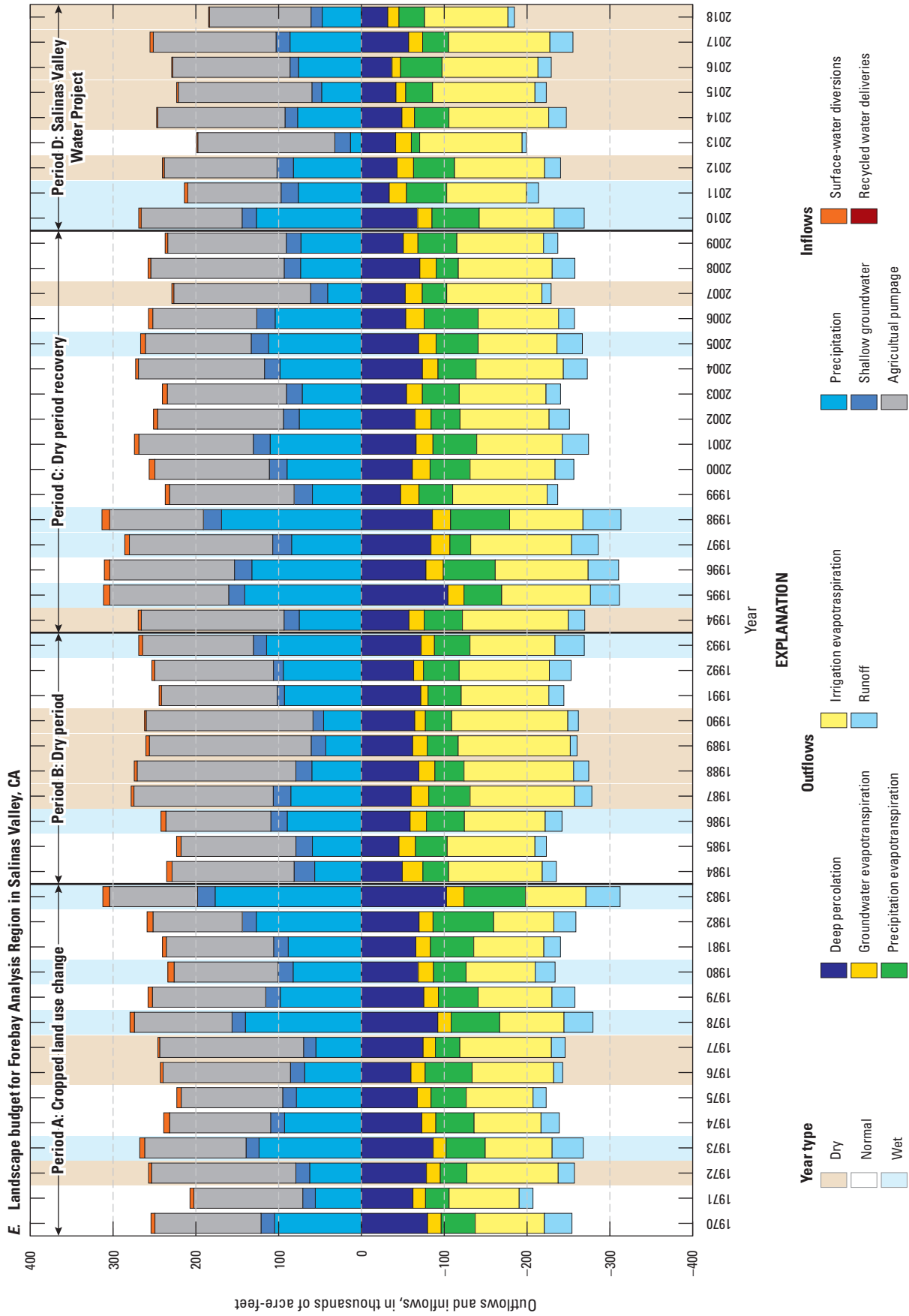
Figure 38. Distribution of landscape-budget inflow and outflow components for the Salinas Valley Integrated Hydrologic Model for water years 1970 to 2018 showing the A) entire integrated hydrologic model domain, B) Riparian analysis region, C) Pressure analysis region, D) East Side-Langley analysis region, E) Forebay analysis region, and F) Upper Valley analysis region (Henson and Culling, 2025).

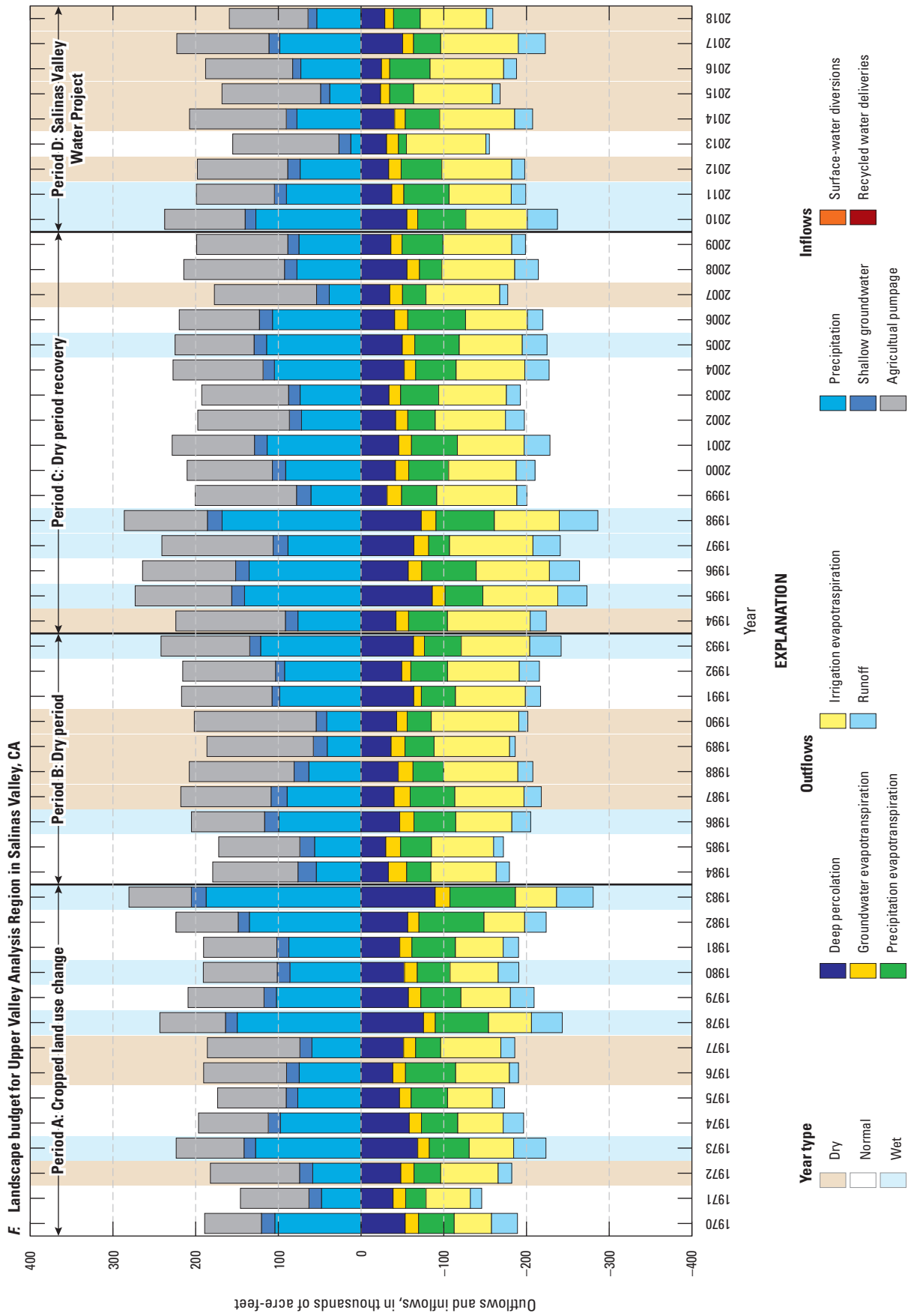






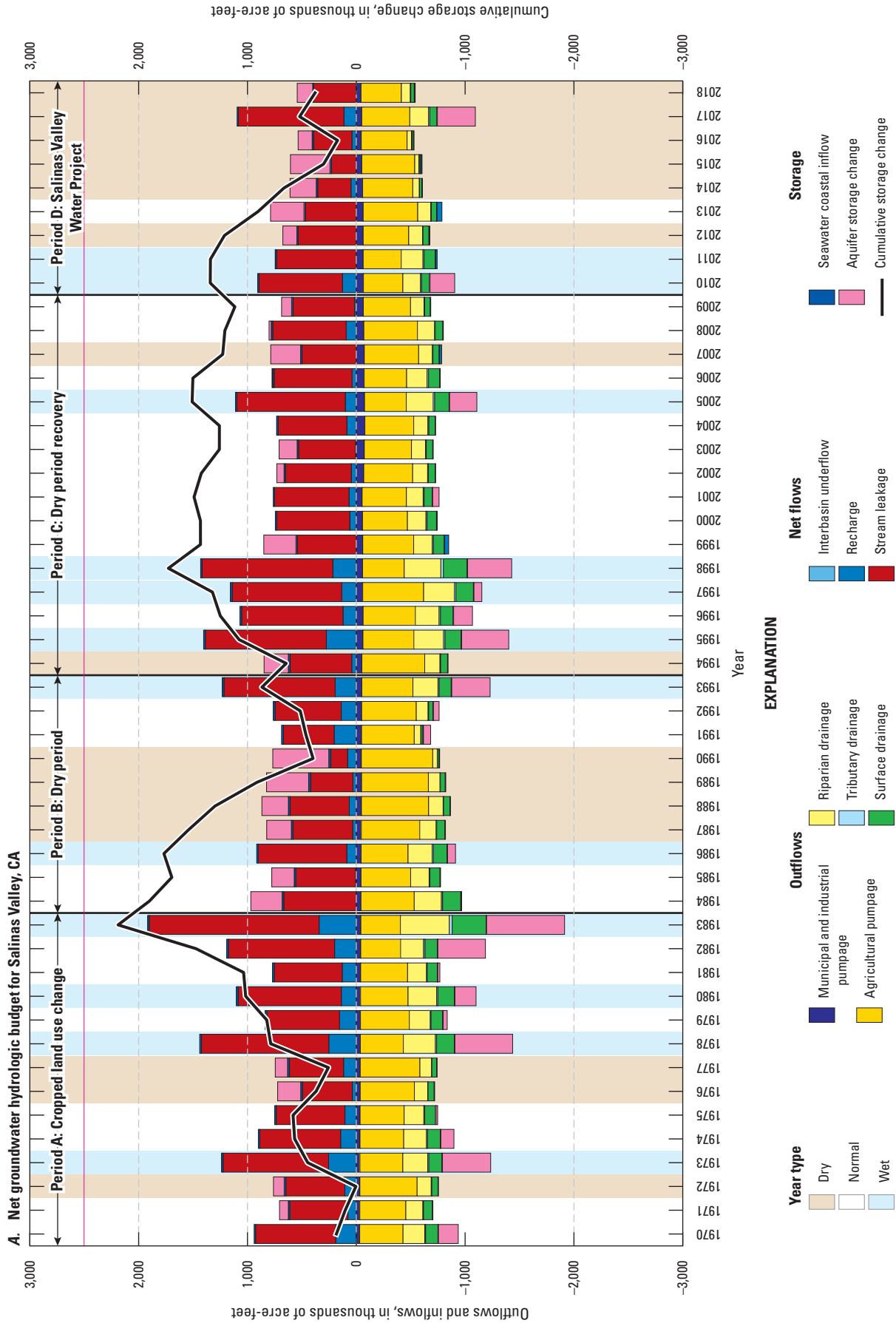


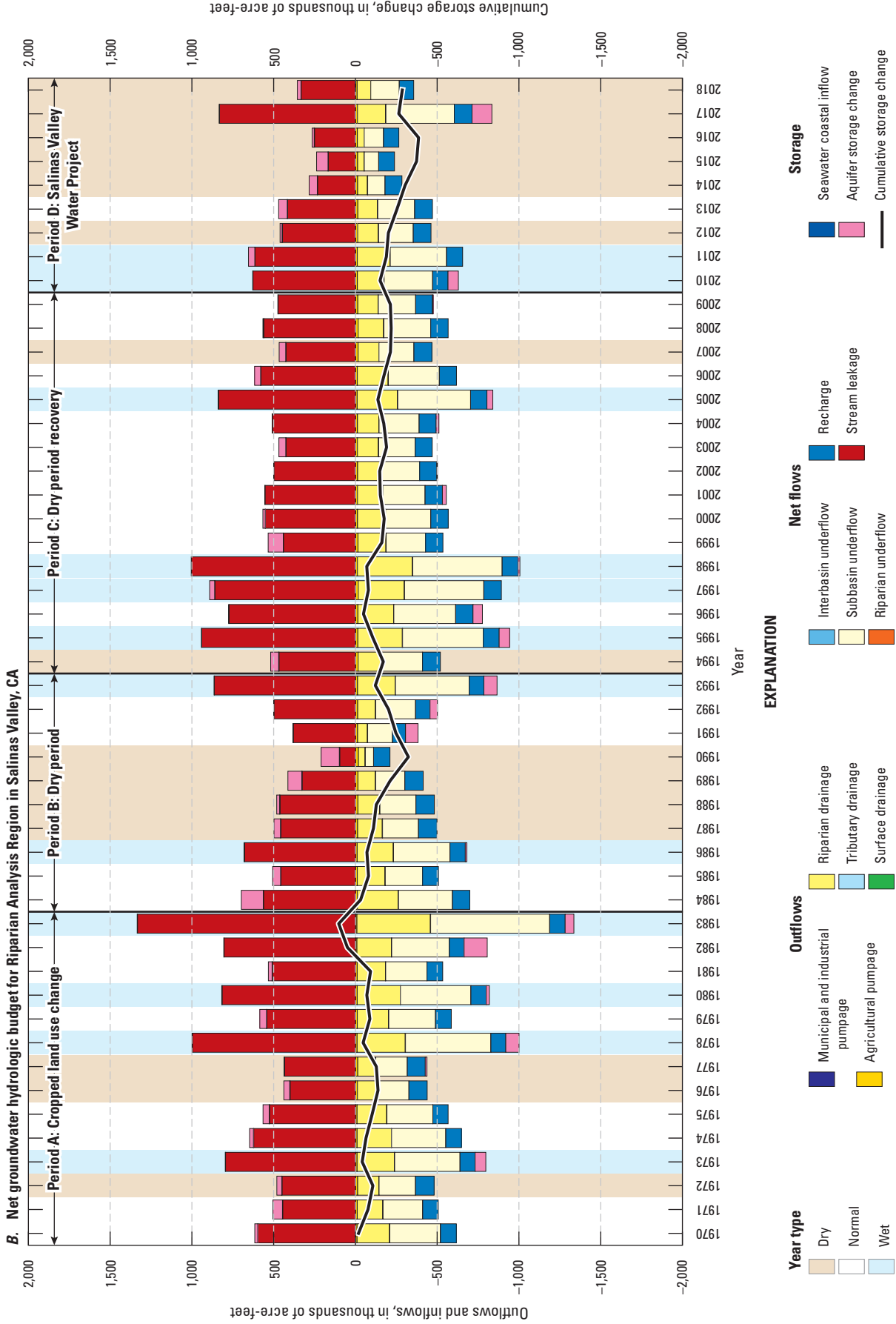




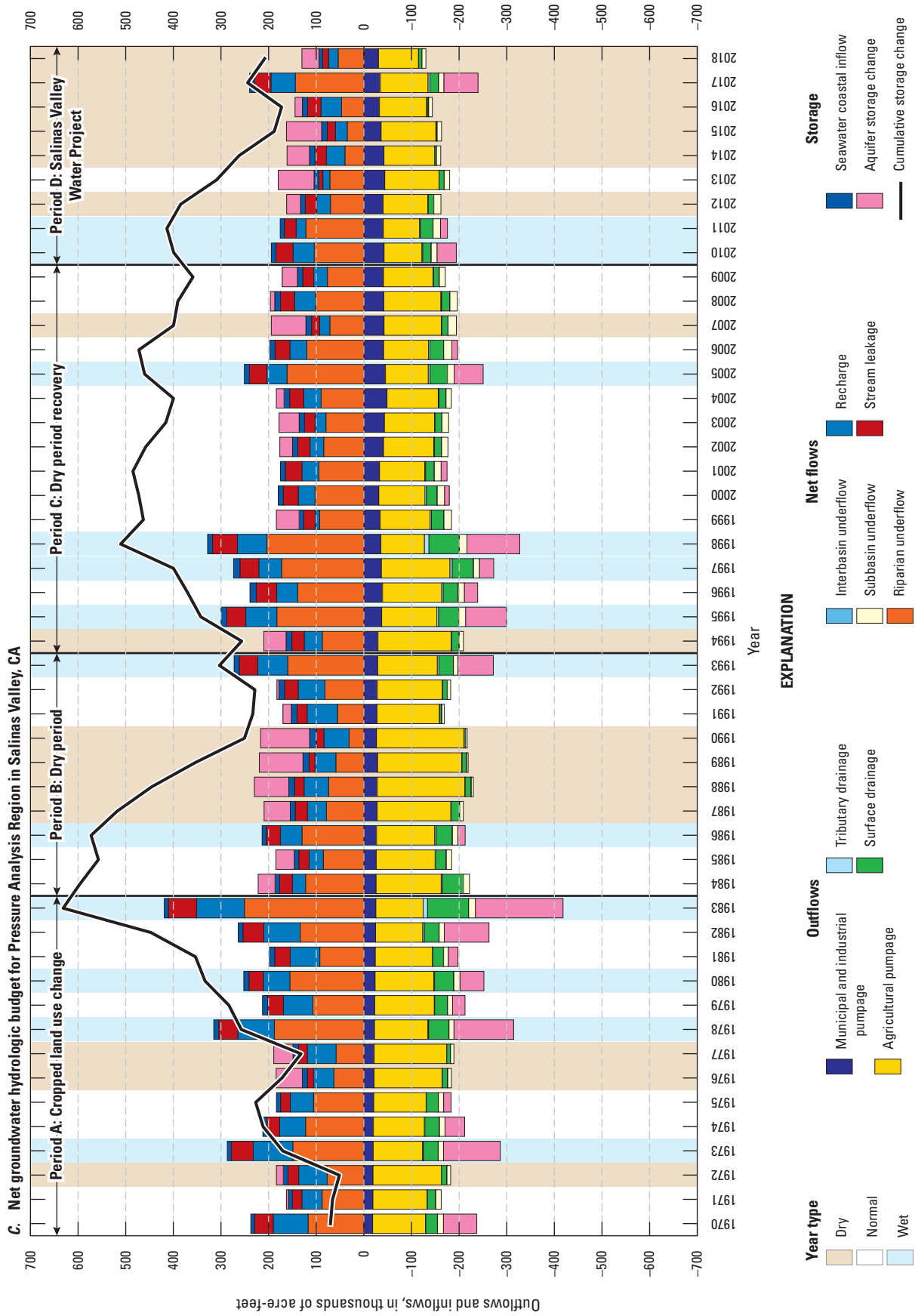
Period A: Cropped land use change  
 Period B: Dry period  
 Period C: Dry period recovery  
 Period D: Salinas Valley Water Project

Figure 39. Distribution of groundwater-budget components of inflows and outflows for the flow system of the Salinas Valley Integrated Hydrologic Model for water year 1970 to 2018. A) Entire integrated hydrologic model domain, B) Riparian analysis region, C) Pressure analysis region, D) East Side-Langley analysis region, E) Forebay analysis region, and F) Upper Valley analysis region (Henson and Culling, 2025).

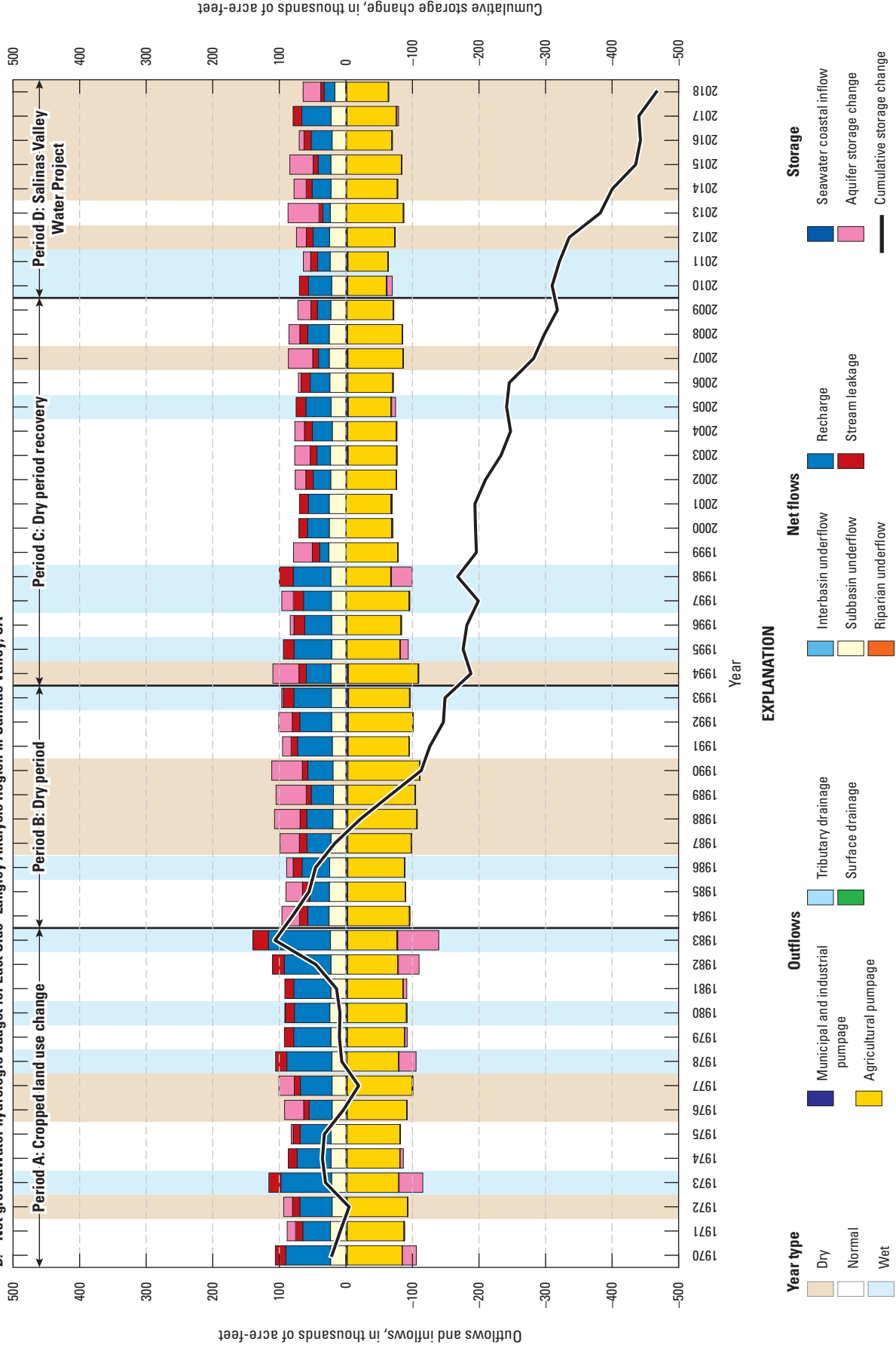


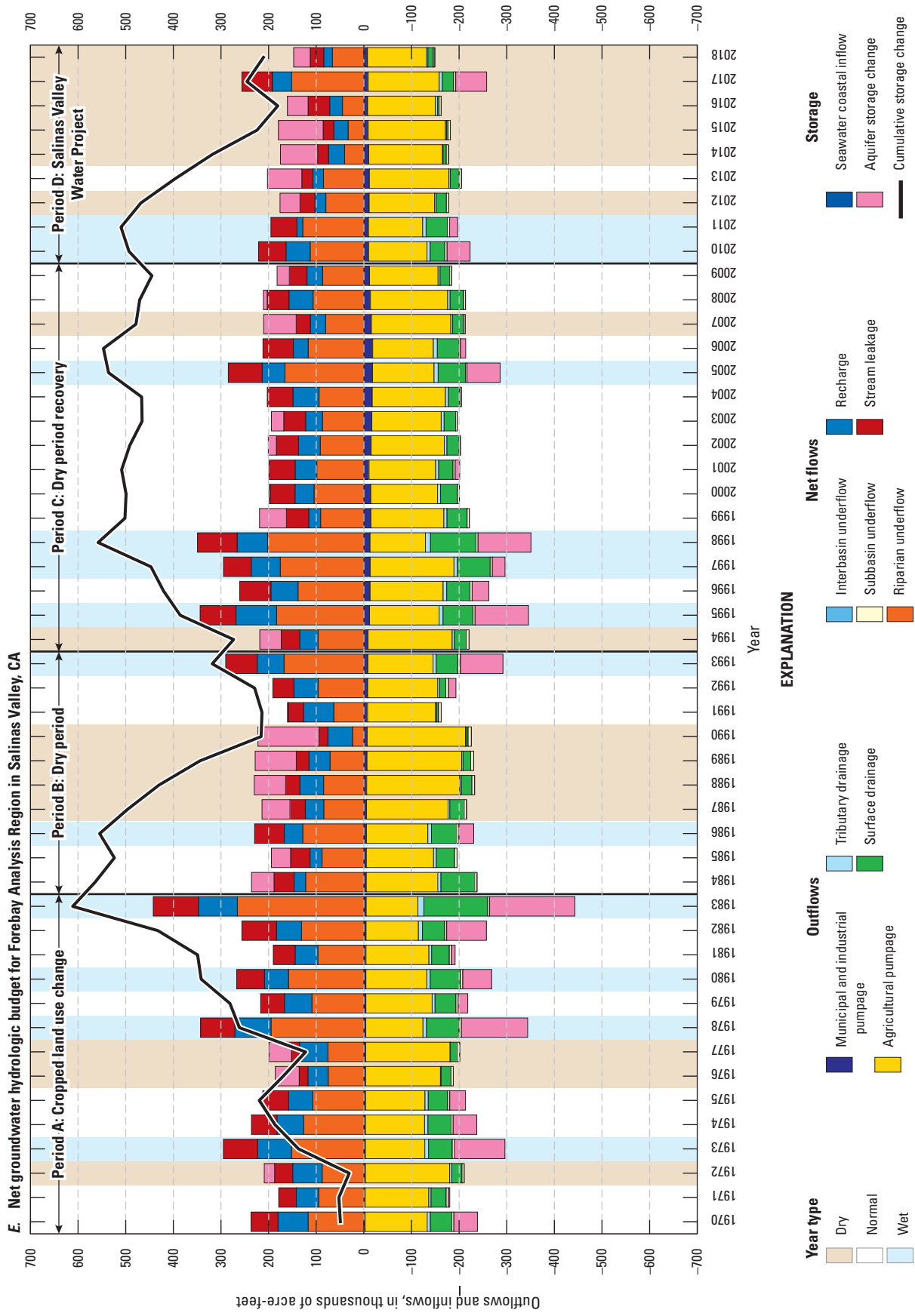




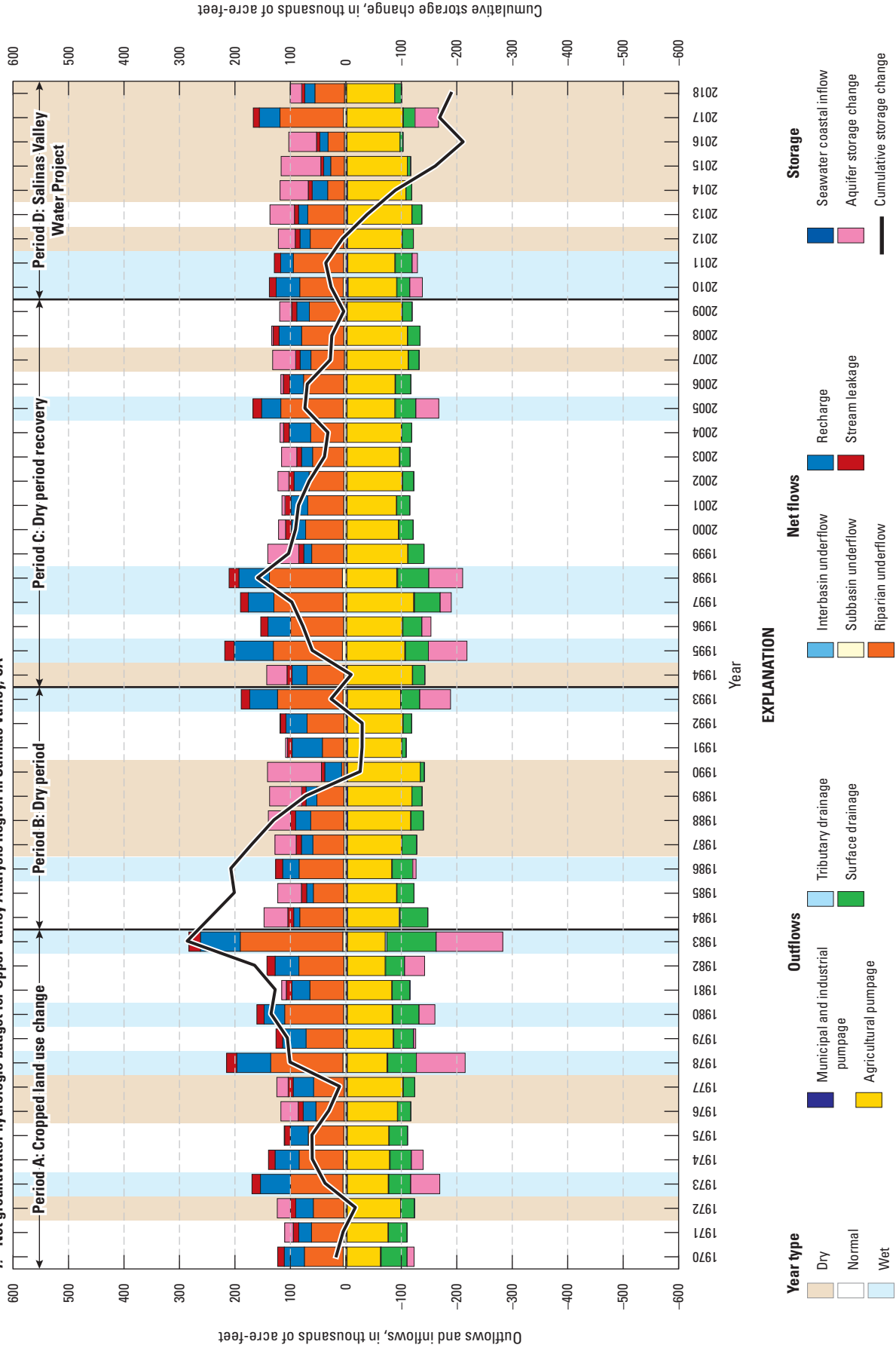


D. Net groundwater hydrologic budget for East Side-Langley Analysis Region in Salinas Valley, CA





F. Net groundwater hydrologic budget for Upper Valley Analysis Region in Salinas Valley, CA



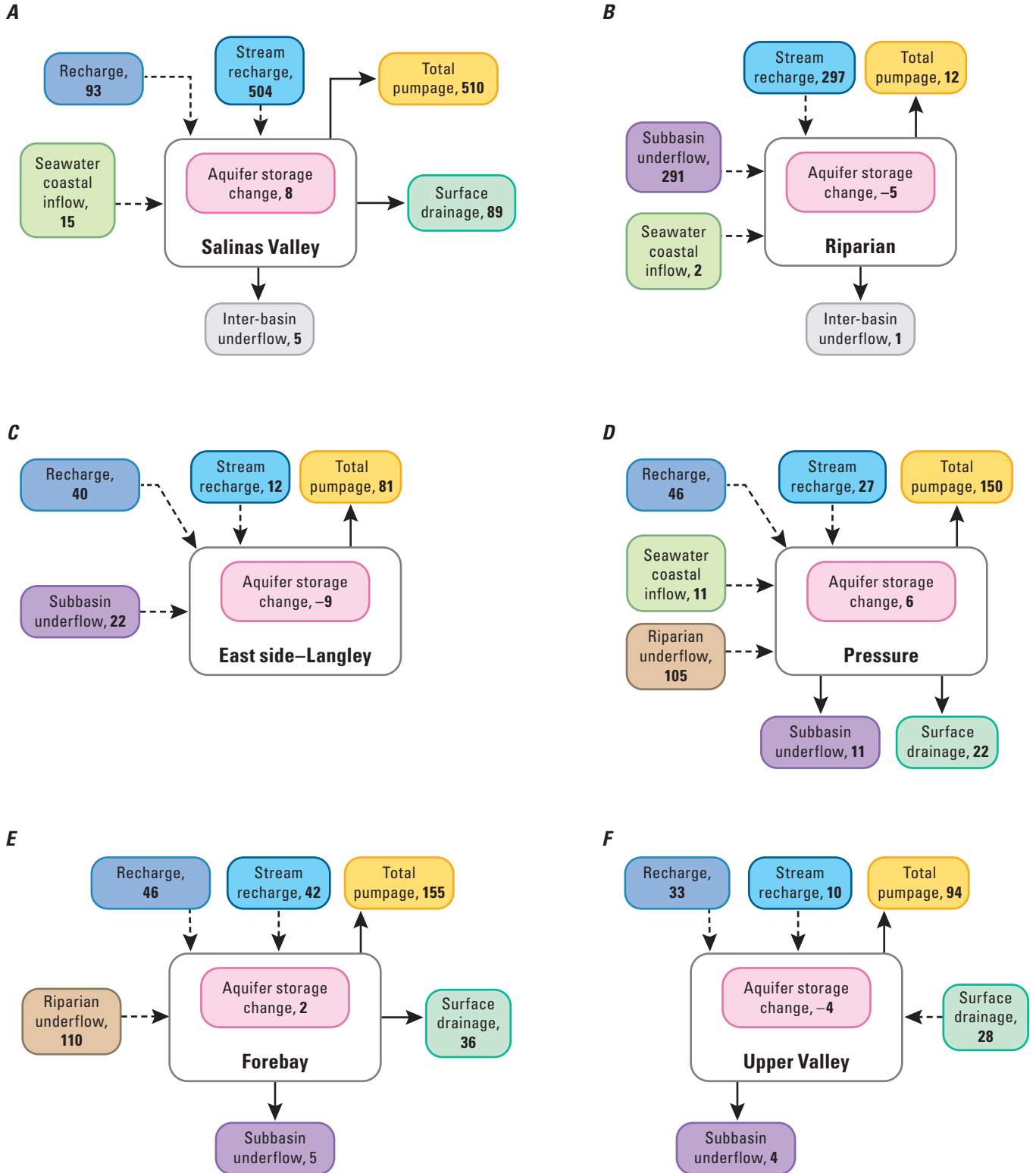


Figure 40. Average groundwater budget from water year 1970 through 2018 showing budget components (in thousands of acre-feet) for the A) entire Salinas Valley Integrated Hydrologic Model domain, B) Riparian analysis region, C) East Side-Langley analysis region, D) Pressure analysis region, E) Forebay analysis region, and F) Upper Valley analysis region (Henson and Culling, 2025).

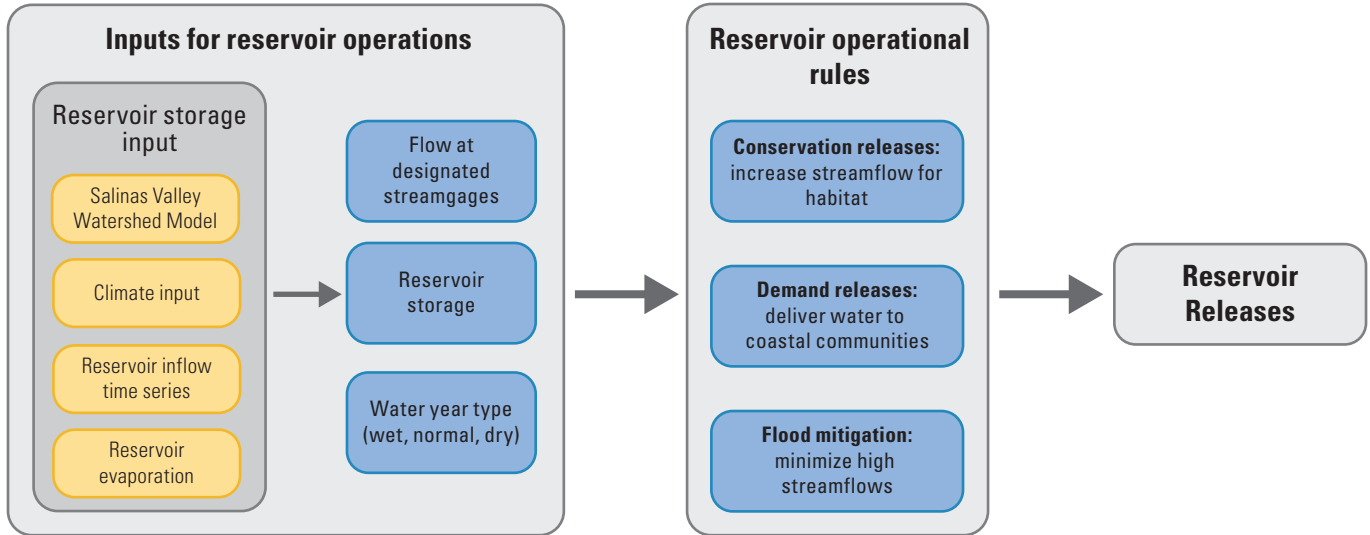


Figure 41. Salinas Valley Operational Model implementation, showing storage parameters that are used to simulate reservoir storage and operational rule parameters that are used to evaluate operational rules for conservation, demand, and floods to generate a time series of reservoir releases.

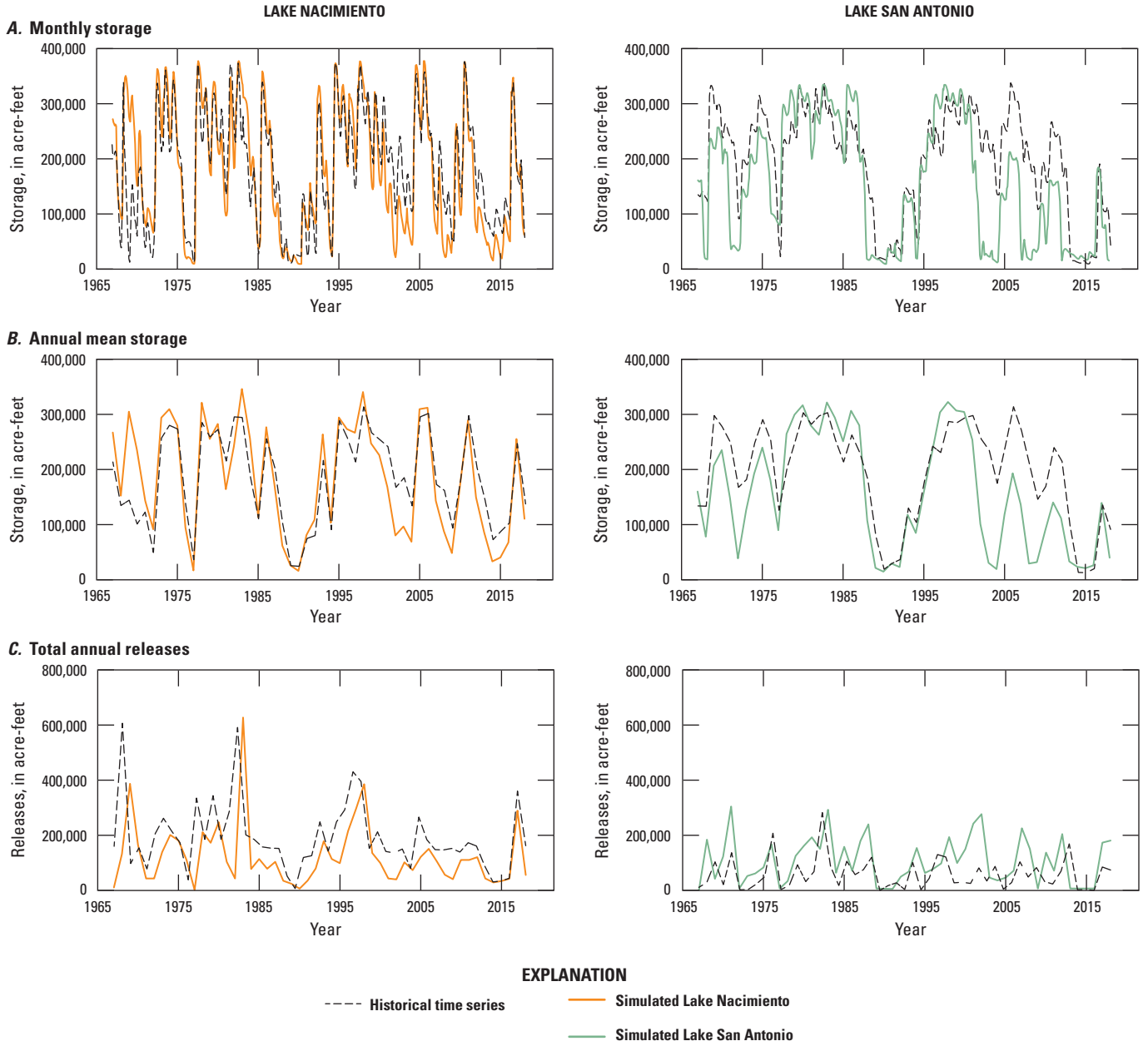


Figure 42. Salinas Valley Operational Model (SVOM) reservoir observed data (Henson and others, 2023) and simulated equivalent values in Lake San Antonio and Lake Nacimiento reservoirs for A) monthly storage, B) annual mean reservoir storage, and C) total annual mean reservoir releases. Reservoir storage and releases in the SVOM are not intended to replicate historical conditions. The historical time series is shown to illustrate that the SVOM results reasonably reproduce flows and storage within the boundaries of historical conditions (Henson and Culling, 2025).

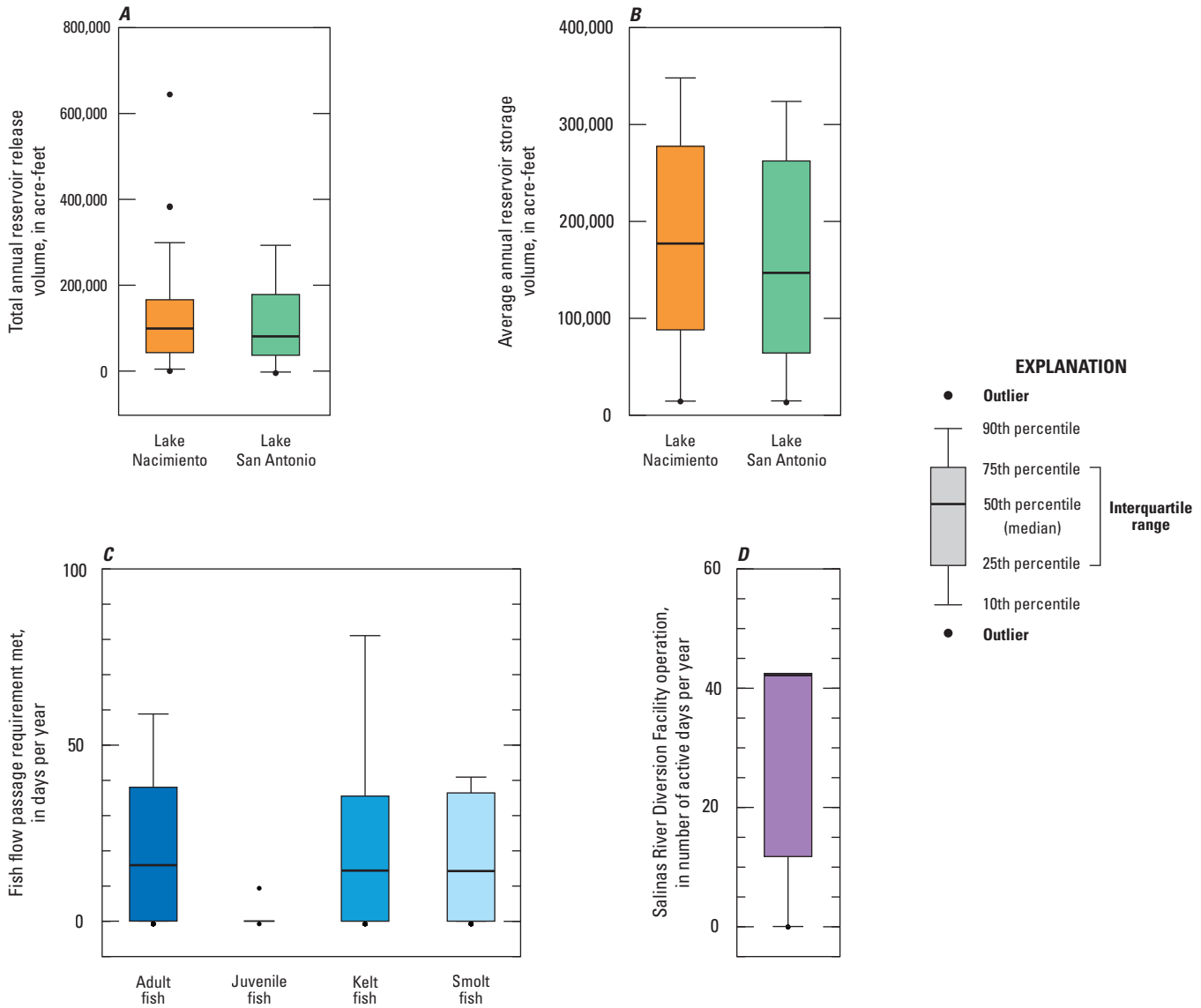


Figure 43. Selected statistics related to reservoir operations describing A) total reservoir releases, B) mean annual reservoir storage, C) simulated days per year where specified streamflow values are met to support phases of steelhead (*Oncorhynchus mykiss*) life cycle, and D) total annual number of days the Salinas River Diversion Facility (SRDF) is active. For each box plot, the shaded box represents the interquartile range, where 50 percent of the data occurs within the range. The lower portion of the shaded box represents the 25th to 50th percentile range, and the upper portion represents the 50th to 75th percentile range. The whiskers display the range that is within 1.5 times the interquartile range. All the data points are plotted on each box plot. Any data points outside of the whisker range are statistical outliers (Henson and Culling, 2025).